frontiers | Research Topics

# Personalized medicine and infectious disease management

**Edited by**
Hadi M. Yassine, Mohamed Emara, Hamdi Mbarek, Nico Marr and Sondes Haddad-Boubaker

**Published in**
Frontiers in Medicine
Frontiers in Molecular biosciences

ISSN 1664-8714
ISBN 978-2-8325-2054-3
DOI 10.3389/978-2-8325-2054-3

## About Frontiers

Frontiers is more than just an open access publisher of scholarly articles: it is a pioneering approach to the world of academia, radically improving the way scholarly research is managed. The grand vision of Frontiers is a world where all people have an equal opportunity to seek, share and generate knowledge. Frontiers provides immediate and permanent online open access to all its publications, but this alone is not enough to realize our grand goals.

## Frontiers journal series

The Frontiers journal series is a multi-tier and interdisciplinary set of open-access, online journals, promising a paradigm shift from the current review, selection and dissemination processes in academic publishing. All Frontiers journals are driven by researchers for researchers; therefore, they constitute a service to the scholarly community. At the same time, the *Frontiers journal series* operates on a revolutionary invention, the tiered publishing system, initially addressing specific communities of scholars, and gradually climbing up to broader public understanding, thus serving the interests of the lay society, too.

## Dedication to quality

Each Frontiers article is a landmark of the highest quality, thanks to genuinely collaborative interactions between authors and review editors, who include some of the world's best academicians. Research must be certified by peers before entering a stream of knowledge that may eventually reach the public - and shape society; therefore, Frontiers only applies the most rigorous and unbiased reviews. Frontiers revolutionizes research publishing by freely delivering the most outstanding research, evaluated with no bias from both the academic and social point of view. By applying the most advanced information technologies, Frontiers is catapulting scholarly publishing into a new generation.

## What are Frontiers Research Topics?

Frontiers Research Topics are very popular trademarks of the *Frontiers journals series*: they are collections of at least ten articles, all centered on a particular subject. With their unique mix of varied contributions from Original Research to Review Articles, Frontiers Research Topics unify the most influential researchers, the latest key findings and historical advances in a hot research area.

Find out more on how to host your own Frontiers Research Topic or contribute to one as an author by contacting the Frontiers editorial office: frontiersin.org/about/contact

# Personalized medicine and infectious disease management

**Topic editors**

Hadi M. Yassine — Qatar University, Qatar
Mohamed Emara — Qatar University, Qatar
Hamdi Mbarek — Qatar Genome, Qatar Foundation, Qatar
Nico Marr — Brandenburg Medical School Theodor Fontane, Germany
Sondes Haddad-Boubaker — Pasteur Institute of Tunis, Tunisia

**Citation**

Yassine, H. M., Emara, M., Mbarek, H., Marr, N., Haddad-Boubaker, S., eds. (2023). *Personalized medicine and infectious disease management*. Lausanne: Frontiers Media SA. doi: 10.3389/978-2-8325-2054-3

# Table of contents

frontiers | Frontiers in Medicine

TYPE Editorial
PUBLISHED 12 May 2023
DOI 10.3389/fmed.2023.1191147



OPEN ACCESS

EDITED AND REVIEWED BY
Alice Chen,
Consultant, Potomac, MD, United States

*CORRESPONDENCE
Sondes Haddad-Boubaker
✉ sondeshaddadboubaker@gmail.com
Hadi M. Yassine
✉ hyassine@qu.edu.qa

RECEIVED 21 March 2023
ACCEPTED 02 May 2023
PUBLISHED 12 May 2023

CITATION
Haddad-Boubaker S, Mbarek H and Yassine HM (2023) Editorial: Personalized medicine and infectious disease management.
*Front. Med.* 10:1191147.
doi: 10.3389/fmed.2023.1191147



# Editorial: Personalized medicine and infectious disease management

Sondes Haddad-Boubaker[1,2,3]*, Hamdi Mbarek[4] and Hadi M. Yassine[5]*

[1]Laboratory of Clinical Virology, WHO Regional Reference Laboratory for Poliomyelitis and Measles for the EMR, Institut Pasteur de Tunis, Tunis, Tunisia, [2]LR20IPT02, Laboratory of Viruses, Hosts and Vectors, Institut Pasteur de Tunis, The University of Tunis El Manar, Tunis, Tunisia, [3]Clinical Investigation Center, Institut Pasteur de Tunis, Université Tunis El Manar, Tunis, Tunisia, [4]Qatar Genome, Qatar Foundation, Doha, Qatar, [5]Biomedical Research Center, Qatar University, Doha, Qatar

KEYWORDS

**infectious diseases, genetics, genetic susceptibility, viruses, SNPs**

Editorial on the Research Topic
Personalized medicine and infectious disease management

The importance of personalized medicine in the healthcare management of several diseases is well-documented. Still, very little is known about the role of genetics in susceptibility or resistance to infectious diseases (1). Following the emergence of SARS-CoV-2, it became prominent that the genetic background of the patient influences the disease prognosis and treatment. Therefore, multiple genetic databases were established to study precision medicine for COVID-19 (2). This Research Topic gathered different contributions demonstrating the impact of genetic determinants in infectious diseases prognosis and clinical outcome. Ten articles were published in this editorial topic, including five research articles, three reviews, and two case studies.

The first article is titled "*Transient receptor potential vanilloid subtype 1: potential role in infection, susceptibility, symptoms and treatment of COVID-19*" (Liviero et al.). This review article focused on the role of the TRPV-1 channel in the pattern of COVID-19 clinical manifestation, susceptibility, pathogenesis, and therapeutic interventions. TRPV-1 is a receptor involved in immune response, and thus, might be involved in the susceptibility/resistance to SARS-CoV-2 infection. Liviero et al. demonstrated that investigating SNPs of the TRPV-1 gene will raise new therapeutic ways that could help the establishment of effective immune responses resulting in a better clinical outcome.

The other study by Saad et al. focused on the role of ACE 1 in the risk and outcome of SARS-CoV-2 infection. Indeed, the study reported a positive correlation between ACE1 I and the risk of acquiring COVID-19 as well as between the ACE1-D allele and its negative impact following SARS-CoV-2 infection. Thus, the authors suggested that genotyping for ACE1 I/D polymorphism could be useful for better management of the disease. Nevertheless, further evaluation studies are required for validation in different ethnic groups (Saad et al.).

Along the same topic, a study by Ahmed et al. discussed the interaction mechanism of the N501Y mutant recorded in some SARS-CoV-2 variants for ACE2. The authors demonstrated an enhanced affinity of the N501Y mutant S1-RBD with ACE2 compared to the wild phenotype interactions. Such findings might have implications for developing anti-viral drugs against SARS-CoV-2 infection (Ahmed et al.).

On the other hand, Angulo-Aguado et al. investigated the impact of LZTFL1 rs11385942 polymorphism on COVID-19 severity in the Colombian population. They investigated the association of three polymorphisms (ACE rs 4646994, ACE2rs 2285666, and LZTFL1 rs11385942) with COVID-19 short- and long-term outcomes. The study highlighted a positive association between LZTFL1 rs11385942 and COVID-19 severity and the role of nongenetic factors such as clinical signs. They also provided an integrative web-based application as a predictive tool for severity risk assessment. Such tools may be impactful for the management of COVID-19 cases. However, the implementation of this integrative application may pose challenges in areas with limited web accessibility. Further validations for this study are necessary in pre-clinical settings and with a larger cohort to strengthen its findings (Angulo-Aguado et al.).

In a case report study, Schaefer and Bittmann reported on "*Individualized pulsed electromagnetic field therapy in a Long COVID patient using the Adaptive Force (AF) as biomarker*". This novel diagnostic approach resulted in positive outcomes for one severely affected patient with long COVID-19. They stated that AF reflects the ability of the neuromuscular system to adjust adequately to external powers in an isometric-holding manner. They also reported that the long COVID-19 symptoms did not return after 6 months. Therefore, this case report indicates that this method should be a valuable diagnostic assay for post-COVID-19 illness. Nonetheless, this study was done on only one patient and did not consider genetic polymorphism as a player in response to the treatment (Schaefer and Bittmann).

Immunogenomic is a growing field that combines immunology and genetics to understand how the immune system responds to infection and vaccination. In a review article, Smatti et al. discussed whether host genetics implicate in the response to COVID-19 vaccination, noting that several studies shed light on the contribution of genetic factors in modaling immune responses after vaccination against measles, hepatitis B, rubella, Influenza, and smallpox. In general, genetic variants in genes related to immune response as well as virus replication may shape the individual response to the vaccination. The review highlited the impact of GWAS and other genomic studies to vaccine reponse and adverse understanding. In summary, identifying genetic markers related to the outcome of SARS-CoV-2 infection or response to vaccination may guide healthcare providers in selecting the appropriate treatment, and probably the most reliable vaccine for an individual or an ethnic group (Smatti et al.).

In another comprehensive review, Atallah and Mansour demonstrated the impact of host response-based molecular diagnostics on the clinical management of viral and bacterial infections. They proposed that host-based response diagnostics could be used as a supplement but not a replacement for commonly used pathogen-based diagnostics. Ultimately, accurate and rapid disease diagnosis will be translated into reduced healthcare burden, lesser adverse effects, reduction in the misuse of antibiotics, improvement of public health measures to a better management of infectious diseases and positive patient outcomes (Atallah and Mansour).

Away from acute infections, Chronic Hepatitis B (CHB) continues to be a significant global health challenge due to high morbidity and mortality, in absence of reliable treatments. In their study, Shang et al. investigated the association and clinical relevance of ALDH2 polymorphisms for HBV susceptibility and persistence in a Chinese population. Indeed, it was previously demonstrated ALDH2 contributes in the way of a variety of liver diseases. Genotyping over 1000 participants, they analyzed the role of rs671 and rs1229984 in HBV infection. Compared to healthy controls, rs671-AA genotype frequency was higher in the HBV-infected individuals, especially in the chronic hepatitis B (CHB) group, demonstrating a significant positive association. They also demonstrated that individuals with CHB who harbor the ALDH2 rs671-AA genotype are at higher risk of developing persistent HBV infection and thus, presenting higher HBV load compared with those with GG/GA genotype. These data suggest the possible harmful role of rs671-AA variant in HBV infection, persistence, and chronicity (Shang et al.).

Testing for specific microbes in the central nervous system (CNS) infectious diseases is often tedious and insensitive. Consequently, the delay in identifying the etiological agents and corresponding treatment in patients with CNS infections leads to worse management and outcomes. Chen et al. reported a case study on herpes simplex encephalitis (HSE). In their case, dual mNGS analysis and multiplex PCR (mPCR) were used to identify and semi-quantify the herpes simplex virus (HSV-1). Utilization of combined mNGS and mPCR methods enabled early diagnosis of the infection and disease management using effective treatment. Furthermore, quantifying the viral load along the treatment process can help for better case management (Chen et al.).

Gu et al. reported preliminary findings on the combined effect of low-dose trimethoprim-sulfamethoxazole (TMP/SMX) and clindamycin on severe pneumocystis pneumonia (PCP) following renal transplantation. Including 20 patients in their study, the authors claimed that the use of this combined treatment on PCP patients was more effective than the single use of TMP/SMX alone. They also demonstrated the safety of such treatment, especially in patients that are intolerant to the standard dose of TMP/SMX. However, Further molecular investigation was required to confirm the improved patient outcome (Gu et al.).

Finally, personalized or precision medicine is a growing approach to improve patient care by applying the right intervention at the right time. According to the GWAS Catalog statistics (OCT 2020), out of 4,761 publications, only eighty-six were related to infectious diseases (ID) (1.8%). Further, only 2,496 associations were ID-related (1.1%) out of 213,519 total associations. With the emergence of SARS-CoV2, most studies have been focused on COVID-19, which was also reflected in this special topic. However, with the significant progress and achievements in this field, we anticipate that other ID, particularly those linked to complex diseases like cancer and neurodegenerative conditions, will be investigated.

The ultimate aim of this Research Topic was to shed light on the importance of genetics and personalized medicine in improving ID management and treatment. Several topics were discussed to highlight the importance of genetic testing in understanding disease susceptibility, prognosis, treatment, as well as drug and vaccine utilization.

## Author contributions

SH-B and HY wrote the initial draft. All authors reviewed and approved the last version.

## Acknowledgments

We would like to acknowledge Dr. Nico Marr and Dr. Mohamed Emara for their contribution to this editorial topic.

## Conflict of interest

The authors declare that the research was conducted in the absence of any commercial or financial relationships that could be construed as a potential conflict of interest.

## Publisher's note



## References

1. Zeberg H, Paabo S. The major genetic risk factor for severe COVID-19 is inherited from Neanderthals. *Nature*. (2020) 587:610–2. doi: 10.1038/s41586-020-2818-3

2. Russo R, Andolfo I, Lasorsa VA, Iolascon A, Capasso M. Genetic analysis of the coronavirus SARS-CoV-2 host protease TMPRSS2 in different populations. *Front Genet*. (2020) 11:872. doi: 10.3389/fgene.2020.00872

frontiers in Medicine

REVIEW
published: 04 November 2021
doi: 10.3389/fmed.2021.753819

# Transient Receptor Potential Vanilloid Subtype 1: Potential Role in Infection, Susceptibility, Symptoms and Treatment of COVID-19

*Filippo Liviero, Manuela Campisi, Paola Mason and Sofia Pavanello**

*Occupational Medicine, Department of Cardiac, Thoracic, Vascular Sciences and Public Health, University Hospital of Padua, Padova, Italy*

The battle against the new coronavirus that continues to kill millions of people will be still long. Novel strategies are demanded to control infection, mitigate symptoms and treatment of COVID-19. This is even more imperative given the long sequels that the disease has on the health of the infected. The discovery that S protein includes two ankyrin binding motifs (S-ARBMs) and that the transient receptor potential vanilloid subtype 1 (TRPV-1) cation channels contain these ankyrin repeat domains (TRPs-ARDs) suggest that TRPV-1, the most studied member of the TRPV channel family, can play a role in binding SARS-CoV-2. This hypothesis is strengthened by studies showing that other respiratory viruses bind the TRPV-1 on sensory nerves and epithelial cells in the airways. Furthermore, the pathophysiology in COVID-19 patients is similar to the effects generated by TRPV-1 stimulation. Lastly, treatment with agonists that down-regulate or inactivate TRPV-1 can have a beneficial action on impaired lung functions and clearance of infection. In this review, we explore the role of the TRPV-1 channel in the infection, susceptibility, pathogenesis, and treatment of COVID-19, with the aim of looking at novel strategies to control infection and mitigate symptoms, and trying to translate this knowledge into new preventive and therapeutic interventions.

**Keywords: TRPV-1, SARS-CoV-2, COVID-19, SNPs, pollution, inflammation, therapy**

OPEN ACCESS

***Edited by:***
*Shisan Bao,*
*The University of Sydney, Australia*

***Reviewed by:***
*Changqing Yang,*
*Tongji University School of Medicine, China*
*Anquan Shang,*
*Tongji University, China*

****Correspondence:***
*Sofia Pavanello*
*sofia.pavanello@unipd.it*

***Specialty section:***
*This article was submitted to Infectious Diseases - Surveillance, Prevention and Treatment, a section of the journal Frontiers in Medicine*

***Received:*** *05 August 2021*
***Accepted:*** *08 October 2021*
***Published:*** *04 November 2021*

***Citation:***
*Liviero F, Campisi M, Mason P and Pavanello S (2021) Transient Receptor Potential Vanilloid Subtype 1: Potential Role in Infection, Susceptibility, Symptoms and Treatment of COVID-19. Front. Med. 8:753819. doi: 10.3389/fmed.2021.753819*

## INTRODUCTION

COVID-19, a new human respiratory disease that continues to kill millions of people, is a worldwide public health challenge. Its infectious agent, SARS-CoV-2, diverges from other coronaviruses in some structural characteristics that render this virus more pathogenic and transmissible. Of the four structural proteins, the spike protein (S) plays the fundamental role in cell receptor recognition and subsequent entry of the virus. The discovery that S protein encompasses two ankyrin binding motifs (S-ARBMs) and some transient receptor potential (TRP) cation channels present the same ankyrin repeat domains (TRPs-ARDs) (1), it may be postulated that the transient receptor potential vanilloid subtype 1 (TRPV-1), the most studied member of the TRPV channel family, can play a role in binding SARS-CoV-2. This hypothesis is strengthened by studies revealing that other respiratory viruses bind the TRPV-1 on sensory nerves and epithelial cells in the airways (2). Furthermore, the pathophysiology in COVID-19 patients is similar to the effects generated by TRPV-1 stimulation (3). Finally, treatment with agonists that down-regulate

or inactivate TRPV-1 may have a beneficial effect on impaired lung function (3–5), and clearance of infection (6). In this review, we explore the role of TRPV-1 channel in the infection, susceptibility, pathogenesis, and treatment of SARS-CoV-2 infection.

## TRPV-1

TRPV-1 is a nonselective cationic ligand-gated channel with high permeability to $Ca^{2+}$, extensively expressed on neuronal and non-neuronal cell membranes, including immune cells and type C sensory nerve fibers of air route (upper and lower lung tract and parenchyma), where they act as molecular sensors to differentiate temperature, noxious substances, and pain. This was a revolutionary discovery which earned David Julius the victory of the 2021 Physiology/Medicine Nobel Prize. TRPV-1 participates (through the generation of $Ca^{2+}$ dependent signals) in mechanisms that contribute to the defense of the airways such as cough and mucociliary clearance (7, 8). The activation of TRPV-1 mainly allows extracellular $Ca^{2+}$ entrances into neuronal cells, with release of neurotransmitters, the excitability of the membrane and contraction of airway smooth muscle (9). It is also considered a "pathological receptor" that plays an important role in the transduction of noxious stimuli and in the maintenance of inflammatory conditions (10). In fact, TRPV-1 is involved in various inflammatory conditions, such as in inflammatory bowel disease (IBD), cutaneous neurogenic inflammation, brain inflammation, allergic asthma, colitis, arthritis, hypersensitivity, chronic obstructive pulmonary disease (COPD), and autoimmune diseases (11).

TRPV-1 works as a multisensory receptor for damage signals and following exposure to inhaled particles, such as allergens, cigarette smoke, air pollutants and virus too. Inflammation of the airways is supported by the transfer of the signal from neuronal fibers TRPV-1-positive to immune cells (12, 13). TRPV-1 can also be triggered by exogenous mediators such as capsaicin (CPS), resiniferatoxin, temperature (higher than 40°C), acidic conditions (e.g., citric acid), and endogenous mediators, including bioactive lipids, mainly produced during inflammation (e.g., prostaglandins E2 (PGE2), thromboxanes, and leukotrienes, three classes of arachidonic acid derivatives). Furthermore, activation of TRPV-1 boosts the release of various pro-inflammatory molecules, including neuropeptides substance P (sP) and cytokines such as interleukin 6 (IL-6), the same involved in the pathophysiological events affecting the COVID-19. All the above hints envisage the involvement of TRPV-1 in COVID-19 infection (3).

**Abbreviations:** IL-6, Interleukin 6; IL-2, Interleukin 2; IL-7, Interleukin 7; IL-10, Interleukin 10; GSCF, Granulocyte colony-stimulating factor; IP-10, Interferon ɤ-induced protein; MCP1, Monocyte chemoattractant protein-1; MIP1A, Macrophage inflammatory protein-1α; TNFα, Tumor Necrosis Factor α; TRPV-1, Transient receptor potential vanilloid subtype 1; CPS, Capsaicin; DEP, Diesel exhaust particulate; ECG, Electrocardiogram; HRV, Heart rate variability; PGE2, Prostaglandin E2; BK, Bradykin; HRV, Human rhinovirus; RSV, Respiratory syncytial virus; MV, Measles virus; HCV, Hepatitis C virus; HSV-2, Herpes simplex virus type 2; HSV-1, Herpes simplex virus type 1; VZV, Varicella-zoster virus.

## TRPV-1 IN VIRAL INFECTIONS

TRPV-1 expression is significantly activated by several viral infections, including those through the respiratory route, i.e., human respiratory rhinovirus (HRV) and syncytial virus (RSV), or even through other routes i.e., measles virus (MV), hepatitis C virus (HCV), herpes simplex virus type 2 (HSV-2), herpes simplex virus type 1 (HSV-1), and varicella-zoster virus (VZV) (14, 15). This therefore suggested that TRPV-1 plays a central role in host-pathogen contacts including the binding, entry and replication of the virus. Recently, the involvement of TRPV-1 during Chikungunya virus (CHIKV) infection was studied in host macrophages (16).

Furthermore, likewise COVID-19, CHIKV is a single-stranded RNA virus, and generates symptoms, fever, including high fever, nausea, vomiting, headache, rashes, polyarthralgia, and myalgia (17–19), comparable to that of COVID-19. Results showed that TRPV-1 was upregulated by CHIKV infection. The involvement of TRPV-1 in CHIKV was confirmed by using specific modulators the 5'-iodoresiniferatoxin (5'-IRTX, a TRPV-1 antagonist) and resiniferatoxin (RTX, a TRPV-1 agonist). The results indicate that TRPV-1 inhibition leads to a reduction in CHIKV infection, whereas TRPV-1 activation significantly enhances CHIKV infection (16). Furthermore, Sanjai Kumar and co-workers demonstrated that CHIKV infection regulated $Ca^{2+}$ influx through TRPV-1 resulting in a higher production of pro-inflammatory TNF and IL-6 the same during COVID-19 infection. These findings, therefore, suggest the involvement of TRPV-1 in other viral infections, including COVID-19 (**Figure 1**).

## INFLAMMATION IN SARS-COV-2 INFECTION AND POTENTIAL ROLE OF TRPV-1

SARS-CoV-2 induces an alveolar-interstitial inflammation with a high risk of acute pulmonary edema or acute respiratory distress syndrome. The clinical signs of COVID-19 are consistent with those observed in viral pneumonia (20). These pulmonary changes are likely responsible for both systemic and localized immune responses leading to a hyperinflammatory state. The mortality rate in patients with SARS-CoV-2 infections is related to virally driven "cytokine storm" that results from a severe immune reaction in the lungs as measured by high levels of inflammatory markers (c-reactive protein, serum ferritin) and cytokine levels (IL-6, IL-2, IL-7, IL-10, GSCF, IP10, MCP1, MIP1A, and TNFα) in the plasma (21). Underlying physiological events leading to mortality have been hypothesized to be closely linked to the TRPV-1 expressing neuronal system in the lungs. The respiratory tract (higher and lower) is densely populated by sensory afferents originating from neurons in the nodose (vagal) ganglia (VG) and dorsal root ganglia (DRG). Many of the neurons in these ganglia express high levels of the TRPV-1 ion channel. The crosstalk between TRPV-1 positive nerve fibers and immune cells is

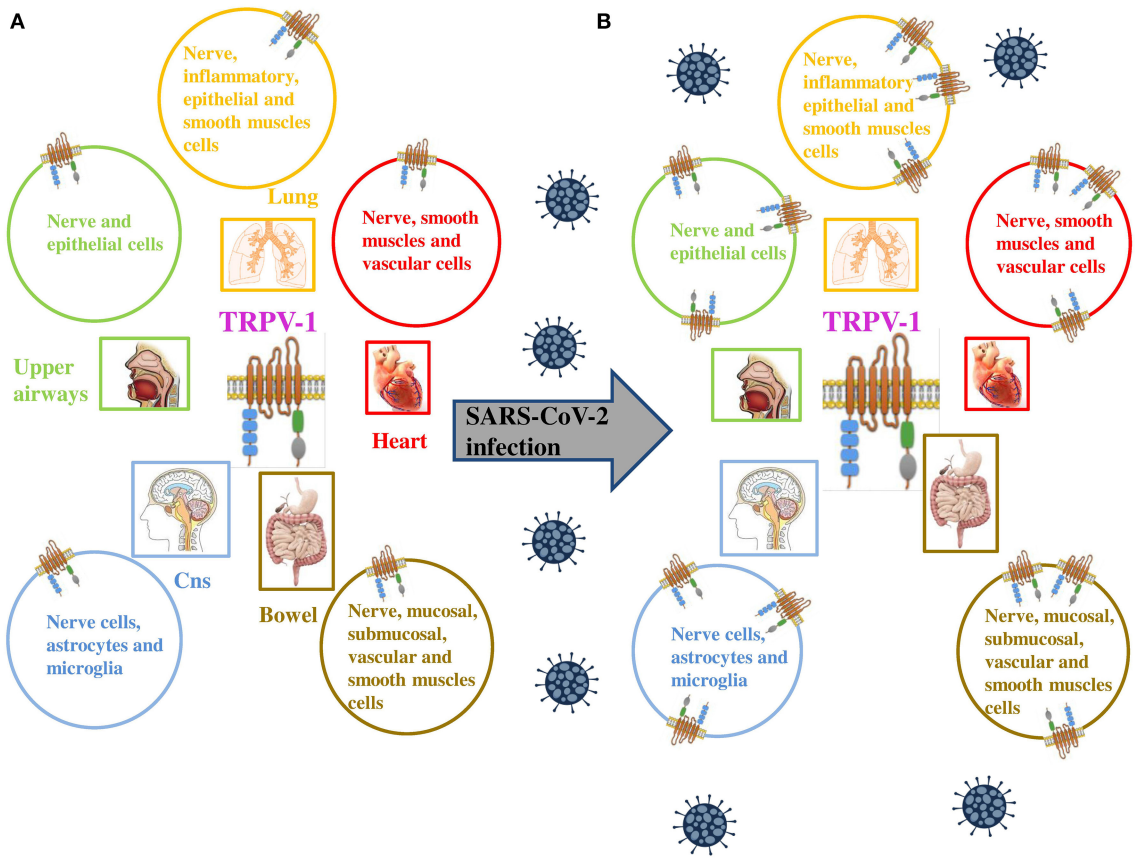


**FIGURE 1 | (A)** TRPV-1 is extensively expressed on neuronal and non neuronal cell membranes, including immune cells and type C sensory nerve fibers of the airways (upper and lower respiratory tract and lung parenchyma). **(B)** TRPV-1 has been found to be significantly upregulated in numerous viral infections, similarly SARS-CoV-2 is proposed to upregulate the expression of the channel on neuronal and non neuronal cell membranes of infected patients. Adapted from (9).

critical in mediating inflammation of the airways following exposure to either inhaled allergens or viral infection (12, 22). A recent study has demonstrated that respiratory viral infections (by rhinovirus, respiratory syncytial virus or measles virus) can upregulate TRPV-1 receptors by channel specific mechanisms (2). This upregulation can drive an inflammatory cascade in the lungs leading to airways hyperactivity and is dependent on the viral load and duration of infection. Interestingly, treatment with TRPV-1 antagonist in this study significantly inhibited TRPV-1 upregulation post viral infection. The interaction of SARS-CoV-2 virus with TRPV-1 receptors has not yet been investigated but given the respiratory pathophysiology in COVID-19 cases, may exhibit similar mechanisms that can result in sensitizing TRPV-1 receptors resulting in hyper-inflamed lungs and associated complications. Indeed activation of TRPV-1 enhances the release of several pro-inflammatory molecules, including sP, and cytokines such as IL-6. Moreover, pro-inflammatory substances have reported to be upregulated in COVID-19 cases and reflect the severity of the disease (23).

## SUSCEPTIBILITY TO COVID-19 INFECTION

### Pollution

Two big studies conducted in France examined the incidence of myocardial infarction (MI) admission during the COVID-19 pandemic, in particular the periods before and after the lockdown in France (24, 25). The first study conducted in 22 centers in France identified a significant decline of admission for MI (including ST-segment and non-ST segment raise MI) during COVID-19 national lockdown. Both studies reported 30% (24) and 20% (25) drop of MI, the latter observed in two region of France ("Hauts-de-France" and "Pays de-la-Loire"). The authors concluded that the reduction in hospital admissions was influenced by the decrease in air pollution, a well-known trigger of acute MI (26).

Numerous epidemiological studies have consistently highlighted associations between mortality and morbidity due to cardiopulmonary diseases and increased air pollutants (27, 28). These relationships, which are more reliable for particulate matter (PM) and are often observed within hours of PM concentration peaks in urban air, suggest that very fast

events should take place (29, 30). A number of authors have suggested neurological mechanisms to explain such short-term toxicity of PM (27, 31–36) with TRPV-1 localized on vagal bronchopulmonary C-fibers endings in the lung, as primarily responsible for eliciting centrally mediated reflexes (37).

*In vitro* and *in vivo* studies showed that TRP channels are activated by air contaminants. We recently demonstrated that air pollutants, such as DEP, directly interact with TRPV-1 and cause channel opening (38). Furthermore, the inhalation of environmental (39) and diesel exhaust particulate (DEP) (36) stimulate TRPV-1 causing changes in cardiac rhythm, electrocardiogram (ECG) morphology, and decreased heart rate variability (HRV). These results may be explained considering an imbalance of autonomic heart control (in favor of sympathetic activity), with centrally-mediated reflexes, *via* the afferent unmyelinated C-fibers, which are in turn activated by PM. In line with this hypothesis, a reduced HRV was observed in susceptible individuals after short-term exposures to PM (40). Furthermore, in patients taking ß-blockers, which regulated the sympathetic activity, HRV reduction by PM exposure was not detected (41). Our recent data (38) indicate that signals from airways sensory nerves (i.e., DEP which directly activate TRPV-1 and also endogenous mediators such as prostaglandin E2 (PGE2) and bradykinin (BK) which are considered to be indirect sensitizers of the channel), when they joined the central nervous system (CNS) can affect the autonomic impulse to the heart (**Figure 2**). All this evidence postulates a proof of concept that explains the indication that peaks of pollutants are associated with short-term cardiovascular adverse events in susceptible subjects, as for example COVID-19 patients.

## Interconnection Between ACE2, TMPRSS2 and TRPV-1

That TRPV-1 interacts with other receptors is not new (42). TRPV-1 may interact with Angiotensin-converting enzyme 2 (ACE2) and transmembrane protease-serine 2 (TMPRSS2) through the activation of cyclooxygenase 2 (COX-2) and kininogen pathways (**Figure 3**). ACE2 and TMPRSS2 are broadly documented as key cellular receptors of SARS-CoV-2 to conquer target cells (43). In particular, SARS-CoV-2 spike protein is processed by TMPRSS2 which favors its binding to ACE2, expressed on epithelial lung cells (44).

In the COX-2 pathway, TRPV-1 sensitization may be achieved when SARS-CoV-2, by interacting with neuroinflammatory cells, increases levels of PGE2, a potent inflammatory mediator that is generated by the effect of COX-2 on arachidonic acid. High PGE2 levels lead to prostaglandin receptors 1 (EP1) and 3 (EP3) stimulation and subsequent TRPV-1 sensitization. The EP1 and EP3 are regarded as stimulatory receptors as their activation leads to stimulation of the cell concerned, such as contraction in the smooth muscle cell or activation of the neuron. ACE2 that is a negative regulator of the classical angiotensin-converting enzyme (ACE) in the renin-angiotensin system (RAS) was discovered to be dysregulated (decreased levels of ACE and increased levels of ACE2 in the lung cells) in patients presenting severe symptoms of COVID-19 (45). In addition, a significant increase of bioactive lipid levels modulating lung inflammation of severe COVID-19 patients, compared to healthy controls, has been reported (46). The Authors highlighted in COVID-19 patients, a predominance of cyclooxygenase metabolites, in particular significant levels of PGE2, and also increased levels of leukotrienes, compared to controls (46). These products of inflammation are able to activate TRPV-1.

In the kininogen pathway SARS-CoV-2, by interacting with neuroinflammatory cells, increases levels of BK, which is produced from an inactive pre-protein kininogen through activation by the serine protease kallikrein. High BK levels lead to BK receptors stimulation and subsequent TRPV-1 sensitization on bronchopulmonary C-fibers. There are two types of receptors for BK in the body, the BKB1 receptor which is inducible and is expressed by the presence of inflammation and tissue damage (47), and the BKB2 receptor which is present constitutively (48). Both BKB1 and BKB2 receptors exert their effect by coupling to G proteins and activating phospholipase C or A2. The activation of phospholipase C leads to the sensitization of TRPV-1 through protein kinase C (49, 50). Furthermore, the upregulation of ACE2, in patients with severe symptoms of COVID-19 (45), increases Angiotensin 1–9 levels that in turn rise the levels of BK in the cells (referred to as a "Bradykinin Storm"), comporting a dysregulated BK signaling in COVID-19 patients (51) with further TRPV-1 sensitization.

Furthermore, we demonstrated that the air pollutant, DEP, directly interacts with TRPV-1 contributing to channel opening (38). Therefore, inhalation exposures to high levels of pollution during SARS-CoV-2 infection could worsen the outcome of COVID-19 in affected patients, directly modulating the activity of TRPV-1.

## Susceptibility of Elder People to SARS-CoV-2

Studies on knockout (TRPV-1–/–) mice or using a pharmacological block with TRPV-1 antagonist (capsazepine) or agonist such (resiniferatoxin) have revealed that TRPV-1 presents an anti-inflammatory function and a decreased systemic inflammatory response, by reducing the production of TNFα, on a systemic inflammatory animal model on which a "cytokine storm" was induced. The anti-inflammatory activity gave however way to a pro-inflammatory activity in elderly rats. In particular, TRPV-1 expression was found to be upregulated in the lungs of rats, in relation to not only the progress of pathology but also with age, revealing a primarily anti-inflammatory role of TRPV-1 in young and a pro-inflammatory function in the elderly (52).

The pro-inflammatory role of TRPV-1 in the elderly might contribute to aggravate the incidence of COVID-19 fatality associated with older patients, especially people over 65-years-old. This, along with an overall deterioration of immune function and the higher rate of comorbidity, making the elderly more susceptive to infections, could help to clarify the progression and unbalanced impact of COVID-19 in the elderly.

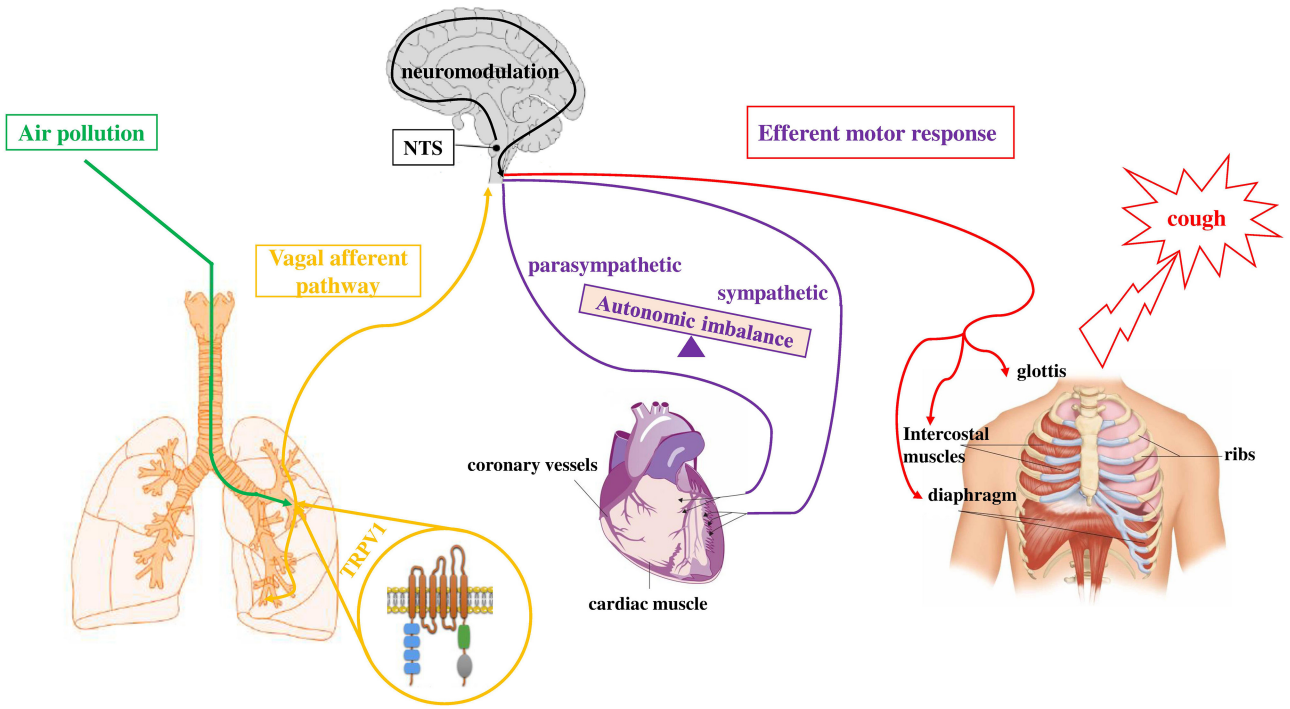


**FIGURE 2 |** Simplified depiction of how exposure to air pollutants is proposed to sensitize the sensory to autonomic reflex arc and alter subsequent responses. Inhaled component of air pollution (i.e., DEP), directly sensitizes TRPV-1 (green pathway) located on vagal bronchopulmonary C-fibers endings. Activation of airways sensory nerves (yellow pathway) stimulates neurons in the midbrain (NTS) and, through a neuromodulation process in the CNS, causes the efferent motor responses (red and violet pathways) to the heart (autonomic imbalance) and to respiratory muscles (cough). Adapted from (141).

## SYMPTOMS

The most common symptoms of COVID-19 are fever, cough, dyspnea, altered sense of taste/smell, palpitations. Less common symptoms include: myalgia and arthralgia, fatigue, rhinorrhea/nasal congestion, chest tightness, chest pain and hemoptysis, gastrointestinal symptoms, sore throat, headache, dizziness, neurological symptoms, ocular symptoms, audio-vestibular symptoms, cutaneous symptoms (53). While in severe cases patients with COVID-19 at admission in the hospital the most common symptoms are fever, cough, and/or shortness of breath, in mild or moderate disease are headache, loss of smell, nasal obstruction with cough. Overall, the prevalence of symptoms was highest in people aged 30–60 years; the most common atypical presentation in older adults was confusion. Most of these symptoms are associated with pathways controlled by TRPV-1.

### Cough

Cough is the major COVID-19 symptom (54), not necessarily associated with severity. The cough reflex is initiated by activation of TRPV-1 receptors on vagal bronchopulmonary C-fibers endings which are mainly involved in airways reflex responses and primarily responsible for "detecting" inhaled toxicants' presence. In effect, TRPV-1 represents a portal of entry to respiratory tract irritation and reflex responses induced by inhaled oxidant agents (55, 56), particulate air pollution (39), and cigarette smoking (57). Moreover, patients suffering from chronic cough exhibit increased levels of TRPV-1 positive cells in the airways. Interestingly, TRPV-1 upregulation in neuronal cell cultures, infected by rhinoviruses, may explain cases of cough hypersensitivity syndrome following airway viral infections (post-viral vagal neuropathy), regardless of inflammation (58). Prevalence of post-COVID-19 cough varied widely between studies (59–61). However, there's a growing opinion that vagal neuroinflammation caused by the virus is closely connected to the development and persistence of COVID-19 cough (62).

A way to quantification cough and evaluate the effect of pharmacological intervention in cough investigation is the cough challenge (63). Inhalation cough challenge, the most commonly employed method to assess cough reflex sensitivity, implicates the inhalation of tussive agents and the subsequent counting of the induced coughs number (64). CPS mainly acts on TRPV-1, thus the CPS cough challenge has been applied to investigate TRPV-1 function *in vivo* measuring cough response (63). During an upper respiratory infection, a temporary increase in cough sensitivity to inhaled CPS has been demonstrated, moreover CPS sensitivity has been positively associated with the cough severity score (65). Our group recently demonstrated that cough reflex induced by CPS can be modulated by inhalation of endogenous mediators of TRPV-1, PGE2, and BK, in healthy subjects (38). The upregulation and subsequent modulation of TRPV-1 by

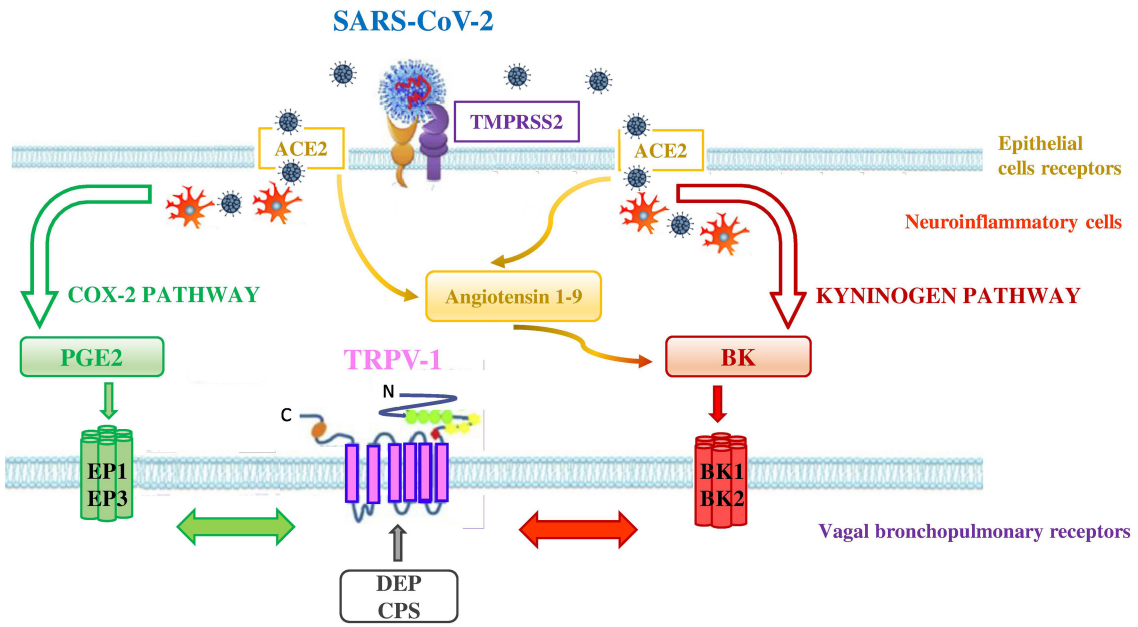


**FIGURE 3 |** Interconnection between ACE2, TMPRSS2, and TRPV-1 in SARS-CoV-2 infection. SARS-CoV-2 uses the ACE2 receptor for entry into lung epithelial cells and the host cell serine protease TMPRSS2 for priming the S protein. ACE2 and TMPRSS2 may interact with TRPV-1 through the activation of COX-2 and kininogen pathways. - COX-2 pathway (green pathway). TRPV-1 sensitization is due to the interaction between TRPV-1 and EP receptors (i.e., EP1 and EP3) stimulated by the increase of PGE2 levels in the lungs of affected COVID-19 patients. SARS-CoV-2 interaction with neuroinflammatory cells increases levels of PGE2 a potent inflammatory mediator that is generated by COX-2 conversion of arachidonic acid.- kininogen pathway (red pathway). TRPV-1 sensitization is due to the interaction between TRPV-1 and BK receptors (i.e,. BKB1 and BKB2) stimulated by the increase of BK levels in the lungs. SARS-CoV-2 interaction with neuroinflammatory cells increases levels of BK, referred to as a "Bradykinin Storm." BK is produced from an inactive pre-protein kininogen through activation by the serine protease kallikrein. The upregulation of ACE2 in patients with severe symptoms of COVID-19 increases Angiotensin 1–9 levels that in turn raise the levels of BK. High levels of PM in air pollution, such as DEP, directly interact with TRPV-1 (gray arrow) by modulating its activity and increasing its sensitization. This interaction could worsen the outcome of COVID-19 disease in affected patients. Adapted from (42).

lung inflammation products, i.e., PGE2, and BK, during and following airways viral infections, including COVID-19, may explain hypersensitivity of the cough reflex during the period of illness and after COVID-19 (post-viral vagal neuropathy).

## Persistent Fatigue

TRPV-1 is involved in persistent fatigue, a common symptom following SARS-CoV-2 infection (66). Particularly interesting is that TRPV-1 ligands, i.e., CPS and n-tert-butylecyclohexanol, are able to alleviate chronic fatigue syndrome's (CFS) symptoms. The inhibition of TRPV-1 channel and the subsequent modulation of pain perception, neuroendocrine function, oxidative stress, and immune function, are believed to be involved in these beneficial effects. N-tert-butylcyclohexanol, an antagonist of the TRPV-1 channel, is more effective in reducing CFS symptoms than CPS (67).

## From Palpitation to Heart Attack

One of the major complications among COVID-19 patients includes cardiac arrhythmias. The commonest arrhythmia is sinus tachycardia which is usually associated with palpitations causing discomfort to patients. One case of COVID-19 with clinical features of autonomic dysfunction in the form of sinus arrhythmia, postural hypotension, intermittent profuse sweating, constipation, erectile dysfunction, and squeezing sensation in the chest, was recently described (68). Another case of a 58-year-old COVID-19 patient with a significant decrease in heart rate and a paradoxical decline in HRV investigated at 24 h ECG monitoring (69) was published. Only one study evaluated the presence of cardiac autonomic dysfunction in hospital COVID-19 patients (70) founding an increased parasympathetic activity in COVID-19 patients compared to healthy controls as demonstrated by the increase in time domain variables of HRV. Unlike the time domain variables, authors found that frequency domains of HRV, specifically the Low Frequency and High Frequency ratio (LF/HF) (traditionally considered a marker of sympathovagal balance in the cardiovascular system), weren't different between the COVID-19 subjects and the healthy subjects. A case of postural tachycardia syndrome was described several months after confirmed SARS-CoV-2 infection (71). Anecdotal cases of autonomic dysfunction (i.e., palpitations, fatigue, dizziness, diarrhea, recurrent presyncope episodes) following viral SARS-CoV-2 infection are emerging (72). Furthermore, a 58% increase of out-of-hospital cardiac arrest in COVID-19 cases out of a total of 9,806 reported in some provinces of Lombardy, the Italian region most affected by SARS-CoV-2 was identified during the first 40 days of the first wave of the outbreak (February 21st through March 31st, 2020), compared with those that occurred

during the same period in 2019. The cumulative incidence of out-of-hospital cardiac arrest in 2020 was strongly associated with the cumulative incidence of COVID-19 and the increase in the number of cases of out-of-hospital cardiac arrest followed the time course of the COVID-19 outbreak (73). Another study conducted in Emilia Romagna region (one of the most severely hit areas of Italy), during the first wave of the COVID-19 pandemic observed an increase in the out-of-hospital cardiac mortality (74). Furthermore, a study conducted in Wuhan, China, reports that cardiac damage also occurs in about 20% of COVID-19 hospitalized patients (75).

TRPV-1 is among the TRP channels involved in the activation of airway sensory nerves causing variability in the autonomic efferent pathways that are resolved centrally at the level of the mid-brain. This causes cardiovascular function changes i.e., alterations of cardiac rhythm and of ECG morphology (36, 39). HRV spectral analysis is a valuable tool for the assessment of cardiovascular autonomic function and to check out fluctuations in autonomic tone. Changes in cardiac autonomic activity are thought to be a common pathway leading to increased morbidity and mortality from various disorders, including cardiovascular disease. Indeed, data from literature sustain the assumption that decreased HRV precedes the evolvement of a number of cardiovascular disease risk factors (76). Plethora of evidence are available in the literature demonstrating autonomic dysfunction in other infectious diseases (77–91).

Recently our group (38) identified a mechanism, which is operative *in vivo* in healthy subjects, by which sensitization of airways sensory TRPV-1 channels by inhalation of endogenous mediators of the channel PGE2 and BK dysregulates autonomic cardiac rhythm increasing sympathetic heart activity. We have demonstrated that an increase in sympathetic activity can be generated by stimuli that are also able to sensitize airways TRPV-1. This brings a proof of concept that signals from vagal bronchopulmonary C-fibers, once they are integrated at the CNS level, can modify autonomic drive to the heart, as was previously demonstrated in animal models.

Therefore, the increase in cardiac arrest that emerged during the COVID-19 pandemic, could be closely related to a potential autonomic dysfunction of cardiac rhythm regulation, caused by TRPV-1 sensitization.

## Gastrointestinal Symptoms

### Smell and Taste Disorders

Smell and taste disorders are very common in COVID-19 (92–96). The nasal cavity expresss high levels of TRPV-1 trigeminal receptors so that the intranasal trigeminal system is considered the third chemical sense with olfaction and gustation (97). TRPV-1 is among the TRP channels mainly involved in the transduction of noxious sensation and is activated by pungent odorous substances (97). TRP channels are also involved in the process of gustation (98). Indeed associations have been observed between TRPV-1 genetic variant rs8065080 (C>T, Val585Ile) polymorphism, the same we analyzed in our previous work (99), in modulation salt taste perception (100). The CPS agonist of TRPV-1 is also implicated in the modulation of smell and taste with sensory (olfactory) and sensitive (trigeminal) perceptions coming together (101). In addition, most aroma compounds have sensitive peculiarities linked to nasal hyper-reactivity to strong aroma (sometimes identified as "hyperosmia" by patients who present sino-nasal inflammation).

Nasal obstruction alone is relatively frequent in COVID-19. In two studies, nasal obstruction was often reported, but not associated with olfactory dysfunction (102, 103). In rhinitis, the nasal itch is related to TRPV-1 (104). Mucus hypersecretion and inflammation are also associated with TRPV-1 sensitization (2, 105). CPS was found to be a choice as therapy for non-allergic rhinitis (106, 107).

### Anorexia

Loss of appetite is frequent and could be severe in COVID-19 (108). TRPV-1 is also involved in appetite through control of appetite hormone levels or stimulation of gastrointestinal vagal afferent signaling (109).

### Nausea, Vomiting, and/or Diarrhea

Nausea, vomiting, and/or diarrhea are rather frequent symptoms of COVID-19 (108). TRPV-1 activation leads to nerve fibers' release of substances such as tachykinins that increase gastric motility and stimulate gastric emptying (110). CPS can promote gastroesophageal and abdominal pain, pyrosis, bloating, and/or dyspepsia through TRPV-1 (111–113).

### Pain

Myalgia, back pain, widespread hyperalgesia, and headache are often concomitant with COVID-19 infection (96, 114). TRPV-1 is implicated in acute and chronic pain and migraine (115, 116).

## GENETIC SUSCEPTIBILITY TO SARS-COV-2 INFECTION AND SYMPTOMS

Genetic factors could explain the variability in COVID-19 symptoms. Single nucleotide polymorphisms (SNPs) in the TRPV-1 gene modulate the functional asset of the channel and contribute to different responsiveness to the agonist CPS *in vitro* (56). Our group recently demonstrated that multiple TRPV-1 polymorphisms explain the variability in cough test sensitivity to CPS in healthy subjects (99). In particular, four combined SNPs: I315M (rs222747); I585V (rs8065080); T469I (rs224534); P91S (rs222749) confer the major CPS sensitivity *in vivo*. Then, the presence of a minimum of two polymorphisms, the 91S combined with 315M or with 585I, was sufficient to produce a significant effect at the CPS concentration causing 2 coughs. The cough response to the modulation of TRPV-1 by endogenous mediators PGE2 and BK, considered to be indirect sensitizers of the channel, was instead irrespective of the presence of TRPV-1 SNPs. That air pollutants, such as DEP, directly interact with TRPV-1 and cause channel opening (38) suggests that genetics variants also are relevant in the interaction between pollutants and TRPV-1 activation too. This fact, in our opinion, could in part explain epidemiological data which highlight higher COVID-19 mortality in most polluted countries. In summary, TRPV-1 genetic variants and their modulation by air pollutants may play a central role in infection and effects of COVID-19.

## THERAPY/TREATMENT

Based on the above, there is the possibility that TRPV-1 has a relevant role in the infection, susceptibility, and symptoms of COVID-19. This encourages looking at therapeutic agents to down-regulate COVID-19 symptoms and responses TRPV-1-associated, including inflammatory response and cough. Identifying a drug that could down-regulate or inactivate TRPV-1 might therefore provide a protective environment to struggle with SARS-CoV-2 infection and COVID-19 disease.

According to recent data, the inhibition of afferent activity, above all the removal of TRPV-1+ afferent fibers from the lung and airways, could exert a beneficial action on the compromised lung function and clearance of infection (3). Moreover, inactivation of the TRPV-1+ innervation could also lead to better prevention or treatment of ventilator-associated lung injury. Furthermore, several active ingredients of spices including pungent (capsaicinoids) CPS, from red pepper (117), resiniferatoxin, from tropical Euphorbia plants (118), allicin, from onion and garlic (119) and non-pungent (capsinoids) including piperine (black pepper) (120, 121), gingerol and zingerone (ginger) (122), cinnamaldehyde, curcumin (123), eugenol (clove), and camphor, are all TRPV-1 agonists. TRPV-1 is also activated by allyl isothiocyanate (AITC), the organosulfur compound present in horseradish, mustard, and wasabi (124). While the first exposure to TRPV-1 activators may induce acute pain, repeated treatment promotes a refractory state of TRPV-1, named as desensitization. This causes the inhibition of receptor function and stops pain perception, underlying a unique form of analgesia (125). This finding was firstly described for CPS and application of CPS as topical ointments has been applied in clinical use to alleviate chronic painful conditions for decades. The acute desensitization of TRVP-1 occurs within few seconds (∼20) after the first administration of vanilloids to the cell. Many signaling pathways including calmodulin, calcineurin, or the decrease of phosphatidylinositol 4,5-bisphosphate, are involved in TRPV-1 desensitization. Oxidative stress reduces phosphatidylinositol 4,5-bisphosphate, and receptor desensitization could be reached at lower doses of agonists in SARS-Cov-2 infection (5). Tachyphylaxis, defined as a reduction in the response after frequent applications of agonists, is another type of desensitization of TRPV-1 by CPS (126).

Patients affected by COVID-19 have been studied in order to evaluate their response to these spices. Consecutive cough-induced challenges were carried out on one of the patients during the recovery phase. The effect of TRPV-1 agonists disappeared in 1–4 h. The duration of this influence increased to around 10 h when small doses of TRPV-1 agonists were added to low-dose broccoli. Paracetamol metabolites, *N*-acetyl-*p*-benzoquinone imine, and *p*-benzoquinone, are TRPV-1 agonists and increased the duration of action of the TRPV-1-broccoli combinations to over 14 h. The results of the challenges suggest a quick short-lasting TRPV-1 desensitization (5, 127). No data until now are available on the treatment of COVID-19 patients with resiniferatoxin (RTX), a known potent agonist of TRPV-1 and active pharmaceutical ingredient that has the potential to be a highly peculiar factor for long-term inactivation of TRPV-1 fibers. Furthermore, COVID-19 patients with mild, moderate, and severe symptoms who received curcumin/piperine treatment promptly recovered from initial symptoms (fever, cough, sore throat, and breathlessness) and exhibited better ability to maintain oxygen saturation above 94% and better clinical outcomes (128). *In silico* drug discovery suggested that curcumin plays as SARS-CoV-2 main protease inhibitor (129). Lastly, some other natural compounds, that are well-known ligands for TRPV-1, may inhibit SARS-CoV-2 as well as lessen some symptoms of COVID-19. Recognized examples are represented by quercetin (130), resveratrol (131), spermidine/spermine (132), naringenin (133), and baicalin. In a prospective, randomized, controlled, and open-label study, a daily dose of 1,000 mg of quercetin was given for 30 days to 152 outpatients affected by COVID-19 to study its adjuvant role in treating the initial symptoms and in preventing the severe effects of the disease. Quercetin was effective in ameliorating COVID-19 early symptoms as well as preventing the severity of the disease (134). Spermidine and spermine, powerful TRPV-1 ligands, have been found to inhibit SARS-CoV-2 infection possibly by promoting viral degradation in the endolysosomes (135). Naringenin, that diminishes TRPV-1 activation channel producing analgesic effect (133), inhibited human coronaviruses infection (136), suggesting that this inhibition can be mediated by TRPV-1. As a final point, baicalin exhibited strong antiviral activities and was recognized as the first non-covalent, non-peptidomimetic inhibitor of SARS-CoV-2 (137). Notably, previous reports showed that baicalin induced down-regulation of TRPV-1 mRNA expression levels in DRG neurons (138). Taken together, evidence gathered from the literature suggests that TRPV-1 can be really considered as target for handling this disease.

## FUTURE CLINICAL APPLICATION

To make our hypothesis clearer and more translational in the clinical setting we envisage future applications that we briefly describe.

### Identify Individuals at Risk of Developing Disease

The analysis of the polymorphic site of the TRPV-1 for deciphering COVID-19 susceptibility could be the key to identify the more vulnerable individuals and those at higher risk for severe disease. As suggested in our previous work (99), the combination of I585, 91S, and 315M modifies the functional properties of the channel and induces an increase in TRPV-1 protein expression due to the multiplied DNA copy number. Furthermore, the corresponding TRPV-1 I585 mutation is associated with a higher risk of wheeze and cough in children with asthma. Since most COVID-19 symptoms are associated with pathways controlled by TRPV-1, we, therefore, expect that the people with 585I, 91S, and 315 M will be more susceptible to adverse effects of COVID-19 infection.

Within the epidemiological area, the identification of TRPV-1 genetic polymorphisms could have important implication

in SARS-CoV-2 susceptibility, infection and spread. TRPV-1 genetic variants by increasing the functional properties of the channel could render people more susceptible to virus access into the cell.

## A Tailored Desensitization Treatment

Capsaicin is a common experimental trigger of cough through TRPV-1 activation. However, one-month treatment with oral capsaicin was found to improve cough through a putative desensitization mechanism (139). A recent study (5) reports that administration of a low dose of oral capsaicin (10 and 30 mg of red pepper in capsules) provokes a rapid decrease in induced cough (1–2 min) and nasal obstruction in a single COVID-19 patient, with ultra-rapid clinical effects, suggesting TRPV-1 channel desensitization as the main mechanism. The duration of the effect was around 2 h with 10 mg and 3 h with 30 mg. However, even if the TRPV-1 desensitization does not last long, the repeated treatments (applications) with oral capsaicin or other TRPV-1 agonists (tachyphylaxis) seems able to reduce permanently the symptoms of cough and nasal obstruction that are prevalent in COVID-19 disease.

Along the same lines, a recent publication shows a strong correlation between grams of spice supply pro-capita per day and a decrease in the total number of COVID-19 cases per million population. This suggests that spice consumption, in particular ginger, curcumin, allicin in garlic, which are all TRPV-1 agonists, play a role in fighting COVID-19 (140).

Alternatively, as proposed by Nahama (3) the therapeutic approaches targeting TRPV-1 containing nerve fibers in the lungs, by use of an ultra-potent TRPV1 agonist could modulate the inflammatory and immune signal activity, leading to reduced mortality and better overall outcomes in COVID-19 disease. The potential use of resiniferatoxin, currently in clinical trials for cancer and osteoarthritis pain, as a possible ablating agent of TRPV-1 positive pulmonary pathways in patients with advanced COVID-19 disease, was recommended.

Despite the preliminary evidence and the proposed hypotheses on the therapeutic role of TRPV-1 agonists, future studies are however warranted to test the efficacy and tolerability of these treatments targeting TRPV-1 on patients with COVID-19 disease. Furthermore, research through the use of tailored doses and timing of administration, should confirm these data and mechanisms in order to develop medications, patch tests (capsaicin), nasal sprays, or food supplements based on TRPV-1 desensitization for the treatment of COVID-19 and its main symptoms, including not only cough but also pain and tachycardia. These studies should be corroborated by the genetic characterization of patients with COVID-19 by six nonsynonymous functional polymorphisms of TRPV-1 (K2N rs9894618, P91S rs222749, I315 M rs222747, T469I rs224534, T505A rs17633288, and I585V rs8065080), that determine a substantial difference in capsaicin sensitivity with levels of SNP-based responsiveness ranging from 2 to 6. Based on our previous study we hypothesized that the most responsive individuals will need a lower dose of agonist (capsaicin) to induce the same effect than fairly ones. This would help to design tailored strategies for SARS-CoV-2 infection too.

## CONCLUSION

The battle against the new coronavirus will be still long, so know the mechanisms of TRPV-1, a receptor involved in lung defense mechanisms, inflammation, and immunomodulation might be relevant in the susceptibility to SARS-CoV-2 infection. Novel target polymorphic TRPV-1 receptor could be the key factor in COVID-19 susceptibility to design not only preventive but also therapeutic strategies in SARS-CoV-2 infections. Exploring the role of multiple SNPs of the TRPV-1 gene in the sensitivity to lung and heart dysfunction in SARS-CoV-2 infection will open new therapeutic approaches targeting TRPV-1 that could modulate the inflammatory and immune signal activity leading to a better overall outcome.

## AUTHOR CONTRIBUTIONS

SP and FL conceived the manuscript. SP, FL, PM, and MC were involved in early discussions and mapping the concepts that led to this paper and wrote the first draft of the manuscript. All authors read and critically reviewed drafts of the manuscript.

## FUNDING

This study was supported by the BIRD175721 funding, provided by the University of Padova, Department of Cardio-Vascular-Thoracic Science and Public Health.

## REFERENCES

1. Xia S, Zhu Y, Liu M, Lan Q, Xu W, Wu Y, et al. Fusion mechanism of 2019-nCoV and fusion inhibitors targeting HR1 domain in spike protein. *Cell Mol Immunol.* (2020) 17:765–7. doi: 10.1038/s41423-020-0374-2
2. Omar S, Clarke R, Abdullah H, Brady C, Corry J, Winter H, et al. Respiratory virus infection up-regulates TRPV1, TRPA1 and ASICS3 receptors on airway cells. *PloS ONE.* (2017) 12:e0171681. doi: 10.1371/journal.pone.0171681
3. Nahama A, Ramachandran R, Cisternas AF, Ji H. The role of afferent pulmonary innervation in ARDS associated with COVID-19 and potential use of resiniferatoxin to improve prognosis: A review. *Med Drug Discov.* (2020) 5:100033. doi: 10.1016/j.medidd.2020.100033
4. Liu Z, Wang P, Lu S, Guo R, Gao W, Tong H, et al. Liquiritin, a novel inhibitor of TRPV1 and TRPA1, protects against LPS-induced acute lung injury. *Cell Calcium.* (2020) 88:102198. doi: 10.1016/j.ceca.2020.102198
5. Bousquet J, Czarlewski W, Zuberbier T, Mullol J, Blain H, Cristol, et al. Potential interplay between Nrf2, TRPA1, and TRPV1 in nutrients for the control of COVID-19. *Int Arch Allergy Immunol.* (2021) 182:324–38. doi: 10.1159/000514204
6. Zhu J, Deng Y-Q, Wang X, Li X-F, Zhang N-N, Liu Z, et al. An artificial intelligence system reveals liquiritin inhibits SARS-CoV-2 by mimicking type I interferon. *bioRxiv [Preprint].* (2020) 2020.05.02.074021. doi: 10.1101/2020.05.02.074021

7. Groneberg DA, Niimi A, Dinh QT, Cosio B, Hew M, Fischer A, et al. Increased expression of transient receptor potential vanilloid-1 in airway nerves of chronic cough. *Am J Respir Crit Care Med.* (2004) 170:1276–80. doi: 10.1164/rccm.200402-174OC
8. McLeod RL, Fernandez X, Correll CC, Phelps TP, Jia Y, Wang X, et al. TRPV1 antagonists attenuate antigen-provoked cough in ovalbumin sensitized guinea pigs. *Cough Lond Engl.* (2006) 2:10. doi: 10.1186/1745-9974-2-10
9. Du Q, Liao Q, Chen C, Yang X, Xie R, Xu J. The role of transient receptor potential vanilloid 1 in common diseases of the digestive tract and the cardiovascular and respiratory system. *Front Physiol.* (2019) 10:1064. doi: 10.3389/fphys.2019.01064
10. Ferrer-Montiel A, Fernández-Carvajal A, Planells-Cases R, Fernández-Ballester G, González-Ros JM, Messeguer À, et al. Advances in modulating thermosensory TRP channels. *Expert Opin Ther Pat.* (2012) 22:999–1017. doi: 10.1517/13543776.2012.711320
11. Xu M, Zhang Y, Wang M, Zhang H, Chen Y, Adcock IM, et al. TRPV1 and TRPA1 in lung inflammation and airway hyperresponsiveness induced by fine particulate matter (PM2.5). *Oxid Med Cell Longev.* (2019) 2019:7450151. doi: 10.1155/2019/7450151
12. Tränkner D, Hahne N, Sugino K, Hoon MA, Zuker C. Population of sensory neurons essential for asthmatic hyperreactivity of inflamed airways. *Proc Natl Acad Sci.* (2014) 111:11515–20. doi: 10.1073/pnas.1411032111
13. Deering-Rice CE, Stockmann C, Romero EG, Lu Z, Shapiro D, Stone BL, et al. Characterization of transient receptor potential vanilloid-1 (TRPV1) variant activation by coal fly ash particles and associations with altered transient receptor potential ankyrin-1 (TRPA1) expression and asthma. *J Biol Chem.* (2016) 291:24866–79. doi: 10.1074/jbc.M116.746156
14. Kitagawa Y, Tamai I, Hamada Y, Usui K, Wada M, Sakata M, et al. The orally administered selective TRPV1 antagonist, JTS-653, attenuates chronic pain refractory to non-steroidal anti-inflammatory drugs in rats and mice including post-herpetic pain. *J Pharmacol Sci.* (2013) 122:128–37. doi: 10.1254/jphs.12276FP
15. Alhmada Y, Selimovic D, Murad F, Hassan, S.-L., Haikel Y, et al. Hepatitis C virus-associated pruritus: etiopathogenesis and therapeutic strategies. *World J Gastroenterol.* (2017) 23:743–50. doi: 10.3748/wjg.v23.i5.743
16. Sanjai Kumar P, Nayak TK, Mahish C, Sahoo SS, Radhakrishnan A, De S, et al. Inhibition of transient receptor potential vanilloid 1 (TRPV1) channel regulates chikungunya virus infection in macrophages. *Arch Virol.* (2021) 166:139–55. doi: 10.1007/s00705-020-04852-8
17. Nayak TK, Mamidi P, Kumar A, Singh LPK, Sahoo SS, Chattopadhyay S, et al. Regulation of viral replication, apoptosis and pro-inflammatory responses by 17-AAG during chikungunya virus infection in macrophages. *Viruses.* (2017) 9:3. doi: 10.3390/v9010003
18. Subudhi BB, Chattopadhyay S, Mishra P, Kumar A. Current strategies for inhibition of chikungunya infection. *Viruses.* (2018) 10:235. doi: 10.3390/v10050235
19. Tanabe ISB, Tanabe ELL, Santos EC, Martins WV, Araújo, I. Cavalcante MC, et al. Cellular and molecular immune response to chikungunya virus infection. *Front Cell Infect Microbiol.* (2018) 8:345. doi: 10.3389/fcimb.2018.00345
20. Huang C, Wang Y, Li X, Ren L, Zhao J, Hu Y, et al. Clinical features of patients infected with 2019 novel coronavirus in Wuhan, China. *Lancet Lond Engl.* (2020) 395:497–506. doi: 10.1016/S0140-6736(20)30183-5
21. Ruan Q, Yang K, Wang W, Jiang L, Song J. Clinical predictors of mortality due to COVID-19 based on an analysis of data of 150 patients from Wuhan, China. *Intensive Care Med.* (2020) 46:846–8. doi: 10.1007/s00134-020-05991-x
22. Talbot S, Abdulnour R-EE, Burkett PR, Lee S, Cronin SJF, Pascal MA, et al. Silencing nociceptor neurons reduces allergic airway inflammation. *Neuron.* (2015) 87:341–54. doi: 10.1016/j.neuron.2015.06.007
23. Wang Z, Yang Y, Yang H, Capó-Aponte JE, Tachado SD, Wolosin JM, et al. NF-κB feedback control of JNK1 activation modulates TRPV1-induced increases in IL-6 and IL-8 release by human corneal epithelial cells. *Mol Vis.* (2011) 17:3137–46. Available online at: https://www.ncbi.nlm.nih.gov/pmc/articles/PMC3235537/
24. Mesnier J, Cottin Y, Coste P, Ferrari E, Schiele F, Lemesle G, et al. Hospital admissions for acute myocardial infarction before and after lockdown according to regional prevalence of COVID-19 and patient profile in France: a registry study. *Lancet Public Health.* (2020) 5:e536–42. doi: 10.1016/S2468-2667(20)30188-2
25. Van Belle E, Manigold T, Piérache A, Furber A, Debry N, Luycx-Bore A, et al. Myocardial infarction incidence during national lockdown in two French provinces unevenly affected by COVID-19 outbreak: an observational study. *Lancet Reg Health - Eur.* (2021) 2:100030. doi: 10.1016/j.lanepe.2021.100030
26. Claeys MJ, Rajagopalan S, Nawrot TS, Brook RD. Climate and environmental triggers of acute myocardial infarction. *Eur Heart J.* (2017) 38:955–60. doi: 10.1093/eurheartj/ehw151
27. Pope CA, Dockery DW. Health effects of fine particulate air pollution: lines that connect. *J Air Waste Manag Assoc.* (2006) 56:709–42. doi: 10.1080/10473289.2006.10464485
28. Sun Q, Hong X, Wold LE. Cardiovascular effects of ambient particulate air pollution exposure. *Circulation.* (2010) 121:2755–65. doi: 10.1161/CIRCULATIONAHA.109.893461
29. Peters A, von Klot S, Heier M, Trentinaglia I, Hörmann A, Wichmann HE, et al. Exposure to traffic and the onset of myocardial infarction. *N Engl J Med.* (2004) 351:1721–30. doi: 10.1056/NEJMoa040203
30. Folino F, Buja G, Zanotto G, Marras E, Allocca G, Vaccari D, et al. Association between air pollution and ventricular arrhythmias in high-risk patients (ARIA study): a multicentre longitudinal study. *Lancet Planet Health.* (2017) 1:e58–e64. doi: 10.1016/S2542-5196(17)30020-7
31. Gordon T, Reibman J. Cardiovascular toxicity of inhaled ambient particulate matter. *Toxicol Sci.* (2000) 56:2–4. doi: 10.1093/toxsci/56.1.2
32. Bernstein JA, Alexis N, Barnes C, Bernstein IL, Bernstein JA, Nel A, et al. Health effects of air pollution. *J Allergy Clin Immunol.* (2004) 114:1116–23. doi: 10.1016/j.jaci.2004.08.030
33. Brook RD, Franklin B, Cascio W, Hong Y, Howard G, Lipsett M, et al. Air pollution and cardiovascular disease: a statement for healthcare professionals from the Expert Panel on Population and Prevention Science of the American Heart Association. *Circulation.* (2004) 109:2655–71. doi: 10.1161/01.CIR.0000128587.30041.C8
34. Schulz H, Harder V, Ibald-Mulli A, Khandoga A, Koenig W, Krombach F, et al. Cardiovascular effects of fine and ultrafine particles. *J Aerosol Med.* (2005) 18:1–22. doi: 10.1089/jam.2005.18.1
35. Vermylen J, Nemmar A, Nemery B, Hoylaerts MF. Ambient air pollution and acute myocardial infarction. *J Thromb Haemost JTH.* (2005) 3:1955–61. doi: 10.1111/j.1538-7836.2005.01471.x
36. Robertson S, Thomson AL, Carter R, Stott HR, Shaw CA, Hadoke PWF, et al. Pulmonary diesel particulate increases susceptibility to myocardial ischemia/reperfusion injury *via* activation of sensory TRPV1 and β1 adrenoreceptors. *Part Fibre Toxicol.* (2014) 11:12. doi: 10.1186/1743-8977-11-12
37. Lee LY, Widdicombe JG. Modulation of airway sensitivity to inhaled irritants: role of inflammatory mediators. *Environ Health Perspect.* (2001) 109 Suppl.4:585–9. doi: 10.1289/ehp.01109s4585
38. Liviero F, Scarpa MC, De Stefani D, Folino F, Campisi M, Mason P, et al. Modulation of TRPV-1 by prostaglandin-E2 and bradykinin changes cough sensitivity and autonomic regulation of cardiac rhythm in healthy subjects. *Sci Rep.* (2020) 10:15163. doi: 10.1038/s41598-020-72062-y
39. Ghelfi E, Rhoden CR, Wellenius GA, Lawrence J, Gonzalez-Flecha B. Cardiac oxidative stress and electrophysiological changes in rats exposed to concentrated ambient particles are mediated by TRP-dependent pulmonary reflexes. *Toxicol Sci.* (2008) 102:328–36. doi: 10.1093/toxsci/kfn005
40. Holguín F, Téllez-Rojo MM, Hernández M, Cortez M, Chow JC, Watson JG, et al. Air pollution and heart rate variability among the elderly in Mexico City. *Epidemiol Camb Mass.* (2003) 14:521–7. doi: 10.1097/01.ede.0000081999.15060.ae
41. Folino AF, Scapellato ML, Canova C, Maestrelli P, Bertorelli G, Simonato L, et al. Individual exposure to particulate matter and the short-term arrhythmic and autonomic profiles in patients with myocardial infarction. *Eur. Heart J.* (2009) 30:1614–20. doi: 10.1093/eurheartj/ehp136
42. Szallasi A, Cortright DN, Blum CA, Eid SR. The vanilloid receptor TRPV1: 10 years from channel cloning to antagonist proof-of-concept. *Nat Rev Drug Discov.* (2007) 6:357–72. doi: 10.1038/nrd2280
43. Hoffmann M, Kleine-Weber H, Schroeder S, Krüger N, Herrler T, Erichsen S, et al. SARS-CoV-2 cell entry depends on ACE2 and TMPRSS2 and is

blocked by a clinically proven protease inhibitor. *Cell.* (2020) *181*:271–80.e8. doi: 10.1016/j.cell.2020.02.052
44. Wrapp D, Wang N, Corbett KS, Goldsmith JA, Hsieh C-L, et al. Cryo-EM structure of the 2019-nCoV spike in the prefusion conformation. *Science.* (2020) 367:1260–63. doi: 10.1126/science.abb2507
45. Garvin MR, Alvarez C, Miller JI, Prates ET, Walker AM, Amos BK, et al. A mechanistic model and therapeutic interventions for COVID-19 involving a RAS-mediated bradykinin storm. *eLife.* (2020) 9:e59177. doi: 10.7554/eLife.59177.sa2
46. Archambault AS, Zaid Y, Rakotoarivelo V, Turcotte C, Doré É, Dubuc I, et al. High levels of eicosanoids and docosanoids in the lungs of intubated COVID-19 patients. *FASEB J.* (2021) 35:e21666. doi: 10.1096/fj.202100540R
47. Ahluwalia J, Urban L, Capogna M, Bevan S, Nagy I. Cannabinoid 1 receptors are expressed in nociceptive primary sensory neurons. *Neuroscience.* (2000) 100:685–8. doi: 10.1016/S0306-4522(00)00389-4
48. Couture R, Harrisson M, Vianna RM, Cloutier F. Kinin receptors in pain and inflammation. *Eur J Pharmacol.* (2001) 429:161–76. doi: 10.1016/S0014-2999(01)01318-8
49. Premkumar LS, Ahern GP. Induction of vanilloid receptor channel activity by protein kinase C. *Nature.* (2000) 408:985–90. doi: 10.1038/35050121
50. Sugiura T, Tominaga M, Katsuya H, Mizumura K. Bradykinin lowers the threshold temperature for heat activation of vanilloid receptor 1. *J Neurophysiol.* (2002) 88:544–8. doi: 10.1152/jn.2002.88.1.544
51. Roche JA, Roche R. A hypothesized role for dysregulated bradykinin signaling in COVID-19 respiratory complications. *FASEB J.* (2020) 34:7265–69. doi: 10.1096/fj.202000967
52. Wanner SP, Garami A, Pakai E, Oliveira DL, Gavva NR, Coimbra CC, et al. Aging reverses the role of the transient receptor potential vanilloid-1 channel in systemic inflammation from anti-inflammatory to proinflammatory. *Cell Cycle.* (2012) 11:343–9. doi: 10.4161/cc.11.2.18772
53. Shah W, Heightman M, O'Brien S. UK guidelines for managing long-term effects of COVID-19. *The Lancet.* (2021) 397:1706. doi: 10.1016/S0140-6736(21)00847-3
54. Hu Y, Sun J, Dai Z, Deng H, Li X, Huang Q, et al. Prevalence and severity of corona virus disease 2019 (COVID-19): A systematic review and meta-analysis. *J Clin Virol.* (2020) 127:104371. doi: 10.1016/j.jcv.2020.104371
55. Caterina MJ, Schumacher MA, Tominaga M, Rosen TA, Levine JD, Julius D. The capsaicin receptor: a heat-activated ion channel in the pain pathway. *Nature.* (1997) 389:816–24. doi: 10.1038/39807
56. Deering-Rice CE, Johansen ME, Roberts JK, Thomas KC, Romero EG, Lee J, et al. Transient Receptor Potential Vanilloid-1 (TRPV1) Is a Mediator of Lung Toxicity for Coal Fly Ash Particulate Material. *Mol Pharmacol.* (2012) 81:411–9. doi: 10.1124/mol.111.076067
57. Kanezaki M, Ebihara S, Gui P, Ebihara T, Kohzuki M. Effect of cigarette smoking on cough reflex induced by TRPV1 and TRPA1 stimulations. *Respir Med.* (2012) 106:406–12. doi: 10.1016/j.rmed.2011.12.007
58. Abdullah H, Heaney LG, Cosby SL, McGarvey LPA. Rhinovirus upregulates transient receptor potential channels in a human neuronal cell line: implications for respiratory virus-induced cough reflex sensitivity. *Thorax.* (2014) 69:46–54. doi: 10.1136/thoraxjnl-2013-203894
59. Petersen MS, Kristiansen MF, Hanusson KD, Danielsen ME, Steigá B, Gaini S, et al. Long COVID in the Faroe Islands - a longitudinal study among non-hospitalized patients. *Clin Infect Dis.* (2020) 30:ciaa1792. doi: 10.1093/cid/ciaa1792
60. Chopra V, Flanders SA, O'Malley M, Malani AN, Prescott HC. Sixty-Day outcomes among patients hospitalized with COVID-19. *Ann Intern Med.* (2021) 174:576–8. doi: 10.7326/M20-5661
61. Stavem K, Ghanima W, Olsen MK, Gilboe HM, Einvik G. Persistent symptoms 1.5–6 months after COVID-19 in non-hospitalised subjects: a population-based cohort *study*. *Thorax.* (2021) 76:405–7. doi: 10.1136/thoraxjnl-2020-216377
62. Song W-J. Confronting COVID-19-associated cough and the post-COVID syndrome: role of viral neurotropism, neuroinflammation, neuroimmune *responses. Lancet Respir Med.* (2021) 9:533–44. doi: 10.1016/S2213-2600(21)00125-9
63. Morice AH, Fontana GA, Belvisi MG, Birring SS, Chung KF, Dicpinigaitis PV, et al. ERS guidelines on the assessment of cough. *Eur. Respir J. (*2007) *29*:1256–76. doi: 10.1183/09031936.00101006
64. Morice AH, Kastelik JA, Thompson R. Cough challenge in the assessment of cough reflex. *Br J Clin Pharmacol.* (2001) 52:365–75. doi: 10.1046/j.0306-5251.2001.01475.x
65. O'Connell F, Thomas VE, Studham JM, Pride NB, Fuller RW. Capsaicin cough sensitivity increases during upper respiratory infection. *Respir Med.* (1996) 90:279–86. doi: 10.1016/S0954-6111(96)90099-2
66. Townsend L, Dyer AH, Jones K, Dunne J, Mooney A, Gaffney F, et al. Persistent fatigue following SARS-CoV-2 infection is common and independent of severity of initial infection. *PloS ONE.* (2020) 15:e0240784. doi: 10.1371/journal.pone.0240784
67. Sarvaiya K, Goswami S. Investigation of the effects of vanilloids in chronic fatigue syndrome. *Brain Res Bull.* (2016) 127:187–94. doi: 10.1016/j.brainresbull.2016.09.015
68. Ghosh R, Roy D, Sengupta S, Benito-León J. Autonomic dysfunction heralding acute motor axonal neuropathy in COVID-19. *J Neurovirol.* (2020) 26:964–6. doi: 10.1007/s13365-020-00908-2
69. Baumann C, Buchhorn R, Willaschek C. Heart Rate Variability in a Patient with Coronavirus *Disease* (2020) 2020050209. doi: 10.20944/preprints202005.0209.v1
70. Kaliyaperumal D, Karthikeyan Rk, Alagesan M, Ramalingam S. Characterization of cardiac autonomic function in COVID-19 using heart rate variability: a hospital based preliminary observational study. *J Basic Clin Physiol Pharmacol*. (2021) 32:247–53. doi: 10.1515/jbcpp-2020-0378
71. Miglis MG, Prieto T, Shaik R, Muppidi S, Sinn, D.-I., et al. A case report of postural tachycardia syndrome after COVID-19. *Clin Auton Res.* (2020) 1–3. doi: 10.1007/s10286-020-00727-9
72. Dani M, Dirksen A, Taraborrelli P, Torocastro M, Panagopoulos D, Sutton R, et al. Autonomic dysfunction in "long COVID": rationale, physiology and management strategies. *Clin Med Lond Engl.* (2021) 21:e63–e67. doi: 10.7861/clinmed.2020-0896
73. Baldi E, Sechi GM, Mare C, Canevari F, Brancaglione A, Primi R, et al. Out-of-Hospital Cardiac Arrest during the Covid-19 Outbreak in Italy. *N Engl J Med.* (2020) 383:496–8. doi: 10.1056/NEJMc2010418
74. Campo G, Fortuna D, Berti E, Palma RD, Pasquale GD, Galvani M, et al. In- and out-of-hospital mortality for myocardial infarction during the first wave of the COVID-19 pandemic in Emilia-Romagna, Italy: a population-based observational study. *Lancet Reg. Health – Eur.* (2021) 3. doi: 10.1016/j.lanepe.2021.100055
75. Shi S, Qin M, Shen B, Cai Y, Liu T, Yang F, et al. Association of cardiac injury with mortality in hospitalized patients with COVID-19 in Wuhan, China. *JAMA Cardiol.* (2020) 5:802–10. doi: 10.1001/jamacardio.2020.0950
76. Thayer JF, Yamamoto SS, Brosschot JF. The relationship of autonomic imbalance, heart rate variability and cardiovascular disease risk factors. *Int J Cardiol.* (2010) 141:122–31. doi: 10.1016/j.ijcard.2009.09.543
77. Idiaquez J. Autonomic dysfunction in diphtheritic neuropathy. *J Neurol Neurosurg Psychiatry.* (1992) 55:159–61. doi: 10.1136/jnnp.55.2.159
78. Bennett JL, Mahalingam R, Wellish MC, Gilden DH. Epstein-Barr virus–associated acute autonomic neuropathy. *Ann Neurol.* (1996) 40:453–5. doi: 10.1002/ana.410400316
79. Becker K, Görlach I, Frieling T, Häussinger D. Characterization and natural course of cardiac autonomic nervous dysfunction in HIV-infected patients. *AIDS Lond Engl.* (1997) 11:751–7. doi: 10.1097/00002030-199706000-00008
80. Alamy AH, Menezes FB, Leite ACB, Nascimento OM, Araújo A. Dysautonomia in human T-cell lymphotrophic virus type I-associated myelopathy/tropical spastic paraparesis. *Ann Neurol.* (2001) 50:681–5. doi: 10.1002/ana.1264
81. Merz B, Bigalke H, Stoll G, Naumann M. Botulism type B presenting as pure autonomic dysfunction. *Clin Auton Res.* (2003) 13:337–8. doi: 10.1007/s10286-003-0118-2
82. Mittal CM, Wig N, Mishra S, Deepak KK. Heart rate variability in human immunodeficiency virus-positive individuals. *Int J Cardiol.* (2004) 94:1–6. doi: 10.1016/j.ijcard.2003.02.002
83. Illarramendi X, Bührer-Sékula S, Sales AM, Bakker MI, Oliveira A, Nery J, et al. High prevalence of vasomotor reflex impairment in newly diagnosed leprosy patients. *Eur J Clin Invest.* (2005) 35:658–65. doi: 10.1111/j.1365-2362.2005.01554.x

84. Bode AV, Sejvar JJ, Pape WJ, Campbell GL, Marfin AA. West Nile virus disease: a descriptive study of 228 patients hospitalized in a 4-county region of Colorado in 2003. *Clin Infect Dis.* (2006) 42:1234–40. doi: 10.1086/503038
85. Lin, T.-S., Chen, L.-K., Lin, T.-Y., et al. -H., Chen, M.-C., Jan, R.-H. Autonomic dysfunction because of severe tetanus in an unvaccinated child. *Pediatr Neonatol.* (2011) 52:169–71. doi: 10.1016/j.pedneo.2011.03.010
86. Junqueira LF. Insights into the clinical and functional significance of cardiac autonomic dysfunction in Chagas disease. *Rev Soc Bras Med Trop.* (2012) 45:243–52. doi: 10.1590/S0037-86822012000200020
87. Vasconcelos DF, Junqueira LF. Cardiac autonomic and ventricular mechanical functions in asymptomatic chronic chagasic cardiomyopathy. *Arq Bras Cardiol.* (2012) 98:111–9. doi: 10.1590/S0066-782X2012005000002
88. Vijayabala J, Attapaththu M, Jayawardena P, de Silva SG, Constantine G. Sympathetic dysfunction as a cause for hypotension in dengue shock syndrome. *Chin Med J.* (2012) *125:*3757–8. doi: 10.3760/cma.j.issn.0366-6999.2012.20.032
89. Carter R, Hinojosa-Laborde C, Convertino VA. Heart rate variability in patients being treated for dengue viral infection: new insights from mathematical correction of heart rate. *Front Physiol.* (2014) 5:46. doi: 10.3389/fphys.2014.00046
90. Chow D, Nakamoto BK, Sullivan K, Sletten DM, Fujii S, Umekawa S, et al. Symptoms of Autonomic Dysfunction in Human Immunodeficiency Virus. *Open Forum Infect Dis.* (2015) 2. doi: 10.1093/ofid/ofv103
91. Nakao K, Namekawa M, Kondo S, Ono S, Nakano I. Subacute autonomic and sensory neuropathy closely related to cytomegalovirus infection preceded by frequent syncopal attacks. *Rinsho Shinkeigaku.* (2016) 56:555–9. doi: 10.5692/clinicalneurol.cn-000863
92. Izquierdo-Dominguez A, Rojas-Lechuga MJ, Mullol J, Alobid I. Olfactory dysfunction in the COVID-19 outbreak. *J Investig Allergol Clin Immunol.* (2020) 30:317–26. doi: 10.18176/jiaci.0567
93. Lechien JR, Chiesa-Estomba CM, De Siati DR, Horoi M, Le Bon SD, Rodriguez A, et al. Olfactory and gustatory dysfunctions as a clinical presentation of mild-to-moderate forms of the coronavirus disease (COVID-19): a multicenter European study. *Eur Arch Oto-Rhino-Laryngol.* (2020) 277:2251–61. doi: 10.1007/s00405-020-06024-5
94. Mullol J, Alobid I, Mariño-Sánchez F, Izquierdo-Domínguez A, Marin C, Klimek L, et al. The loss of smell and taste in the COVID-19 outbreak: a tale of many countries. *Curr Allergy Asthma Rep.* (2020) 20:61. doi: 10.1007/s11882-020-00961-1
95. Salmon Ceron D, Bartier S, Hautefort C, Nguyen Y, Nevoux J, Hamel L, et al. Self-reported loss of smell without nasal obstruction to identify COVID-19. *The multicenter Coranosmia cohort study. J Infect.* (2020) 81:614–20. doi: 10.1016/j.jinf.2020.07.005
96. Whittaker A, Anson M, Harky A. Neurological manifestations of COVID-19: a systematic review and current update. *Acta Neurol Scand.* (2020) 142:14–22. doi: 10.1111/ane.13266
97. Poletti SC, Hausold J, Herrmann A, Witt M, Hummel T. Topographical distribution of trigeminal receptor expression in the nasal cavity. *Rhinology.* (2019) 57:147–52. doi: 10.4193/Rhin18.181
98. Piochi M, Cabrino G, Morini G, Torri L. Individual differences in the perception of orthonasal irritation induced by food. *Appetite.* (2020) 144:104460. doi: 10.1016/j.appet.2019.104460
99. Liviero F, Campisi M, Scarpa MC, Mason P, Guarnieri G, Maestrelli P, et al. Multiple single nucleotide polymorphisms of the transient receptor potential vanilloid 1 (TRPV1) genes associate with cough sensitivity to capsaicin in healthy subjects. *Pulm Pharmacol Ther.* (2020) 61:101889. doi: 10.1016/j.pupt.2020.101889
100. Dias AG, Rousseau D, Duizer L, Cockburn M, Chiu W, Nielsen D, et al. Genetic variation in putative salt taste receptors and salt taste perception in humans. *Chem Senses.* (2013) 38:137–45. doi: 10.1093/chemse/bjs090
101. Cecchini MP, Riello M, Sandri A, Zanini A, Fiorio M, Tinazzi M. Smell and taste dissociations in the modulation of tonic pain perception induced by a capsaicin cream application. *Eur J Pain.* (2020) 24:1946–55. doi: 10.1002/ejp.1644
102. Parma V, Ohla K, Veldhuizen MG, Niv MY, Kelly CE, Bakke AJ, et al. More than Smell-COVID-19 is associated with severe impairment of smell, taste, and chemesthesis. *Chem Senses.* (2020) 45:609–22. doi: 10.1093/chemse/bjaa041
103. Speth MM, Singer-Cornelius T, Oberle M, Gengler I, Brockmeier SJ, Sedaghat AR. Olfactory dysfunction and sinonasal symptomatology in COVID-19: prevalence, severity, timing, associated characteristics. *Otolaryngol–Head Neck Surg.* (2020) 163:114–20. doi: 10.1177/0194599820929185
104. Alenmyr L, Högestätt ED, Zygmunt PM, Greiff L. TRPV1-mediated itch in seasonal allergic rhinitis. *Allergy.* (2009) 64:807–10. doi: 10.1111/j.1398-9995.2009.01937.x
105. Zhang X, Ye L, Huang Y, Ding X, Wang L. The potential role of TRPV1 in pulmonary hypertension: Angel or demon? *Channels.* (2019) 13:235–46. doi: 10.1080/19336950.2019.1631106
106. Mounsey A, Feller CM. Capsaicin for nonallergic rhinitis. *Am Fam Physician.* (2016) 94:217–218. Available online at: https://www.aafp.org/afp/2016/0801/p217.html
107. Gerven LV, Steelant B, Alpizar YA, Talavera K, Hellings PW. Therapeutic effect of capsaicin nasal treatment in patients with mixed rhinitis unresponsive to intranasal steroids. *Allergy.* (2018) 73:248–50. doi: 10.1111/all.13245
108. Mao R, Qiu Y, He J-S, Tan J-Y, Li X-H, Liang J, et al. Manifestations and prognosis of gastrointestinal and liver involvement in patients with COVID-19: a systematic review and meta-analysis. *Lancet Gastroenterol. Hepatol.* (2020) 5:667–78. doi: 10.1016/S2468-1253(20)30126-6
109. Christie S, Wittert GA, Li H, Page AJ. Involvement of TRPV1 channels in energy homeostasis. *Front Endocrinol.* (2018) 9:420. doi: 10.3389/fendo.2018.00420
110. de Man JG, Boeckx S, Anguille S, de Winter BY, de Schepper HU, Herman AG, et al. Functional study on TRPV1-mediated signalling in the mouse small intestine: involvement of tachykinin receptors. *Neurogastroenterol Motil.* (2008) 20:546–56. doi: 10.1111/j.1365-2982.2007.01064.x
111. Kindt S, Vos R, Blondeau K, Tack J. Influence of intra-oesophageal capsaicin instillation on heartburn induction and oesophageal sensitivity in man. *Neurogastroenterol Motil.* (2009) 21:1032–e82. doi: 10.1111/j.1365-2982.2009.01332.x
112. Holzer P. Transient receptor potential (TRP) channels as drug targets for diseases of the digestive system. *Pharmacol Ther.* (2011) 131:142–70. doi: 10.1016/j.pharmthera.2011.03.006
113. Patcharatrakul T, Gonlachanvit S. Chili peppers, curcumins, and prebiotics in gastrointestinal health and disease. *Curr Gastroenterol Rep.* (2016) 18:19. doi: 10.1007/s11894-016-0494-0
114. Abdullahi A, Candan SA, Abba MA, Bello AH, Alshehri MA, Afamefuna VE, et al. Neurological and musculoskeletal features of COVID-19: a systematic review and meta-analysis. *Front Neurol.* (2020) 11:687. doi: 10.3389/fneur.2020.00687
115. Ro JY, Lee J-S, Zhang Y. Activation of TRPV1 and TRPA1 leads to muscle nociception and mechanical hyperalgesia. *PAIN®.* (2009) 144:270–7. doi: 10.1016/j.pain.2009.04.021
116. Moore C, Gupta R, Jordt S-E, Chen Y, Liedtke WB. Regulation of pain and Itch by TRP Channels. *Neurosci Bull.* (2018) 34:120–42. doi: 10.1007/s12264-017-0200-8
117. Yang F, Zheng J. Understand spiciness: mechanism of TRPV1 channel activation by capsaicin. *Protein Cell.* (2017) 8:169–77. doi: 10.1007/s13238-016-0353-7
118. Szallasi A, Szab,ó T, Bír,ó T, Modarres S, Blumberg PM, Krause JE, et al. Resiniferatoxin-type phorboid vanilloids display capsaicin-like selectivity at native vanilloid receptors on rat DRG neurons and at the cloned vanilloid receptor VR1. *Br J Pharmacol.* (1999) 128:428–34. doi: 10.1038/sj.bjp.0702810
119. Ogawa N, Kurokawa T, Mori Y. Sensing of redox status by TRP channels. *Cell Calcium.* (2016) 60:115–22. doi: 10.1016/j.ceca.2016.02.009
120. Okumura Y, Narukawa M, Iwasaki Y, Ishikawa A, Matsuda H, Yoshikawa M, et al. Activation of TRPV1 and TRPA1 by black pepper components. *Biosci Biotechnol Biochem.* (2010) 74:1068–72. doi: 10.1271/bbb.90964
121. Dong Y, Yin Y, Vu S, Yang F, Yarov-Yarovoy V, Tian Y, et al. A distinct structural mechanism underlies TRPV1 activation by piperine. *Biochem Biophys Res Commun.* (2019) 516:365–72. doi: 10.1016/j.bbrc.2019.06.039
122. Yin Y, Dong Y, Vu S, Yang F, Yarov-Yarovoy V, Tian Y, et al. Structural mechanisms underlying activation of TRPV1 channels by

pungent compounds in gingers. *Br J Pharmacol.* (2019) 176:3364–77. doi: 10.1111/bph.14766
123. Nalli M, Ortar G, Schiano Moriello A, Di Marzo V, De Petrocellis. L. Effects of curcumin and curcumin analogues on TRP channels. *Fitoterapia.* (2017) 122:126–31. doi: 10.1016/j.fitote.2017.09.007
124. Everaerts W, Gees M, Alpizar YA, Farre R, Leten C, Apetrei A, et al. The capsaicin receptor TRPV1 is a crucial mediator of the noxious effects of mustard oil. *Curr Biol CB.* (2011) 21:316–21. doi: 10.1016/j.cub.2011.01.031
125. Nilius B, Appendino G. "Spices: The Savory Beneficial Science of Pungency.". In: Nilius B, Amara SG, Lill R, et al. editors. *Reviews of Physiology, Biochemistry Pharmacology*, *Vol. 164* Reviews of Physiology, Biochemistry Pharmacology., eds. Cham: Springer International Publishing (2013). p. 1–76.
126. Vyklick,ý L, Nováková-Tousov,á K, Benedikt J, Samad A, Touska F, Vlachov,á V. Calcium-dependent desensitization of vanilloid receptor TRPV1: a mechanism possibly involved in analgesia induced by topical application of capsaicin. *Physiol Res.* (2008) 57 Suppl.3:S59–S68. doi: 10.33549/physiolres.931478
127. Bousquet J, Le MV, Blain H, Czarlewski W, Zuberbier T, de la Torre R, et al. Efficacy of broccoli and glucoraphanin in COVID-19: From hypothesis to proof-of-concept with three experimental clinical cases. *World Allergy Organ J.* (2021) *14:*100498. doi: 10.1016/j.waojou.2020.100498
128. Pawar KS, Mastud RN, Pawar SK, Pawar SS, Bhoite RR, Bhoite RR, et al. Oral Curcumin With Piperine as Adjuvant Therapy for the Treatment of COVID-19: A Randomized Clinical Trial. *Front. Pharmacol.* (2021) 12:669362. doi: 10.3389/fphar.2021.669362
129. Ibrahim MAA, Abdelrahman AHM, Hussien TA, Badr EAA, Mohamed TA, El-Seedi HR, et al. In silico drug discovery of major metabolites from spices as SARS-CoV-2 main protease inhibitors. *Comput Biol Med.* (2020) 126:104046. doi: 10.1016/j.compbiomed.2020.104046
130. Gao W, Zan Y, Wang Z-J, Hu X-Y, et al. Quercetin ameliorates paclitaxel-induced neuropathic pain by stabilizing mast cells, and subsequently blocking PKCε-dependent activation of TRPV1. *Acta Pharmacol. Sin.* (2016) 37:1166–77. doi: 10.1038/aps.2016.58
131. Zhang Y, Huang F, Xu Y, Xiang W, Xie C. TRPV1 is involved in the antinociceptive effects of resveratrol in paclitaxel-induced neuropathic pain. *Life.* (2021) 14:66–74. doi: 10.1080/26895293.2020.1861111
132. Ahern GP, Wang X, Miyares RL. Polyamines are potent ligands for the capsaicin receptor TRPV1. *J Biol Chem.* (2006) 281:8991–5. doi: 10.1074/jbc.M513429200
133. Straub I, Mohr F, Stab J, Konrad M, Philipp SE, Oberwinkler J, et al. Citrus fruit and fabacea secondary metabolites potently and selectively block TRPM3. *Br J Pharmacol.* (2013) 168:1835–50. doi: 10.1111/bph.12076
134. Di Pierro F, Derosa G, Maffioli P, Bertuccioli A, Togni S, Riva A, et al. Possible therapeutic effects of adjuvant quercetin supplementation against early-stage COVID-19 infection: a prospective, randomized, controlled, open-label study. *Int J Gen Med.* (2021) 14:2359–66. doi: 10.2147/IJGM.S318720
135. Gassen NC, Papies J, Bajaj T, Emanuel J, Dethloff F, Chua RL, et al. SARS-CoV-2-mediated dysregulation of metabolism and autophagy uncovers host-targeting antivirals. *Nat. Commun.* (2021) 12. doi: 10.1038/s41467-021-24007-w
136. Clementi N, Scagnolari C, D'Amore A, Palombi F, Criscuolo E, Frasca F, et al. Naringenin is a powerful inhibitor of SARS-CoV-2 infection *in vitro*. *Pharmacol Res.* (2021) 163:105255. doi: 10.1016/j.phrs.2020.105255
137. Su H, Yao S, Zhao W, Li M, Liu J, Shang W, et al. Discovery of baicalin and baicalein as novel, natural product inhibitors of SARS-CoV-2 3CL protease *in vitro*. *bioRxiv [Preprint].* (2020). doi: 10.1101/2020.04.13.038687
138. Sui F, Zhang, C.-B., Yang N, Li, L.-F., et al. -Y., Huo, H.-R., et al. Anti-nociceptive mechanism of baicalin involved in intervention of TRPV1 in DRG neurons *in vitro*. *J Ethnopharmacol.* (2010) 129:361–6. doi: 10.1016/j.jep.2010.03.039
139. Ternesten-Hasséus E, Johansson, E.-L., Millqvist E. Cough reduction using capsaicin. *Respir Med.* (2015) 109:27–37. doi: 10.1016/j.rmed.2014.11.001
140. Elsayed Y, Khan NA. Immunity-Boosting Spices and the Novel Coronavirus. *ACS Chem Neurosci.* (2020) 11:1696–8. doi: 10.1021/acschemneuro.0c00239
141. Undem BJ, Kajekar R, Hunter DD, Myers AC. Neural integration and allergic disease. *J. Allergy Clin Immunol.* (2000) 106:S213–220. doi: 10.1067/mai.2000.110153

**Conflict of Interest:** The authors declare that the research was conducted in the absence of any commercial or financial relationships that could be construed as a potential conflict of interest.

**Publisher's Note:** All claims expressed in this article are solely those of the authors and do not necessarily represent those of their affiliated organizations, or those of the publisher, the editors and the reviewers. Any product that may be evaluated in this article, or claim that may be made by its manufacturer, is not guaranteed or endorsed by the publisher.

frontiers in Medicine

ORIGINAL RESEARCH
published: 23 December 2021
doi: 10.3389/fmed.2021.798571

# The Role of Angiotensin Converting Enzyme 1 Insertion/Deletion Genetic Polymorphism in the Risk and Severity of COVID-19 Infection

*Halim Saad*[1†], *Karna Jabotian*[1†], *Carine Sakr*[2], *Rami Mahfouz*[3], *Imad Bou Akl*[4*‡] and *Nathalie K. Zgheib*[1*‡]

[1] Department of Pharmacology and Toxicology, American University of Beirut Faculty of Medicine, Beirut, Lebanon,
[2] Employee Health Unit, Department of Family Medicine, American University of Beirut Faculty of Medicine, Beirut, Lebanon,
[3] Department of Pathology and Laboratory Medicine, American University of Beirut Faculty of Medicine, Beirut, Lebanon,
[4] Division of Pulmonary, Department of Internal Medicine, American University of Beirut Faculty of Medicine, Beirut, Lebanon

OPEN ACCESS

**Edited by:**
Hamdi Mbarek,
Qatar Foundation, Qatar

**Reviewed by:**
Mohamad Saad,
Qatar Computing Research Institute, Qatar
Massimiliano Cocca,
Institute for Maternal and Child Health Burlo Garofolo (IRCCS), Italy

***Correspondence:**
Imad Bou Akl
ib08@aub.edu.lb
Nathalie K. Zgheib
nk16@aub.edu.lb

[†]These authors share first authorship

[‡]These authors share senior authorship

**Specialty section:**
This article was submitted to Precision Medicine, a section of the journal Frontiers in Medicine

**Received:** 20 October 2021
**Accepted:** 29 November 2021
**Published:** 23 December 2021

**Citation:**
Saad H, Jabotian K, Sakr C, Mahfouz R, Akl IB and Zgheib NK (2021) The Role of Angiotensin Converting Enzyme 1 Insertion/Deletion Genetic Polymorphism in the Risk and Severity of COVID-19 Infection. Front. Med. 8:798571. doi: 10.3389/fmed.2021.798571

**Background:** Individuals infected with the COVID-19 virus present with different symptoms of varying severity. In addition, not all individuals are infected despite exposure. Risk factors such as age, sex, and comorbidities play a major role in this variability; however, genetics may also be important in driving the differences in the incidence and prognosis of the disease. An *Insertion/Deletion* (*I/D*) polymorphism in the *ACE1* gene (rs1799752) may explain these genetic differences. The aims of this study were to determine the potential role of *ACE1 I/D* genetic polymorphism in the risk of contracting COVID-19 as well as predicting the severity of COVID-19 infection.

**Methods:** Three-hundred and eighty-seven non-related Lebanese subjects, 155 controls and 232 cases, who presented to the American University of Beirut Medical Center (AUBMC) for COVID-19 PCR testing were recruited. Clinical data were collected via filling a questionnaire and accessing the medical records. Peripheral blood was withdrawn for DNA isolation, and genotyping performed with standard PCR followed by band visualization on agarose gel.

**Results:** In our study population, previously described risk factors such as gender, age, and comorbidities were associated with increase in disease susceptibility and severity. *ACE1 I* was the least common allele, and there was a positive association between *ACE1 I* and the risk of contracting the COVID-19 disease. More specifically, the frequency of *II* genotype was significantly higher among cases when compared to controls ($P = 0.035$) with individuals with the *II* genotype having greater risk for contracting the COVID-19 disease: OR = 2.074, $P = 0.048$ in the multivariate analysis. As for disease severity, the *DD* genotype and *D* allele were associated with increased risk for developing severe symptoms (OR = 2.845, $P = 0.026$ and OR = 2.359, $P = 0.014$, respectively), and the *DD* genotype with necessitating hospitalization (OR = 2.307, $P = 0.042$). In parallel, *D* allele carriers showed a significantly increased risk for developing hypoxia: OR = 4.374, $P = 0.045$.

**Conclusion:** We found a positive association between *ACE1 I* and the risk of contracting the COVID-19 disease, and between *ACE1 D* and a worse outcome of the COVID-19 infection. Therefore, genotyping for *ACE1 I/D* polymorphism could be used to assess risk and predict severity for better prognosis and management of the disease.

**Keywords: *ACE1*, COVID, risk, severity, genetic polymorphism**

## INTRODUCTION

Severe acute respiratory syndrome coronavirus 2 (SARS-CoV-2) is a positive-sense single-stranded RNA virus that is responsible for the globally transmissible coronavirus disease of 2019 (COVID-19) (1). It has been observed across infected populations worldwide that symptoms are displayed with dissimilar presentations of varying severity. In addition, not all individuals are infected despite a history of exposure, including multiple direct exposures, to COVID-19. Several factors have been described in the literature for their potential role in the risk of contracting COVID-19 as well as that of developing complications. These include age, sex, blood group, smoking history, comorbidities, obesity, and intake of ACE inhibitors (ACEI) or angiotensin receptor blockers (ARBs) (2–8). In addition to these risk factors, genetics may play a contributing role in COVID-19 infection (9). With inconclusive data, few studies have highlighted the roles of transmembrane protease serine 2 (*TMPRSS2*), angiotensin converting enzyme 1 (*ACE1*), and *ACE2* gene variants in the susceptibility and severity of SARS-CoV-2 infection (10–12).

TMPRSS2 expression facilitates the entry of the virus into host cells through *ACE2* (13). Both *ACE1* and *ACE2* are endogenous proteins involved in the renin-angiotensin system (RAS), which regulates the homeostasis of blood pressure and fluid electrolyte balance (14). In lung vascular endothelium, *ACE1* converts Angiotensin I into Angiotensin II that promotes vasoconstriction, inflammation, and thrombosis (14). *ACE2* converts Angiotensin II into Angiotensin 1–7 that acts inversely to Angiotensin II and hence promotes vasodilation (14). When SARS-CoV-2 enters human cells by binding its spike (S) protein to *ACE2*, lower levels of this membrane receptor become available for the suppression of Angiotensin II (15). Consequently, the balance of the RAS can be distorted in favor of vasoconstriction, inflammation, and thrombosis, potentially complicating the outcome of COVID-19 infection (14, 15).

An Insertion/Deletion (*I/D*) polymorphism in the *ACE1* gene (rs1799752) may explain the differences in genetic susceptibilities across variable geographic populations. The *ACE1 D/D* genotype correlates with a higher activity of the *ACE1* enzyme, hence increasing the levels of Angiotensin II with secondary lowering of *ACE2* expression (16). Despite some negative results (17), few studies showed the *DD* genotype to be associated with a significantly higher risk for COVID-19 morbidity and mortality (18, 19). Moreover, a higher *I/D*-allele frequency ratio has been associated with higher recovery rates despite an increase in infectivity (20). A comprehensive review done in 2021 regarding the association between *ACE1* (*I/D*) polymorphism and COVID-19 symptoms is referenced for the reader (21). The data are less conclusive concerning the association between *ACE1* (*I/D*) genetic polymorphism and risk of contracting the disease. For instance, an initial analysis by Delanghe et al. (22) of disease spread in 25 European countries with *ACE1* historical genetic data showed a significant association between COVID-19 cases and higher frequency of the *ACE1 I* allele (22). In contrast, Yamamoto et al. (23) observed that the Europeans have a higher probability of being infected by SARS-CoV-2 compared to Asian populations who have a higher frequency of the *ACE1 II* genotype. Importantly, the negative correlation between COVID-19 incidence and *ACE1 II* genotype was weakened when they added data from the Middle East, stating that the Middle East should be considered an important factor for future studies (23). This is especially the case since, and as per Saab et al. (24), the Middle Eastern population such as the Lebanese, have a lower frequency of the *ACE1 I* allele when compared to the *D* allele.

The aims of this study were to determine the potential role of *ACE1 I/D* genetic polymorphism in the risk of contracting COVID-19 as well as predicting the severity of COVID-19 infection. We hypothesized that the *ACE1 I* allele is associated with an increased risk of contracting the SARS-CoV-2 virus, while the *ACE1 D* allele is associated with a worse prognosis depicted as increased severity of signs, symptoms, and sequelae following COVID-19 infection.

## METHODS

### Human Subjects

This study was approved by the Institutional Review Board (IRB) of the American University of Beirut (AUB). Three-hundred and eighty-seven Lebanese adult subjects were recruited given they had presented to the AUB Medical Center (AUBMC) for COVID-19 PCR testing (irrespective of result), COVID-19 hospitalization, or post-COVID-19 persistent symptoms. The recruitment process entailed a one-time participation that included informed consent process, data collection, and peripheral blood withdrawal for DNA isolation and *ACE1* genotyping.

### Data Collection

Data for this study were obtained via a questionnaire and access through medical records on the electronic heath information system EPIC. Information collected included demographics, comorbidities, medications intake, date of PCR testing, and COVID-19 disease presentation, management, and progression for each participant.

## ACE1 I/D Genotyping

Peripheral blood was collected in EDTA containing tubes, processed into aliquots and stored at −80°C. DNA was then isolated using FlexiGene® DNA Kit by QIAGEN® (Germany) as per the manufacturer's guidelines. Isolated DNA was read using the DS-11 Spectrophotometer (DeNovix®, USA) for quantification and purity assessment and stored at −20°C. Genotyping for *ACE1 insertion/deletion* polymorphism was carried out by polymerase chain reaction (PCR) followed by gel visualization with primers and experimental conditions as previously described (25). Individuals homozygous for the *D* allele and *I* allele were identified by a single 190 bp fragment and a single 490 bp fragment, respectively. Heterozygous individuals were identified by the presence of both fragments.

## Statistical Analysis

The collected data were transcribed onto Microsoft Excel then exported to SPSS® (IBM, USA) for description and analysis. A $P < 0.05$ was considered statistically significant.

The *ACE1* polymorphism was analyzed using four separate associations: one for the alleles (*I* vs. *D*), and the remaining three for the genotypes (*II* vs. *DI* vs. *DD*, *D*-carriers, and *I*-carriers). The *D*-carrier association was (*II* vs. *DI* + *DD*), and that of the *I*-carrier was (*DD* vs. *DI* + *II*). The genotype frequencies in controls were checked for Hardy Weinberg Equilibrium (HWE) using chi-square test.

Baseline characteristics included in the analysis were age, body mass index (BMI), sex, blood group (containing *A* or not), smoking (never, ever), comorbidities, and intake of ACEI or ARBs. Comorbidities were classified as follows: dyslipidemia, hypertension, diabetes, heart disease (coronary artery disease or heart failure), kidney disease (chronic kidney disease or end-stage renal disease), lung disease (chronic obstructive pulmonary disease or interstitial lung disease or asthma), cerebrovascular disease (stroke or carotid stenosis), coagulation disorders (hemophilia or von Willebrand disease), and cancer.

For the association of *ACE1* (*I/D*) polymorphism with contracting COVID-19 disease, participants infected with COVID-19 (cases) were compared to those who were not (controls). For the association of *ACE1* (*I/D*) polymorphism with severity and outcome of COVID-19 infection, three comparisons were carried out: mild vs. moderate vs. severe disease, hospitalized vs. non-hospitalized, and hypoxic ($SpO_2$ <94%) vs. non-hypoxic ($SpO_2$ ≥94%) upon hospitalization. Disease severity was classified according to the WHO clinical progression scale into three stages: stage I (mild), stage II (moderate), and stage III (severe) (26). Mild presentation included any combination of the following: fever and/or chills, cough, shortness of breath, sore throat, congestion and/or rhinorrhea, fatigue, myalgias, headache, nausea and/or vomiting, diarrhea, anosmia, and ageusia. The moderate disease stage included symptomatic patients who were hospitalized with evident radiographic lung inflammation and a blood oxygen saturation ($SpO_2$) ≥94% with minimal or no oxygen therapy required (26). Severe disease included critically ill patients with marked lung infiltrates on Chest X-Ray or CT scan and hypoxia ($SpO_2$ <94%) who required hospitalization with essential oxygen therapy by either nasal cannula, face mask, non-invasive ventilation (NIV), and/or mechanical ventilation with intubation (26).

Association analyses were carried out using Fisher's Exact test for categorical variables and independent sample *t*-test or one-way ANOVA with *post-hoc* Bonferroni for continuous variables as applicable. Binary or multinomial logistic regressions were used for the associations with *ACE1* (*I/D*) polymorphism at both the univariate and multivariate level since these are the main focus of the study. Multivariate regression entailed adjustment for all statistically significant covariates at the univariate level. Results are presented as number (percentage) *N* (%), mean ± standard deviation (SD) at the univariate level, and odds ratios (OR) (adjusted and unadjusted) with 95% confidence intervals.

Additional analysis was performed to explore previously reported association(s) of the *ACE1* polymorphism with comorbidities.

# RESULTS

Three-hundred and eighty-seven non-related Lebanese subjects, 155 controls and 232 cases, who presented to AUBMC for COVID-19 PCR testing were recruited and included in this study. The three genotypes were in HWE ($P = 0.281$). *ACE1 I* allele was the least common with a frequency of 31.0% and a *II* genotype frequency of 7.8% in controls (**Table 1**). These numbers are in line with the literature stating that the *I* allele is least common in Caucasians and Middle Easterners, and most common in Asians [**Supplementary Table 1**; (24, 27)].

## Disease Susceptibility

When comparing baseline characteristics to predict disease susceptibility in cases vs. controls (**Table 1**), the cases were both older and of higher BMI. There was a larger proportion of males in the infected group compared to that of the uninfected group. Hypertension, diabetes, heart disease, and cancer were all significant comorbid predictors for COVID-19 susceptibility. Moreover, there was a greater proportion of participants taking $ACEI/ARB_s$ among the case group when compared to controls (**Table 1**).

Compared to *ACE1 D*, the frequency of the *II* genotype was significantly higher among individuals infected with COVID-19 (14.2 vs. 7.8%; $P = 0.035$; **Table 1**). After adjusting for age, BMI, sex, hypertension, diabetes, heart disease, cancer, and $ACEI/ARB_s$ intake, binary logistic regression showed that, compared to *D* allele carriers, individuals with the *II* genotype were at increased risk for contracting the virus (OR = 2.074; $P = 0.048$; **Supplementary Table 2** and **Figure 1**).

## Disease Severity

Among the 232 cases, 223 were symptomatic: 136 (61.0%) had mild symptoms, 26 (11.7%) had moderate symptoms and 61 (27.3%) had severe symptoms. The mean ± SD of symptoms' duration was 10.14 ± 8.56 days.

As show in **Table 2**, compared to cases with mild infection, those with moderate and severe infection were older and of higher BMI. There were larger proportions of males among

**TABLE 1 |** Association between baseline characteristics and *ACE1* polymorphism in COVID-19 positive cases vs. COVID-19 negative controls.

| | | | **Controls** ***N* = 155** | **Cases** ***N* = 232** | ***P*-Value**[a] |
|---|---|---|---|---|---|
| Age (years) | Mean ± SD | | 37.14 ± 11.48 | 43.75 ± 15.85 | **<0.001** |
| BMI[b] (kg/m$^2$) | Mean ± SD | | 25.79 ± 4.14 | 27.82 ± 5.51 | **<0.001** |
| Sex | Female | *N* (%) | 86 (55.5) | 106 (45.7) | **0.037** |
| | Male | *N* (%) | 69 (44.5) | 126 (54.3) | |
| Blood group A+ | Yes | *N* (%) | 75 (48.4) | 118 (50.9) | 0.354 |
| | No | *N* (%) | 80 (51.6) | 114 (49.1) | |
| Smoking | Ever | *N* (%) | 63 (40.6) | 98 (42.2) | 0.418 |
| | Never | *N* (%) | 92 (59.4) | 134 (57.8) | |
| Dyslipidemia | Yes | *N* (%) | 19 (12.3) | 40 (17.2) | 0.116 |
| | No | *N* (%) | 136 (87.7) | 192 (82.8) | |
| Hypertension | Yes | *N* (%) | 11 (7.1) | 46 (19.8) | **<0.001** |
| | No | *N* (%) | 144 (92.9) | 186 (80.2) | |
| Diabetes | Yes | *N* (%) | 4 (2.6) | 29 (12.5) | **<0.001** |
| | No | *N* (%) | 151 (97.4) | 203 (87.5) | |
| Heart disease[c] | Yes | *N* (%) | 2 (1.3) | 15 (6.5) | **<0.001** |
| | No | *N* (%) | 153 (98.7) | 217 (93.5) | |
| Kidney disease[d] | Yes | *N* (%) | 1 (0.6) | 8 (3.4) | 0.068 |
| | No | *N* (%) | 154 (99.4) | 224 (96.6) | |
| Lung disease[e] | Yes | *N* (%) | 5 (3.2) | 13 (5.6) | 0.202 |
| | No | *N* (%) | 150 (96.8) | 219 (94.4) | |
| Cerebrovascular disease[f] | Yes | *N* (%) | 0 (0.0) | 2 (0.9) | 0.359 |
| | No | *N* (%) | 155 (100) | 230 (99.1) | |
| Coagulation disorders[g] | Yes | *N* (%) | 1 (0.6) | 4 (1.7) | 0.335 |
| | No | *N* (%) | 154 (99.4) | 228 (98.3) | |
| Cancer | Yes | *N* (%) | 3 (1.9) | 21 (9.1) | **0.003** |
| | No | *N* (%) | 152 (98.1) | 211 (90.9) | |
| ACEI[h]/ARB[i] intake | Yes | *N* (%) | 9 (5.8) | 27 (11.6) | **0.037** |
| | No | *N* (%) | 146 (94.2) | 205 (88.4) | |
| *ACE* genotype | *II* | *N* (%) | 12 (7.8) | 33 (14.2) | 0.141 |
| | *DI* | *N* (%) | 72 (46.4) | 104 (44.8) | |
| | *DD* | *N* (%) | 71 (45.8) | 95 (41.0) | |
| | *II* | *N* (%) | 12 (7.8) | 33 (14.2) | **0.035** |
| | *DI + DD* | *N* (%) | 143 (92.3) | 199 (85.8) | |
| | *DI + II* | *N* (%) | 84 (54.2) | 137 (59.1) | 0.200 |
| | *DD* | *N* (%) | 71 (45.8) | 95 (41.0) | |
| *ACE* allele | *I* | *N* (%) | 96 (31.0) | 170 (36.6) | 0.060 |
| | *D* | *N* (%) | 71 (69.0) | 95 (63.4) | |

[a] *P-values defined using independent t-test for continuous variables and Fisher exact for categorical variables.*
[b] *Body mass index.*
[c] *Coronary artery disease; heart failure.*
[d] *Chronic kidney disease, end-stage renal disease.*
[e] *Chronic obstructive pulmonary disease, interstitial lung disease, asthma.*
[f] *Stroke, carotid stenosis.*
[g] *Hemophilia, von Willebrand disease.*
[h] *Angiotensin converting enzyme inhibitor.*
[i] *Angiotensin receptor blocker.*
*The statistically significant P values are in bold.*

moderate and severe cases compared to mild cases. Dyslipidemia, hypertension, diabetes, heart disease, kidney disease, coagulation disorders, and cancer were significant comorbid predictors for moderate and severe disease vs. mild disease. There was also a larger proportion of ACEI/ARB$_s$ intake among moderate and severe cases when compared to controls (**Table 2**).

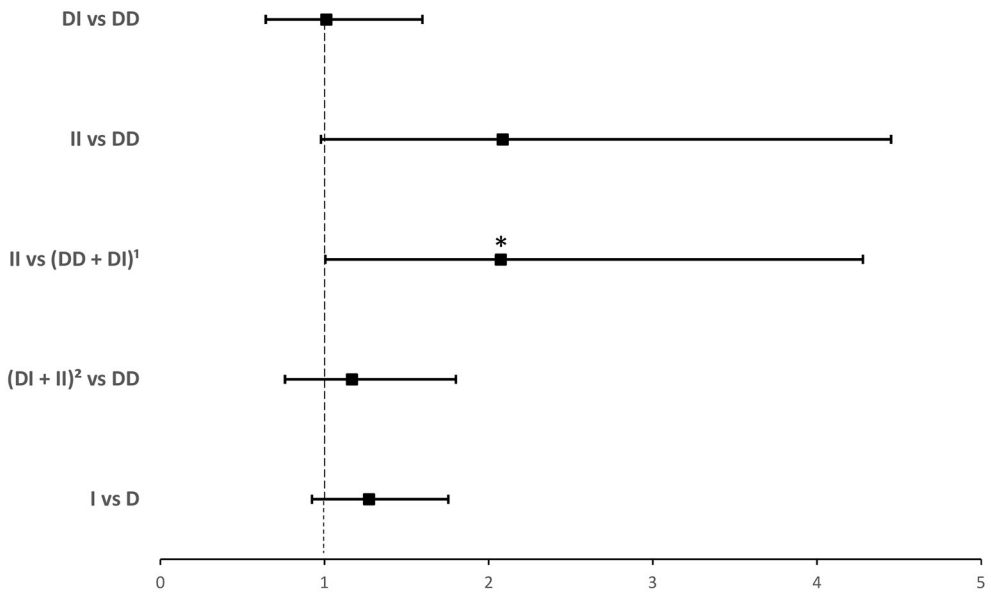


**FIGURE 1 |** Forest plot showing adjusted odds ratios ± 95% confidence intervals of *ACE1* polymorphism for contracting SARS-CoV-2. Multivariate analysis included variables that were statistically significant in the association analysis shown in **Table 1**; *$P < 0.05$. [1]*D* allele carriers. [2]*I* allele carriers.

*ACE1 I/D* genotype and allele frequencies were not significantly associated with disease severity although there was a trend of higher *DD* genotype and *D* allele frequencies in cases with severe symptoms of COVID-19 disease (**Table 2**). After adjusting for age, BMI, sex, significant comorbidities, and ACEI/$ARB_s$ intake, multinomial logistic regression showed that symptomatic cases with the *DD* genotype had a higher risk of developing severe disease following SARS-CoV-2 infection (OR = 5.751; $P = 0.038$) when compared to symptomatic *II* individuals. In addition, and compared to symptomatic *I* carriers, symptomatic cases with the *DD* genotype were more likely to develop severe disease following infection (OR = 2.845; $P = 0.026$). Similarly, the *D* allele was significantly associated with more severe disease presentation (OR =2.359; $P = 0.014$: **Supplementary Table 3** and **Figure 2**).

## Hospitalization

Among the 232 cases, 144 (62.1%) were non-hospitalized while 88 (37.9%) were hospitalized. The mean ± SD of length of stay was 13.45 ± 13.73 days.

It is shown in **Table 3** that hospitalized patients were older and of higher BMI. There was a significantly larger proportion of hospitalized males compared to non-hospitalized males. Dyslipidemia, hypertension, diabetes, heart disease, kidney disease, coagulation disorders, and cancer were significant comorbid predictors for hospitalization. Additionally, there was a larger proportion of ACEI/$ARB_s$ intake among hospitalized cases (**Table 3**).

*ACE1 I/D* genotype and allele frequencies were not significantly associated with hospitalization although there was a trend of higher *DD* genotype and *D* allele frequencies in hospitalized cases with COVID-19 disease (**Table 3**). After adjusting for age, BMI, sex, significant comorbidities, and ACEI/$ARB_s$ intake, binary logistic regression showed that, compared to *I* carriers, individuals with the *DD* genotype were at higher risk for hospitalization following infection (OR = 2.307; $P = 0.042$; **Supplementary Table 4** and **Figure 3**).

## Hypoxia

Among the 88 hospitalized patients, 26 (29.5%) were not hypoxic as opposed to 62 (70.5%) that were.

As shown in **Table 4**, hypoxic patients only had significantly higher BMI when compared to admitted patients without hypoxia. There was a slightly larger proportion of hypoxic males compared to non-hypoxic males, but this result was not statistically significant. There were no significant comorbid predictors for developing hypoxia; nevertheless, there was an increasing trend for dyslipidemia, hypertension, diabetes, and ACEI/$ARB_s$ intake among hypoxic patients (**Table 4**).

*ACE1 I/D* genotype and allele frequencies were not significantly associated with hypoxia although there was a trend of higher *DD* genotype and *D* allele frequencies in hypoxic hospitalized cases with COVID-19 disease (**Table 4**). After adjusting for BMI, binary logistic regression showed that, compared to the *II* genotype, *D* allele carriers were at an increased risk for developing hypoxia following infection (OR = 4.374; $P = 0.045$; **Supplementary Table 5** and **Figure 4**).

# DISCUSSION

Ever since the outbreak, people realized that the SARS-CoV-2 virus hits every individual differently with varying symptoms and severity. There has been a plethora of articles from

**TABLE 2 |** Association between baseline characteristics and *ACE1* polymorphism with disease severity[1] in symptomatic COVID-19 cases.

| | | | **Mild** ***N* = 138** | **Moderate** ***N* = 26** | **Severe** ***N* = 61** | ***P*-Value[2]** |
|---|---|---|---|---|---|---|
| Age (years) | Mean ± SD | | 36.51 ± 11.06[a,b] | 54.00 ± 15.03 | 56.98 ± 15.33 | **<0.001** |
| BMI[3] (kg/m$^2$) | Mean ± SD | | 26.55 ± 4.87[b] | 27.85 ± 4.56[c] | 31.05 ± 6.18 | **<0.001** |
| Sex | Female | *N* (%) | 75 (55.1) | 7 (26.9) | 18 (29.5) | **0.001** |
| | Male | *N* (%) | 61 (44.9) | 19 (73.1) | 43 (70.5) | |
| Blood group A+ | Yes | *N* (%) | 70 (51.5) | 11 (42.3) | 32 (52.5) | 0.682 |
| | No | *N* (%) | 66 (48.5) | 15 (57.7) | 29 (47.5) | |
| Smoking | Ever | *N* (%) | 57 (41.9) | 11 (42.3) | 25 (41.0) | 1.000 |
| | Never | *N* (%) | 79 (58.1) | 15 (57.7) | 36 (59.0) | |
| Dyslipidemia | Yes | *N* (%) | 14 (10.3) | 6 (23.1) | 20 (32.8) | **0.001** |
| | No | *N* (%) | 122 (89.7) | 20 (76.9) | 41 (67.2) | |
| Hypertension | Yes | *N* (%) | 10 (7.4) | 8 (30.8) | 28 (45.9) | **<0.001** |
| | No | *N* (%) | 126 (92.6) | 18 (69.2) | 33 (54.1) | |
| Diabetes | Yes | *N* (%) | 5 (3.7) | 6 (23.1) | 18 (29.5) | **<0.001** |
| | No | *N* (%) | 131 (96.3) | 20 (76.9) | 43 (70.5) | |
| Heart disease[4] | Yes | *N* (%) | 1 (0.7) | 4 (15.4) | 10 (16.4) | **<0.001** |
| | No | *N* (%) | 135 (99.3) | 22 (84.6) | 51 (83.6) | |
| Kidney disease[5] | Yes | *N* (%) | 1 (0.7) | 3 (11.5) | 4 (6.6) | **0.003** |
| | No | *N* (%) | 135 (99.3) | 23 (88.5) | 57 (93.4) | |
| Lung disease[6] | Yes | *N* (%) | 7 (5.1) | 3 (11.5) | 3 (4.9) | 0.367 |
| | No | *N* (%) | 129 (94.9) | 23 (88.5) | 58 (95.1) | |
| Cerebrovascular disease[7] | Yes | *N* (%) | 0 (0.0) | 1 (3.8) | 1 (1.6) | 0.077 |
| | No | *N* (%) | 136 (100.0) | 25 (96.2) | 60 (98.4) | |
| Coagulation disorders[8] | Yes | *N* (%) | 0 (0.0) | 0 (0.0) | 4 (6.6) | **0.010** |
| | No | *N* (%) | 136 (100.0) | 26 (100.0) | 57 (93.4) | |
| Cancer | Yes | *N* (%) | 1 (0.7) | 9 (34.6) | 11 (18.0) | <**0.001** |
| | No | *N* (%) | 135 (99.3) | 17 (65.4) | 50 (82.0) | |
| ACEI[9]/ARB[10] intake | Yes | *N* (%) | 9 (6.6) | 4 (15.4) | 14 (23.0) | **0.005** |
| | No | *N* (%) | 127 (93.4) | 22 (86.4) | 47 (77.0) | |
| *ACE* genotype | *II* | *N* (%) | 23 (16.9) | 5 (19.2) | 5 (8.2) | 0.348 |
| | *DI* | *N* (%) | 62 (45.6) | 12 (46.2) | 26 (42.6) | |
| | *DD* | *N* (%) | 51 (37.5) | 9 (34.6) | 30 (49.2) | |
| | *II* | *N* (%) | 23 (16.9) | 5 (19.2) | 5 (8.2) | 0.200 |
| | *DI + DD* | *N* (%) | 113 (83.1) | 21 (80.8) | 56 (91.8) | |
| | *DI + II* | *N* (%) | 85 (62.5) | 17 (65.4) | 31 (50.8) | 0.259 |
| | *DD* | *N* (%) | 51 (37.5) | 9 (34.6) | 30 (49.2) | |
| *ACE* allele | *I* | *N* (%) | 108 (39.7) | 22 (42.3) | 36 (29.5) | 0.15 |
| | *D* | *N* (%) | 164 (60.3) | 30 (57.7) | 86 (70.5) | |

[1]*Rated as mild, moderate, or severe according to the WHO clinical progression scale for COVID-19.*
[2]*P-values defined using one-way ANOVA with post-hoc Bonferroni for continuous variables and Fisher exact for categorical variables.*
[a]*P < 0.05 for Mild vs. Moderate with post-hoc Bonferroni.*
[b]*P < 0.05 for Mild vs. Severe with post-hoc Bonferroni.*
[c]*P < 0.05 for Moderate vs. Severe with post-hoc Bonferroni.*
[3]*Body mass index.*
[4]*Coronary artery disease; heart failure.*
[5]*Chronic kidney disease, end-stage renal disease.*
[6]*Chronic obstructive pulmonary disease, interstitial lung disease, asthma.*
[7]*Stroke, carotid stenosis.*
[8]*Hemophilia, von Willebrand disease.*
[9]*Angiotensin converting enzyme inhibitor.*
[10]*Angiotensin receptor blocker.*
*The statistically significant P values are in bold.*

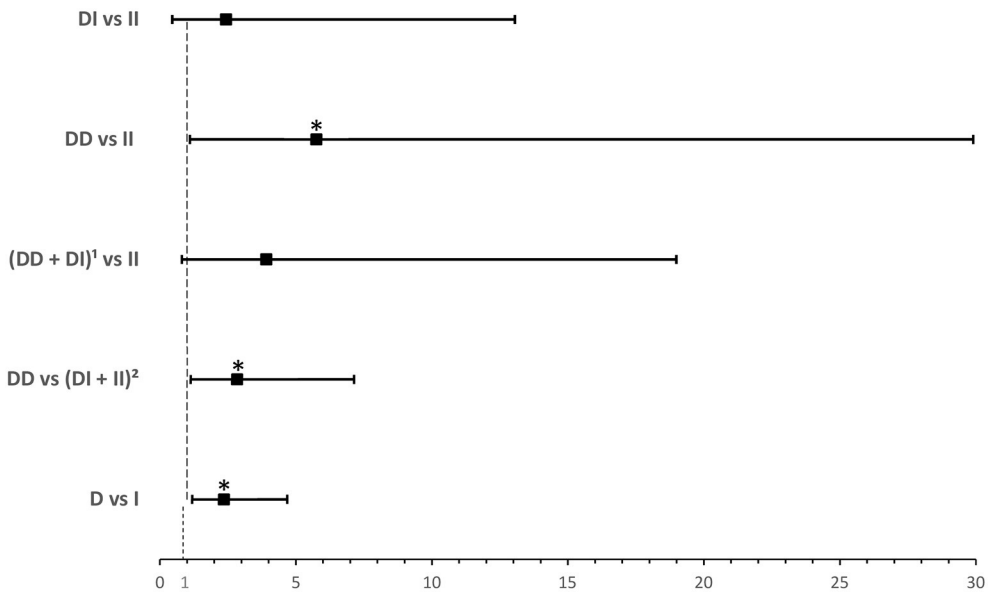


**FIGURE 2 |** Forest plot showing odds ratios ± 95% confidence intervals of *ACE1* polymorphism for developing severe[a] disease in symptomatic COVID-19 cases. Multivariate analysis included variables that were statistically significant in the association analysis shown in **Table 2**; *$P < 0.05$. [a]Rated as mild, moderate, or severe according to WHO clinical progression scale for COVID-19 with mild disease as Reference. [1]*D* allele carriers. [2]*I* allele carriers.

different populations and ethnicities discussing the factors that are considered to be risk factors for both symptoms and severity of the COVID-19 disease, but with only few related to genetics. This study is the first to evaluate these factors in Lebanese Arabs. We show that almost all previously reported factors and comorbidities also predict disease susceptibility and severity in the Lebanese population. We also show a positive correlation between *ACE1 I* and the risk of contracting the COVID-19 disease, and between *ACE1 D* and worse COVID-19 infection. These results suggest that genotyping for *ACE1 I/D* polymorphism could be used to assess risk and predict severity for better prognosis and management of the disease. This is especially important for Middle Easterners in general and the Lebanese in particular who, and similarly to the results of the current study, have a higher frequency of the *ACE1 D* allele when compared to the *I* allele (24, 25).

## Demographics, Health Related Behaviors, and Comorbidities

Most of the associated demographics, health-related behaviors, and comorbidities can be explained at the physiological level. For instance for age, *ACE2* receptor, being the key factor in the entry of the virus, is more highly expressed in well-differentiated ciliated epithelial cells found in adults (2). Moreover, the immunity of an older individual is weaker than the immunity of children due to immunosenescence and the presence of central memory T cells rather than naïve T cells (2). Our results agree with the literature since the mean age (in years) is significantly higher in the infected cases when compared to the non-infected controls, and it is significantly higher with disease severity. Concerning sex, *ACE2* being an X-linked gene can be considered as a disadvantage for infected males, since lower *ACE2* expression may correlate with lesser conversion of Angiotensin II into Angiotensin 1–7 (28). Moreover, testosterone suppresses the immune system in males, which affects the T cell responses (29). These findings are compatible with our results that show that the majority of cases and those with worse outcome are males. In our study, the mean BMI ($kg/m^2$) was also significantly higher in the infected cases and associated with more severe disease. This can be explained by the fact that the adipose tissue expresses *ACE2* receptors as much as the pulmonary tissues (7). Accordingly, obese individuals have higher levels of circulating *ACE2* with secondarily higher disease susceptibility and adverse outcome (30). As for blood group, data are still non-conclusive. For example, it has been shown that carriage of blood group A was associated with a higher rate of COVID-19 infection when compared to blood group O (31). However, it is felt that individuals with blood group A also have more underlying comorbidities (29), which could be the reason behind the significance seen in infected patients. In our study, blood group did not show any significant difference with neither risk nor severity of the disease.

Concerning health-related behavior, smoking is one of the most common risk factor for many diseases. That is why smoking is expected to further complicate the symptoms of COVID-19. Smoking is shown to increase the gene expression of *ACE2* in the lungs (4). Moreover, nicotine upregulates the activity of renin and *ACE1* thus activating ACE/Angiotensin II/AT1R

**TABLE 3 |** Association between baseline characteristics and *ACE1* polymorphism with hospitalized vs. non-hospitalized COVID-19 cases.

| | | | Not hospitalized $N = 144$ | Hospitalized $N = 88$ | *P*-Value[a] |
|---|---|---|---|---|---|
| Age (years) | Mean ± SD | | 36.49 ± 11.28 | 55.64 ± 15.09 | **<0.001** |
| BMI[b] (kg/m$^2$) | Mean ± SD | | 26.50 ± 4.81 | 29.98 ± 5.92 | **<0.001** |
| Sex | Female | *N* (%) | 79 (54.9) | 27 (30.7) | **<0.001** |
| | Male | *N* (%) | 65 (45.1) | 61 (69.3) | |
| Blood group A+ | Yes | *N* (%) | 75 (52.1) | 43 (48.9) | 0.367 |
| | No | *N* (%) | 69 (47.9) | 45 (51.1) | |
| Smoking | Ever | *N* (%) | 62 (43.1) | 36 (40.9) | 0.428 |
| | Never | *N* (%) | 82 (56.9) | 52 (59.1) | |
| Dyslipidemia | Yes | *N* (%) | 15 (10.4) | 25 (28.4) | **<0.001** |
| | No | *N* (%) | 129 (89.6) | 63 (71.6) | |
| Hypertension | Yes | *N* (%) | 10 (6.9) | 36 (40.9) | **<0.001** |
| | No | *N* (%) | 134 (93.1) | 52 (59.1) | |
| Diabetes | Yes | *N* (%) | 4 (2.8) | 25 (28.4) | **<0.001** |
| | No | *N* (%) | 140 (97.2) | 63 (71.6) | |
| Heart disease[c] | Yes | *N* (%) | 1 (0.7) | 14 (15.9) | **<0.001** |
| | No | *N* (%) | 143 (99.3) | 74 (84.1) | |
| Kidney disease[d] | Yes | *N* (%) | 1 (0.7) | 7 (8.0) | **0.005** |
| | No | *N* (%) | 143 (99.3) | 81 (92.0) | |
| Lung disease[e] | Yes | *N* (%) | 7 (4.9) | 6 (6.8) | 0.362 |
| | No | *N* (%) | 137 (95.1) | 82 (93.2) | |
| Cerebrovascular disease[f] | Yes | *N* (%) | 0 (0.0) | 2 (2.3) | 0.143 |
| | No | *N* (%) | 144 (100) | 86 (97.7) | |
| Coagulation disorders[g] | Yes | *N* (%) | 0 (0.0) | 4 (4.5) | **0.020** |
| | No | *N* (%) | 144 (100) | 84 (95.5) | |
| Cancer | Yes | *N* (%) | 1 (0.7) | 20 (22.7) | **<0.001** |
| | No | *N* (%) | 143 (99.3) | 64 (77.3) | |
| ACEI[h]/ARB[i] | Yes | *N* (%) | 9 (6.3) | 18 (20.5) | **0.001** |
| | No | *N* (%) | 135 (93.8) | 70 (79.5) | |
| *ACE* genotype | *II* | *N* (%) | 22 (15.3) | 11 (12.5) | 0.555 |
| | *DI* | *N* (%) | 67 (46.5) | 37 (42.0) | |
| | *DD* | *N* (%) | 55 (38.2) | 40 (45.5) | |
| | *II* | *N* (%) | 22 (15.3) | 11 (12.5) | 0.351 |
| | *DI + DD* | *N* (%) | 122 (84.7) | 77 (87.5) | |
| | *DI + II* | *N* (%) | 89 (61.8) | 48 (54.5) | 0.170 |
| | *DD* | *N* (%) | 55 (38.2) | 40 (45.5) | |
| *ACE* allele | *I* | *N* (%) | 111 (38.5) | 59 (33.5) | 0.161 |
| | *D* | *N* (%) | 177 (61.5) | 117 (66.5) | |

[a] *P-values defined using independent t-test for continuous variables and Fisher exact for categorical variables.*
[b] *Body mass index.*
[c] *Coronary artery disease; heart failure.*
[d] *Chronic kidney disease, end-stage renal disease.*
[e] *Chronic obstructive pulmonary disease, interstitial lung disease, asthma.*
[f] *Stroke, carotid stenosis.*
[g] *Hemophilia, von Willebrand disease.*
[h] *Angiotensin converting enzyme inhibitor.*
[i] *Angiotensin receptor blocker.*
*The statistically significant P values are in bold.*

pathway, and decreases the activity of AT2R by downregulating the activity of *ACE2* (32). A systematic review has shown that current smokers had a lower risk for developing severe outcome when compared to former smokers (33). However, a preliminary meta-analysis on five studies in China, and similarly to our results, has shown that active smoking is not significantly related

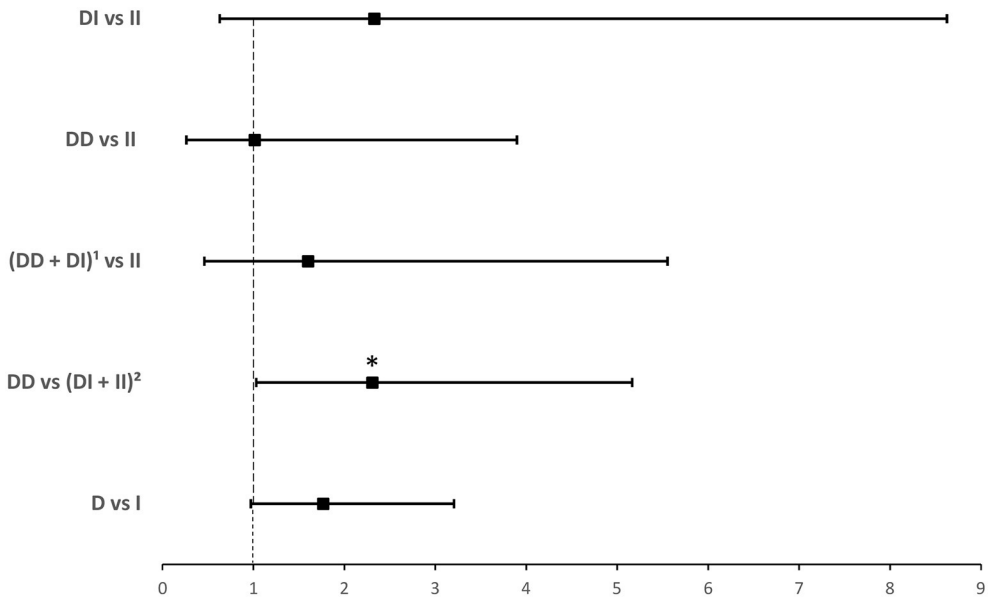


**FIGURE 3 |** Forest plot showing adjusted odds ratios ± 95% confidence intervals of *ACE1* polymorphism for hospitalization for COVID-19. Multivariate analysis included variables that were statistically significant in the association analysis shown in **Table 3**; *$P < 0.05$. [1]*D* allele carriers, [2]*I* allele carriers.

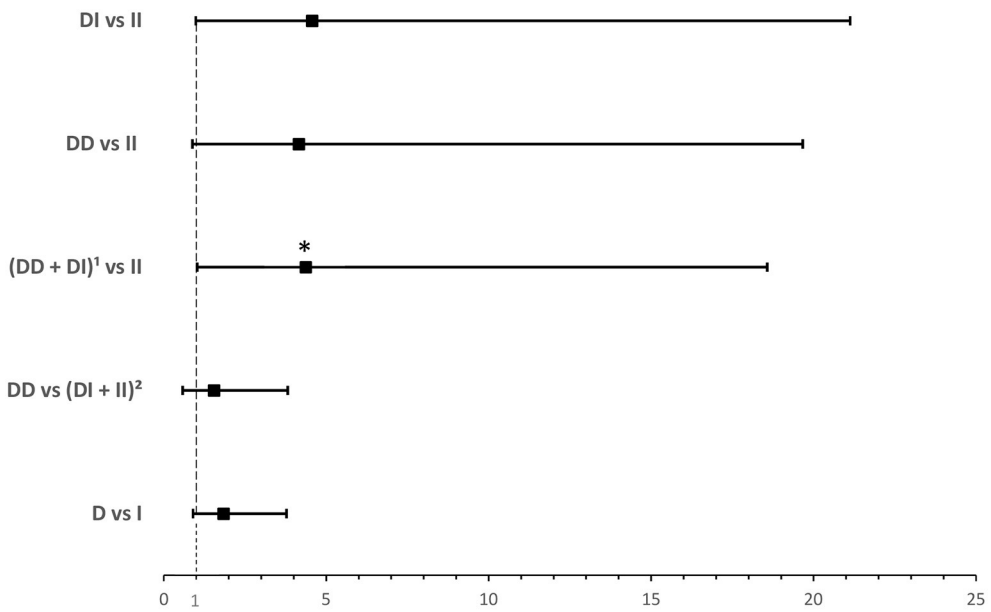


**FIGURE 4 |** Forest plot showing adjusted odds ratios ± 95% confidence intervals of *ACE1* polymorphism for developing hypoxia in hospitalized COVID-19 cases. Multivariate analysis adjusted for BMI; *$P < 0.05$. [1]*D* allele carriers. [2]*I* allele carriers.

to the severity of COVID-19 (34). Further data are needed to resolve this controversy.

To date, it is still unclear whether ACEI and/or $ARB_s$ should be kept in patients who contract COVID-19. There are currently two contradicting hypotheses in the literature that RAS inhibition could be both harmful and protective (8). In our study, ACEI/$ARB_s$ were significantly more frequently taken in the worse disease outcome group. However, it is possible that these results

**TABLE 4 |** Association between baseline characteristics and *ACE1* polymorphism with hypoxic vs. non-hypoxic hospitalized COVID-19 cases.

| | | | Not hypoxic $N = 26$ | Hypoxic $N = 62$ | *P*-Value[a] |
|---|---|---|---|---|---|
| Age (years) | Mean ± SD | | 52.08 ± 14.38 | 57.13 ± 15.24 | 0.146 |
| BMI[b] (kg/m$^2$) | Mean ± SD | | 27.27 ± 4.35 | 31.12 ± 6.15 | **0.001** |
| Sex | Female | *N* (%) | 9 (34.6) | 18 (29.0) | 0.391 |
| | Male | *N* (%) | 17 (65.4) | 44 (71.0) | |
| Blood group A+ | Yes | *N* (%) | 11 (42.3) | 32 (51.6) | 0.287 |
| | No | *N* (%) | 15 (57.7) | 30 (48.4) | |
| Smoking | Ever | *N* (%) | 11 (42.3) | 25 (40.3) | 0.523 |
| | Never | *N* (%) | 15 (57.7) | 37 (59.7) | |
| Dyslipidemia | Yes | *N* (%) | 4 (15.4) | 21 (33.9) | 0.064 |
| | No | *N* (%) | 22 (84.6) | 41 (66.1) | |
| Hypertension | Yes | *N* (%) | 7 (26.9) | 29 (46.8) | 0.067 |
| | No | *N* (%) | 19 (73.1) | 33 (53.2) | |
| Diabetes | Yes | *N* (%) | 6 (23.1) | 19 (30.6) | 0.328 |
| | No | *N* (%) | 20 (76.9) | 43 (69.4) | |
| Heart disease[c] | Yes | *N* (%) | 5 (15.4) | 10 (16.1) | 0.603 |
| | No | *N* (%) | 22 (84.6) | 52 (83.9) | |
| Kidney disease[d] | Yes | *N* (%) | 3 (11.5) | 4 (6.5) | 0.339 |
| | No | *N* (%) | 23 (88.5) | 58 (93.5) | |
| Lung disease[e] | Yes | *N* (%) | 3 (11.5) | 3 (4.8) | 0.242 |
| | No | *N* (%) | 23 (88.5) | 59 (95.2) | |
| Cerebrovascular disease[f] | Yes | *N* (%) | 0 (0.0) | 2 (3.2) | 0.494 |
| | No | *N* (%) | 26 (100.0) | 60 (96.8) | |
| Coagulation disorders[g] | Yes | *N* (%) | 0 (0.0) | 4 (6.5) | 0.239 |
| | No | *N* (%) | 26 (100.0) | 58 (93.5) | |
| Cancer | Yes | *N* (%) | 9 (34.6) | 11 (17.7) | 0.077 |
| | No | *N* (%) | 17 (65.4) | 51 (82.3) | |
| ACEI[h]/ARB[i] | Yes | *N* (%) | 3 (11.5) | 15 (24.2) | 0.145 |
| | No | *N* (%) | 23 (88.5) | 47 (75.8) | |
| *ACE* genotype | *II* | *N* (%) | 6 (23.1) | 5 (8.1) | 0.171 |
| | *DI* | *N* (%) | 10 (38.5) | 27 (43.5) | |
| | *DD* | *N* (%) | 10 (38.5) | 30 (48.4) | |
| | *II* | *N* (%) | 6 (23.1) | 5 (8.1) | 0.060 |
| | *DI + DD* | *N* (%) | 20 (76.9) | 57 (91.9) | |
| | *DI + II* | *N* (%) | 16 (61.5) | 32 (51.6) | 0.269 |
| | *DD* | *N* (%) | 10 (38.5) | 30 (48.4) | |
| *ACE* allele | *I* | *N* (%) | 22 (42.3) | 37 (29.8) | 0.078 |
| | *D* | *N* (%) | 30 (57.7) | 87 (70.2) | |

[a] *P-values defined using independent t-test for continuous variables and Fisher exact for categorical variables.*
[b] *Body mass index.*
[c] *Coronary artery disease; heart failure.*
[d] *Chronic kidney disease, end-stage renal disease.*
[e] *Chronic obstructive pulmonary disease, interstitial lung disease, asthma.*
[f] *Stroke, carotid stenosis.*
[g] *Hemophilia, von Willebrand disease.*
[h] *Angiotensin converting enzyme inhibitor.*
[i] *Angiotensin receptor blocker.*
*The statistically significant P values are in bold.*

relate to the fact that this group of subjects has underlying comorbidities that necessitate ACEI/ARB$_s$ treatment. As a matter of fact, people with underlying comorbidities such as diabetes, hypertension (HTN), cardiovascular diseases (CVD), chronic kidney diseases (CKD), lung diseases (COPD and asthma), cerebral vascular disease, and coagulation disorders are at a

higher risk of worse COVID-19 severity and outcome (35–37). Our results clearly show that comorbidities are risk factors for contracting the virus and developing a worse COVID-19 disease outcome.

## *ACE1* I/D Genetic Polymorphism

In relation to disease susceptibility, available data, most of which are literature and database searches, are at times contradictory (21). For example on one hand, Yamamoto et al. (23) showed that countries with higher frequency of the *ACE1 I* allele had less susceptibility to COVID-19. On the other hand, Delanghe et al. (22) showed that a high frequency of *ACE1 I* allele increases the prevalence of COVID-19 cases. Nevertheless, when Yamamoto et al. (23) specifically looked at Middle Eastern populations, they found a weaker association with the *D* allele, hence the need for further investigations. To our knowledge, we are the first to evaluate such an association in patients. We confirmed Delanghe et al.'s (22) simulations by showing that the frequency of *II* was significantly highest in infected cases when compared to controls coupled with a significantly higher risk of contracting the COVID-19 disease after adjusting for confounders.

As for disease outcome, *ACE1 DD* genotype leads to higher activity of *ACE1* enzyme thus lowering *ACE2* causing an increase in the amount of angiotensin II left active. Although lower levels of *ACE2* could mean that there is less chance for SARS-CoV-2 to bind and enter the host cell, high levels of angiotensin II would act through AT1R and further cause cardiovascular and lung pathologies (16). As a matter of fact, Gomez et al. (16) found that *ACE1 DD* genotype was more frequent in severe COVID-19 cases, suggesting that there is an association between *ACE1 DD* genotype and the severity of COVID-19. Furthermore, *ACE1 DD* genotype has been correlated with respiratory failure (12) and increased death rate (38) in patients infected with COVID-19. In addition, an ecologic meta-regression showed that there is a link between *ACE1 I/D* polymorphism and the recovery rate of COVID-19 whereby faster recovery was correlated with higher frequency ratio of the *I/D* allele (20). Our results are in agreement with the literature. Notably, it could be argued that the latter association is due to the known associations of the *ACE1 D* allele with cardiovascular comorbidities. In our cohort of infected cases however, we found no significant associations with any of the comorbidities (**Supplementary Table 6**).

## Limitations

This study has few limitations. First, the sample size is limited to a single country and institution, and is relatively small. Of note that we did not estimate needed sample size at study initiation because of lack of such data at the time and the study being exploratory. Nevertheless, our sample size for the severity outcome is very similar to two recent investigations, one with Spanish Caucasians (16) and another with Indians (39). Second, the study entailed multiple testing, the adjustment of which could lead to loss of statistical significance. In fact for the severity outcome whereby we assessed three independent outcomes, it may be relevant to set the significance level at 0.016 (0.05/3). With such adjustment, only the association between the *D* allele and disease severity remains statistically significant (OR =2.359; $P = 0.014$). Notably, disease severity was classified as mild, moderate, and severe as per the WHO progression scale scoring system (26), a scoring system that is based on a constellation of assessment tools for severity following infection that includes hospitalization status, oxygen saturation, and need for oxygen therapy. With a larger representative sample, it is possible to have independently increased risks for both hospitalization and hypoxia with the *D* allele after accounting for multiple testing ($P < 0.016$). Additional data from other institutions and populations may address these two limitations with the opportunity to perform a meta-analysis. Third, the study only evaluated the *ACE1 I/D* polymorphism and did not look at other possible SNPs in *ACE1*. Moreover, it would be relevant to look at *ACE2* and *TMPRSS2* variants, as these two genes are important factors in the entry of SARS-CoV-2 (40). Finally, the role of ACEI/$ARB_s$ in COVID-19 disease is still unresolved and it would be interesting to evaluate whether there is any interaction between *ACE* polymorphisms and these drugs in the SARS-COV2 setting (41).

# CONCLUSION

To our knowledge, we are the first to evaluate the association of *ACE1* genetic polymorphism with COVID-19 disease susceptibility and outcome in a Middle Eastern Arab population such as the Lebanese. Despite its limitations, results of this study suggest that genotyping for *ACE1 I/D* polymorphism could be used to elicit the disease risk and severity for better prognosis and management. Further studies are needed to evaluate additional genetic variants in different ethnicities and populations.

# DATA AVAILABILITY STATEMENT

The original contributions presented in the study are included in the article/**Supplementary Material**, further inquiries can be directed to the corresponding author/s.

# ETHICS STATEMENT

The studies involving human participants were reviewed and approved by the American University of Beirut Institutional Review Board under protocol: BIO-2020-0259. The patients/participants provided their written informed consent to participate in this study.

# AUTHOR CONTRIBUTIONS

CS, RM, IA, and NZ contributed conception and design of the study. HS recruited study subjects and collected data. KJ performed the experiments. HS, KJ, and NZ organized the database, performed the statistical analysis, and wrote the first draft of the manuscript. All authors

contributed to manuscript revision, read, and approved the submitted version.

## FUNDING

This work was supported by National Council for Scientific Research Lebanon: The flash call COVID-19 management in Lebanon. Diana Tamari Sabbagh Scholars Program (DTSSP)—Award for MS Graduate Students in biomedical research.

## SUPPLEMENTARY MATERIAL

The Supplementary Material for this article can be found online at: https://www.frontiersin.org/articles/10.3389/fmed.2021.798571/full#supplementary-material

## REFERENCES

1. Cevik M, Kuppalli K, Kindrachuk J, Peiris M. Virology, transmission, and pathogenesis of SARS-CoV-2. *BMJ.* (2020) 371:m3862. doi: 10.1136/bmj.m3862
2. Yuki K, Fujiogi M, Koutsogiannaki S. COVID-19 pathophysiology: a review. *Clin Immunol.* (2020) 215:108427. doi: 10.1016/j.clim.2020.108427
3. Goel R, Bloch EM, Pirenne F, Al-Riyami AZ, Crowe E, Dau L, et al. ABO blood group and COVID-19: a review on behalf of the ISBT COVID-19 Working Group. *Vox Sang.* (2021) 116:849–61. doi: 10.1111/vox.13076
4. Cai G, Bosse Y, Xiao F, Kheradmand F, Amos CI. Tobacco smoking increases the lung gene expression of ACE2, the receptor of SARS-CoV-2. *Am J Respir Crit Care Med.* (2020) 201:1557–9. doi: 10.1164/rccm.202003-0693LE
5. Ejaz H, Alsrhani A, Zafar A, Javed H, Junaid K, Abdalla AE, et al. COVID-19 and comorbidities: deleterious impact on infected patients. *J Infect Public Health.* (2020) 13:1833–9. doi: 10.1016/j.jiph.2020.07.014
6. Froldi G, Dorigo P. Endothelial dysfunction in Coronavirus disease (2019) (COVID-19): gender and age influences. *Med Hypotheses.* (2020). 144:110015. doi: 10.1016/j.mehy.2020.110015
7. Sattar N, McInnes IB, McMurray JJV. Obesity is a risk factor for severe COVID-19 infection: multiple potential mechanisms. *Circulation.* (2020) 142:4–6. doi: 10.1161/CIRCULATIONAHA.120.047659
8. Patel AB, Verma A. COVID-19 and angiotensin-converting enzyme inhibitors and angiotensin receptor blockers: what is the evidence? *JAMA.* (2020) 323:1769–70. doi: 10.1001/jama.2020.4812
9. Zeberg H, Paabo S. The major genetic risk factor for severe COVID-19 is inherited from Neanderthals. *Nature.* (2020) 587:610–2. doi: 10.1038/s41586-020-2818-3
10. Russo R, Andolfo I, Lasorsa VA, Iolascon A, Capasso M. Genetic analysis of the coronavirus SARS-CoV-2 host protease TMPRSS2 in different populations. *Front Genet.* (2020) 11:872. doi: 10.3389/fgene.2020.00872
11. Wooster L, Nicholson CJ, Sigurslid HH, Lino Cardenas CL, Malhotra R. Polymorphisms in the ACE2 locus associate with severity of COVID-19 infection. *MedRxiv.* (2020). doi: 10.1101/2020.06.18.20135152
12. Annunziata A, Coppola A, Lanza M, Simioli F, Imitazione P, Pepe N, et al. ACE DD polymorphism in severe COVID-19. *J Transl Sci.* (2020) 7:1. doi: 10.15761/JTS.1000396
13. Hou Y, Zhao J, Martin W, Kallianpur A, Chung MK, Jehi L, et al. New insights into genetic susceptibility of COVID-19: an ACE2 and TMPRSS2 polymorphism analysis. *BMC Med.* (2020) 18:216. doi: 10.1186/s12916-020-01673-z
14. D'Ardes D, Boccatonda A, Rossi I, Guagnano MT, Santilli F, Cipollone F, et al. COVID-19 and RAS: unravelling an unclear relationship. *Int J Mol Sci.* (2020) 21:3003. doi: 10.3390/ijms21083003
15. Cao Y, Li L, Feng Z, Wan S, Huang P, Sun X, et al. Comparative genetic analysis of the novel coronavirus (2019-nCoV/SARS-CoV-2) receptor ACE2 in different populations. *Cell Discov.* (2020) 6:11. doi: 10.1038/s41421-020-0147-1
16. Gomez J, Albaiceta GM, Garcia-Clemente M, Lopez-Larrea C, Amado-Rodriguez L, Lopez-Alonso I, et al. Angiotensin-converting enzymes (ACE, ACE2) gene variants and COVID-19 outcome. *Gene.* (2020) 762:145102. doi: 10.1016/j.gene.2020.145102
17. Karakas CS, Cakmak GG, Piskin N, Acikgoz B, Altinsoy B, Kurucu IB, et al. Polymorphisms of ACE (I/D) and ACE2 receptor gene (Rs2106809, Rs2285666) are not related to the clinical course of COVID-19: a case study. *J Med Virol.* (2021) 93:5947–52. doi: 10.1002/jmv.27160
18. Zheng H, Cao JJ. Angiotensin-converting enzyme gene polymorphism and severe lung injury in patients with coronavirus disease 2019. *Am J Pathol.* (2020) 190:2013–7. doi: 10.1016/j.ajpath.2020.07.009
19. Liu Y, Yang Y, Zhang C, Huang F, Wang F, Yuan J, et al. Clinical and biochemical indexes from 2019-nCoV infected patients linked to viral loads and lung injury. *Sci China Life Sci.* (2020) 63:364–74. doi: 10.1007/s11427-020-1643-8
20. Hatami N, Ahi S, Sadeghinikoo A, Foroughian M, Javdani F, Kalani N, et al. Worldwide ACE (I/D) polymorphism may affect COVID-19 recovery rate: an ecological meta-regression. *Endocrine.* (2020) 68:479–84. doi: 10.1007/s12020-020-02381-7
21. Yamamoto N, Nishida N, Yamamoto R, Gojobori T, Shimotohno K, Mizokami M, et al. Angiotensin-Converting Enzyme (ACE) 1 gene polymorphism and phenotypic expression of COVID-19 symptoms. *Genes.* (2021) 12:1572. doi: 10.3390/genes12101572
22. Delanghe JR, Speeckaert MM, De Buyzere ML. The host's angiotensin-converting enzyme polymorphism may explain epidemiological findings in COVID-19 infections. *Clin Chim Acta.* (2020) 505:192–3. doi: 10.1016/j.cca.2020.03.031
23. Yamamoto N, Ariumi Y, Nishida N, Yamamoto R, Bauer G, Gojobori T, et al. SARS-CoV-2 infections and COVID-19 mortalities strongly correlate with ACE1 I/D genotype. *Gene.* (2020) 758:144944. doi: 10.1016/j.gene.2020.144944
24. Saab YB, Gard PR, Overall AD. The geographic distribution of the ACE II genotype: a novel finding. *Genet Res.* (2007) 89:259–67. doi: 10.1017/S0016672307009019
25. Akra-Ismail M, Makki RF, Chmaisse HN, Kazma A, Zgheib NK. Association between angiotensin-converting enzyme insertion/deletion genetic polymorphism and hypertension in a sample of Lebanese patients. *Genet Test Mol Biomarkers.* (2010) 14:787–92. doi: 10.1089/gtmb.2010.0096
26. WHO Working Group on the Clinical Characterisation and Management of COVID-19 infection. A minimal common outcome measure set for COVID-19 clinical research. *Lancet Infect Dis.* (2020) 20:e192–7. doi: 10.1016/S1473-3099(20)30483-7
27. Han C, Han XK, Liu FC, Huang JF. Ethnic differences in the association between angiotensin-converting enzyme gene insertion/deletion polymorphism and peripheral vascular disease: a meta-analysis. *Chronic Dis Transl Med.* (2017) 3:230–41. doi: 10.1016/j.cdtm.2017.07.002
28. Gemmati D, Bramanti B, Serino ML, Secchiero P, Zauli G, Tisato V. COVID-19 and individual genetic susceptibility/receptivity: role of ACE1/ACE2 genes, immunity, inflammation and coagulation. Might the double X-chromosome in females be protective against SARS-CoV-2 compared to the single X-chromosome in males? *Int J Mol Sci.* (2020) 21:3474. doi: 10.3390/ijms21103474
29. Peckham H, de Gruijter NM, Raine C, Radziszewska A, Ciurtin C, Wedderburn LR, et al. Male sex identified by global COVID-19 meta-analysis as a risk factor for death and ITU admission. *Nat Commun.* (2020) 11:6317. doi: 10.1038/s41467-020-19741-6
30. Emilsson V, Gudmundsson EF, Aspelund T, Jonsson BG, Gudjonsson A, Launer LJ, et al. Serum levels of ACE2 are higher in patients with obesity and diabetes. *Obes Sci Pract.* (2021) 7:239–43. doi: 10.1002/osp4.472
31. Li J, Wang X, Chen J, Cai Y, Deng A, Yang M. Association between ABO blood groups and risk of SARS-CoV-2 pneumonia. *Br J Haematol.* (2020) 190:24–7. doi: 10.1111/bjh.16797

32. Oakes JM, Fuchs RM, Gardner JD, Lazartigues E, Yue X. Nicotine and the renin-angiotensin system. *Am J Physiol Regul Integr Comp Physiol.* (2018) 315:R895–906. doi: 10.1152/ajpregu.00099.2018
33. Farsalinos K, Barbouni A, Poulas K, Polosa R, Caponnetto P, Niaura R. Current smoking, former smoking, and adverse outcome among hospitalized COVID-19 patients: a systematic review and meta-analysis. *Ther Adv Chronic Dis.* (2020) 11:2040622320935765. doi: 10.1177/2040622320935765
34. Lippi G, Henry BM. Active smoking is not associated with severity of coronavirus disease 2019. (COVID-19). *Eur J Intern Med.* (2020) 75:107–8. doi: 10.1016/j.ejim.2020.03.014
35. Sanyaolu A, Okorie C, Marinkovic A, Patidar R, Younis K, Desai P, et al. Comorbidity and its impact on patients with COVID-19. *SN Compr Clin Med.* (2020) 1–8. doi: 10.1007/s42399-020-00363-4
36. Iniguez M, Perez-Matute P, Villoslada-Blanco P, Recio-Fernandez E, Ezquerro-Perez D, Alba J, et al. ACE gene variants rise the risk of severe COVID-19 in patients with hypertension, dyslipidemia or diabetes: a spanish pilot study. *Front Endocrinol.* (2021) 12:688071. doi: 10.3389/fendo.2021.688071
37. Vetter P, Vu DL, L'Huillier AG, Schibler M, Kaiser L, Jacquerioz F. Clinical features of covid-19. *BMJ.* (2020) 369:m1470. doi: 10.1136/bmj.m1470
38. Adamzik M, Frey U, Sixt S, Knemeyer L, Beiderlinden M, Peters J, et al. ACE I/D but not AGT (-6)A/G polymorphism is a risk factor for mortality in ARDS. *Eur Respir J.* (2007) 29:482–8. doi: 10.1183/09031936.00046106
39. Verma S, Abbas M, Verma S, Khan FH, Raza ST, Siddiqi Z, et al. Impact of I/D polymorphism of angiotensin-converting enzyme 1 (ACE1) gene on the severity of COVID-19 patients. *Infect Genet Evol.* (2021) 91:104801. doi: 10.1016/j.meegid.2021.104801
40. Torre-Fuentes L, Matias-Guiu J, Hernandez-Lorenzo L, Montero-Escribano P, Pytel V, Porta-Etessam J, et al. ACE2, TMPRSS2, and furin variants and SARS-CoV-2 infection in Madrid, Spain. *J Med Virol.* (2021) 93:863–9. doi: 10.1002/jmv.26319
41. Sienko J, Kotowski M, Bogacz A, Lechowicz K, Drozdzal S, Rosik J, et al. COVID-19: the influence of ACE genotype and ACE-I and ARBs on the course of SARS-CoV-2 infection in elderly patients. *Clin Interv Aging.* (2020) 15:1231–40. doi: 10.2147/CIA.S261516


**Conflict of Interest:** The authors declare that the research was conducted in the absence of any commercial or financial relationships that could be construed as a potential conflict of interest.

**Publisher's Note:** All claims expressed in this article are solely those of the authors and do not necessarily represent those of their affiliated organizations, or those of the publisher, the editors and the reviewers. Any product that may be evaluated in this article, or claim that may be made by its manufacturer, is not guaranteed or endorsed by the publisher.

frontiers in Medicine

REVIEW
published: 03 February 2022
doi: 10.3389/fmed.2022.805107

# Implications of Using Host Response-Based Molecular Diagnostics on the Management of Bacterial and Viral Infections: A Review

*Johnny Atallah*[1,2] *and Michael K. Mansour*[1,2]*

[1] *Division of Infectious Diseases, Massachusetts General Hospital, Boston, MA, United States,* [2] *Department of Medicine, Harvard Medical School, Boston, MA, United States*

Host-based diagnostics are a rapidly evolving field that may serve as an alternative to traditional pathogen-based diagnostics for infectious diseases. Understanding the exact mechanisms underlying a host-immune response and deriving specific host-response signatures, biomarkers and gene transcripts will potentially achieve improved diagnostics that will ultimately translate to better patient outcomes. Several studies have focused on novel techniques and assays focused on immunodiagnostics. In this review, we will highlight recent publications on the current use of host-based diagnostics alone or in combination with traditional microbiological assays and their potential future implications on the diagnosis and prognostic accuracy for the patient with infectious complications. Finally, we will address the cost-effectiveness implications from a healthcare and public health perspective.

**Keywords: infections, host-response, biomarkers, proteomics, transcriptomics, RT-PCR**

OPEN ACCESS

***Edited by:***
*Hadi M. Yassine,*
*Qatar University, Qatar*

***Reviewed by:***
*Nicolas Leveque,*
*University of Poitiers, France*
*Hossein Yousofi Darani,*
*Isfahan University of Medical Sciences, Iran*
*Meghna Verma,*
*AstraZeneca, United States*

***Correspondence:**
*Michael K. Mansour*
*mkmansour@mgh.harvard.edu*

***Specialty section:***
*This article was submitted to Precision Medicine, a section of the journal Frontiers in Medicine*

***Received:*** *29 October 2021*
***Accepted:*** *03 January 2022*
***Published:*** *03 February 2022*

***Citation:***
*Atallah J and Mansour MK (2022) Implications of Using Host Response-Based Molecular Diagnostics on the Management of Bacterial and Viral Infections: A Review. Front. Med. 9:805107. doi: 10.3389/fmed.2022.805107*

## INTRODUCTION

The complexity of the human immune response in the setting of disease has made it difficult to assign the contribution from the underlying pathologic process in the background of the host immune response. The difficulty in such determination frequently leads to misdiagnoses, antibiotic misuse leading to antimicrobial resistance (AMR), increased healthcare expenses and direct adverse effects affecting the health of patients.

The clinical manifestations of pathogen-specific disease vary across a wide spectrum of symptoms including fever, myalgias, respiratory symptoms, weakness and altered mental status among many others. In fact, pathogen-based diagnostic testing has been the traditional and a convenient method for the identification of the causative pathogen linked with specific clinical manifestations, such as fever. This process is usually performed using traditional based culture systems, immunoassays, and molecular-based testing. Pathogen detection can usually be achieved by polymerase chain reaction (PCR) that can amplify the nucleic acid of pathogens directly from blood culture. However, a limitation to PCR is the necessity for a minimum pathogen burden in the bloodstream, which in turn results in several false-negative outcomes. Another limitation is the time constraint on laboratory staff performing repeat pathogen-based diagnostics in an attempt to improve sensitivity and detection.

The purpose of the immune system is to recognize and eliminate invading pathogens making a host response-based immunodiagnostic an attractive adjunct to pathogen-based diagnostics

with the potential for improved diagnostics accuracy and efficiency. These techniques represent a step closer toward precision and personalized medicine capable of providing the best treatment matched for the specific patient in a timely manner (1). As such, the "omics" platforms have proliferated around host immunodiagnostics and several promising molecular host biomarkers show potential in the rapid diagnosis in critical diseases (2). Unlike pathogen-based testing, host immunodiagnostics present the capability of differentiating non-infectious immune triggers including sterile inflammatory processes, autoimmune diseases, or malignancy.

These techniques involve platform assays such as RT-PCR, RNA sequencing and others to test for specific host gene expression signatures and transcripts as well as metabolic and protein biomarkers directly related to susceptibility and response to infection. These technological advances have made it possible to integrate multiple biomarkers into single predictive models, and thus there is progress in the integration of genomics, transcriptomics, and proteomics with recent expansion into epigenomics, lipidomics, and metabolomics (3). While these approaches have the prospect of a more precise identification of an infectious trigger based on the host immune response, none to date have undergone clinical trial testing or achieved approval for clinical application.

Here, we review the current state of novel host response-based diagnostic testing on the identification of the causative processes underlying an activated immune response, on the influence on patient outcome, on reduction of healthcare cost, and on the possibility of redefining the standard of care for specific clinical presentations. This article will shed light on possible benefits of using host-based diagnostics from a public health perspective regarding pandemics and endemics, and finally, we examine techniques of integrating both, host-based and pathogen-based diagnostics for improving clinical outcomes.

## METHODS

Publications on host immune response and role of immune based diagnostics were collected from the PubMed database. MeSH terms included host response, immune based diagnostics, transcriptomics, proteomics, infection, and sepsis were used to conduct this search. The articles were reviewed by the authors. Articles were limited to English language only and results were filtered by date of publication to include all articles published from 2015 through 2021.

**Abbreviations:** AMR, Antimicrobial resistance; AUROC, Area under the receiver operating characteristic curve; CAP, Community acquired pneumonia; PSI, Pneumonia severity index; RSV, Respiratory syncytial virus; RT-PCR, Real time polymerase chain reaction; LRTI, Lower respiratory tract infection; CRP, C-Reactive protein; FAM89A, Family With Sequence Similarity 89 Member A; IFI44L, Interferon Induced Protein 44 Like; mNGS, Metagenomics next generation sequencing; Tb, Tuberculosis; ED, Emergency Department; WHO, World Health Organization; NPV, Negative predictive value; PPV, Positive predictive value; PCT, Procalcitonin; IMKX-BWN-1, Inflammatix-bacterial-viral-non-infected-version 1; NAAT, Nucleic acid amplification test; RT-LAMP, Reverse transcription loop-mediated isothermal amplification; NTS, Nose and throat swabs; IP-10, Interferon-Inducible Protein 10; BCA-1, B-Cell attracting chemokine; OASL, Oligoadenylate synthetases-like; NP, Nasopharyngeal samples.

## RESULTS

### Host-Based Diagnostics for Identifying the Infectious Etiology

The initial management of suspected infection is pathogen identification, which subsequently dictates the treatment approach. In this section, we will review the use of host-based diagnostics in determining and identifying the infectious etiology. MeSH terms yielded 12 studies.

The host response to bacterial vs. viral test was examined. The study compared transcriptional analysis to a host immune biomarker, procalcitonin (PCT), which rises in the setting of bacterial but not viral infection (4). Results of the BioFire FilmArray system using RT-PCR to measure 45 transcript signatures were compared to standard PCT, yielded accurate discrimination between bacterial and viral infections superior to PCT performance. Six hundred twenty-three subjects with suspected respiratory infection or sepsis had blood testing for transcriptional profiling. The results provided 80.1% accuracy for bacterial infection and 86.8% accuracy for viral infection with a mean turnaround time of ∼45 min compared to an accuracy of 68.7% for PCT alone (5). In addition to accurately detecting infectious processes, the BioFire FilmArray correctly identified ill patients without infection (no positive microbiology) with an 86% accuracy (6).

Several studies focused on using detection of host mRNA signatures to differentiate infectious from non-infectious processes in patients with acute infections and sepsis. The InSep$^{TM}$ test (Inflammatix, Burlingame, CA, formerly known as HostDx$^{TM}$ Sepsis) is a 29-host mRNA blood-based test that allows for rapid diagnosis of acute infections and sepsis using machine-learning algorithms. The patterns interpreted using InSep allows for differentiation of acute host response to bacterial vs. viral infections as well as prognosticating disease severity using whole blood. Following whole blood RNA extraction from patients with suspected sepsis in the emergency department, amplifying and quantitating the 29-mRNAs; these transcriptional signatures are then fed into machine learning algorithms to produce measurable scores. The 3 measurable scores (scale from 0 to 40) assess the likelihood of bacterial infection, the likelihood of viral infection, and the infection severity prediction score. However, one limitation is that some of the information presented was in some cases preliminary or hypothetical. An attractive feature of the InSep test is a rapid turnaround time of <30 min.

The 29 mRNAs that the InSep test consists of are classified into 3 separate, validated subpanels: a 7-mRNA "Bacterial-Viral Metascore," an 11-mRNA "Stanford Mortality Score" and an 11-mRNA "Sepsis Metascore." The 7-gene "Bacterial-Viral Metascore" subpanel consists of 4 genes (HK3, TNIP1, GPAA1, and CTSB) that have shown to be significantly higher in bacterial infections, and 3 genes (IFI27, JUP, and LAX1) shown to be higher in viral infections. The "Sepsis Metascore" subpanel on another hand, consists of a sepsis-specific transcripts including CEACAM1, C3AR1, GNA15, and HLA-DPB1 which have previously been linked to sepsis. Furthermore, neutrophil-related antimicrobial proteins genes such as DEFA4, CTSG, MPO, and

BPI constitute the "Stanford Mortality Score" subpanel, along with additional genes related to energy metabolism and hypoxia (TRIB1, HIF1A, and NDUFV2).

Given the breadth of signatures included in the InSep platform, the potential exists to differentiate detection of bacterial or viral infection. The authors propose that application of RNA transcriptional analysis early in the presentation of a patient with a suspected infection reduces the ordering of multiple unnecessary diagnostics (7). The InSep assay showed a specificity of 98% and a sensitivity of 94% for detecting bacterial infections, and a specificity of 93% and a sensitivity of 96% for viral infections (8).

A similar platform using 29 host mRNA signatures analysis, a neural network classifier: Inflammatix-Bacterial-Viral-Non-infected-Version 1 (IMX-BWN-1) shows similar discriminatory results. The IMX-BVN-1 was used to assess patients with presumed infection and sepsis through the combination of mRNA host-response profiling combined with a machine learning algorithm. IMX-BWN-1 showed excellence diagnostic accuracy for bacterial and viral infection differentiation with a sensitivity of 97% and a specificity of 99%. The area under the curve (AUROC) for IMX-BWN-1 for identifying bacterial infections and viral infections was 0.87 and 0.86, respectively. The combination of mRNA expression analysis and machine learning proved superior to classic infection biomarkers such as PCT with an AUROC of 0.83 for bacterial infections and 0.27 for viral infections, and C-reactive protein (CRP) with an AUROC of 0.7 for bacterial infections and 0.38 for viral infections (9, 10).

In another pooled analysis of 1,057 samples from 20 cohorts, a set of 7 genes was derived for discriminating bacterial and viral infections. The 20 cohorts that were included either bacterial or viral infections, but not both. These cohorts represent a wide variety of clinical conditions, including a range of infection types (gram-positive, gram-negative, atypical bacteria, common respiratory viruses) as well as a range of severities (from mild infections to severe septic shock). This multicohort analysis aimed to use gene expression datasets for identifying a biomarker that can discriminate between viral and bacterial infections. Using this set alongside the 11-gene Sepsis MetaScore (Please see section "d" for more information) yielded a sensitivity of 94% and a specificity of 59.8% for identifying bacterial infections (11).

## Infectious Etiology in the Pediatric Population

Infections are a leading cause for life-threatening events in the pediatric population. The WHO reports a global mortality rate of 5.9 million children under the age of 5 due to infections (12). Thus, host-response assays have emerged as promising diagnostics in this population.

In a prospective observational study febrile infants 60 days or younger were enrolled. The transcriptional assessment of 66 genes accurately identified infants with bacterial infections with a sensitivity of 87% and a specificity of 89%. Moreover, when 66 genes were reduced to 10 classifier genes, data continued to yield high diagnostic performance with a sensitivity of 94% and a specificity of 95% in distinguishing bacteremia in infants from those without infection as compared to confirmed bacterial blood cultures (13).

Furthermore, in a similar study, total blood RNA expression signature for distinguishing bacterial from viral infection in febrile children was compared with clinical and microbiological diagnostics. Subjects were classified into one of 3 groups: definite bacterial infection, definite viral infection and indeterminate state. These groups were stratified by culture or molecular detection of pathogens A two-transcript RNA signature (*FAM89A* and *IFI44L*) was identified from a larger 38-transcript screen. Then, the performance of a 2-transcript RNA signature expression was evaluated among the groups. The Family with Sequence Similarity 89 Member A (*FAM89A*) and the Interferon Induced Protein 44 Like (*IFI44L*) are both protein coding genes that have been linked to a rare mild immunodeficiency (immunodeficiency 38 with basal ganglia calcification). Upon implementation, this 2-transcript signature yielded favorable results for detection of definite bacterial with a sensitivity of 100%, and a specificity of 96.4% and definite viral with a sensitivity of 100%, and a specificity of 97.1%. IFI44L and FAM89A expression values were combined into a disease risk score. IFI4L was noted to be increased in antiviral responses mediated by interferons, while FAM89A was increased in bacterial infections and septic shock thus forming a reciprocal relationship of upregulation between both genes in viral and bacterial infections.

One interesting outcome was regarding the indeterminate groups where the 2-transcript signature detected 46.3% of those cases as having bacterial infection although 94.9% received antibiotic treatment by standard care (14, 15).

This 2-gene signature was further validated when applied to data from the RNA expression signatures used by the study described above. This validation study aimed to assess the accuracy of the 2-gene signature, previously tested in children with a mean age of 19 months, in infants aged 60 days or younger. The results were promising and showed a sensitivity of 88.8% and a specificity of 93.7% when compared to definite bacterial infections with positive cultures and confirmed viral infections. These data demonstrate the translatable potential of this 2-gene transcript signature into a simple bedside diagnostic test although a larger sample of subjects is needed for confirmation (16).

The application of technology amenable to bedside conditions show promise as a point of care RNA diagnostic. Use of reverse transcription-loop mediated isothermal amplification (RT-LAMP) technology demonstrated that the 2-gene RNA signature has the potential of being translated into a rapid and portable platform convenient for the use as a point-of-care test. A laboratory-on-a-chip platform that uses reverse transcription-loop mediated isothermal amplification (RT-LAMP) technology. RT-LAMP technology uses the mechanism of auto cycling strand displacement DNA synthesis using a polymerase with 2 pairs of primers used. Using 6 independent sequences at the start and 4 independent sequences toward the latter stages, RT-LAMP can recognize and amplify target sequences. This RT-LAMP uses numerous microsensors that can detect hydrogen ions released and thus detect changes in pH during NAAT under same experimental conditions of the previous studies (14–16). The results of translating this 2-gene signature to RT-LAMP were very similar to using microarray data used in the previous

studies. Sensitivity and specificity were 100% for confirmed viral and bacterial infections. In addition to RT-LAMP platform being simple, the assay time required was <25 min which is considerably more rapid than microarray (17).

The application of RNA signatures to determine microbial composition and prognostic outcomes has been examined. In a retrospective study aiming to evaluate the use of microbial signatures of specific microbiota to prognosticate the severity of influenza virus infection, 36 pediatric (mean age of 3 years) subjects infected with influenza and presenting with symptoms for <2 days were recruited. RNA-gene sequencing, mNGS and computational analysis workflow were used to assess nasopharyngeal samples (NP) collected from these subjects. Results indicated that subjects having an increased bacterial diversity in their NP samples experienced milder disease. On the contrary, subjects with diminished abundance of *S. aureus* on one hand, and increased presence of Streptobacillus, Prevotella, Porphyromonas, Granulicatealla, Veillonella, Fusobacterium, and Haemophilus in their NP samples experienced severe respiratory or neurological influenza outcomes. These data demonstrate that use of RNA transcript as a reflection of microbiome diversity in the setting of influenza can potentially serve as an accurate prognostic indicator (18) (see **Table 1**).

Some limitations arise due to the special considerations of the pediatric population, which include difficulty of sample collection. In addition, some studies aimed to recruit equal numbers of children with confirmed bacterial and viral infections and then assess for diagnostic accuracy of the host-response assay. Thus, a limitation around possible bias in misrepresentation of infectious etiology and frequency in febrile children presenting to healthcare facilities.

## Host-Based Diagnostics for Identifying Respiratory Infections

### Respiratory Infections

One of the most common causes of hospitalization and mortality in adults is lower respiratory tract infection (LRTI). Evaluation of whole blood gene expression profiling using RNA sequencing and qPCR for the discrimination bacterial from non-bacterial infection was performed. Using MeSH terms for host-based diagnostics for identifying bacterial vs. viral respiratory infections including tuberculosis yielded 13 studies.

Despite being a common cause of morbidity, mortality and hospitalization, LRTI-causing pathogens are infrequently identified due to limitations of traditional pathogen-based detection methods. In one study, an 11-host gene pathway set from nose and throat swabs, sputum, urine, and blood samples obtained from potential patients with symptoms of LRTI was used as an optimal marker. Quantitative PCR assay [e.g., Film Array Respiratory Panel, Idaho Technologies Inc. for nose and throat swabs (NTS) and sputum] was used for all the samples, and the difference in gene expression was tested by Wilcoxon Rank test. The Respiratory Panel offers a run time of about 45 min for rapid PCR detection of respiratory infections, and it integrates sample purification, amplification, detection, and analysis in one automated multiplex PCR system for detection of many pathogens within rapid time. RNA sequencing was also used and differences in gene expression between bacterial and non-bacterial infected subjects were assessed by a similar statistical approach. The results of this study showed promising outcomes with a sensitivity of 90% and a specificity of 83% for identifying bacterial LRTI as compared to confirmed microbiological testing (19).

Other studies have utilitzed metagenomic next-generation sequencing (mNGS) for DNA and RNA (see section "f" for more information) to define host signatures in response etiologic pathogens resulting in LRTI. In a prospective observational study comparing mNGS from patients with and without LRTI to traditional assays, this novel host-based platform detected more viruses and fungi and at a more rapid rate with an approximate 2-day turnaround time. It showed a positive predictive value (PPV) of 78.5%, sensitivity of 66.7% and specificity of 75.4%. Such results will provide insight regarding the impact of the host transcriptome data in the accurate diagnosis of LRTI (20).

In addition to PCR and transcriptional analysis, circulating host biomarker have also been explored as diagnostic and prognostic indicators of infection. One such molecular is proadrenomedulin, a receptor expressed on myeloid cells showing encouraging results for predicting complicated community acquired pneumonia (CAP) in the pediatric population. Proadrenomedullin is a member of the calcitonin peptide family that has been shown to be expressed proportionately during severe infections and is widely expressed by many tissues and organs. It increases microvasculature flow to maintain adequate vascular supply to vital organs during sepsis (21). A proadrenomedullin level above 0.16 nmol/L generated using TRACE (time-resolved amplified cryptase emission) showed a sensitivity of 100% and a specificity of 70% for bacteraemia in children (0–18 years of age) presenting with community acquired pneumonia (22, 30).

The evaluation of proadrenomedullin in the assessment of adult patients with CAP shows similar results when compared to pneumonia severity index (PSI) and CURB65 scores, as a prognostic indicator. Eighty-one patients with suspected CAP were enrolled and followed up to a 28-day duration. Results showed an increased prognostic accuracy for CAP when CURB65 scores were used in combination with proadrenomedullin levels. In fact, for the highest risk patients with upper score classes of PSI and CURB65, proadrenomedullin levels provided additional risk stratification. This result provided valuable accuracy and guidance to the patients' need for intubation, non-invasive ventilation and ICU admission. Using specific proadrenomedullin levels for predicting outcomes yielded a sensitivity of 77.8% and a specificity of 76.5% for death when the value is 1.6 nmol/L, a sensitivity of 83.3% and a specificity of 88.7% for endotracheal intubation when the value is 2.4 nmol/L, and a sensitivity of 87.5% and a specificity of 77% for non-invasive mechanical ventilation at a value of 1.5 nmol/L (31).

### Coronavirus Disease 2019

SARS-CoV-2 is the causative respiratory viral pathogen responsible for the COVID-19 (32). Given the need for rapid diagnostics, multiple studies explored the use of host-based

**TABLE 1 |** Use of host-response diagnostics for discrimination of bacterial vs. viral infections.

| References | Objective | Assay | Comparison | Genes | Sample size | Sensitivity | Specificity | PPV | NPV | Notes |
|---|---|---|---|---|---|---|---|---|---|---|
| Tsalik et al. (5) de Jonge et al. (4) | Bacterial vs. viral discrimination | BioFire FilmArray system using RT-PCR | PCT | 45 transcript signatures | 623 adults with suspected respiratory infections | - | 80.1% for bacterial 86.8% for viral 86% for no infection | - | - | Turnaround time of 45 min |
| Ducharme et al. (7) Safalika et al. (8) | Infectious vs. non-infectious discrimination | InSep Test using whole blood mRNA for host mRNA signatures | Traditional microbiology assays | 29-host mRNA signatures | - | 98% for bacterial 93% for viral | 94% for bacterial 96% for viral | - | - | Turnaround time of 30 min |
| Mayhew (9) Bauer et al. (10) | Bacterial vs. viral discrimination | IMX-BWN-1 using whole blood mRNA for host mRNA signatures | Traditional microbiology assays + PCT + CRP | 29-host mRNA signatures | 1,069 adults with suspected infections | 97% | 99% | - | - | Performance superior to PCT and CRP |
| Sweeney et al. (11) | Bacterial vs. viral discrimination | Multicohort analysis using gene expression datasets to derive a biomarker | | 7-gene dataset | 1,057 adults with suspected infections | 94% | 59.8% | - | - | - |
| Mahajan et al. (13) | Detection of Bacterial infections in febrile infants 60 days or younger | Transcriptional assessment of RNA biosignatures | Traditional microbiology assays | 10-classifier genes | 279 randomly selected febrile infants | 94% | 95% | - | - | - |
| Herberg et al. (15) | Bacterial vs. viral infection in febrile children | Microarray | Traditional microbiology assays and clinical assessment | 2-gene transcript signature | 455 children with fever | 100% for bacterial 100% for viral | 96.4% for bacterial 97.% for viral | - | - | The 2-transcript gene signature detected 46.3% of indeterminate subjects as having infection although 94.9% received antibiotics as per standard care. |
| Kafourou et al. (16) | Bacterial vs. viral infection in febrile infants <60 days old | Microarray | Traditional microbiology assays and clinical assessment | 2-gene transcript signature | 279 randomly selected febrile infants | 88.8% | 93.7% | - | - | Potential of being used as a simple bedside diagnostic test |
| Pennisi et al. (17) | Bacterial vs. viral infection in febrile children | RT-LAMP | Traditional microbiology assays and clinical assessment | 2-gene transcript signature | 455 children with fever | 100% | 100% | - | - | Turnaround time of 25 min significantly faster than microarray |

**TABLE 2 |** Results of using host-response diagnostics for identifying respiratory infections.

| References | Objective | Assay | Comparison | Genes | Sample size | Sensitivity | Specificity | PPV | NPV | Notes |
|---|---|---|---|---|---|---|---|---|---|---|
| Bhattacharya et al. (19) | Identifying bacterial LRTI | PCR assays and RNA sequencing | Standard of care | 11 gene pathways | 94 adults with suspected LRTI | 90% | 83% | - | - | Turnaround time of 45 min |
| Chen et al. (20) | Diagnosing LRTI | mNGS | Traditional microbiological assays | | 162 adults with and without LRTI | 66.7% | 75.4% | 78.5% | - | - |
| Alcoba et al. (21) Saleh et al. (22) | Diagnosing bacteremia in children (0–18 years old) presenting with community acquired pneumonia | TRACE | Traditional microbiological assays | Proadrenomedullin levels | 88 children | 100% | 70% | - | - | - |
| Li et al. (23) | Diagnosing COVID-19 | RT-qPCR | CRP and leukocyte count | 3-gene transcript signature | 228 adults | 88.6% | 94.1% | - | - | |
| McClain et al. (24) | Early detection and treatment of influenza (in the pre-symptomatic phase) | GeneChip Human Genome U133A Array (microarray) | Standard methods | 50-gene signature | 21 healthy adults inoculated with influenza | - | - | - | | Demonstrating temporal dynamics between gene signatures and early treatment |
| Tang et al. (25) | Influenza vs. bacterial infections | Integrated genomic analysis | Standard methods | 1-gene (IFI27) | 1,071 individuals | 88% | 90% | - | - | Diagnostic accuracy of this 1 gene signature equivalent to using multi-gene biomarkers |
| Barral-Arca et al. (26) | Diagnosing RSV infection | Meta-analysis of 7-transcriptome microarrays from whole blood samples | | 17-transcript host genes | 922 samples | 81.3% | 93% | - | - | - |
| Sweeney et al. (27) | Non-sputum host-based diagnostics for active Tb | Integrated multicohort analysis of existing gene expression microarray from peripheral blood | Traditional growth-based microbiology diagnostics | 3-gene signature | 2,572 patients | 93% | 97% | - | - | - |
| Warsinske et al. (28) | Using the 3-gene signature in Rossi et al. (29) for studying treatment response and progression of latent to active Tb | qPCR and RNA sequencing | Traditional sputum conversion | 3-gene signature | 363 subjects | 86% | 84% | - | 99.3% | This assay showed accurate diagnosis of active to latent Tb progression 6 months earlier than traditional sputum conversion |

diagnostics for the detection of COVID-19. In one study, the aim was to derive a transcriptional signature to detect multiple viral infection among including COVID-19. Whole-blood RNA sequencing on samples from subjects was performed with confirmed bacterial, viral or no infection cases. Signature host genes were derived and validated using RT-qPCR. Three-signature genes (*IGF1R*, *NAGK,* and *HERC6*) were derived from the subjects enrolled by differential gene expression analyses using forward selection-partial least squares. The *IFG1R* represents an insulin signaling tyrosine kinase protein that has shown to act as an entry receptor for respiratory syncytial virus (RSV) as well as macrophage and phagocytosis activation. *NAGK* is an enzyme responsible for amino acid metabolism, and *HERC6* has been reported to have antiviral activity when induced by interferon. These gene transcripts distinguished bacterial from viral infections with a 97.3% sensitivity and 100% specificity with superior performance to CRP and leukocyte count. A second validation analysis was done, and the 3 gene signature distinguished between bacterial and COVID-19 positive subjects with a sensitivity of 88.6% and a specificity of 94.1% also outperforming CRP levels and leukocyte count (23).

In one recent study of COVID-19 infected subjects, RNA-sequencing was used to assess the host response in nasopharyngeal and whole blood samples. This technique allowed the derivation of a 19-gene host-response classifier that can differentiate COVID-19 infection from other infections with an accuracy of 86.5%, sensitivity of 80% and specificity of 90% using NP samples. The dysregulated immune response with COVID-19 showed a distinct pattern of activation and inhibition of immune pathways as compared to other infections such as influenza, seasonal coronaviruses, and bacterial sepsis. Moreover, the magnitude of the host-response was found to be directly proportional with clinical severity of the disease. Remarkably, an increased expression of genes involved in interferon responses and decreased expression of IL-6 and IL-18 signaling was noted. Other genes such as ACE2 and TMPRSS2 have shown an association with the need of oxygen therapy during COVID-19 as well as predicting disease severity. However, these genes did not necessarily prove to be upregulated in COVID-19, whether from whole blood or nasopharyngeal swab. The results show that the expression of both genes can serve a prognostic rather than diagnostic role (29, 33).

Such a study points out to the potential of using classifiers of host-response for diagnosis of COVID-19 in the pre-symptomatic or asymptomatic stage during which 38% of pathogen-based PCR will turn out negative (33).

## Influenza and Respiratory Syncytial Virus

Influenza virus, known as "the flu" is one of the most common seasonal respiratory infections worldwide (34). The average pre-symptomatic incubation period of influenza is 2 days. Oseltamivir, a neuraminidase inhibitor, is a therapeutic intervention used in the pre-symptomatic phase shows reduction in the progression of disease, decrease symptoms, infectivity, and accelerated resolution of disease. Early identification of influenza-infected individuals would permit more effective use of antiviral interventions. The use of host-based immune response for early detection of influenza was examined including the implications on management and therapy. Subjects were intranasally inoculated with influenza A and host gene expression was then assessed in peripheral blood samples every 8 h for 7 days using the GeneChip Human Genome U133A Array (Affymetrix, Santa Clara, CA), which is a single array representing 14,500 genes. This process led to the derivation of a gene signature expression for influenza virus composed of 50 genes. The host inflammatory response represented by the gene signature derived was then monitored after the early therapeutic use of oseltamivir in inoculated subjects. It was noted that the markers of host response were significantly reduced upon early treatment with oseltamivir demonstrating a correlation between disease activity, symptoms over time and overall expression of gene-signature levels. The level of host-gene expression was in agreement with the trajectory of symptom progression, thus showing the significance of the impact of time on host-response diagnostics. Although the application of such a technology is complex, the use of a potential rapid and accessible platform (i.e., PCR-based assays) as described in this article could help overcome this limitation. This study is important for providing insight on the correlation of disease severity and gene signatures as well as demonstrating the temporal dynamics of genomic signatures and their response to early treatment (24).

The number of gene biomarkers required has also been examined. A single gene biomarker, IFI27, was used for discriminating between influenza and bacterial infections was identified using integrated genomic analysis. *In vitro* experiments have shown that IFI27 was expressed by antigen presenting cells responding to influenza virus. *In vivo* studies confirmed expression of IFI27 in influenza patients. In fact, in this prospective study enrolling patients with suspected respiratory illness, IFI27 showed high diagnostic accuracy of 88% and a specificity of 90% for distinguishing between influenza and bacterial infections equivalent to accuracy obtained by using multi-gene biomarkers (25).

Although IFI27 has demonstrated the potential of differentiating influenza virus from bacterial infections, other studies using the same gene marker in the context of other viral respiratory infections show similar results. In one study of preterm RSV-infected infants, IFI27 was highly expressed, and its expression correlated with the severity of the disease (35).

Moreover, in another multi-cohort observational study, IFI27 was shown to be expressed in COVID-19 infected patients, and its level of expression was associated with the presence of a high viral load (36). These results are promising although further validation is required to achieve high specificity of this gene marker to a particular disease.

Since IFI27 has been found to be upregulated in influenza, RSV and COVID-19, an effort to identify a single-gene biomarker with a high diagnostic accuracy and specificity to influenza virus in one study was attempted. XGBoost integrated bioinformatics analysis was used to identify 14 genes specifically related

to influenza infection using data from obtained from the gene expression Omnibus database. One gene, oligoadenylate synthetases-like (OASL), was further identified from the 14 gene set and was shown to differentiate between influenza and non-influenza viral and bacterial respiratory infections sharing comparable clinical features outperforming IFI27 with an AUC of 0.85 vs. 0.76, respectively. OASL is known to possess antiviral mediated roles and has been recently shown to have a role in antiviral innate immunity, and it has been previously studied in the context of differentiating viral from bacterial infections. However, OASL's expression value measured by qRT-PCR can be sufficient to differentiate influenza from other non-influenza viral infections. Thus, this study presented significant results to identify OASL as a single biomarker for accurate and specific influenza virus identification (37).

Host-response profiling is not limited to diagnostic potential but also for predicting disease severity. In a study of RSV, the association between nasopharyngeal microbiota and host response profiles predicted the disease severity in RSV-infected children. Nasopharyngeal microbiota was characterized from children with mild and severe RSV using RNA sequencing. In turn, whole blood transcriptome profiles were analyzed to find the potential relationship between the microbiota, RSV host response and consequently, disease severity. RNA from whole blood was hybridized onto Illumina HT12-V4 bead chips.

The data revealed different nasopharyngeal microbiota clusters correlated with interferon related genes from the host response to RSV infections. A significant result overexpression of interferon genes related to neutrophil and macrophage activation in RSV infected children with *H. influenza* and Streptococcus dominant microbiota. This provides a demonstration of the possible interaction between the nasopharyngeal microbiota and the host response in RSV infected children ultimately in determining disease severity (35, 38).

A multi-cohort analysis approach for exploring host transcriptome biomarkers to derive a transcript-gene signature was undertaken as a better RSV diagnostic. Meta-analysis of 7 transcriptome microarray studies consisting of 922 whole blood samples from RSV, healthy, coronaviruses, rhinoviruses infected adults and children identified over 1,500 expressed genes from RSV-infected patients. Furthermore, selectively studying various pathways significantly affected by RSV yielded a 17 transcript host gene signature that is specific for RSV and can differentiate it from other respiratory infections. The results showed a sensitivity of 81.3% and a specificity of 93% for distinguishing RSV from other viral infections using this 17-transcript host signature (26).

In a similar manner, one study used whole blood mRNA signatures to assess the severity and pathogenicity of influenza virus. Certain signatures related to interferon antiviral pathways proved to be common in influenza cases not requiring intubation. As for those requiring mechanical ventilation support, inflammatory, activated neutrophil pattern was seen as early as possible in the course of the disease. Thus, using host-based profiling can potentially project the clinical course of influenza and provide insight on therapeutic tools for severe cases (38, 39).

## Host-Based Diagnostics for Identifying *Mycobacterium tuberculosis*

*Mycobacterium tuberculosis* (*M. tuberculosis*) is a potentially life-threatening infectious disease with typical pulmonary primary infection. The use of host-immune based diagnostics to support the identification of *M. tuberculosis*, disease severity and treatment response was assessed. The focus of these novel diagnostic models was on the ability of improved sensitivity for the detection of smaller disease signatures with higher discriminatory power (40).

The World Health Organization (WHO) identified the need for non-sputum-based diagnostic tests for better diagnosis of *M. tuberculosis* and for differentiating active from latent disease states. The need for new non-sputum diagnostics for active *M. tuberculosis* is realized by the difficulty and poor sensitivity of traditional growth-based microbiology approaches. In an integrated multicohort analysis of existing gene expression microarray from peripheral blood of patients with active *M. tuberculosis* composed of 2,572 patient samples, deriving a diagnostic gene set was attempted. Patients with latent *M. tuberculosis* and other diseases (i.e., sarcoidosis, autoimmune infections, lung cancer) were compared to those with active *M. tuberculosis* using the available multicohort analysis framework. Following analysis, a three gene set out of 266 demonstrated significantly higher diagnostic accuracy for active vs. latent *M. tuberculosis* from whole blood. These 3 genes were *GBP5*, *DUSP3,* and *KLF2*. *GBP5* is a protein coding gene known to activate inflammasome assembly and reported to have a role in innate immunity and inflammation. Similarly, *DUSP3*, a protein phosphatase, and *KLF2* play a role in modulating innate immunity. This dataset distinguished active *M. tuberculosis* from healthy subjects with a sensitivity of 93% and a specificity of 97%. Such a gene set could potentially offer a framework for better diagnosis and treatment response to active *M. tuberculosis* (27).

In a similar study, published gene signatures for active *M. tuberculosis* diagnosis were identified using unbiased screens. Sixteen gene signatures were found. Twenty-four datasets containing 3,083 transcriptome profiles from whole and peripheral blood of healthy, active *M. tuberculosis*, latent *M. tuberculosis* and other diseases subjects were screened. A similar conclusion was made with the 3 signature genes (*GBP5*, *DUSP3,* and *KLF2*) described above demonstrating significant discrimination in identifying subjects with active *M. tuberculosis* and in predicting those with high risk of progression from latent to active *M. tuberculosis* with a sensitivity of 90%. These results demonstrated superiority over traditional sputum tests with a sensitivity of 53.3% (28).

This three-gene *M. tuberculosis* score was further tested in a cohort study for performance, not only as a diagnostic, but as an indicator for *M. tuberculosis* treatment response and on post-treatment residual inflammation. The three-gene *M. tuberculosis* score detected patients with active *M. tuberculosis* with a negative predictive value (NPV) of 99.3% at a prevalence of 4%. Additionally, with a sensitivity of 86% and a specificity of 84%, the three-gene mRNA expression score measured by qPCR or RNA sequencing showed accurate diagnosis of progression of

latent to active Tb with an 86% sensitivity and 84% specificity, 6 months earlier than traditional sputum conversion which has a lower sensitivity of 45–61% (41) (see **Table 2**).

Moreover, soluble protein biomarkers such as interferon-inducible protein 10 (IP-10) have shown high sensitivity (98%) and specificity (87%) for Tb infection with superior sensitivity compared to interferon gamma-based IGRA test (42). In fact, in a recent study of *M. tuberculosis* infection, the aim was to identify host biomarkers for discrimination between latent and active *M. tuberculosis*. Using PCR assays on serum and saliva samples from active *M. tuberculosis* patients and their contacts, numerous chemokines, cytokines, and growth factors were assessed. Results were favorable for differentiating latent and active *M. tuberculosis* using interferon-inducible protein 10 IP-10 and B-Cell attracting chemokine (BCA-1) in serum with an AUC of 0.83, specificity of 88% and sensitivity of 72%. Moreover, testing for IP-10 in saliva showed an AUC of 0.68, sensitivity of 52% and specificity of 68%. This provides additional insight on the role of host-response diagnostics on differentiating latent vs. active *M. tuberculosis* infections (43, 44).

## Host-Based Immunodiagnostics in Sepsis

Host immune-based diagnostics have also been studied in sepsis, a potentially life-threatening process in the setting of serious infections. Using MeSH terms for sepsis, host-response, and infections we have found 5 citations of studies.

The InSep test (previously mentioned in section "a") provides better insight to guide decision making. The host data, reflecting activation of immunity, can offer more real-time guidance for antimicrobial stewardship programs in management of appropriate antibiotic usage reduction of antimicrobial resistance and drug side effect. In addition, the rapid turnaround time allows for efficient diagnosis of sepsis along with determination of prognosis and disease severity (7, 8).

Multiple clustering analysis from host transcriptomics in a retrospective study of patients with bacterial sepsis revealed three robust clusters. These subtypes were derived from a unified clustering analysis across 14 discovery datasets. The three robust clusters were termed "Inflammopathic," "Coagulopathic," and "Adaptive." Such clusters represent the heterogeneity of sepsis, and each subtype is associated with different mortality rates and different clinical coagulopathy rates. The "Inflammopathic" cluster was associated with higher mortality and an innate immune activation; the "Coagulopathic" cluster was associated with higher mortality, older patients and evidence of coagulopathy, and the "Adaptive" cluster showed an association with lower mortality and adaptive immune activation. These results represent a broad definition of the host-response to sepsis (45).

In a similar manner, studies using single-cell RNA sequencing of peripheral blood from subjects with sepsis defined 16 immune cell states. Using monocytes and dendritic cells, the outcome attained was identification of a sepsis specific CD14+ monocyte state. This monocyte state has specific surface markers and ultimately demonstrates that use of single-cell RNA sequencing can lead to the identification of unique disease associated cytologic signatures in bacterial sepsis (46).

Sepsis is a process that is not just limited to the adult population; in fact, neonates are at increased risk for developing sepsis. The complexity and ambiguity of the neonatal immune response has made it difficult to diagnose infections. There is no single biomarker that has yet proven to perform with sufficient accuracy for ruling out pediatric sepsis. Using host whole blood expression for 11 gene (Sepsis MetaScore, company, city, state), pediatric patients with sepsis were evaluated. The Sepsis MetaScore showed higher accuracy in diagnosing sepsis among 3 cohorts of neonates from several different countries as compared to standard neonatal lab tests. The sensitivity and specificity were 95 and 60%, respectively, as compared to standard microbiological testing with a sensitivity of 70% for a leukocyte count>15,000 and <3,000, and a sensitivity of 90% for CRP>10 mg/L. As for adults, implementing such improved diagnostics would lead to less AMR as well as decreased neonatal mortality rates (47).

## Effect of Host-Based Diagnostics on Healthcare Cost and Public Health Measures

The impact of host-based diagnostics has also been studied economic and public health outcomes in four studies.

Host-based immunodiagnostics were used to examine high risk close contact exposures. Participants who were in proximity of patients diagnosed with a respiratory viral infection were recruited, and a blood based 36 gene RT-PCR assay as a transcriptomic biomarker was used in an attempt for early identification of viral infection. The results were promising and have shown that such an assay can serve as an accurate prediction for viral infection at both the time of maximum symptom severity as well as up to 3 days before symptoms arise when compared to definite viral infection confirmed by PCR. This transcriptomic assay predicted viral infection at the peak symptom severity with an AUROC of 0.94, at 1, 2, and 3 days before symptoms arise with an AUROC of 0.87, 0.85, and 0.74, respectively. This study was the first real-world study to show that a host gene expression-based assay can accurately predict a respiratory viral infection before typical symptoms are present (48).

From an economic point of view, HostDx™ Sepsis (Inflammatix, Inc., city, state), a multi-RNA host response expression platform, was compared to the standard of care including procalcitonin. Results showed substantial reduction of average cost estimated to be around a $1974 USD per patient. Excluding the cost of the test itself, this overall healthcare cost reduction was attributed to a shorter stay at the hospital, decrease mortality rates at 30 days and less antibiotics being prescribed (7, 49). Additionally, a decline in the number of blood cultures drawn can be achieved, as well as mechanical ventilation and ICU stay days.

Moreover, platforms utilizing two-gene transcript RNA signature translated to RT-LAMP can prove to be cost-effective (due to absence of fluorescent label) with an average assay cost of, $1.33 USD per chip (17).

## Integrating Host-Based Diagnostics With Pathogen-Based Testing for Improved Clinical Outcomes

Despite the recent rise attention on host-based diagnostics, pathogen-based diagnostics continue to be the gold standard and the most frequently used assays for infectious disease detection. Therefore, being able to integrate host-based with pathogen-based diagnostics for increased sensitivity and better outcomes is an area of active investigation.

In a prospective cohort study of critically ill patients with acute respiratory failure, a combination of three elements: pathogen, host gene expression signatures and the airway microbiome using a developed sequencing-based approach was studied. The hypothesis of the study states that the combination of host response testing with simultaneous detection of possible respiratory pathogens and measurement of lung microbiome diversity could serve as a more precise and accurate platform for infection. In the host-response, upregulation of pathways related to 414 expressed genes was shown in the LRTI patients. These sets of transcriptional signatures differentiated LRTI subjects from the non-LRTI group which showed another set of upregulated pathways. On the other hand, the LRTI prediction using pathogen diagnostics was based on a logistic regression model. A logistic regression model microbial score was derived to classify subjects as having lower respiratory tract infection or not. The third element was lung microbiome diversity, and the rationale based on several studies is that a reduction in the diversity of the airway microbiome occurs in the setting of an active infection. This diversity was denoted by α and was measured using a diversity index using RNA-sequencing which showed more diversity for LRTI than non-LRTI enrolled patients.

Metagenomics next generation sequencing was next applied to integrate these three core elements. mNGS was used to identify microbial species. However, the presence of bacterial components in a blood specimen does not necessarily explain the cause of the patient's disease due to possibility of contamination or translocation of commensal bacteria to the bloodstream. In a similar manner, viral sequencing can detect clinically irrelevant or latent viruses in the bloodstream and thus would not explain the patient's disease. Therefore, complementing mNGS that detect microbes with host RNA transcript-based profiling using RNA signatures can provide better results in detecting infected patients, differentiating bacterial vs. viral infections.

The results of this integration resulted in a 36% reduction in antibiotics use, higher accuracy for identifying LRTI positive patients as compared to the standard of care. The detection of pathogens otherwise not usually tested for using classic viral PCR assays (i.e., influenzae C). The specificity and sensitivity of this assay were 87.5 and 100%, respectively. Therefore, the results of this study suggested using an integration protocol for these three elements of LRTI can operate as a promising and superior tool in the management and outcomes of LRTI patients (50–52).

Similarly, integrating mNGS for detecting bacterial DNA, host response profiling using previously defined host response transcript signatures and viral capture sequencing was performed in a prospective study of 200 patients enrolled from the ED with suspected sepsis. Study results show that each of the 3 techniques used showed an improvement of diagnosis of sepsis, and when used in combination, an even better improvement in diagnosis and management of sepsis was noted. One notable result of this study was that host response profiling led physicians to change their diagnostic decisions in 46 out of 100 patients highlighting the impact of host response profiling in the management of patients with suspected sepsis (52).

## Other Diagnostic Methods

Finally, the focus of this review is molecular assays based on the host immune response, although it is noteworthy to mention that advances in specific imaging modalities utilizing "omics" technology have contributed to improved microbial detection. A major step in the technological progress may be the implementation of 7T MRI imaging to investigate microbiological processes by sampling parameters of cell and tissue metabolism that are dynamic and subject to changes within certain cellular conditions such as infections (53).

# DISCUSSION

A dynamic and temporal relationship between infectious processes and the host-immune response has been described in this review. Taking into consideration the impact of the host-response, attempts of using it as a reference for applying a more individualized approach of precision medicine has become the focus of many research studies. Using advanced assays that include RT-PCR, single cell RNA sequencing, mNGS, microarrays and RT-LAMP were reviewed and show high levels of accuracy compared to gold standard. Host-gene signatures, transcriptomics, proteomics, and expressed biomarkers used demonstrate promising results for a systematic integration of host immunodiagnostics with conventional microbial detection for improved management of infectious diseases. Host-based response may serve to be an alternative of the traditional time-consuming microbiological assays. However, a more holistic approach would be the integration of both host and pathogen-based diagnostics into one single platform. Future studies and clinical trials will be required to measure the true impact of combining these approaches.

One of the most important uses of the host-response as a tool for improving diagnostics has been the focus on the discrimination between bacterial and viral infections. Several studies were described in this review article that allow for the accurate discrimination of bacterial vs. viral etiologies in suspected infection. In fact, potential results of host-based diagnostics in this matter can achieve the WHO goal of ending tuberculosis in 2,035 if correctly implemented for superior pathogen diagnosis (27).

Accurate and rapid discrimination between bacterial and viral infections can also direct management by permitting proper antibiotics usage and prescription in a timely and directed manner. Ultimately, the improved patient outcome with higher and more rapid cure rates may translate into decreased mortality rate, healthcare costs for prolonged hospital stay, and the decrease in antibiotics misuse.

Host-based diagnostics have also shown major success in the diagnosis of sepsis. Considered a life-threatening process, sepsis calls for immediate life-saving intervention measures. Applying host-based diagnostics was shown to assist with the determination of the underlying etiology of sepsis as well as providing insight on the severity and prognosis.

Another important manifestation of host-immune diagnostics that has been highlighted in this review is the ability to distinguish latent infection from active infection as well as predicting the progression from latent to active infection at an earlier stage than standard microbiological tests. This should be an important aspect for future consideration that may necessitate a different approach with latent infections' management and prognosis.

Additionally, host gene signatures contribute to identification of treatment response over elapsed time as well as disease progression. This ability to measure response can prove to play an important role in determining staging of an infectious disease, its severity and its response to treatment.

This review also highlighted the potential of host-microbiota signatures to provide a perception of the severity and prognosis of certain infections. Although further future validation is required, such a link could facilitate the implementation of assays using microbial signatures to prognosticate respiratory infections concurrently with diagnostics for such infections.

From an economic perspective, host-based diagnostics may significantly reduce healthcare costs. Through improved definition of host response, more sensible use of antibiotics will ultimately lead to a reduction in the drug cost as well as antibiotic administration. Moreover, improved accuracy will likely lead to a decrease in the usage of consultation services as well as excessive procedures and laboratory tests being ordered (e.g., interventional radiology procedures, inflammatory markers, tumor markers, biopsies). These interventions may result in an overall decrease in cost on the individualized patient level and on the overall healthcare industry, although additional clinical trials will be required. In future applications, immunodiagnostics, unlike pathogen-based testing, may present the capability of differentiating non-infectious immune triggers including sterile inflammatory processes, autoimmune diseases, or malignancy. Further improvement in the currently existing platforms is required before such a claim can be translated into clinical practice and to possibly supersede and replace standard pathological techniques for such non-infectious causes.

One other advantage for host-response diagnostics as compared to pathogen-based diagnostics arises from the ability of viruses to mutate at a fast rate with emergence of different variants. Some RNA viruses can have a mutation rate up to a million times higher than their hosts and can incorporate mutated nucleotides at a rate of $10^{-6}$-$10^{-4}$ substitutions per nucleotide per cell infection (54). This ability of viruses to rapidly mutate and transfer between hosts imposes a limitation for their detection and requires the development of dynamic means to detect current and emergent viral strains. Using the host as the diagnostic subject overcomes this limitation and proves yet another firm basis for adopting such methods.

Finally, host-based diagnostics can help resolve multiple public health issues. A major effect of adopting more recent host-based diagnostics is preventing further AMR which is one of the most serious global public health threats. By providing accurate diagnostic outcomes, more precise and targeted therapies could be applied, thus, reducing the risk antibiotic overuse and the emergence of AMR. At a hospital, country or global scale, host-response diagnostics may also play a role in the rapid identification of exposure which can result in containment and improved infection control measures, especially in the setting of epidemics and/or pandemics. Several studies have shown more rapid results of testing the host response for infectious processes than traditional microbiology assays. This approach has proven to be essential in the case of viral infections with long incubation periods and those characterized with pre-symptomatic yet highly contagious phases. Using such assays could prove to help with infection containment during viral pandemics or influenza season. The early detection of the nature of an infectious disease would help aid determining which patients require early quarantine, and this would ultimately be reflected as better patient care during possible pandemics such as COVID-19 (7). Detecting such affected individuals will help in the quarantine process and put a limit for the transmission of diseases. The COVID-19 pandemic has uncovered the severe lack of means and the desperate need of public health measures that deal with phenomena of such impact and scale (see **Figure 1**).

## POTENTIAL DOWNFALLS

As with other assays, host-based diagnostics have shortcomings. An important limitation in multiple studies is lack of adequate sample size and concern for appropriate power resulting in a possible increase in the margin of error. Larger cohorts in prospective studies are required to improve the robustness of study performance estimates.

Another limitation is the absence of special populations including immunocompromised hosts such as solid organ, stem cell transplant recipients and those individuals with autoimmune disorders. These patients are at risk for expanded infections including invasive fungal pathogens, which are not represented in current studies and require future investigation.

Among the drawbacks of host response-based diagnostics is the lack of precise identification of the pathogen involved. This prevents directed and specific treatment of the causative agent (19). Moreover, despite promising outcomes in differentiating bacterial vs. viral infections and thus limiting the use of antibiotics in case of viral infections, the lack of precise identification of the causative pathogen and ultimately the lack of isolation of such pathogen in the case of bacterial infection prevents the assessment of its sensitivity to antibiotics. This would impose a limitation to reducing antimicrobial resistance.

Cost and technical limitations exist to these assays. For RNA-sequencing techniques, high cost are major barriers to adoption, specifically in areas with limited resources. The development of inexpensive platforms would improve the prospects of more rapid utilization in

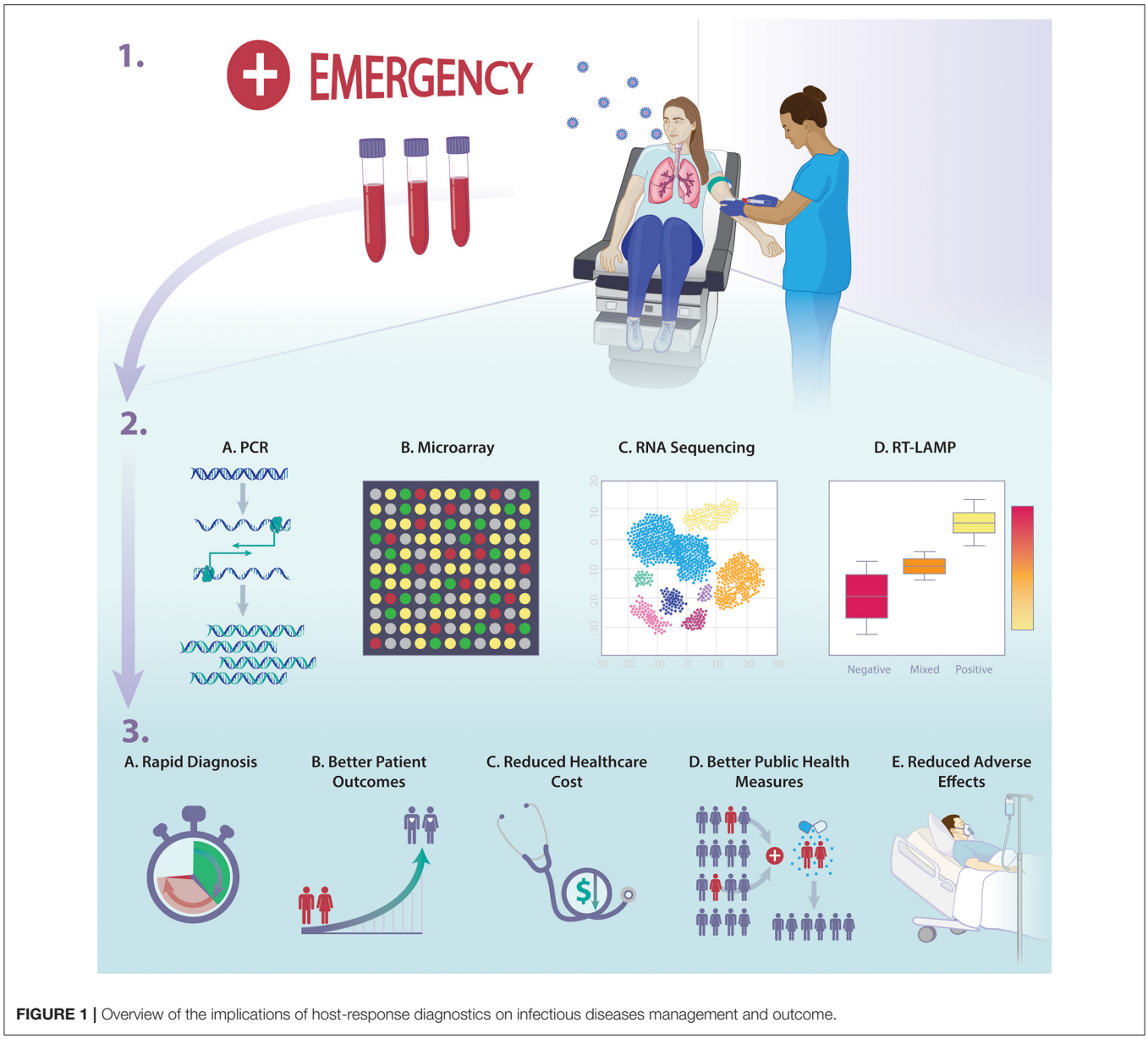


**FIGURE 1 |** Overview of the implications of host-response diagnostics on infectious diseases management and outcome.

healthcare setting. Additionally, some platforms are tuned to specific set of biomarkers, which make generalizability for detection of other diseases potentially difficult. Finally, microarrays are currently far too time-consuming with a turnaround time of about 1–2 weeks to be applied in a clinical setting (55). Thus, further laboratory validation should be attained before any of these assays can be used in clinical settings.

## CONCLUSION

This review describes multiple aspects of host-based response diagnostics as an adjunct to pathogen-based diagnostics and not as a replacement. However, favorable outcomes show that there are advantages of using host-based diagnostics as compared to pathogen-based diagnostics. Over 30 trials have focused on the use of host-response diagnostics for improved diagnosis of acute infection. Rapid and accurate diagnosis and prognosis can result in reduced healthcare costs, fewer adverse effects, reduction in antibiotic misuse and lower rates of antimicrobial resistance, improvement in public health measures for rapidly spreading endemics and pandemics, and ultimately better management with positive patient outcomes are potentials of adopting host immunodiagnostics. However, there remains some pitfalls including accessibility, cost, laboratory practicality and further clinical validation. While host immunodiagnostics show excellent promise, further investigations are needed to define the

possible implications of adopting these novel modalities for the advancement in the field of infectious diseases.

## AUTHOR CONTRIBUTIONS

JA drafted the original manuscript, responsible for article curation, and investigation. JA and MM revised and edited the draft. MM supervised and validated the final product. All authors gave final approval of this version to be published and agreed to be guarantor of the work.

## FUNDING

This work was supported, in part, by grants from the National Institute of Allergy and Infectious Diseases (RO1 AI132638) to MM.

## REFERENCES

1. Ramilo O, Mejias A. Host transcriptomics for diagnosis of infectious diseases: one step closer to clinical application. *Eur Respir J.* (2017) 49:1700993. doi: 10.1183/13993003.00993-2017
2. Sweeney TE, Khatri P. Generalizable biomarkers in critical care. *Crit Care Med.* (2017) 45:934–9. doi: 10.1097/CCM.0000000000002402
3. Ross MH, Zick BL, Tsalik EL. Host-based diagnostics for acute respiratory infections. *Clin Ther.* (2019) 41:1923–38. doi: 10.1016/j.clinthera.2019.06.007
4. de Jonge JC, de Lange DW, de Vaate EAB, van Leeuwen H, Arends JE. [Procalcitonin as biomarker for infections]. *Ned Tijdschr Genees.* (2016) 160:D282. doi: 10.3904/kjim.2013.28.3.285
5. Tsalik EL, Henao R, Montgomery JL, Nawrocki JW, Aydin M, Lydon EC, et al. Discriminating bacterial and viral infection using a rapid host gene expression test*. *Crit Care Med.* (2021) 49:1651–63. doi: 10.1097/CCM.0000000000005085
6. Tsalik EL, Henao R, Aydin M, Bullard C, Montgomery J, Nawrocki J, et al. 2012 FilmArray® measurement of host response signatures rapidly discriminates viral, bacterial, and non-infectious etiologies of illness. *Open Forum Infect Dis.* (2018) 5:S586. doi: 10.1093/ofid/ofy210.1668
7. Ducharme J, Self WH, Osborn TM, Ledeboer NA, Romanowsky J, Sweeney TE, et al. A multi-mRNA host-response molecular blood test for the diagnosis and prognosis of acute infections and sepsis: proceedings from a clinical advisory panel. *J Personalized Med.* (2020) 10:266. doi: 10.3390/jpm10040266
8. Safarika A, Wacker JW, Katsaros K, Solomonidi N, Giannikopoulos G, Kotsaki A, et al. A 29-mRNA host response test from blood accurately distinguishes bacterial and viral infections among emergency department patients. *Intensive Care Med Exp.* (2020) 8:31. doi: 10.21203/rs.3.rs-128429/v1
9. Mayhew MB. A generalizable 29-mRNA neural-network classifier for acute bacterial and viral infections. *Nat Commun.* (2020) 11:1117. doi: 10.1038/s41467-020-14975-w
10. Bauer W, Kappert K, Galtung N, Lehmann D, Wacker J, Cheng HK, et al. A novel 29-messenger RNA host-response assay from whole blood accurately identifies bacterial and viral infections in patients presenting to the emergency department with suspected infections: a prospective observational study*. *Crit Care Med.* (2021) 49:1664–73. doi: 10.1097/CCM.0000000000005119
11. Sweeney TE, Wong HR, Khatri P. Robust classification of bacterial and viral infections via integrated host gene expression diagnostics. *Sci Transl Med.* (2016) 8:346ra91. doi: 10.1126/scitranslmed.aaf7165
12. Liu L, Oza S, Hogan D, Chu Y, Perin J, Zhu J, et al. Global, regional, and national causes of under-5 mortality in 2000-15: an updated systematic analysis with implications for the Sustainable Development Goals. *Lancet Lond Engl.* (2016) 388:3027–35. doi: 10.1016/S0140-6736(16)31593-8
13. Mahajan P, Kuppermann N, Mejias A, Suarez N, Chaussabel D, Casper TC, et al. Association of RNA biosignatures with bacterial infections in febrile infants aged 60 days or younger. *JAMA.* (2016) 316:846–57. doi: 10.1001/jama.2016.9207
14. Gómez-Carballa A, Cebey-López M, Pardo-Seco J, Barral-Arca R, Rivero-Calle I, Pischedda S, et al. A qPCR expression assay of IFI44L gene differentiates viral from bacterial infections in febrile children. *Sci Rep-uk.* (2019) 9:11780. doi: 10.1038/s41598-019-48162-9
15. Herberg JA, Kaforou M, Wright VJ, Shailes H, Eleftherohorinou H, Hoggart CJ, et al. Diagnostic test accuracy of a 2-transcript host RNA signature for discriminating bacterial vs viral infection in febrile children. *JAMA.* (2016) 316:835–45. doi: 10.1001/jama.2016.11236
16. Kaforou M, Herberg JA, Wright VJ, Coin LJM, Levin M. Diagnosis of bacterial infection using a 2-transcript host RNA signature in febrile infants 60 days or younger. *JAMA.* (2017) 317:1577–8. doi: 10.1001/jama.2017.1365
17. Pennisi I, Rodriguez-Manzano J, Moniri A, Kaforou M, Herberg JA, Levin M, et al. Translation of a host blood RNA signature distinguishing bacterial from viral infection into a platform suitable for development as a point-of-care test. *JAMA Pediatr.* (2021) 175:417–9. doi: 10.1001/jamapediatrics.2020.5227
18. Langevin S, Pichon M, Smith E, Morrison J, Bent Z, Green R, et al. Early nasopharyngeal microbial signature associated with severe influenza in children: a retrospective pilot study. *J Gen Virol.* (2017) 98:2425–37. doi: 10.1099/jgv.0.000920
19. Bhattacharya S, Rosenberg AF, Peterson DR, et al. Transcriptomic biomarkers to discriminate bacterial from nonbacterial infection in adults hospitalized with respiratory illness. *Sci Rep-uk.* (2017) 7:6548. doi: 10.1038/s41598-017-06738-3
20. Chen H, Yin Y, Gao H, Guo Y, Dong Z, Wang X, et al. Clinical utility of in-house metagenomic next-generation sequencing for the diagnosis of lower respiratory tract infections and analysis of the host immune response. *Clin Infect Dis.* (2020) 71:S416–26. doi: 10.1093/cid/ciaa1516
21. Saeed K, Legramante JM, Angeletti S, Curcio F, Miguens I, Poole S, et al. Mid-regional pro-adrenomedullin as a supplementary tool to clinical parameters in cases of suspicion of infection in the emergency department. *Expert Rev Mol Diagn.* (2021) 21:1–8. doi: 10.1080/14737159.2021.1902312
22. Saleh MAA, van de Garde EMW, van Hasselt CJG. Host-response biomarkers for the diagnosis of bacterial respiratory tract infections. *Clin Chem Lab Med Cclm.* (2019) 57:442–51. doi: 10.1515/cclm-2018-0682
23. Li HK, Kaforou M, Rodriguez-Manzano J, Channon-Wells S, Moniri A, Habgood-Coote D, et al. Discovery and validation of a three-gene signature to distinguish COVID-19 and other viral infections in emergency infectious disease presentations: a case-control and observational cohort study. *Lancet Microbe.* (2021) 2:e594–603. doi: 10.1016/S2666-5247(21)00145-2
24. McClain MT, Nicholson BP, Park LP, Liu TY, Hero AO, Tsalik EL, et al. A genomic signature of influenza infection shows potential for presymptomatic detection, guiding early therapy, and monitoring clinical responses. *Open Forum Infect Dis.* (2016) 3:ofw007. doi: 10.1093/ofid/ofw007
25. Tang BM, Shojaei M, Parnell GP, Huang S, Nalos M, Teoh S, et al. A novel immune biomarker IFI27 discriminates between influenza and bacteria in patients with suspected respiratory infection. *Eur Respir J.* (2017) 49:1602098. doi: 10.1183/13993003.02098-2016
26. Barral-Arca R, Gómez-Carballa A, Cebey-López M, Bello X, Martinón-Torres F, Salas A. A meta-analysis of multiple whole blood gene expression data unveils a diagnostic host-response transcript signature for respiratory syncytial virus. *Int J Mol Sci.* (2020) 21:1831. doi: 10.3390/ijms21051831
27. Sweeney TE, Braviak L, Tato CM, Khatri P. Genome-wide expression for diagnosis of pulmonary tuberculosis: a multicohort analysis. *Lancet Respir Med.* (2016) 4:213–24. doi: 10.1016/S2213-2600(16)00048-5
28. Warsinske H, Vashisht R, Khatri P. Host-response-based gene signatures for tuberculosis diagnosis: A systematic comparison of 16 signatures. *PLoS Med.* (2019) 16:e1002786. doi: 10.1371/journal.pmed.1002786
29. Rossi ÁD, de Araújo JLF, de Almeida TB, Ribeiro-Alves M, de Almeida Velozo C. Association between ACE2 and TMPRSS2 nasopharyngeal expression and COVID-19 respiratory distress. *Sci Rep-uk.* (2021) 11:9658. doi: 10.1038/s41598-021-88944-8
30. Alcoba G, Manzano S, Lacroix L, Galetto-Lacour A, Gervaix A. Proadrenomedullin and copeptin in pediatric pneumonia: a

prospective diagnostic accuracy study. *BMC Infect Dis.* (2015) 15:347. doi: 10.1186/s12879-015-1095-5
31. Legramante JM, Mastropasqua M, Susi B, Porzio O, Mazza M, Miranda Agrippino G, et al. Prognostic performance of MR-pro-adrenomedullin in patients with community acquired pneumonia in the Emergency Department compared to clinical severity scores PSI and CURB. *PLoS ONE.* (2017) 12:e0187702. doi: 10.1371/journal.pone.0187702
32. Konings F, Perkins MD, Kuhn JH, Pallen MJ, Alm EJ, Archer BN, et al. SARS-CoV-2 Variants of Interest and Concern naming scheme conducive for global discourse. *Nat Microbiol.* (2021) 6:821–3. doi: 10.1038/s41564-021-00932-w
33. Ng DL, Granados AC, Santos YA, Servellita V, Goldgof GM, Meydan C, et al. A diagnostic host response biosignature for COVID-19 from RNA profiling of nasal swabs and blood. *Sci Adv.* (2021) 7:eabe5984. doi: 10.1126/sciadv.abe5984
34. Dangi T, Jain A. Influenza virus: a brief overview. *Proc Nat Acad Sci India Sect B Biol Sci.* (2012) 82:111–21. doi: 10.1007/s40011-011-0009-6
35. Gao J, Zhu X, Wu M, Jiang L, Wang F, He S. IFI27 may predict and evaluate the severity of respiratory syncytial virus infection in preterm infants. (2020) *Hereditas.* 158:1–14. doi: 10.21203/rs.3.rs-42880/v3
36. Shojaei M, Shamshirian A, Monkman J, Grice L, Tran M. IFI27 transcription is an early predictor for COVID-19 outcomes; a multi-cohort observational study. *Medrxiv.* (2021) 2021:10.29.21265555. doi: 10.1101/2021.10.29.21265555
37. Li Y, Liu H, Xu Q, Wu R, Zhang Y, Li N, et al. OASL as a diagnostic marker for influenza infection revealed by integrative bioinformatics analysis with XGBoost. *Front Bioeng Biotechnol.* (2020) 8:729. doi: 10.3389/fbioe.2020.00729
38. de Steenhuijsen Piters WA, Heinonen S, Hasrat R, Bunsow E, Smith B, Suarez-Arrabal MC, et al. Nasopharyngeal microbiota, host transcriptome, and disease severity in children with respiratory syncytial virus infection. *Am J Resp Crit Care.* (2016) 194:1104–15. doi: 10.1164/rccm.201602-0220OC
39. Dunning J, Blankley S, Hoang LT, Cox M, Graham CM, James PL, et al. Progression of whole-blood transcriptional signatures from interferon-induced to neutrophil-associated patterns in severe influenza. *Nat Immunol.* (2018) 19:625–35. doi: 10.1038/s41590-018-0111-5
40. Burel JG, Babor M, Pomaznoy M, Lindestam Arlehamn CS, Khan N, Sette A, et al. Host transcriptomics as a tool to identify diagnostic and mechanistic immune signatures of tuberculosis. *Front Immunol.* (2019) 10:221. doi: 10.3389/fimmu.2019.00221
41. Warsinske HC, Rao AM, Moreira FMF, Santos PCP, Liu AB, Scott M, et al. Assessment of validity of a blood-based 3-gene signature score for progression and diagnosis of tuberculosis, disease severity, and treatment response. *JAMA Netw Open.* (2018) 1:e183779. doi: 10.1001/jamanetworkopen.2018.3779
42. Blauenfeldt T, Villar-Hernández R, García-García E, Latorre I, Holm LL, Muriel-Moreno B, et al. Diagnostic accuracy of interferon gamma-induced protein 10 mRNA release assay for tuberculosis. *J Clin Microbiol.* (2020) 58:10. doi: 10.1128/JCM.00848-20
43. Estévez O, Anibarro L, Garet E, Pallares Á, Pena A, Villaverde C, et al. Identification of candidate host serum and saliva biomarkers for a better diagnosis of active and latent tuberculosis infection. *PLoS ONE.* (2020) 15:e0235859. doi: 10.1371/journal.pone.025859
44. Estévez O, Anibarro L, Garet E, Pallares Á, Barcia L, Calviño L, et al. An RNA-seq based machine learning approach identifies latent tuberculosis patients with an active tuberculosis profile. *Front Immunol.* (2020) 11:1470. doi: 10.3389/fimmu.2020.01470
45. Sweeney TE, Azad TD, Donato M, Haynes WA, Perumal TM, Henao R, et al. Unsupervised analysis of transcriptomics in bacterial sepsis across multiple datasets reveals three robust clusters. *Crit Care Med.* (2018) 46:915–25. doi: 10.1097/CCM.0000000000003084
46. Reyes M, Filbin MR, Bhattacharyya RP, Billman K, Eisenhaure T, Hung DT, et al. An immune-cell signature of bacterial sepsis. *Nat Med.* (2020) 26:333–40. doi: 10.1038/s41591-020-0752-4
47. Sweeney TE, Wynn JL, Cernada M, Serna E, Wong HR, Baker HV, et al. Validation of the sepsis metascore for diagnosis of neonatal sepsis. *J Pediatric Infect Dis Soc.* (2017) 7:129–35. doi: 10.1093/jpids/pix021
48. McClain MT, Constantine FJ. A blood-based host gene expression assay for early detection of respiratory viral infection: an index-cluster prospective cohort study. *Lancet Infect Dis.* (2021) 21:396–404. doi: 10.1016/S1473-3099(20)30486-2
49. Schneider JE, Romanowsky J, Schuetz P, Stojanovic I, Cheng HK, Liesenfeld O, et al. Cost impact model of a novel multi-mRNA host response assay for diagnosis and risk assessment of acute respiratory tract infections and sepsis in the emergency department. *J Heal Econ Outcomes Res.* (2020) 7:24–34. doi: 10.36469/jheor.2020.12637
50. Langelier C, Kalantar KL, Moazed F, Wilson MR, Crawford ED, Deiss T, et al. Integrating host response and unbiased microbe detection for lower respiratory tract infection diagnosis in critically ill adults. *Proc National Acad Sci USA.* (2018) 115:201809700. doi: 10.1101/341149
51. Penaranda C, Hung DT. Single-cell RNA sequencing to understand host-pathogen interactions. *Acs Infect Dis.* (2019) 5:336–44. doi: 10.1021/acsinfecdis.8b00369
52. Cheng HK. Combined use of metagenomic sequencing and host response profiling for the diagnosis of suspected sepsis. *Biorxiv.* (2019) 2019:854182. doi: 10.1101/854182
53. Hoerr V, Faber C. Magnetic resonance imaging characterization of microbial infections. *J Pharmaceut Biomed.* (2014) 93:136–46. doi: 10.1016/j.jpba.2013.10.034
54. Cassedy A, Parle-McDermott A, O'Kennedy R. Virus detection: a review of the current and emerging molecular and immunological methods. *Front Mol Biosci.* (2021) 8:637559. doi: 10.3389/fmolb.2021.637559
55. Savage MS, Mourad MJ, Wapner RJ. Evolving applications of microarray analysis in prenatal diagnosis. *Curr Opin Obstetrics Gynecol.* (2011) 23:103–8. doi: 10.1097/GCO.0b013e32834457c7

**Conflict of Interest:** MM reports consultation fees from Safi Biosolutions, Clear Creek Bio, Vericel, NED biosystems, GenMark Diagnostics, and Day Zero Diagnostics; grant support from Thermo Fisher Scientific and Genentech; medical editing/writing fees from UpToDate, outside the submitted work. MM also reports patents 14/110,443 and 15/999,463 pending.

The remaining author declares that the research was conducted in the absence of any commercial or financial relationships that could be construed as a potential conflict of interest.

**Publisher's Note:** All claims expressed in this article are solely those of the authors and do not necessarily represent those of their affiliated organizations, or those of the publisher, the editors and the reviewers. Any product that may be evaluated in this article, or claim that may be made by its manufacturer, is not guaranteed or endorsed by the publisher.

frontiers in Medicine

ORIGINAL RESEARCH
published: 14 February 2022
doi: 10.3389/fmed.2022.811639

# Genetic Variations of ALDH (rs671) Are Associated With the Persistence of HBV Infection Among the Chinese Han Population

*Dabao Shang[1,2†], Peng Wang[1,3†], Weiliang Tang[1,2†], Ruidong Mo[1,2], Rongtao Lai[1,2], Jie Lu[1,2], Ziqiang Li[1,2], Xiaolin Wang[1,2], Wei Cai[1,2], Hui Wang[1,2], Gangde Zhao[1,2*], Qing Xie[1,2*] and Xiaogang Xiang[1,2*]*

[1] Department of Infectious Diseases, Ruijin Hospital, Shanghai Jiaotong University School of Medicine, Shanghai, China, [2] Translational Laboratory of Liver Diseases, Department of Infectious Diseases, Ruijin Hospital, Shanghai Jiaotong University School of Medicine, Shanghai, China, [3] Department of Hepatobiliary Medicine, Eastern Hepatobiliary Surgery Hospital, Naval Medical University, Shanghai, China

OPEN ACCESS

**Edited by:**
*Shisan Bao,*
*The University of Sydney, Australia*

**Reviewed by:**
*Yiguang Lin,*
*University of Technology Sydney, Australia*
*Brett David Hambly,*
*Torrens University Australia, Australia*

***Correspondence:**
*Gangde Zhao*
*zhaogd1016@foxmail.com*
*Qing Xie*
*xieqingrjh@163.com*
*Xiaogang Xiang*
*shine-xxg@163.com*

*[†]These authors have contributed equally to this work*

**Specialty section:**
*This article was submitted to Infectious Diseases – Surveillance, Prevention and Treatment, a section of the journal Frontiers in Medicine*

**Received:** *09 November 2021*
**Accepted:** *10 January 2022*
**Published:** *14 February 2022*

**Citation:**
*Shang D, Wang P, Tang W, Mo R, Lai R, Lu J, Li Z, Wang X, Cai W, Wang H, Zhao G, Xie Q and Xiang X (2022) Genetic Variations of ALDH (rs671) Are Associated With the Persistence of HBV Infection Among the Chinese Han Population. Front. Med. 9:811639. doi: 10.3389/fmed.2022.811639*

Alcohol dehydrogenase 1B (ADH1B) and aldehyde dehydrogenase 2 (ALDH2), members of the alcohol dehydrogenase family, have important roles in liver diseases. The roles of the polymorphisms of ADH1B rs1229984 and ALDH2 rs671 in hepatitis B virus (HBV) susceptibility and persistent infection were investigated in the present study. Total 1,034 patients with hepatitis B [99 acute hepatitis B (AHB), 521 chronic hepatitis B (CHB), 158 acute-on-chronic liver failure (ACLF), 159 liver cirrhosis (LC), and 97 hepatocellular carcinoma (HCC)] and 1,262 healthy controls (HCs) of the Chinese Han population were recruited, and single nucleotide polymorphisms (SNPs) of rs671 and rs1229984 were genotyped. Independent and joint roles of rs671 and rs1229984 in HBV infection were analyzed. The results showed that rs671 genotypes had a significantly different distribution among different subgroups. Compared with HCs, the frequency of rs671-AA genotype was higher in hepatitis B individuals, especially in the CHB group [adjusted OR (95%CI) = 1.899 (1.232–2.928), $p = 0.003$, in the co-dominant model], which showed a significant positive association. It was further confirmed that CHB individuals who carried ALDH2 rs671-AA genotype had a higher risk of persistent HBV infection and higher HBV-DNA quantitation compared with those with GG/GA genotype. In addition, the rs671-AA genotype might predict HCC incidence in patients with CHB. There were no different distributions of alleles or genotypes in rs671 mutant among AHB, ACLF, LC, or HCC groups compared with HCs. These data suggested the possible hazardous role of rs671-AA variant in HBV infection and persistence.

**Keywords: HBV, rs671, ALDH, polymorphism, association study**

## INTRODUCTION

Chronic hepatitis B (CHB) remains an important global health challenge due to high morbidity (∼240 million hepatitis B virus (HBV) surface antigen carriers) (1) and mortality (7,86,000 people die each year from related complications) (2). The prevalence of HBV infection is still very high at about 7.18% in China, though huge improvements have been achieved *via* universal vaccination

programs and effective antiviral treatments (3). Patients with chronic HBV infection have about a 10-fold higher incidence of hepatocellular carcinoma (HCC) and liver-related mortality than those without HBV infection (4). HBV infection is still a critical public health burden worldwide due to limited curable therapeutic options for HBV-related HCC and liver cirrhosis/failure.

It has been reported that HBV can enhance its DNA replication through the autophagy pathway mediated by HBV × protein (5, 6). Adenosine monophosphate-activated protein kinase (AMPK) is a crucial energy sensor in macroautophagy/autophagy and can restrict HBV replication through the promotion of autophagic degradation (7). The persistent activation of autophagy in hepatocytes during HBV infection might influence the persistence of HBV infection (8). This indicates that certain genes in the human body may have an impact on HBV infection.

Alcohol dehydrogenase 1B (ADH1B) and aldehyde dehydrogenase 2 (ALDH2), members of the alcohol dehydrogenase family, are crucial enzymes for alcohol metabolism (9). Recently, multiple studies have suggested that ALDH2 is involved in the course of autophagy in a variety of liver diseases. ALDH2 may inhibit metastasis in HCC cells by regulating the AMPK signaling pathway (10) and also ameliorate chronic alcohol-induced hepatic steatosis and inflammation through up-regulation of the autophagy pathway (11). The ALDH2 rs671 (Glu504Lys) mutant, a common missense mutation in the ALDH2 gene (12), has been found to increase protein turnover and promote hepatocarcinogenesis *in vivo* (13). Moreover, individuals with the ALDH2 rs671-AA genotype exhibit severely decreased activity of the ALDH2 enzyme and an elevated level of gamma-glutamyl transpeptidase (GGT) in patients with non-alcoholic fatty liver disease (NAFLD) (14), indicating that the polymorphism of ALDH2 might have an important influence on liver diseases.

However, there have been no studies focused on the relationship between ALDH2 rs671 mutant and HBV infection to date, and the role of the ALDH2 rs671 polymorphism in the pathogenesis of HBV infection. Therefore, the present study investigated the association and clinical relevance of ALDH2 polymorphisms with respect to HBV susceptibility and persistence in the Chinese Han population.

# METHODS

## Subjects

A total cohort of 1,034 patients with HBV infection in the Southeastern China region was recruited from June 2011 to December 2014 in the Department of Infectious Diseases, Ruijin Hospital, Shanghai Jiaotong University School of Medicine. The Ethnically and geographically matched 1,262 HCs for a routine checkup were recruited from the Center of Health Examination of Ruijin Hospital in the same period.

The diagnosis of CHB was established by seropositivity of hepatitis B surface antigen (HBsAg) over 6 months according to the Chinese guideline of prevention and treatment for CHB (2010 version) (15) and did not have any other type of liver diseases, such as chronic hepatitis C, hepatitis D, hepatitis E, drug-induced liver diseases, and alcoholic or autoimmune liver disease. All participants were identified as Han Chinese. The demographic information included gender, age, birthplace, and past and current residency. The clinic data were collected from clinical records and/or telephone interviews. The study is approved by the Ethics Committee of Shanghai Ruijin Hospital, School of Medicine, Shanghai Jiaotong University in accordance with the Helsinki Declaration. The characteristics of AHB, CHB, LC, HCC, and HC are presented in **Table 1**.

## Single Nucleotide Polymorphism Selection

Single nucleotide polymorphisms were selected using HapMap Data Rel 27 Phase II+III, February 2009, on NCBI B36 assembly, dbSNP b126 of Han Chinese Beijing (http://hapmap.ncbi.nlm.nih.gov/) and Haploview software 4.2 (Mark Daly's Lab of Broad Institute, Cambridge, MA, USA). The criteria used for the SNP selection were population-frequency and multiple, high-profile or inconsistent submitters. The core criterion was determined based on the alteration of ADH1B and ALDH2 transcription, translation, or function. Two SNPs (rs1229984 and rs671) were finally selected for the evaluation.

## Genomic DNA Extraction

Genomic DNA was extracted from 5 ml venous blood, using the DNA Extraction Kit (Tiangen Biotech Co., Ltd., Beijing, China) according to the manufacturer's instructions. After the determination of genomic DNA concentration, the samples were stored at −80°C until genetic polymorphism analyses.

## Genotyping

Rs671 was identified in the region of the ALDH2 gene on chromosome 12 (location on 111803962). Rs1229984 was identified in the region of the ADH1B gene on chromosome 4 (location on 99318162). SNP ID numbers and sequence are available at http://www.ncbi.nlm.nih.gov/snp/ (**Supplementary Table 1**). The primers used for the corresponding SNP PCR amplification and SNaPshot extension reactions were designed using the Primer 5 software (**Supplementary Table 1**). SNPs were confirmed by multiplex SNaPshot technology as previously described (16) using an ABI fluorescence-based assay allelic discrimination method (Applied Biosystems, Bedford, MA, USA).

The PCR was performed as described previously (17). Briefly, in a total volume of 20 μl containing 1×ExTaq 0.2 μl, 25 Mm $MgCl_2$ 2 μl, 25 mM dNTP mix 2 μl, (TaKaRa Bio, Dalian, China), 2 μl genomic DNA, and 4 μl of each primer. The PCR product was purified by 1 U shrimp alkaline phosphatase (SAP) and 1 U Exonuclease I. The product was processed according to the ABI SNaPshot protocol. The extension was performed in a total volume of 10 μl containing 5 μl SNaPshot Multiplex Kit (ABI), 2 μl PCR product, 1 μl mixed extension primer, and 2 μl $H_2O$. The samples were put through 28 cycles of denaturation at 96°C, annealing at 50°C, elongation at 60°C, and a final

**TABLE 1 |** Demographic and clinical features of the patients and healthy controls in the study.

| Characteristic | HC ($n$ = 1,262) | Total Hepatitis B ($n$ = 1,034) | I AHB ($n$ = 99) | II CHB ($n$ = 521) | III HBV-ACLF ($n$ = 158) | IV HBV-LC ($n$ = 159) | V HBV-HCC ($n$ = 97) | $P_1$ | $P_2$ |
|---|---|---|---|---|---|---|---|---|---|
| **Mean age**† | 46.49 ± 13.82 | 45.24 ± 13.45 | 39.78 ± 12.05 | 44.16 ± 13.72 | 45.06 ± 11.39 | 50.78 ± 9.836 | 55.94 ± 10.69 | 0.3276 | <0.0001 |
| **Gender**†† (Male/female) | 734 (58.16)/ 527 (41.74) | 628 (60.74)/ 406 (39.26) | 56 (56.57)/ 43 (43.43) | 331 (63.53)/ 190 (36.47) | 87 (55.06)/ 71 (44.94) | 91 (57.23)/ 68 (42.77) | 63 (64.95)/ 34 (35.05) | 0.455 | 0.0254 |
| **ALT** (IU/ml)† | 22.05 ± 9.095 | 283.6 ± 448.3 | 706.9 ± 668.6 | 290.9 ± 397.3 | 320.5 ± 577.1 | 90.24 ± 156.0 | 60.92 ± 53.93 | <0.0001 | <0.0001 |
| **AST** (IU/ml)† | 19.39 ± 4.951 | 175.4 ± 240.0 | 300.2 ± 325.2 | 165.2 ± 224.3 | 255.1 ± 316.1 | 89.71 ± 108.7 | 104.7 ± 1111.3 | < 0.0001 | <0.0001 |
| **Tbil** (umol/L)† | 15.23 ± 4.265 | 139.9 ± 194.7 | 107.1 ± 117.2 | 80.10 ± 133.0 | 386.3 ± 198.4 | 96.41 ± 172.1 | 138.7 ± 235.8 | <0.0001 | <0.0001 |
| **GGT (**IU/ml**)**† | 18.47 ± 11.05 | 91.54 ± 99.15 | 145.2 ± 109.8 | 93.27 ± 84.86 | 74.98 ± 83.93 | 60.22 ± 72.33 | 111.9 ± 170.4 | < 0.0001 | <0.0001 |
| **AFP** (ug/L)† | 1.982 ± 1.683 | 505.6 ± 3032 | 20.45 ± 45.33 | 203.9 ± 967 | 119.7 ± 167.9 | 110.4 ± 347.4 | 2,392 ± 6,529 | 0.0067 | <0.0001 |
| **eAg +** (no, %)†† | / | 550 (53.20) | 52 (52.53) | 237 (45.49) | 69 (43.67) | 49 (30.82) | 28 (28.87) | / | 0.0049 |
| **HBV-DNA** [$Log_{10}$ (copies)/ml] | / | 5.491 ± 1.732 | 4.639 ± 1.46 | 5.971 ± 1.676 | 5.129 ± 1.549 | 5.022 ± 1.743 | 4.532 ± 1.731 | / | <0.0001 |
| $<10^3$†† | / | 300 (29.05) | 33 (33.33) | 104 (19.96) | 38 (24.05) | 69 (43.40) | 57 (58.76) | / | / |
| $10^3$-$10^5$†† | / | 279 (26.99) | 43 (43.44) | 125 (23.99) | 51 (32.28) | 43 (27.04) | 18 (18.56) | / | / |
| $>10^5$†† | / | 455 (43.96) | 23 (23.23) | 292 (56.05) | 69 (43.67) | 47 (29.56) | 22 (22.68) | / | / |
| **Genotype**†† | | | | | | | | | |
| GG | 709 (56.23) | 547 (53.06) | 59 (59.60) | 260 (49.90) | 79 (50.0) | 92 (57.86) | 60 (61.86) | / | / |
| GA | 496 (39.33) | 417 (40.45) | 36 (36.36) | 222 (42.61) | 71 (44.94) | 56 (35.22) | 32 (32.99) | / | / |
| AA | 56 (4.45) | 67 (6.5) | 4 (4.04) | 39 (7.49) | 8 (5.06) | 11 (6.92) | 5 (5.15) | / | / |

*HC, health control; AHB, acute hepatitis B; CHB, chronic hepatitis B without ACLF, LC, and HCC; LC, HBV-related liver cirrhosis; HCC, HBV-related hepatocellular carcinoma; †Date presented as (mean ± SD); ††Date presented as (n, %); $P_1$, t-test for all of the patients with CHB compared to HC individuals; $P_2$, One-way ANOVA test for all of hepatitis B groups (groups I–V); Hepatitis B group is the sum of groups I–V.*

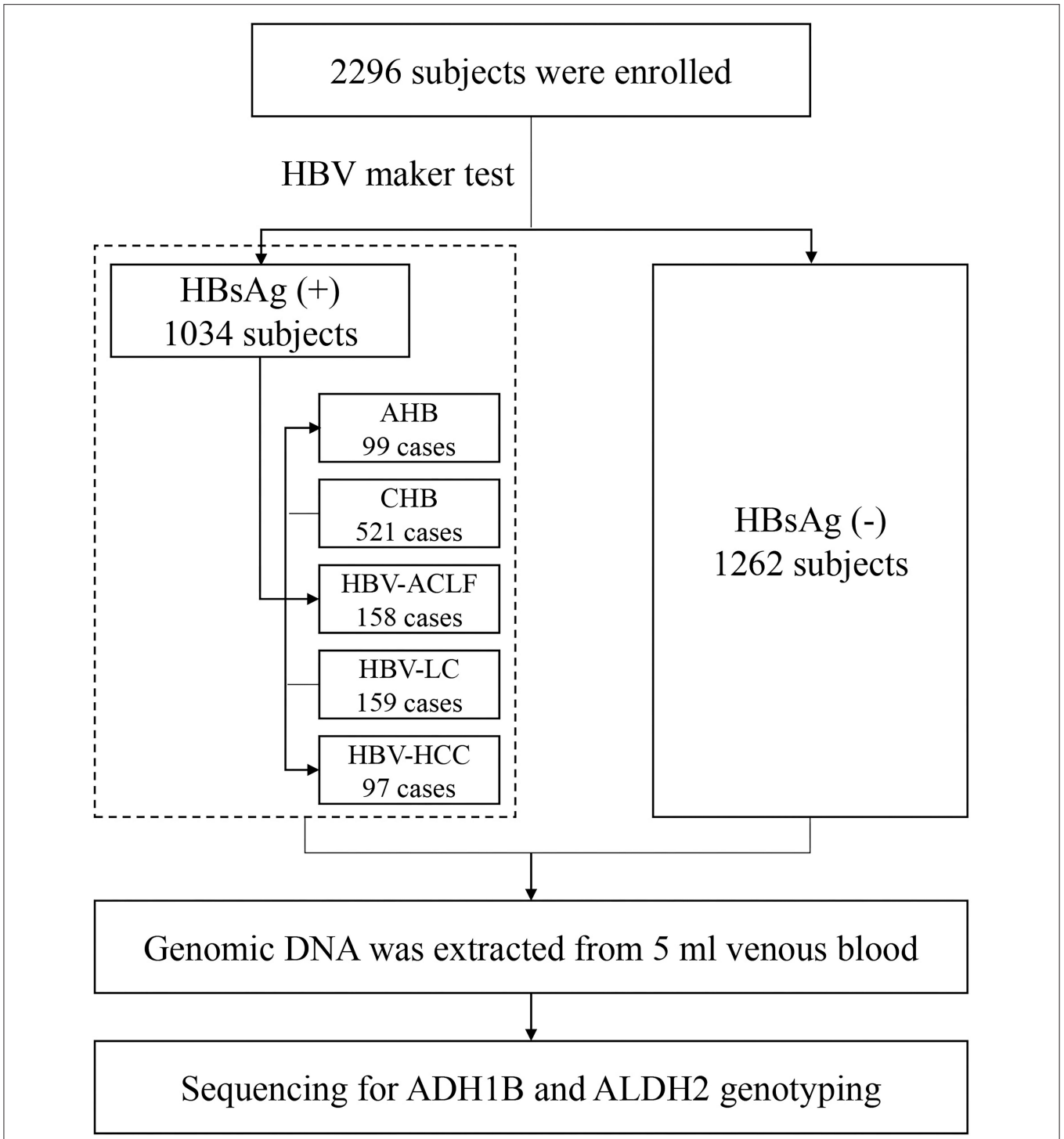


**FIGURE 1 |** Flow chart of subjects included. HC, health control; AHB, acute hepatitis B; CHB, chronic hepatitis B without ACLF, LC, and HCC; LC, HBV-related liver cirrhosis; HCC, HBV-related hepatocellular carcinoma.

extension at 72°C. The extension product was purified by 1 U SAP. The SNP genotype was confirmed using an ABI3130 genetic analyzer. Genotypes were determined automatically using the Genemapper 4.0 software (Applied Biosystems).

## Statistical Analysis

The significance was determined using Student's *t*-test or *Z*-test in demographic and clinical data for two groups or continuous variables. The $\chi^2$ test or the Fisher exact tests (two-sided)

were used to compare the categorical variables. The differences between groups were examined using the respective genetics models of codominant, dominant, recessive, and additive, as appropriate. Statistical significance was performed using the SPSS software version 18.0 (SPSS Inc., Chicago, IL, USA) and GraphPad Prism 5 (GraphPad Software Inc., La Jolla, CA, USA). Hardy–Weinberg disequilibrium, the odds ratio with a 95% CI, logistic regression adjusted for age and gender were calculated by PLINK (v.1.07, http://pngu.mgh.harvard.edu/purcell/plink/, 5 February 2015, date last accessed) (18).

# RESULTS

## Demographic and Clinical Characteristics

In total, 2,296 participants were recruited in the present study, including 1,034 patients infected with HBV [99 acute hepatitis B (AHB), 521 CHB without liver cirrhosis (LC) and HCC, 158 acute-on-chronic liver failure (ACLF), 159 HBV-associated liver cirrhosis (LC), and 97 HBV-associated HCC] and 1,262 HCs. The general demographic characteristics of the study population are shown in **Table 1** and **Figure 1**. There were no significant differences in age and gender between the HBV group and the HCs. The mean age of the HBV group was similar to the HCs (45.24 ± 13.45 vs. 46.49 ± 13.82 years, $p = 0.328$). The levels of serum alanine aminotransferase (ALT), aspartate aminotransferase (AST), gamma-glutamyl transpeptidase (GGT), total bilirubin (TBIL), and alpha-fetoprotein (AFP) in the HBV group were significantly higher than that in HCs (all of $p < 0.0001$).

Similar to the clinical situation, there were different distributions of HBV-DNA quantity among the various subgroups (groups I, II, III, IV, and V). The quantity of HBV-DNA in patients with HCC was lower than that in the AHB, CHB, ACLF, or LC groups ($p < 0.001$). The positive percentage of hepatitis B e antigen (HBeAg) in the HCC group was also the lowest among all subgroups ($p < 0.0049$) (**Table 1**).

## Quality Assessment

In total, 2,849 variants of the 2 loci were successfully genotyped in the 2,296 samples. The rates of successful genotyping (call rate) were about 100% (**Supplementary Table 2**). Hardy–Weinberg disequilibrium was assessed using the Haploview 4.2 test. The genotype distributions of the 2 SNPs were consistent with the Hardy–Weinberg equilibrium in the HC and HBV groups (**Supplementary Table 2**). These results were suitable for further genetic analysis based on these quality control assessments.

## Positive Correlation Between ALDH2 rs671 AA/GA Mutants and HBV Infection

Minor allele frequency (MAF) between the patients with hepatitis B and HCs was compared in **Table 2**. The frequency of the A allele at rs671 in the HBV group was significantly higher than that in HCs [OR (95%CI) = 1.148 (1.004–1.312), $p = 0.043$]. The genetic models (codominant, dominant, recessive, and additive) were then applied to calculate genotype frequencies. The binary logistic regression was performed to analyze whether the variant on rs671 was independently associated with HBV infection. Age and gender covariates were included in the logistic regressions (19), which were previously reported to be significantly associated with HBV infection. In the codominant model, the frequency of the rs671-AA genotype in patients with hepatitis B accounted for a relatively high proportion [adjusted OR = 1.551 (1.069–2.25), $p = 0.02$], compared to HCs (**Table 2**). Similarly, the frequency of the GA + AA genotypes in patients with hepatitis B was significantly higher than that in HCs (43.77 vs. 46.94%, adjusted OR = 1.454, $p = 0.046$) in the recessive model (**Table 2**). Moreover, in the additive model, the frequency of the GA and AA genotypes at rs671 in patients with hepatitis B was significantly higher compared to HCs (adjusted OR was 1.226, $p = 0.033$) (**Table 2**).

## Positive Association Between ALDH2 rs671-AA Mutant and HBV Persistence

When subgroup analysis was undertaken, different distributions of allele frequencies or genotypes in the rs671 mutant were only found between the HC group and CHB group (group II). When compared to HCs, a significantly higher frequency of the A allele at rs671 in the CHB group (group II) was found [OR (95%CI) = 1.273(1.082–1.497), $p = 0.003$]. Using the codominant genetic model, the AA genotype of rs671 significantly increased the risk of HBV infection in the CHB group (adjusted OR = 1.899, 95% CI = 1.232–2.928, $p = 0.003$), compared with the GG genotype. There was no significant difference in the rs671-GA genotype between the CHB group and HCs (adjusted OR = 1.221, 95% CI = 0.987–1.51, $p = 0.066$). The additional genetic model analysis also demonstrated that the rs671-AA mutant was positively associated with CHB, regardless of using the dominant model (GG vs. GA + AA, adjusted OR = 1.272, $p = 0.023$), recessive model (GG + GA vs. AA, adjusted OR = 1.621, $p = 0.027$) or additive model (adjusted OR = 1.328, $p = 0.011$) (**Table 2**). Additionally, compared with the rs671-GA genotype, the distribution of the rs671-AA genotype within the CHB group was also higher than that in HCs (adjust OR is 1.556, 95%CI: 1.004–2.412, $p = 0.046$), which suggested that the rs671-AA genotype was the dominant effect in patients with CHB (**Table 2**).

## Association Between ALDH2 rs671 Mutant and AHB, ACLF, LC, or HCC

For patients with AHB, ACLF, LC, and HCC, there were no differences in the rs671 allele frequencies, genotypes, or genetics models between patients and HCs, respectively. Binary logistic regression, adjusted for age and gender, also did not show any significant association between rs671 GA/AA and the risks of AHB, ACLF, LC, or HCC (**Table 2**).

When patients with CHB without LC/HCC (group II) were used as controls, there was a significantly decreased frequency of the rs671-AA genotype in patients with HCC [adjusted OR (95%CI) = 0.619 (0.385–0.994), $p = 0.041$ in the dominant model] (**Table 3**). These data suggest that the rs671-AA genotype might have a potential value for predicting a lower incidence of HCC in patients with CHB.

**TABLE 2 |** Association between rs671 and hepatitis B virus (HBV) infection in different hepatitis B groups.

| Model | HC | Hepatitis B | AOR | *P* | I | $OR_1$ | $P_1$ | II | $OR_2$ | $P_2$ | III | $OR_3$ | $P_3$ | IV | $OR_4$ | $P_4$ | V | $OR_5$ | $P_5$ |
|---|---|---|---|---|---|---|---|---|---|---|---|---|---|---|---|---|---|---|---|
| **Alleles** | | | | | | | | | | | | | | | | | | | |
| G | 1914 (75.89) | 1511 (73.29) | 1 | | 154 (77.78) | 1 | | 742 (71.21) | 1 | | 229 (74.47) | 1 | | 240 (75.47) | 1 | | 152 (77.55) | 1 | |
| A | 608 (24.11) | 551 (26.71) | **1.148 (1.004–1.312)** | **0.043** | 44 (22.22) | 0.899 (0.636–1.273) | 0.55 | 300 (28.79) | **1.273 (1.082–1.497)** | **0.003** | 87 (27.53) | 1.196 (0.919–1.556) | 0.182 | 78 (24.53) | 1.023 (0.78–1.342) | 0.867 | 42 (22.45) | 0.742 (0.513–1.074) | 0.112 |
| **Codominant** | | | | | | | | | | | | | | | | | | | |
| GG | 709 (56.23) | 547 (53.06) | 1 | | 59 (59.60) | 1 | | 260 (49.90) | 1 | | 79 (50) | 1 | | 92 (57.86) | 1 | | 60 (61.86) | 1 | |
| GA | 496 (39.33) | 417 (40.45) | 1.09 (0.918–1.294) | 0.326 | 36 (36.36) | 0.872 (0.567–1.341) | 0.533 | 222 (42.61) | 1.221 (0.987–1.51) | 0.066 | 71 (44.94) | 1.285 (0.914–1.806) | 0.148 | 56 (35.22) | 0.87 (0.612–1.237) | 0.437 | 32 (32.99) | 0.648 (0.412–1.019) | 0.041 |
| AA | 56 (4.44) | 67 (6.49) | **1.551 (1.069–2.25)** | **0.020** | 4 (4.04) | 0.858 (0.301–2.45) | 0.775 | 39 (7.49) | **1.899 (1.232–2.928)** | **0.003** | 8 (5.06) | 1.282 (0.589–2.787) | 0.529 | 11 (6.92) | 1.514 (0.765–2.994) | 0.23 | 5 (5.15) | 0.791 (0.278–2.253) | 0.66 |
| **Dominant** | | | | | | | | | | | | | | | | | | | |
| GG+GA | 1205 (95.56) | 964 (93.51) | 1 | | 95 (95.96) | 1 | | 482 (92.51) | 1 | | 150 (94.94) | 1 | | 148 (93.08) | 1 | | 92 (94.85) | 1 | |
| AA | 56 (4.44) | 67 (6.49) | 1.125 (0.951–1.329) | 0.169 | 4 (4.04) | 0.838 (0.547–1.285) | 0.418 | 39 (7.49) | **1.272 (1.033–1.566)** | **0.023** | 8 (5.06) | 1.276 (0.915–1.78) | 0.15 | 11 (6.92) | 0.936 (0.666–1.315) | 0.703 | 5 (5.15) | 0.867 (0.562–1.336) | 0.516 |
| **Recessive** | | | | | | | | | | | | | | | | | | | |
| GG | 709 (56.23) | 547 (53.06) | 1 | | 40 (40.40) | 1 | | 261 (50.10) | 1 | | 79 (50.00) | 1 | | 67 (42.14) | 1 | | 32 (32.99) | 1 | |
| AA+GA | 552 (43.77) | 484 (46.94) | **1.454 (1.006–2.1)** | **0.046** | 59 (59.60) | 0.855 (0.298–2.454) | 0.771 | 260 (49.90) | **1.621 (1.056–2.488)** | **0.027** | 79 (50.00) | 1.072 (0.499–2.302) | 0.858 | 92 (57.86) | 1.61 (0.813–3.186) | 0.171 | 65 (67.01) | 1.306 (0.499–3.41) | 0.586 |
| Additive | | | **1.226 (1.016–1.479)** | **0.033** | | 0.862 (0.597–1.245) | 0.429 | | **1.328 (1.066–1.654)** | **0.011** | | 1.095 (0.741–1.617) | 0.65 | | 1.234 (0.872–1.748) | 0.236 | | 1.103 (0.677–1.795) | 0.694 |

*Data were presented as number (percentage) for every group. The differences in genotype frequencies between any two groups were analyzed using logistic regression models (codominant, recessive, dominant, and additive). Age and sex were included as covariates. ORs (adjusted odds ratio) were calculated and reported within the 95% CI. Groups I, II, III, IV, and V represented the AHB, CHB, ACLF, LC, and HCC groups, respectively. Hepatitis B group was all of the groups I, II, III, IV, and V. $OR_1$, $P_1$; $OR_2$, $P_2$; $OR_3$, $P_1$; $OR_4$, $P_4$; and $OR_5$, $P_5$ were respectively calculated for groups I, II, III, IV, and V compared to the HC group. Significant p-values (<0.05) are highlighted in bold.*

**TABLE 3 |** Association between rs671 and hepatitis B virus (HBV) persistence among hepatitis B subgroups.

| Model | II | I | $OR_1$ | $P_1$ | III | $OR_2$ | $P_2$ | IV | $OR_3$ | $P_3$ | V | $OR_4$ | $P_4$ |
|---|---|---|---|---|---|---|---|---|---|---|---|---|---|
| **Alleles** | | | | | | | | | | | | | |
| G | 742 (71.21) | 154 (77.78) | 1 | | 229 (74.47) | 1 | | 240 (75.47) | 1 | | 152 (77.55) | 1 | |
| A | 300 (28.79) | 44 (22.22) | 0.707 (0.493–1.014) | 0.058 | 87 (27.53) | 0.939 (0.71–1.245) | 0.664 | 78 (24.53) | 0.804 (0.602–1.073) | 0.138 | 42 (22.45) | **0.683 (0.473–0.987)** | **0.041** |
| **Codominant** | | | | | | | | | | | | | |
| GG | 260 (49.90) | 59 (59.60) | 1 | | 79 (50) | 1 | | 92 (57.86) | 1 | | 60 (61.86) | 1 | |
| GA | 222 (42.61) | 36 (36.36) | 0.717 (0.455–1.123) | 0.144 | 71 (44.94) | 1.053 (0.729–1.52) | 0.785 | 56 (35.22) | 0.713 (0.489–1.04) | 0.078 | 32 (32.99) | **0.625 (0.392–0.994)** | **0.044** |
| AA | 39 (7.49) | 4 (4.04) | 0.452 (0.155–1.314) | 0.136 | 8 (5.06) | 0.675 (0.303–1.505) | 0.334 | 11 (6.92) | 0.797 (0.392–1.622) | 0.531 | 5 (5.15) | 0.556 (0.21–1.469) | 0.231 |
| **Dominant** | | | | | | | | | | | | | |
| GG+GA | 482 (92.51) | 95 (95.96) | 1 | | 150 (94.94) | 1 | | 148 (93.08) | 1 | | 92 (94.85) | 1 | |
| AA | 39 (7.49) | 4 (4.04) | 0.653 (0.419–1.016) | 0.058 | 8 (5.06) | 0.977 (0.682–1.398) | 0.897 | 11 (6.92) | 0.748 (0.513–1.089) | 0.129 | 5 (5.15) | **0.619 (0.385–0.994)** | **0.041** |
| **Recessive** | | | | | | | | | | | | | |
| AA+GA | 261 (50.10) | 40 (40.40) | 1 | | 79 (50.00) | 1 | | 67 (42.14) | 1 | | 32 (32.99) | 1 | |
| GG | 260 (49.90) | 59 (59.60) | 0.485 (0.169–1.397) | 0.18 | 79 (50.00) | 0.692 (0.314–1.524) | 0.361 | 92 (57.86) | 1.104 (0.536–2.275) | 0.789 | 65 (67.01) | 1.119 (0.409–3.063) | 0.827 |
| Additive | | | 0.647 (0.378–1.106) | 0.111 | | 0.836 (0.559–1.252) | 0.386 | | 0.98 (0.677–1.419) | 0.916 | | 0.949 (0.568–1.584) | 0.841 |

*Data were presented as number (percentage) for every group. The differences in genotype frequencies between any two groups were analyzed using logistic regression models (codominant, recessive, dominant, and additive). Age and sex were included as covariates. ORs (adjusted odds ratio) were calculated and reported within the 95% CI. Groups I, II, III, IV, and V represented the AHB, CHB, ACLF, LC, and HCC groups, respectively. $OR_1$, $P_1$; $OR_2$, $P_2$; $OR_3$, $P_3$, and $OR_4$, $P_4$ were respectively calculated for Group I, III, IV, and V compared to the II group. Significant p-values (<0.05) are highlighted in bold.*

## No Association Between ADH1B rs1229984 Mutant and HBV Infection

Genotyping of rs1229984 (His48Arg) of ADH1B and rs671 (Glu504Lys) of ADH1B were performed using 266 patients with CHB without LC/HCC and 287 HCs of the Chinese Han population (**Table 4**). The results are shown in **Table 4** and **Supplementary Table 3**. The call rates for rs1229984 and rs671 were 100%. Those variants in the control and case-patient group were in accord with Hardy–Weinberg equilibrium ($p > 0.05$).

The variant of ADH1B rs1229984 showed no association with CHB in allele frequencies analysis [$p = 0.996$, OR (95%CI) = 1.001 (0.771–1.299)], or genotype models analysis [adjusted $p = 0.785$, OR (95%CI) = 0.947 (0.662–1.353), in the co-dominant model] (**Supplementary Table 3**). The joint effects of the combined variants of ADH1B (rs1229984) and ALDH2 (rs671) on the HBV persistent infection were investigated. Based on the enzyme activity (20), the His carrier (His+) and non-His carrier (His–) models were selected for the association analysis between CHB and rs1229984 (His48Arg) of ADH1B. The His carrier is mainly represented as rs671-AA/GA genotypes and the non-His carrier is mainly represented as the rs671-GG genotype. Regarding the association analysis between CHB and rs671 (Glu504Lys) of ALDH2, we adopted the non-Lys carrier (Lys–) and the Lys carrier (Lys+) models as described previously (21). The non-Lys carrier or the Lys carrier respectively represented AA or GG/GA genotypes. There are no significant differences in the distribution of alleles and genotypes between HCs and CHBs, according to a subgroup analysis of His–/Lys+, His–/Lys–, His+/Lys+, and His+/Lys+, as shown in **Table 4** ($p = 0.675$, 0.849, and 0.324, respectively). There were also no significantly combined effects in CHB of the variants of ADH1B (rs1229984) and ALDH2 (rs671).

## Positive Association Between ALDH2 rs671-AA Mutant and the HBV-DNA Quantitation

The CHB subjects with the rs671-AA genotype were found to have a significantly higher quantity of circulating HBV-DNA [6.745 ± 1.603 $Log_{10}$ (copies)/ml] than those with rs671-GG [5.877 ± 1.651 $Log_{10}$ (copies)/ml] or rs671-GA [5.980 ± 1.650 $Log_{10}$ (copies)/ml] genotype ($p = 0.0046$), as shown in **Table 5** and **Figure 2A**. There was a higher percentage of patients with CHB with a high quantitation of HBV-DNA ($>10^5$ copies/ml) in the individuals with rs671-AA (58.97%), compared with patients with rs671-GG (50.45%) or rs671-GA (49.23%) (**Table 5** and **Figure 2B**). It was demonstrated that the rs671-AA mutant was positively correlated with the quantitation of HBV-DNA.

As for age, gender, liver function (including ALT, AST, GGT, and TBIL), AFP, and rate of positive HBeAg, there were no significant differences among patients with CHB with GG, GA, or AA genotype (**Table 5**).

## DISCUSSION

In the current study, the association between polymorphisms within the ADH1B/ALDH2 genes and HBV susceptibility

**TABLE 4 |** CHB risk due to the combination of ADH1B and ALDH2 genotypes.

| rs1229984 (His48Arg) | rs671(Glu504Lys) | HC ($n = 287$)†† | CHB ($n = 266$)†† | OR (95%CI) | *p*-value |
|---|---|---|---|---|---|
| AA | GG | 77 | 60 | 1 | / |
| AA | GA | 52 | 60 | 1.481 (0.896–2.446) | 0.245 |
| AA | AA | 7 | 5 | 0.917 (0.277–3.033) | 0.194 |
| AG | GG | 59 | 54 | 1.175 (0.712–1.937) | 0.618 |
| AG | GA | 57 | 57 | 1.283 (0.779–2.113) | 0.974 |
| AG | AA | 7 | 2 | 0.367 (0.073–1.830) | 0.849 |
| GG | GG | 16 | 15 | 1.203 (0.551–2.628) | 0.298 |
| GG | GA | 12 | 12 | 1.283 (0.538–3.059) | 0.940 |
| GG | AA | 0 | 1 | 3.843 (0.154–96.09) | 0.649 |
| His+ (AA/AG) | Lys- (GG) | 136 | 114 | 1 | / |
| His- (GG) | Lys+ (AA/GA) | 12 | 13 | 1.292 (0.567–2.944) | 0.675 |
| His- (GG) | Lys- (GG) | 16 | 15 | 1.118 (0.53–2.361) | 0.849 |
| His+ (AA/AG) | Lys+ (AA/GA) | 123 | 124 | 1.203 (0.923–1.294) | 0.324 |

*HC, health control; CHB, chronic hepatitis B; His, histidine; Lys, lysine; OR, odds ratio; CI, confidence interval. *In the analysis of rs1229984 (His48Arg), "His+" and "His–" mean His carrier (His/His or His/Arg) and non-His carrier (Arg/Arg), respectively. In the analysis of rs671 (Glu504Lys), "Lys+" and "Lys–" mean Lys carrier (Lys/Lys or Lys/Glu) and non-Lys carrier (Glu/Glu), respectively. We investigated the combined effects of rs1229984 and rs671 on CHB as compared with "His +/Lys–". ††Data were presented as number (percentage) for every group. The differences in genotype frequencies between any two groups were analyzed using logistic regression models. Age and sex were included as covariates. The P-values were calculated for CHB patients compared to HC individuals.*

**TABLE 5 |** Comparison of clinical features levels between subjects with different genotypes at rs671 in the CHB ($n = 521$) group.

| Characteristic | GG ($n = 260$) | GA ($n = 222$) | AA ($n = 39$) | *P** |
|---|---|---|---|---|
| **Mean age**† | 42.01 ± 13.88 | 43.81 ± 14.18 | 43.46 ± 13.90 | 0.169 |
| **Gender**†† (Male/female) | 157 (60.38)/ 103 (39.62) | 148 (66.67)/ 74 (33.33) | 28 (71.79)/ 11 (28.21) | 0.115 |
| **ALT** (IU/ml)† | 282.7 ± 379.0 | 308.2 ± 424.3 | 385.7 ± 448.3 | 0.338 |
| **AST** (IU/ml)† | 162.3 ± 217.7 | 173.1 ± 237.2 | 213.1 ± 243.2 | 0.512 |
| **Tbil** (umol/L)† | 78.01 ± 127.5 | 87.61 ± 142.7 | 98.90 ± 150.3 | 0.974 |
| **GGT (**IU/ml**)**† | 94.34 ± 84.63 | 92.20 ± 82.72 | 91.91 ± 101.3 | 0.962 |
| **AFP** (ug/L)† | 210.2 ± 931.5 | 242.0 ± 1,144 | 86.04 ± 211.4 | 0.743 |
| **eAg +** (no, %)†† | 171 (65.77)/ 89 (34.23) | 145 (65.32)/ 77 (34.68) | 29 (74.36)/ 10 (25.64) | 0.161 |
| **HBVDNA** [$Log_{10}$ (copies)/ml] | 5.877 ± 1.651 | 5.980 ± 1.650 | 6.745 ± 1.603 | **0.0046** |
| $<10^3$†† | 74 (28.46) | 60 (27.03) | 9 (23.08) | / |
| $10^3$-$10^4$†† | 26 (10.00) | 19 (8.56) | 3 (7.69) | / |
| $10^4$-$10^5$†† | 32 (12.31) | 31 (13.96) | 4 (10.26) | / |
| $>10^5$†† | 128 (49.23) | 112 (50.45) | 23 (58.97) | **<0.0001** |

†*Data presented as (mean ± SD).* ††*Data were presented as number (percentage) for every group. *Difference in clinical features levels was tested between different genotypes (AA, AG, and GG) by one-way ANOVA test. Significant p-values (<0.05) are highlighted in bold.*

was investigated in the Chinese Han population. It was the first investigation that focused on the relationship between the ALDH2 rs671 polymorphism and HBV susceptibility of individuals till now. It was also the first study that has demonstrated that individuals who carried ALDH2 rs671-AA genotype might have a higher risk of persistent HBV infection and higher HBV-DNA level compared to those with GG/GA genotype. Our results suggest the possible hazardous role of this variant during persistent HBV infection. Based on the fact that the rs671 (Glu504Lys) SNP has been shown to be a well-known dysfunctional SNP in a previous study (22), which has been confirmed in the present data, it is reasonable to conclude that the rs671-AA genotype is a potential hazardous HBV-associated functional SNP.

In addition, the rs671-AA variant might be a risk predicator for the incidence of HCC in patients with CHB, suggesting that patients with CHB with the rs671-AA genotype might have a lower risk of HCC incidence. However, there was no significant different distribution of allele or genotypes in the rs671 mutant among patients with AHB, ACLF, LC, or HCC, compared with HCs. The results further indicate that patients with CHB with persistent high HBV-DNA replication might be influenced by the

rs671 polymorphism of ALDH2, whereas HBV-DNA replication in AHB, ACLF, LC, or HCC was lower than in CHB. It is worth initiating studies to reveal the underlying mechanism of the rs671 mutants and HBV replication.

The ALDH2 is a crucial enzyme in the hepatocyte, which takes part in alcohol metabolism. Alcohol is oxidized to acetaldehyde by ADH, and acetaldehyde is further metabolized to acetate by ALDH, which largely depends on ALDH2 (22). ALDH2 also plays important role in other liver diseases, including ameliorating chronic alcohol-induced hepatic steatosis and inflammation (11), inhibiting aggressive behavior of HCC (10), and increased risk for NAFLD with a mutation in ALDH2 (14).

The ALDH2 rs671 (Glu504Lys) is a common missense SNP, mainly in East Asians (40–50%), resulting in a Gly-to-Lys amino acid substitution in exon 12 (23). Individuals with the ALDH2 rs671-AA genotype exhibit severely decreased activity of the ALDH2 enzyme and have only 6.25% of the normal protein encoded by the ALDH2 rs671-GG variant, indicating the dominant effect of the ALDH2 A allele (24–26). Murine models with the rs671-AA mutant on ALDH2 could increase protein turnover and would promote murine hepatocarcinogenesis *in vivo* (13). It had been reported that the ALDH2 rs671-AA, which is associated with the GGT level, might potentially be a novel risk factor for NAFLD (14). In our study, we also found that individuals who carried the ALDH2 rs671-AA genotype had a higher risk of persistent HBV infection and higher HBV-DNA levels, compared to subjects with the rs671-GG genotype.

At first, we found that the distribution frequency of the A allele on ALDH2 rs671 was increased in patients with hepatitis B, especially in the CHB group, compared with HCs. However, no significant difference in the distribution of allele or genotype was found in rs671 mutants among patients with AHB, ACLF, LC, or HCC, compared with HCs, suggesting that the potential role of the rs671-AA variant is mainly related to the persistent HBV infection (CHB). We further found that the ALDH2 rs671-AA genotype was significantly increased in the CHB group compared with HCs, whereas the rs671-GA genotype was not significantly increased. The results demonstrated that the rs671-AA genotype might play a dominant effect on the HBV persistent infection. In addition, compared to the rs671-GA genotype, individuals with the rs671-AA genotype were significantly higher in the CHB group than that in HCs, which also suggested the dominant effect on CHB. We reasonably concluded that the rs671-AA genotype, not the rs671-GA genotype, might have an influence on the persistence of HBV infection.

Recently, cumulative evidence has revealed that ALDH2 plays an important role in liver diseases associated with the autophagy signal pathway (27, 28). ALDH2 could ameliorate chronic alcohol intake-induced hepatic steatosis and inflammation through the regulation of autophagy (11). Moreover, upregulating the expression of ALDH2 in HCC cells leads to the inhibition of tumor aggressive behavior *in vitro* and *in vivo*, largely exerted by modulating the activity of the ALDH2–acetaldehyde–redox–AMPK axis, which is an important autophagy pathway (10).

It has been reported that the enhancement of autophagy could increase HBV-DNA replication mediated by HBV × protein (5, 6), and the promotion of autophagic degradation by AMPK could restrict HBV replication (7). Meanwhile, HBV evaded antiviral immunity and permitted survival of virus-infected cells through triggering autophagy by the degradation of the TNFSF10/TRAIL response, which targets the TNFRSF10B/death receptor 5 (29). Moreover, the inhibition of ALDH2 activity could result in upregulated inflammatory molecules, including an increase of nuclear translocation of NF-κB and the enhancement of phosphorylation of NF-κB, p65, AP-1 c-Jun, Jun-N terminal kinase, and p38 MAPK (30). The persistent activation of autophagy and the inflammatory response in hepatocytes, which is mediated by ALDH2 during chronic HBV infection, might take part in the regulation of HBV infection and lead to persistent infection (8).

In the present study, individuals with a high HBV-DNA level accounted for a larger proportion of patients with CHB with the rs671-AA genotype compared to the rs671-GG/GA genotype, indicating a significant positive association between HBV-DNA level and the ALDH2 rs671-AA genotype. We reasonably conclude that the decreased activity of the ALDH2 enzymes in patients with CHB, which resulted from the rs671-AA mutant (24), might activate the autophagy signal pathway (10), triggering autophagy then promoting HBV to evade antiviral immunity (29), permitting the survival of virus-infected cells (29), further enhancing the HBV replication (5, 6), and ultimately promoting the persistence of HBV infection (8). The present study demonstrates the possible hazardous role of the rs671-AA variant during HBV infection and persistence (**Figure 3**).

However, the decreased activity of ALDH2 resulting from the rs671-AA mutant could trigger contrary effects in the incidence of HCC. There were lower distribution frequencies of the rs671-AA genotype in the HCC group compared with the CHB group in subgroup analysis, which was in accordance with the lower HBV-DNA quantitation in the patients with HCC. Combined with the lower HBV-DNA level in the HCC group, we speculate that the rs671-AA mutant might be a potential risk predictor of HCC incidence in the CHB group. Thus, CHB individuals with ALDH rs671-AA genotype potentially have a lower risk of incidence of HCC. Recently, Seo et al. (31) have reported that the progression of HCC was mainly observed in patients with the ALDH2-rs671-GG genotype rather than the GA/AA genotype (31).

There are some limitations to our study. First, the selected hot spots (rs671 and rs1229984) might miss other important mutant sites, including sites that may be in linkage disequilibrium with the selected sites. It would be better to sequence the whole genome of ADH1B and ALDH2 to discover new loci that might play significant roles in the pathogenesis of CHB or other HBV-related liver diseases. Second, we did not assess the influence of ALDH2 expression mediated by rs671 mutants in liver tissues due to the limited acquisition of liver biopsies in these patients. Third, there were only 97 patients with HCC enrolled in the present study, the statistical conclusion that subjects with rs671-AA genotype might have a lower risk of HCC

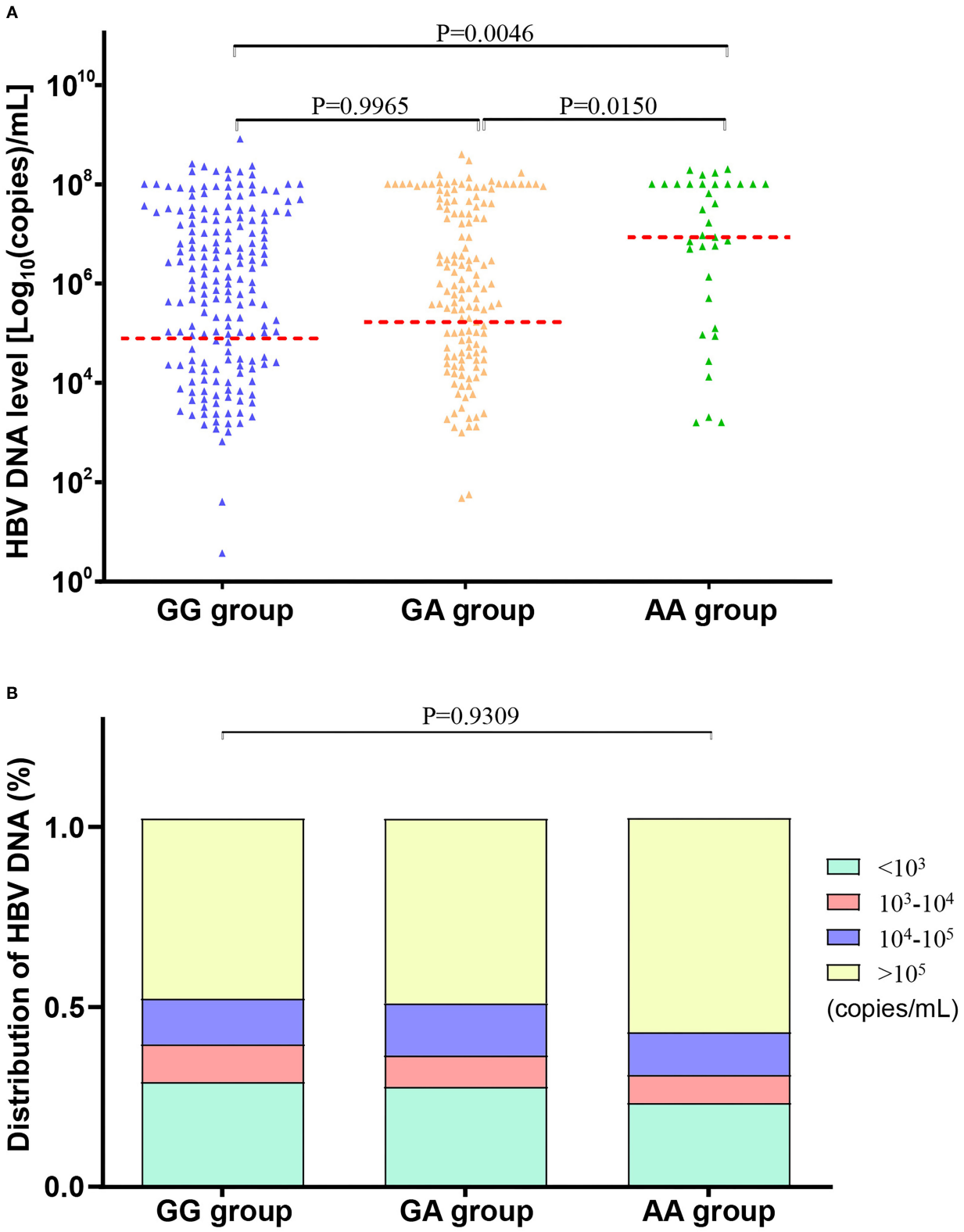


**FIGURE 2 |** HBV-DNA levels were the highest in patients with chronic hepatitis B (CHB) with rs671-AA genotype. **(A)** Comparison of HBV-DNA mean levels among subjects with AA, AG, and GG genotypes at rs671 in the CHB group. HBV-DNA levels were analyzed by converting to $Log_{10}$ (copies)/ml. Data were presented as

*(Continued)*

**FIGURE 2 |** (mean ± SD), unpaired *t*-test, and one-way ANOVA were used. **(B)** Comparison of HBV-DNA distribution among subjects with AA, AG, and GG genotypes at rs671 in the CHB group. Patients with CHB with rs671-AA genotype showed the highest proportion (58.97%) of HBV-DNA levels at more than $10^5$ copies/ml, compared to patients with rs671-GG (50.45%) or rs671-GA (49.23%). Data were presented as a percentage for each group. Fisher's exact test was used.

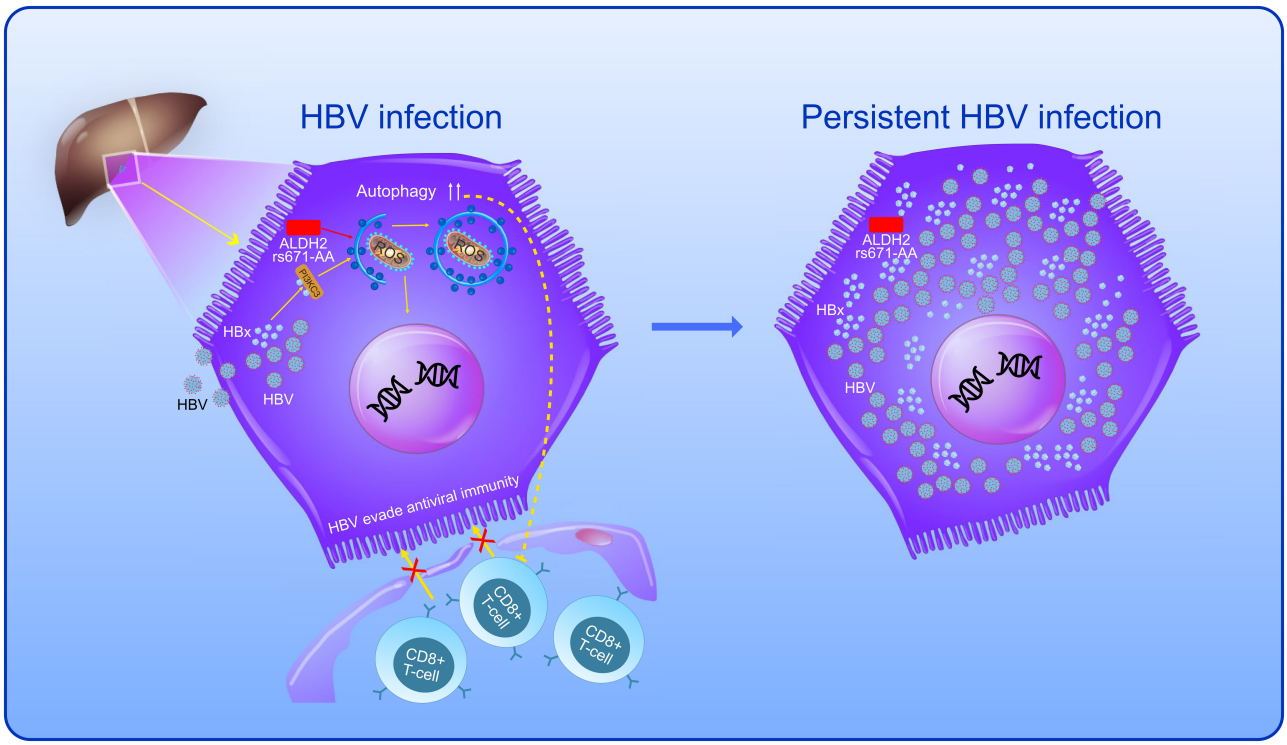


**FIGURE 3 |** The possible hazardous role of the rs671-AA variant during HBV infection and persistence. The autophagic pathway in HBV-infected hepatocytes is enhanced by hepatitis B virus × protein (HBx) *via* the binding to phosphatidylinositol 3-kinase class III (PI3KC3). Meanwhile, ALDH2-rs671-AA mutant in individuals with decreased activity of ALDH2 enzymes might also activate the autophagy signal pathway, triggering autophagy then promoting HBV to evade antiviral immunity, permitting the survival of virus-infected hepatocytes, further enhancing the HBV replication and ultimately promoting the persistence of HBV infection.

incidence needs a larger sample size to confirm this conclusion. Finally, we did not verify the underlying mechanism of ALDH2 rs671 mutant *in vivo* or *in vitro*, it would be performed in our future studies.

In conclusion, the present study provides evidence for the perspective that the ALDH2-rs671 variant was correlated with HBV infection and persistence. It is the first time that the positive association between rs671 polymorphism and HBV infection has been investigated. Currently, the hot site rs671-AA imparts a hazardous role during persistent HBV infection. These results might shed light on the study of HBV susceptibility of individuals and the prevention of persistent HBV infection, and the targeting of drugs for a functional cure of patients with CHB.

## DATA AVAILABILITY STATEMENT

The datasets presented in this study can be found in online repositories. The names of the repository/repositories and accession number(s) can be found in the article/**Supplementary Material**.

## ETHICS STATEMENT

The studies involving human participants were reviewed and approved by the Ethics Committee of Shanghai Ruijin Hospital, School of Medicine, Shanghai Jiaotong University. The patients/participants provided their written informed consent to participate in this study.

## AUTHOR CONTRIBUTIONS

QX, XX, and GZ conceived, designed, and directed the overall project, reviewed the manuscript, and approved the final version. HW and WC directed partial experiments. PW, GZ, WT, and DS collected samples. RL, ZL, and XW collected data. PW and RM performed experiments and analyzed the data. PW and XX wrote the manuscript. All the authors had access to the study data and have reviewed and approved the final manuscript.

## FUNDING

This study was supported by the National Natural Science Foundation of China (Nos. 82170619, 81970544, 82070604, 81770587, 81770578, and 81900527), the Three-Year Public Health Action Plan (2020–2022) of Shanghai (No. GWV-10.1-XK13), the Shanghai Municipal Key Clinical Specialty (shslczdzk01103), the Shanghai Ruijin Hospital Clinical Skills and Innovations (2018CR005), the Shanghai talent development fund (2020097), the Shanghai Rising Stars of Medical Talent Youth Development Program Outstanding Youth Medical Talents [SHWJRS(2021)-99], the Shanghai Outstanding Academic Leader Youth Program (20XD1422600) and the Shanghai Sailing Program (No. 19YF1429200).

## SUPPLEMENTARY MATERIAL

The Supplementary Material for this article can be found online at: https://www.frontiersin.org/articles/10.3389/fmed.2022.811639/full#supplementary-material

## REFERENCES

1. Schweitzer A, Horn J, Mikolajczyk RT, Krause G, Ott JJ. Estimations of worldwide prevalence of chronic hepatitis B virus infection: a systematic review of data published between 1965 and 2013. *Lancet*. (2015) 386:1546–55. doi: 10.1016/S0140-6736(15)61412-X
2. EASL 2017 Clinical Practice Guidelines on the management of hepatitis B virus infection. *J Hepatol*. (2017) 67:370–98. doi: 10.1016/j.jhep.2017.03.021
3. Cui Y, Jia J. Update on epidemiology of hepatitis B and C in China. *J Gastroenterol Hepatol.* (2013) 28 Suppl 1:7–10. doi: 10.1111/jgh.12220
4. Yu MW, Lin CL, Liu CJ, Yang SH, Tseng YL, Wu CF. Influence of metabolic risk factors on risk of hepatocellular carcinoma and liver-related death in men with chronic hepatitis B: a large cohort study. *Gastroenterology*. (2017) 153:1006–17.e5. doi: 10.1053/j.gastro.2017.07.001
5. Sir D, Tian Y, Chen WL, Ann DK, Yen TS, Ou JH. The early autophagic pathway is activated by hepatitis B virus and required for viral DNA replication. *Proc Natl Acad Sci U S A*. (2010) 107:4383–8. doi: 10.1073/pnas.0911373107
6. Tang H, Da L, Mao Y, Li Y, Li D, Xu Z, et al. Hepatitis B virus X protein sensitizes cells to starvation-induced autophagy *via* up-regulation of beclin 1 expression. *Hepatology.* (2009) 49:60–71. doi: 10.1002/hep.22581
7. Xie N, Yuan K, Zhou L, Wang K, Chen HN, Lei Y, et al. PRKAA/AMPK restricts HBV replication through promotion of autophagic degradation. *Autophagy.* (2016) 12:1507–20. doi: 10.1080/15548627.2016.1191857
8. Sir D, Ann DK, Ou JH. Autophagy by hepatitis B virus and for hepatitis B virus. *Autophagy.* (2010) 6:548–9. doi: 10.4161/auto.6.4.11669
9. Li D, Zhao H, Gelernter J. Strong protective effect of the aldehyde dehydrogenase gene (ALDH2) 504lys (*2) allele against alcoholism and alcohol-induced medical diseases in Asians. *Hum Genet.* (2012) 131:725–37. doi: 10.1007/s00439-011-1116-4
10. Hou G, Chen L, Liu G, Li L, Yang Y, Yan HX, et al. Aldehyde dehydrogenase-2 (ALDH2) opposes hepatocellular carcinoma progression by regulating AMP-activated protein kinase signaling in mice. *Hepatology*. (2017) 65:1628–44. doi: 10.1002/hep.29006
11. Guo R, Xu X, Babcock SA, Zhang Y, Ren J. Aldehyde dedydrogenase-2 plays a beneficial role in ameliorating chronic alcohol-induced hepatic steatosis and inflammation through regulation of autophagy. *J Hepatol.* (2015) 62:647–56. doi: 10.1016/j.jhep.2014.10.009
12. Cui R, Kamatani Y, Takahashi A, Usami M, Hosono N, Kawaguchi T, et al. Functional variants in ADH1B and ALDH2 coupled with alcohol and smoking synergistically enhance esophageal cancer risk. *Gastroenterology.* (2009) 137:1768–75. doi: 10.1053/j.gastro.2009.07.070
13. Jin S, Chen J, Chen L, Histen G, Lin Z, Gross S, et al. ALDH2(E487K) mutation increases protein turnover and promotes murine hepatocarcinogenesis. *Proc Natl Acad Sci U S A.* (2015) 112:9088–93. doi: 10.1073/pnas.1510757112
14. Oniki K, Morita K, Watanabe T, Kajiwara A, Otake K, Nakagawa K, et al. The longitudinal effect of the aldehyde dehydrogenase 2*2 allele on the risk for nonalcoholic fatty liver disease. *Nutr Diabetes.* (2016) 6:e210. doi: 10.1038/nutd.2016.17
15. [The guideline of prevention and treatment for chronic hepatitis B (2010 version)]. *Zhonghua gan zang bing za zhi.* (2011) 19:13–24. doi: 10.3760/cma.j.issn.1007-3418.2011.01.007
16. Yan H, Yuan W, Velculescu VE, Vogelstein B, Kinzler KW. Allelic variation in human gene expression. *Science.* (2002) 297:1143. doi: 10.1126/science.1072545
17. Gohl DM, Vangay P, Garbe J, MacLean A, Hauge A, Becker A, et al. Systematic improvement of amplicon marker gene methods for increased accuracy in microbiome studies. *Nat Biotechnol.* (2016) 34:942–9. doi: 10.1038/nbt.3601
18. Purcell S, Neale B, Todd-Brown K, Thomas L, Ferreira MA, Bender D, et al. PLINK: a tool set for whole-genome association and population-based linkage analyses. *Am J Hum Genet.* (2007) 81:559–75. doi: 10.1086/519795
19. Stroffolini T, Esvan R, Biliotti E, Sagnelli E, Gaeta GB, Almasio PL. Gender differences in chronic HBsAg carriers in Italy: evidence for the independent role of male sex in severity of liver disease. *J Med Virol.* (2015) 87:1899–903. doi: 10.1002/jmv.24243
20. Sakiyama M, Matsuo H, Akashi A, Shimizu S, Higashino T, Kawaguchi M, et al. Independent effects of ADH1B and ALDH2 common dysfunctional variants on gout risk. *Sci Rep.* (2017) 7:2500. doi: 10.1038/s41598-017-02528-z
21. Sakiyama M, Matsuo H, Nakaoka H, Yamamoto K, Nakayama A, Nakamura T, et al. Identification of rs671, a common variant of ALDH2, as a gout susceptibility locus. *Sci Rep.* (2016) 6:25360. doi: 10.1038/srep25360
22. Takeuchi F, Isono M, Nabika T, Katsuya T, Sugiyama T, Yamaguchi S, et al. Confirmation of ALDH2 as a major locus of drinking behavior and of its variants regulating multiple metabolic phenotypes in a Japanese population. *Circ J.* (2011) 75:911–8. doi: 10.1253/circj.CJ-10-0774
23. Wu C, Kraft P, Zhai K, Chang J, Wang Z, Li Y, et al. Genome-wide association analyses of esophageal squamous cell carcinoma in Chinese identify multiple susceptibility loci and gene-environment interactions. *Nat Genet.* (2012) 44:1090–7. doi: 10.1038/ng.2411
24. Matsuo K, Wakai K, Hirose K, Ito H, Saito T, Tajima K. Alcohol dehydrogenase 2 His47Arg polymorphism influences drinking habit independently of aldehyde dehydrogenase 2 Glu487Lys polymorphism: analysis of 2,299 Japanese subjects. *Cancer Epidemiol Biomarkers Prev.* (2006) 15:1009–13. doi: 10.1158/1055-9965.EPI-05-0911
25. Li Y, Zhang D, Jin W, Shao C, Yan P, Xu C, et al. Mitochondrial aldehyde dehydrogenase-2 (ALDH2) Glu504Lys polymorphism contributes to the variation in efficacy of sublingual nitroglycerin. *J Clin Invest.* (2006) 116:506–11. doi: 10.1172/JCI26564
26. Larson HN, Weiner H, Hurley TD. Disruption of the coenzyme binding site and dimer interface revealed in the crystal structure of mitochondrial aldehyde dehydrogenase "Asian" variant. *J Biol Chem.* (2005) 280:30550–6. doi: 10.1074/jbc.M502345200
27. Stachowicz A, Olszanecki R, Suski M, Wisniewska A, Toton-Zuranska J, Madej J, et al. Mitochondrial aldehyde dehydrogenase activation by Alda-1 inhibits atherosclerosis and attenuates hepatic steatosis in apolipoprotein E-knockout mice. *J Am Heart Assoc.* (2014) 3:e001329. doi: 10.1161/JAHA.114.001329
28. Hao X, Zeng Q. The association and interaction of aldehyde dehydrogenase 2 polymorphisms with food group intake and probability of having non-alcoholic fatty liver disease. *Diabetes Metab Syndr Obes.* (2020) 13:5049–57. doi: 10.2147/DMSO.S290491
29. Shin GC, Kang HS, Lee AR, Kim KH. Hepatitis B virus-triggered autophagy targets TNFRSF10B/death receptor 5 for degradation to limit TNFSF10/TRAIL response. *Autophagy.* (2016) 12:2451–66. doi: 10.1080/15548627.2016.1239002
30. Pan C, Xing JH, Zhang C, Zhang YM, Zhang LT, Wei SJ, et al. Aldehyde dehydrogenase 2 inhibits inflammatory response and regulates atherosclerotic plaque. *Oncotarget.* (2016) 7:35562–76. doi: 10.18632/oncotarget.9384
31. Seo W, Gao Y, He Y, Sun J, Xu H, Feng D, et al. ALDH2 deficiency promotes alcohol-associated liver cancer by activating oncogenic pathways

*via* oxidized DNA-enriched extracellular vesicles. *J Hepatol.* (2019) 71:1000–11. doi: 10.1016/j.jhep.2019.06.018

**Conflict of Interest:** The authors declare that the research was conducted in the absence of any commercial or financial relationships that could be construed as a potential conflict of interest.

**Publisher's Note:** All claims expressed in this article are solely those of the authors and do not necessarily represent those of their affiliated organizations, or those of the publisher, the editors and the reviewers. Any product that may be evaluated in this article, or claim that may be made by its manufacturer, is not guaranteed or endorsed by the publisher.

frontiers in Medicine

REVIEW
published: 11 March 2022
doi: 10.3389/fmed.2022.802312

# Will Host Genetics Affect the Response to SARS-CoV-2 Vaccines? Historical Precedents

*Maria K. Smatti*[1,2], *Hebah A. Alkhatib*[2], *Asmaa A. Al Thani*[2] *and Hadi M. Yassine*[1,2]*

[1] College of Health and Life Sciences, Hamad Bin Khalifa University, Doha, Qatar, [2] Biomedical Research Center, Qatar University, Doha, Qatar

Recent progress in genomics and bioinformatics technologies have allowed for the emergence of immunogenomics field. This intersection of immunology and genetics has broadened our understanding of how the immune system responds to infection and vaccination. While the immunogenetic basis of the huge clinical variability in response to the severe acute respiratory syndrome coronavirus 2 (SARS-CoV-2) infection is currently being extensively studied, the host genetic determinants of SARS-CoV-2 vaccines remain largely unknown. Previous reports evidenced that vaccines may not protect all populations or individuals equally, due to multiple host- and vaccine-specific factors. Several studies on vaccine response to measles, rubella, hepatitis B, smallpox, and influenza highlighted the contribution of genetic mutations or polymorphisms in modulating the innate and adaptive immunity following vaccination. Specifically, genetic variants in genes encoding virus receptors, antigen presentation, cytokine production, or related to immune cells activation and differentiation could influence how an individual responds to vaccination. Although such knowledge could be utilized to generate personalized vaccine strategies to optimize the vaccine response, studies in this filed are still scarce. Here, we briefly summarize the scientific literature related to the immunogenetic determinants of vaccine-induced immunity, highlighting the possible role of host genetics in response to SARS-CoV-2 vaccines as well.

**Keywords: SARS-CoV-2, COVID-19, vaccines, SNPs, host genetics**

OPEN ACCESS

***Edited by:***
*Renan Pedra de Souza, Federal University of Minas Gerais, Brazil*

***Reviewed by:***
*Gualberto Ruaño, University of Connecticut, United States*
*Alexandre Bolze, Helix Opco LLC, United States*

***Correspondence:**
*Hadi M. Yassine*
*hyassine@qu.edu.qa*

***Specialty section:***
*This article was submitted to Precision Medicine, a section of the journal Frontiers in Medicine*

***Received:*** *26 October 2021*
***Accepted:*** *10 February 2022*
***Published:*** *11 March 2022*

***Citation:***
*Smatti MK, Alkhatib HA, Al Thani AA and Yassine HM (2022) Will Host Genetics Affect the Response to SARS-CoV-2 Vaccines? Historical Precedents. Front. Med. 9:802312. doi: 10.3389/fmed.2022.802312*

## INTRODUCTION

Vaccination has become one of the most effective public health strategies to prevent infectious diseases in the modern medicine. Undeniably, it has saved millions of lives by reducing the burden of many serious infections such as polio, tuberculosis, measles, and tetanus. Currently, the entire world is in a battle against SARS-CoV-2, which emerged at the end of 2019 and caused the coronavirus disease 19 (COVID-19). The virus has affected almost 400 million people and has claimed over 5 million lives worldwide (1). Yet, there is no decisive therapy to treat SARS-CoV-2 infection until now, and therefore, vaccines are considered the only hope to control the spread of the virus.

Despite the great success of vaccines throughout the history, the field of vaccinology is still dominated by the traditional empiric model of "isolate-inactivate-inject," which translates into a population-level model of "same dose for everyone for every disease" (2). Clearly, this approach is limited by the incomplete knowledge on immunogenetic determinants of vaccine effectiveness as

well as the population and individual heterogeneity in vaccine-induced immunity. Therefore, the poor immune response in some individuals to vaccines remains unexplained.

Population based studies highlighted the relatively high percentages of vaccine failure and the possible role of genetic factors in that. It was found that ∼2–10% of individuals receiving the measles vaccine fail to produce protective immunity (3). Also, vaccination against rubella indicated that 2–5% of vaccinated individuals do not seroconvert. Not only that, but also those who respond to the vaccine showed a great variability in the immune response, which is believed to be heritable (4). Moreover, Hepatitis B vaccine failure was estimated to be 5–10% (5). Ganczak et al. reported an association between the homozygous genotype of CCR5Δ32 of the *CCR5* gene and reduced HBV vaccine immunogenicity (6). This genetic mutation exhibits a characteristic ethnical distribution, being more frequent in Europeans, and thus, may influence their response to the HBV vaccine. Inter-individual differences in response to Anthrax Vaccine Adsorbed (AVA) had also suggested the potential host genetic influences, as evidenced by the observed variability in the protective antigen-specific antibodies level between Europeans and African-Americans (7). Furthermore, genetic polymorphisms of the HLA, cytokines, innate immunity and viral receptor, and other genes, were found to account for almost 30% of the inter-individual variation in measles vaccine-specific humoral immunity (8).

It is now well-acknowledged that an individualized medicine approach mandates the integration of the mechanistic understanding of all the factors that could contribute to vaccine effectiveness, including host immunogenomics. This, in turn, aims to provide the right vaccine to the right patient, with the right reason, at the right dose (2). Although researches had begun looking into the host genetics, aiming to find immunogenomic clues to vaccine-response and factors behind vaccine failure, investigations in this field are still very limited.

The paradigm of personalized medicine has been applied in the current SARS-CoV-2 in an effort to understand the large clinical variability observed between individuals as well as populations. While several large-scale studies highlighted the crucial role of genetic diversity in response to COVID-19, the contribution of host genetics in response to SARS-CoV-2 vaccines is unknown. Importantly, the need for personalized approaches could be more crucial for SARS-CoV-2 vaccines compared to other vaccines. The reason behind this is the large inter-individual differences that was reported in response to SARS-CoV-2 infection, where host genetics factors showed to contribute to SARS-CoV-2 clinical variability and modulate response to infection. This variability could also be translated into vaccine responsiveness. Moreover, the global spread of SARS-CoV-2 pandemic, which in turn, led to the wide administration of SARS-CoV-2 vaccines, could increase the chance of low vaccine efficacy or high risk of adverse reactions at certain populations or individuals. Hence, it is significant to understand the immunogenetic factors underlying SARS-CoV-2 vaccine effectiveness and adverse responses at both individual and population levels.

Here, we review the role of genetics in response to vaccination to other pathogens, aiming to draw attention to this important field, especially that SARS-CoV-2 vaccines are currently being distributed and evaluated.

## OVERVIEW ON THE IMMUNE RESPONSE TO VIRAL INFECTIONS

It is well-known that immune responses to viral infections involve all arms of the immune system. This begins with pathogen recognition and antigen presentation and is then followed by a cascade of immune defense mechanisms of innate and adaptive immunity. The innate immune system is the first line of defense. It is triggered by encountering damage-associated molecular patterns (DAMPs) released from infected tissue or dead cells or pathogen-associated molecular patterns (PAMPs), such as viral RNA and DNA (9). Virally induced DAMPs and PAMPs stimulate tissue-resident macrophages and activate multiple innate immune pathways through Toll-Like receptors (TLRs), NLRP3/inflammasome activation, or by triggering cytoplasmic DNA sensors such as cGAS-STING and RIG-I-MAVS. This, in turn, derives the production of pro-inflammatory cytokines and chemokines, which subsequently leads to the stimulation of antiviral gene expression and the recruitment of more innate and adaptive immune cells for viral control and tissue hemostasis. The production of type I and type III interferons (IFNs) as a part of innate immunity initiates intracellular antiviral defense pathways while the release of IL-6 and IL-1β stimulates the recruitment of neutrophils and cytotoxic T cells (10). Paradoxically, the dysregulated inflammatory cascade initiated by macrophages could contribute to tissue damage leading to cytokine storm as previously reported from different viral infections, including SARS-CoV-2 (9).

Following and complementing the innate immune response, the adaptive immune system responds to pathogens by producing pathogen-specific humoral and cellular immunity, with T and B cells acting as the key players. T-cell mediated immune response represents an essential arm in mediating adaptive immunity to a variety of pathogens. Pathogen peptides presented by the MHC complexes on the surface of antigen-presenting cells (APCs), such as dendritic cells (DCs), stimulate the activation, proliferation, and differentiation of naïve $CD8^+$ and $CD4^+$ T-cells. Subsequently, these cells undergo clonal expansion by interleukin-2 (IL-2), and differentiate into effector T cells in the presence of a set of cytokines engaging and activating their respective cytokine receptors (11, 12). Importantly, achieving an effective viral clearance requires $CD8^+$ effector T cell-mediated killing of infected cells in addition to $CD4^+$ T cell-mediated enhancement of $CD8^+$ and B cell responses.

On the other hand, humoral immunity, particularly the production of neutralizing antibodies, is of a central importance in combating viral infections. It is evidenced that T-independent B cell response contribute substantially to highly stable antibody repertoires, providing humoral barriers to protect against invading pathogens. However, producing humoral memory through long-lived plasma cells that elicit specific antibodies of

adapted avidity and function is T-cell dependent (13). Taken together, an efficient immunological memory is achieved by the collective involvement of both T and B cells responses.

## OVERVIEW ON THE IMMUNE RESPONSE TO VACCINATION

The innate immune system can sense vaccines through the pattern-recognition receptors (PRRs), such as TLRs. For instance, the influenza virus live-attenuated vaccine activates plasmacytoid DCs (pDCs) *via* TLR7 (14). Another example is the yellow fever vaccine (YF-17D), which stimulates multiple TLRs on DCs, including TLR2, TLR3, TLR7, TLR8, and TLR9 (15). Importantly, it was shown that deficiency in any TLR substantially impaired the cytokine production in mice model (15). Vaccines based on synthetic nanoparticles containing TLR ligand have also shown to induce a synergistic enhancement of both the affinity of neutralizing antibodies as well as specialized T-cell responses (16). Most importantly, polymorphisms in TLR genes have been previously linked to immune response following vaccination. For example, variants in the *TLR3* gene and its associated signaling genes were associated with low measles antibody and lymphoproliferative immune responses in vaccinated individuals (17). This highlights the central role of TLRs in vaccine-induced innate and adaptive immunity.

Most vaccines are believed to confer protection by inducing B-cells mediated immunity that results in antibody production, although they can induce T cell responses as well. Polysaccharide vaccines, particularly, are completely T-cell independent, in contrast to vaccines based on proteins combined with polysaccharides, which can induce B and T cell responses (18). Recently, there has been an increasing interest in understanding the role of T cells in vaccine-induced protection; especially that antibodies level is not the only indicator of vaccine effectiveness. The main goal of any T-cell-based vaccine is to induce antigen-specific memory T cells. Following vaccination, naïve CD4+ T cells differentiate to functionally distinct populations of helper T cells (Th1, Th2, Th17, Th21, T follicular helper, Th22, or Th9), which are involved in different defense mechanisms. On the other hand, naïve CD8+ T cells can differentiate into effector cells, while memory T cells reside as precursor cells in lymphoid organs and differentiate rapidly to effector cells upon stimulation (14). New vaccine platforms such as lipid nanoparticles (LNP) based vaccines induce T cells responses that depend on the DC subsets and PRRs involved. For instance, mRNA-LNP vaccines have been shown to induce Th1 and T follicular helper cells (Tfh), most probably through the engagement of TLRs (19). Adenovirus vectors, on the other hand, are considered one of the most potent vaccines in inducing CD8+ T cell responses in addition to sustained B and CD4+ T cell responses (20). However, the absence of individual TLRs does not seem to affect antigen-specific CD8+ T cell responses elicited by adenovirus vectors, suggesting that this type of vaccine involves multiple redundant MyD88 (TLR adapter protein)-dependent signaling pathways (14).

## HETEROGENEITY IN VACCINE-INDUCED IMMUNE RESPONSE

The influence of host genetics on vaccine response occurs if polymorphisms or mutations exist in genes related directly or indirectly to the host immune response to the vaccine. This involves but is not limited to genes related to cellular receptors of viral proteins/adjuvants, antigen presentation, innate immunity (such as TLRs), signaling molecules, cytokine genes, cytokine receptor genes, HLA, immunoglobulin Gm and Km allotypes, vitamin A and D receptor genes, and many other genes (21). **Figure 1** illustrates the main pathways where genetic polymorphisms could modulate response to vaccination.

### Twin Studies

A considerable clue for the influence of genetics on vaccine- and natural-induced immunity comes from twin studies. These studies represented a pivotal model to differentiate genetics from environmental and other factors affecting immune response phenotypes. Heritability, which is estimated as the ratio of genetic variance to total variance within pairs, was used to assess genetics-vaccines associations (21). Using this approach, very early studies pinpointed the heritability to measles-mumps-rubella-II (MMRII) vaccine response. For instance, through examining the antibody level in 100 healthy twins who received MMRII vaccine, a study found that heritability to measles almost reached 90%, while heritability to rubella and mumps was 46 and 39%, respectively (22). Similarly, other reports evidenced the heritability of vaccine-induced antibody response to hepatitis viruses, ranging from 60% for recombinant hepatitis B surface antigen (HBsAg) vaccine, to 36% in the inactivated hepatitis A vaccine (23). Of note, only 40% of this heritability pattern was explained by HLA genes, compared to non-HLA genes, which contributed to 60% of the cases. This underscores the importance of exploring genetic polymorphisms with a broad prospect and at the whole genome level in order to better identify genetic factors contributing to vaccine responsiveness. Additional twin studies had confirmed the dominant role of non-HLA genes in the humoral response to vaccination to hepatitis B, oral polio, tetanus, and diphtheria, which all had high heritabilities (77, 60, 44, and 49%, respectively). In addition to the antibody response, interferon-$\gamma$ and interleukin-13 responses also showed a high degree of heritability to some BCG vaccine antigens (39–65%). Yet, these responses were mainly modulated by HLA class II genes (24). Taken together, these studies provided a glimpse on the importance of gene variation in the modulating the humoral immune response to different vaccines, and opened the door for a more comprehensive research in this field.

### Genome-Wide Association Studies

In recent years, the advancements in genomics and bioinformatics have paved the way for implementing genome-wide association studies (GWAS) to investigate the link between host genetics and response to vaccines. Several GWAS have

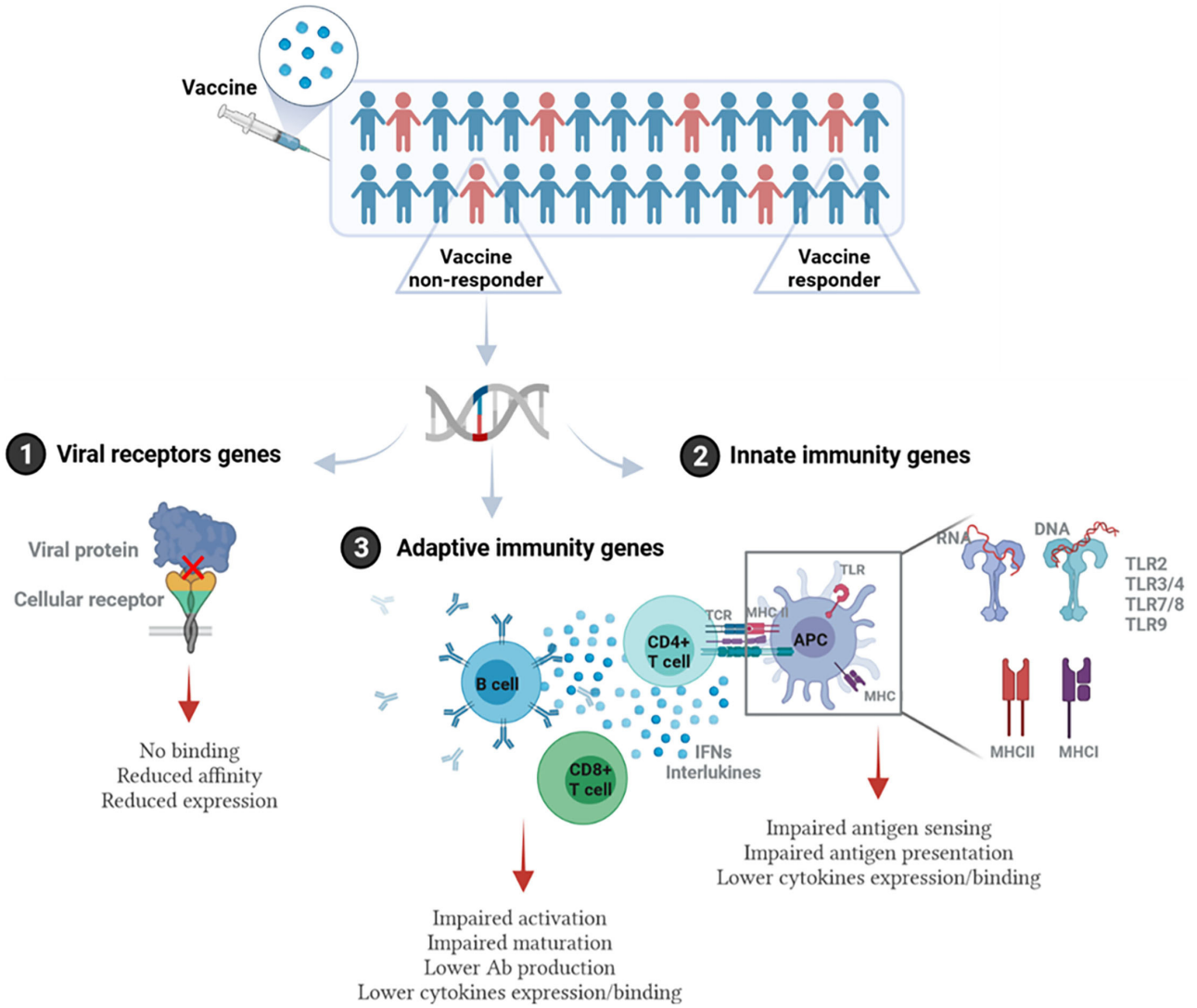


**FIGURE 1 |** Immunogenetic pathways involved in vaccine response. Individuals/populations with lower vaccine efficacy could carry genetic polymorphisms in: (1) Genes encoding viral receptors on the host cells. This could affect the binding affinity of viral antigen and cellular receptor, virus entry, or the level of receptor expression. (2) Genes related to the innate immunity. This includes genes encoding pathogen recognition receptors (PRRs) such as different types of TLRs, and MHC (HLA) genes that are essential for antigen presentation, as well as genes encoding cytokines and cytokine receptors. (3) Genes related to adaptive immune response such as T and B cell receptors, genes related to activation or differentiation of adaptive immune cells, and antibody production. This figure was generated using Biorender.

discovered single nucleotide polymorphisms (SNPs) in genes related to the innate and adaptive immune responses. However, despite the continuously growing number of vaccine-associated GWASs, these studies are either clustered within specific ethnic groups, or focused on a limited number of pathogens. Most of the currently available reports are on vaccine response to hepatitis B, measles, rubella, influenza A, smallpox, anthrax, and mumps (4, 5, 7, 25–29).

Overall, our search on "response to vaccine" phenotype at the GWAS catalog revealed various associations. The strongest genetic associations were linked to chromosome 6, particularly the HLA gene (**Figure 2**). Different associations, yet less significant, were found at different chromosomal locations, mapped to immune and non-immune related genes. **Table 1** summarizes all the vaccine-related studies registered at the GWAS catalog, while the detailed list of reported SNPs is presented in **Supplementary Table 1**. Remarkably, most (around 65%) of the studies were conducted on the European or Asian populations. Moreover, the main trait for phenotypic classification was the antibodies or cytokines level after vaccine administration. In addition to the GWAS catalog, we used "Open Targets Genetics" portal to search for genetic associations with vaccine response. **Figure 3** shows all the genes with an association score >0.11, along with

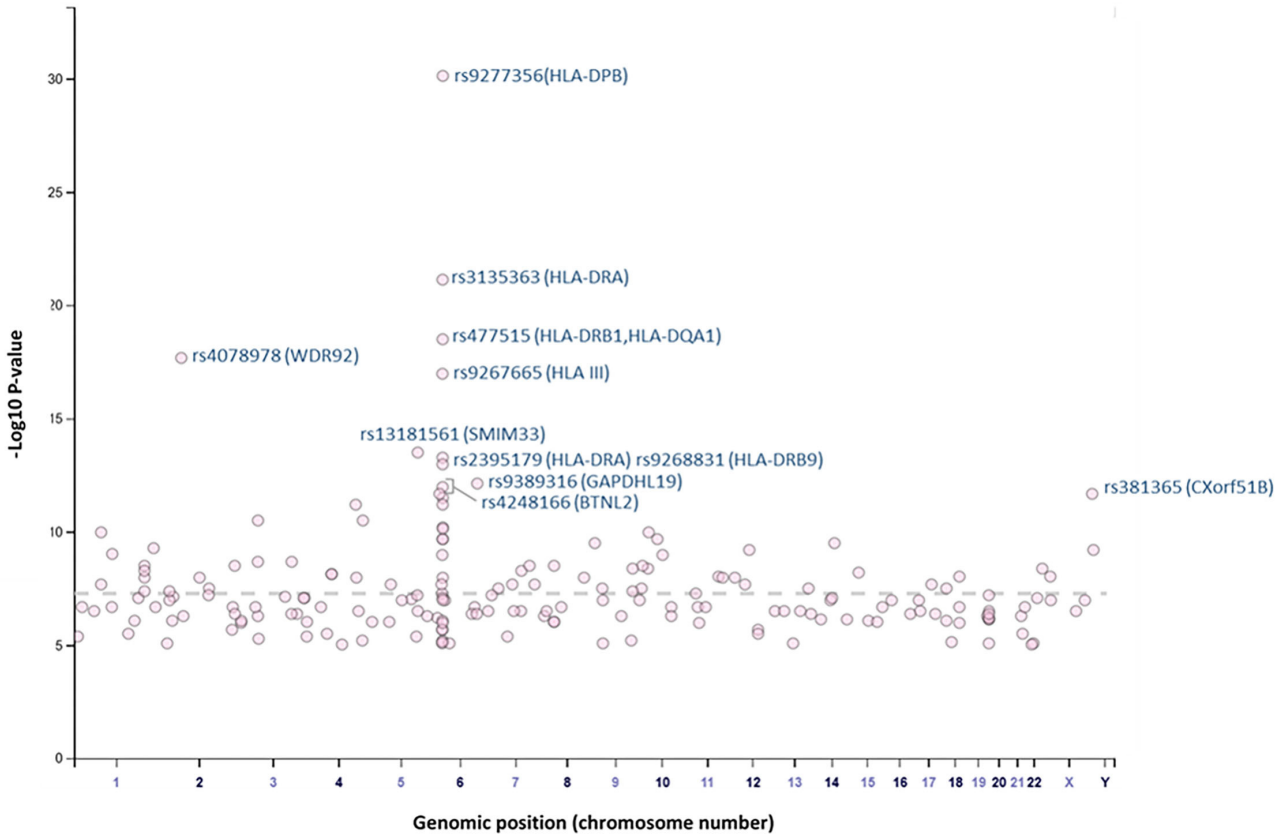


**FIGURE 2 |** Plot of GWAS Catalog associations for vaccine response related SNPs. The data and plot were retrieved from the GWAS catalog, an open database. All associations with "response to vaccine" phenotype are plotted. The top 10 SNPs are labeled with the rs identifiers.

the corresponding pathogen, while the details of the top 10 associations are summarized in **Supplementary Table 2**. This data again highlights the limitation in the currently available studies, as most of the significant associations are reported on few viruses only (smallpox, hepatitis B, measles, MMR, and rubella).

Using genotype-phenotype association approach, several highly significant SNPs were reported. These polymorphisms are located in genes that are linked directly or indirectly to the immune response. For instance, variants in the interferon-induced protein 44 like (*IFI44L*) and the cluster of differentiation 46 (*CD46*) genes were associated with measles-specific neutralizing antibody titers in response to MMR vaccine (3). *IFI44L* encoded proteins are stimulated by interferon type 1 and hence, are possibly involved in the innate immune response (3). On the other hand, CD46 glycoprotein is involved in the regulation of complement and antibody-mediated lysis. Additionally, it is a cellular receptor for attenuated measles virus strains, group B and D adenoviruses, human herpesvirus 6, bovine viral diarrhea virus, and other pathogens (34). Interestingly, variants in these two genes have been previously associated with adverse events/febrile seizures following MMR vaccination (28). Additionally, genetic variants in *IFI44L* have shown to increase the susceptibility of mice to Coxsackievirus B3 virus, confirming the possible association of this gene to innate immunity (35). Other GWA studies identified genetic variants that could modulate the adaptive immune responses to MMR vaccinations. Kennedy et al. reported significant associations in the protein tyrosine phosphatase delta (*PTPRD*) and the iron regulatory protein (*ACO1*) genes, in response to MMR vaccine (4). These variants explained the inter-individual variations in IFNγ response to rubella virus stimulation. However, the exact role of these genes in vaccine-response still requires further explanation. Additionally, a variant in the Wilms Tumor Gene (*WT1*) has been linked to rubella-specific interleukin 6 secretion following MMRII vaccination (30). Although *WT1* gene is not typically associated with immunity, it has been shown that it can directly bind to IL-10 promoter and induce IL-10 expression, which is important for tumor necrosis factor-α- (TNF- α) induced IL-10 stimulation in macrophages (36).

In addition to MMR, smallpox vaccine is one the commonly studied vaccines in the context of host genetics. Multiple GWAs identified genetic variants in genes that modulated the humoral (neutralizing antibodies) or cellular (cytokine secretion) following vaccination (31, 32). More than 50 significant

**TABLE 1 |** List of all GWA studies on vaccine response retrieved from the GWAS catalog as of June 2021.

| Vaccine against | Phenotype | Study title | Trait | No. of associations | Discovery sample size and ancestry | References |
|---|---|---|---|---|---|---|
| Rubella | Cellular immune response | Polymorphisms in the Wilms Tumor Gene Are Associated With Interindividual Variations in Rubella Virus-Specific Cellular Immunity After Measles-Mumps-Rubella II Vaccination. | Interferon-gamma secretion | 0 | 1,643 European | (30) |
| | | | Interleukin-6 secretion | 1 | 1,643 European 202 African American or Afro-Caribbean | |
| Hepatitis B | Antibody response | Key HLA-DRB1-DQB1 haplotypes and role of the BTNL2 gene for response to a hepatitis B vaccine. | Anti-HBV surface antigen IgG level | 20 | 1,193 East Asian | (5) |
| Hepatitis B | Antibody response | GWAS identifying HLA-DPB1 gene variants associated with responsiveness to hepatitis B virus vaccination in Koreans | Anti-HBV surface antigen IgG level | 1 | 6,867 East Asian | (25) |
| Measles-mumps-rubella | Cytokine production | Genome-wide SNP associations with rubella-specific cytokine responses in measles-mumps-rubella vaccine recipients. | IL-6 level | 2 | 883 European | (4) |
| | | | IFN gamma level | 8 | 883 European | |
| Measles | Neutralizing antibodies level | Genome-wide associations of CD46 and IFI44L genetic variants with neutralizing antibody response to measles vaccine. | IFN gamma level | 1 | 2,555 European | (3) |
| | | | Neutralizing antibodies titer | 6 | 317 African American or Afro-Caribbean | |
| Smallpox | Antibody response | Genome-wide association study of antibody response to smallpox vaccine. | IL-6 level | 37 | 580 European 217 African American or Afro-Caribbean 217 Hispanic or Latin American | (31) |
| Smallpox | Cytokine production | Genome-wide analysis of polymorphisms associated with cytokine responses in smallpox vaccine recipients. | Secreted IFN-alpha level | 32 | 512 European 199 African American or Afro-Caribbean | (32) |
| | | | Secreted IL-10 level | 6 | | |
| | | | Secreted IL-12p40 level | 10 | | |
| | | | Secreted IL-1beta level | 13 | | |
| | | | Secreted IL-2 level | 17 | | |
| | | | Secreted TNF-alpha level | 6 | | |
| | | | Secreted IL-6 level | 9 | | |
| Multiple vaccines | Antibody response | Common Genetic Variations Associated with the Persistence of Immunity following Childhood Immunization. | Haemophilus influenza type b polyribosylribitol phosphate IgG level | 0 | 967 European | (33) |
| | | | Meningococcal C functional antibody titers | 6 | 1,585 European | |
| | | | Meningococcal C IgG concentrations | 1 | 1,203 European | |
| | | | Tetanus toxoid IgG concentrations | 1 | 549 European | |

*(Continued)*

**TABLE 1** | Continued

| Vaccine against | Phenotype | Study title | Trait | No. of associations | Discovery sample size and ancestry | References |
|---|---|---|---|---|---|---|
| Anthrax | Antibody response | A genome-wide association study of host genetic determinants of the antibody response to Anthrax Vaccine Adsorbed. | Anti-protective antigen (PA) ab | 8 | 726 European | (7) |
| Hepatitis B | Antibody response | A genome-wide association study of hepatitis B vaccine response in an Indonesian population reveals multiple independent risk variants in the HLA region. | Anti HBs titer | 3 | 1,683 Asian unspecified | (27) |
| Hepatitis B | Antibody response | A genome-wide association study identifies polymorphisms in the HLA-DR region associated with non-response to hepatitis B vaccination in Chinese Han populations. | Anti HBs titer | 2 | 185 East Asian | (26) |

polymorphisms (reached the GWAS significance of $5 \times 10^{-8}$) in different genes have been reported (**Supplementary Table 1**). These variants were found to affect the levels of anti-smallpox antibodies, IFN-alpha, IL-10, IL-12p40, TNF-alpha, and IL-6 (31, 32). Importantly, many if these variants are located genes that have never been linked to immunity. Hence, the pathways by which these variants affect antibody and cytokines production is largely unknown, and necessitates additional functional characterization.

Considering that 5–10% of individuals who receive hepatitis B virus (HBV) vaccine fail to produce protective antibodies, several GWASs were conducted to investigate the genetic factors behind this variability (5). The most significant associations were linked to *HLA* polymorphisms. Multiple *HLA* alleles were associated with anti-hepatitis surface antigen IgG levels including *HLA-DPB1* and *HLA-DRAB5* and *HLA-DQA1* (5, 25–27). *HLA* genes are known to be the most polymorphic region of human genes, and encodes surface proteins which are essential in self and non-self-antigen presentation (37). Therefore, it is expected that certain *HLA* haplotypes correlate to response to vaccination. Notably, *HLA* genes have been linked to the susceptibility or resistance of multiple infections, including HBV, SARS-CoV, and SARS-CoV-2 (38–40). In Addition to *HLA* types, significant associations were found in other genes such as the Butyrophilin Like 2 (*BTNL2*) gene, which is involved in the regulation of T cell activation (5, 41).

## GENETICS AND VACCINE ADVERSE EVENTS

In the past decade, a new terminology, called "Adversomics" has been introduced by Whitaker et al. (42). This term refers to the study of vaccine-related adverse reactions using immunogenomics and systems biology approaches (42). Typically, the design of vaccines is based on stimulating the immune system to an antigen. This usually induces an inflammatory reaction, which ranges from a mild local to a serious systematic adverse reaction in rare cases. Indeed, vaccine adverse effects—whether real or unreal- have been one of the major barriers in public acceptance and trust in vaccines. Thus, the identification of factors that contribute to the unwanted vaccine adverse effects is crucial to increase the safety as well as to maintain public trust in vaccines.

It is well-acknowledged now that heterogeneity in vaccine response is a multifactorial trait influenced by external (environmental), and internal (host immunogenetics) factors. However, the field of adversomics is still relatively new compared to other fields and only a very few studies has been conducted so far (**Table 2**). Additionally, multiple studies that looked into the underlying genetic factors in individuals experiencing adverse effects did not report any GWAS significant associations (45). This could be attributed to the small sample sizes, which reflects the infrequency of serious adverse vaccines or the complexity of such analysis. On the other hand, few significant associations were found and replicated. For instance, Hallberg et al., reported a novel association between Pandemrix

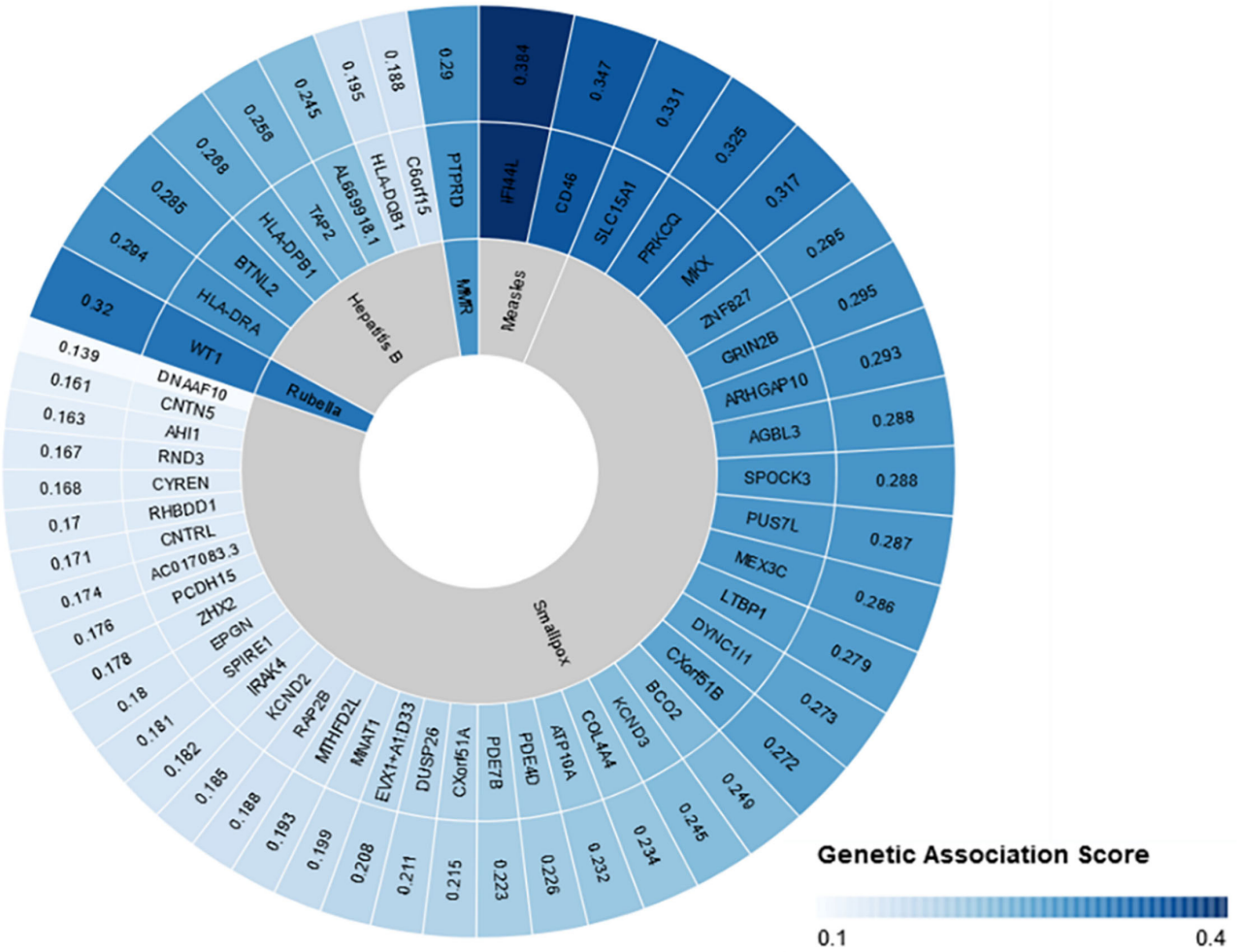


**FIGURE 3 |** Open Targets genetics association scores for genes linked to vaccine response. Open target platform was used to search for all the associations under "response to vaccine" phenotype. The top 50 associations are plotted with the association score, the name of the corresponding gene, and the pathogen name to which vaccine was given. This figure was generated using Rawgraphs.

(influenza vaccine)-induced narcolepsy and the non-coding RNA gene (*GDNF-AS1*) (29). This gene is involved in regulating the expression of GDNF and have been linked to neurodegenerative diseases (29). Similarly, a GWAS identified significant risk variants for developing febrile seizures following MMR vaccine (28). These variants are located in *CD46* and *IFI44L* genes, and have also been linked to the humoral immune response to MMR vaccine as mentioned earlier. Rare variants have also played a major underlying factor in life-threatening disease following vaccinations with live-attenuated vaccines. For instance, inborn errors of IFN-γ, B-cell Immunity, IFN-α/β and IFN-λ, and adaptive immunity, were leading to Bacille Calmette-Guerin (BCG), oral poliovirus (OPV), vaccine measles virus (vMeV), and Oral rotavirus vaccine (ORV) diseases, respectively (49).

Taken together, these studies, as well as others, reveal an important insight on the role of common and rare genetic variants in vaccine-related adverse events and underscore the need for more and larger studies.

# IMMUNOGENOMICS AND VACCINOMICS OF SARS-COV-2

## Immune Response to SARS-CoV-2 Infection

SARS-CoV-2 primarily attacks the respiratory system leading to pneumonia and lymphopenia in severe disease. However, in most cases, a 1-week, self-limiting respiratory disease occurs (50). Viral antigens, recognized by pathogen recognition receptors (PRRs), mainly TLR 3, 7, and 8, induce the enhanced production of IFNs. Similar to other coronaviruses, viral antigens trigger the development of antibody production, as well as CD4+ and CD8+ T-cells immunity.

Generally, SARS-CoV-2 infection leads to the production of anti-N and anti-S antibodies, with antibodies targeting the receptor-binding domain (RBD, in S1) being crucial for viral neutralization (51). Studies showed that most SARS-CoV-2 patients seroconvert, and neutralizing antibodies (nAbs) activity

**TABLE 2 |** List of all genome wide associaitons on vaccine adverse events.

| Vaccine against | Type of vaccine | Phenotype | Region | Main annotated gene | References |
|---|---|---|---|---|---|
| SARS-CoV-2 | mRNA vaccines: Pfizer/BioNTech (BNT162b1) and Moderna (mRNA-1273) | Vaccine-related adverse events: severe/extreme difficulties with daily routine | 6p22.1 | *HLA-A*03:01* | (43) |
| SARS-CoV-2 | mRNA vaccines: Pfizer/BioNTech (BNT162b1) and Moderna (mRNA-1273) | Vaccine-related adverse events: | Multiple | Multiple genes including: *HLA, NOTCH4*, and *RPS18* | (44) |
| Influenza | Pandemrix | Vaccine-related adverse events: narcolepsy | 5p13.2 | *(GDNF) anti-sense 1 (AS1)* | (29) |
| Influenza | Intranasal trivalent live attenuated influenza vaccine (LAIV) intramuscular trivalent inactivated vaccine (TIV) | Vaccine-related adverse events: Wheezing | 1q23.2 | *CRP - AL445528.1* | (45) |
| | | Vaccine-efficacy: Influenza infection | 7p11.2 | *LINC02854 - AC092848.2* | |
| Measles-mumps-rubella | Priorix or MMR II | Vaccine-related febrile seizures | 1p31.1 | *IFI44L* | (28) |
| | | | 1q32.2 | *CD46, CD34* | |
| Smallpox | Aventis Pasteur Smallpox vaccine | Fever, generalized rash, lymphadenopathy | 1p36.3 | *THFR* | (46) |
| | | | 5q31.1 | *IRF1* | |
| | | | 5q31.1 | *IRF1* | |
| Smallpox | Dryvax | Fever, acute Vaccinia syndrome | Multiple | *IL1, IL4*, and *IL18* | (47) |
| Yellow fever | YF-17D | Viscerotropic disease - Persistent viremia, | Multiple | *CCR5* and its ligand *RANTES* | (48) |
| Yellow fever | YF-17D | Viscerotropic and Neurotropic disease | Multiple | *RANTES, IL-6, IL-8, MIG, GRO, MCP-1, TGF-β,* and *TNF-β* | (43) |

persists up to 6 months (51, 52). Interestingly, although there is an evidence of the beneficial role of nAb in protection against SARS-CoV-2, the peak-neutralizing activity was found to correlate positively with disease severity (52, 53). In fact, despite the numerous amount of studies in this field, there is still a knowledge gap in understanding the durability and effect of these antibodies on disease outcomes and re-infection.

A growing evidence highlights the important role of T-cell immunity in SARS-CoV-2, especially in patients with an underdeveloped humoral response. It was previously found that in contrast to anti- SARS-CoV-1 antibodies that wane after 2–3 years, T-cell responses are long lasting, and can be detected up to 17 years post recovery (54, 55). T-cells recognize viral peptides that are presented on the MHC class I (HLA in humans), which stimulates cytokine release and cytotoxic activity of CD8+ T cells (56). MHC class II can also present antigens to CD4+ T cells (56).

Importantly, as HLA system is known to be highly polymorphic, some haplotypes were found to influence individuals' susceptibility to many infections by modulating the immune response (37, 57). Certain polymorphisms at these loci encode for cell receptors that could lower the binding efficiency to some viral peptides and, therefore, blunt the immune system's normal defenses against the virus in vulnerable individuals (58).

## Heterogeneity in Response to SARS-CoV-2 Infection

Since the start of the current SARS-CoV-2 pandemic, scientists have been puzzling over the factors underlying the inter-individual and inter-population differences in COVID-19 clinical manifestations. Although the infection with SARS-CoV-2 principally attacks the respiratory system, it can also trigger a systematic immune reaction that leads to multiple organ failure. According to the reported data, SARS-CoV-2 can lead to extra-pulmonary diseases, including renal dysfunction, gastrointestinal complications, liver dysfunction, cardiac manifestations, mediastinal findings, neurological abnormalities, and hematological manifestations (59). Epidemiologists have identified age as the main factor for developing COVID-19 related complications, especially among patients over 65 years of age (60). On the other hand, younger individuals (<20 years) almost exclusively experienced another severe condition that has been linked to COVID-19, which is Multisystem Inflammatory Syndrome (MIS-C), that mimics Kawasaki disease (KD) (60). Importantly, this condition is believed to occur in genetically predisposed children following exposure to trigger such as viral infection (61, 62). Besides, black and Hispanic children showed an increase risk of developing MIS-C (63). Although this could be due to the increased burden of SARS-CoV-2 in the black and Hispanic populations, it does not rule out the possible role of population genetics in influencing SARS-CoV-2 related diseases.

Although inter-host clinical variability is the rule in the course of any human infection, the response to SARS-CoV-2 showed a great variability that was not explained by the commonly known factors such as age, sex, and comorbidities. While more than 80% experience mild/asymptomatic illness, 20% experience severe respiratory syndrome, which further progresses to critical illness requiring ventilation in 5% (64). Importantly, severe clinical presentation was observed even in young and previously healthy individuals (65). Hence, neither age nor the lack of comorbidity can guarantee a mild manifestation of the infection. In a study that investigated the transmission of SARS-CoV-2 among asymptomatic carriers, it was shown that family members who are living together tend to develop severe infection (66). This suggested the potential role of genetics in the manifestation of COVID-19.

The striking heterogeneity in the response to SARS-CoV-2 highlighted the crucial need to comprehend the underlying causes of interindividual differences, including host genetics. This area of research has expanded by the combined efforts of global consortiums as well as individual efforts. For instance, the COVID-19 Human Genetics Effort was rapidly launched at the beginning of this pandemic. Their aim was to identity monogenic errors of immunity that could lead to severe COVID-19 in young individuals who were previously well and developed life-threatening disease, such as pneumonia or MIC-S (67). On the contrary, the Host Genetics Initiative (HGI) was established to support the collection and sharing of GWAS data and results to understand the common variants contributing to susceptibility and severity to COVID-19 (68). These two groups, as well as others, have identified several genetic determinants that affect the response to SARS-CoV-2 infection.

The first case report that identified rare variants linked to COVID-19 applied rapid whole-exome sequencing approach on four young male patients (below 35 years) who had a severe SARS-CoV-2 infection. The study revealed rare putative loss-of-function variants of X-chromosomal *TLR7*, which resulted in impaired type I and II IFN responses (65). Additional following studies had also highlighted the role of variants related to IFN signaling in severe COVID-19. Using a larger sample size, Zhang et al. performed whole-genome or exome sequencing of 659 and 534 with life-threatening and mild SARS-CoV-2, respectively. Inborn errors of *TLR3*, interferon regulatory factor 7 (*IRF7*), and interferon regulatory factor 9 (*IRF9*) genes were investigated in life-threatening COVID-19 pneumonia patients who were previously healthy. These genes were selected as they were previously linked to critical influenza-associated pneumonia. The study identified rare variants predicted to be loss-of-function (LOF) related to TLR3- and IRF7-dependent type I IFN immunity in patients with severe SARS-CoV-2 infection (69). Notably, patients who had these mutations or had neutralizing autoantibodies to type I IFNs showed lower levels of IFNs, which possibly contributed to increased viral replication and pathogenesis (70).

On the other hand, the Host Genetics Initiative (HGI) provides the largest set of GWA studies and meta-analyses in history. The latest release (R6 – June 2021) included 125,584 SARS-CoV-2 cases and over 2.56 million controls. A total of 23 genome-wide significant loci ($P < 5 \times 10^{-8}$) were found to either associate with disease susceptibility (7 loci) or disease severity (16 loci). These variants were located in multiple genes related to viral entry, host immune response, lung function, and others. The severity lead variant was located in chromosome 3 (rs35508621), that is in LD with *LZTFL1* and has *CXCR6* as

the highest gene prioritized by OpenTargetGenetics'V2G. The *LZTFL1* gene is involved in regulating protein trafficking to ciliary membranes and has a role in immune response, while *CXCR6* plays a role in chemokine signaling (71, 72). The most statistically significant variant on chromosome 1 was rs67579710, which was also associated with COVID-19 severity. This is an intronic variant in Thrombospondin 3 (*THBS3*) gene, which is related to lung function. Similarly, genetic variants in *SFTPD* (rs721917), *SLC22A31* (rs117169628), *FOXP4* (rs41435745), and *MUC5B* (rs35705950), which are all related to lung function and lung diseases, have been significantly associated with COVID-19 severity. *SFTPD* gene encodes the surfactant protein D (SP-D) that has a role in the innate immunity, while SLC22A31 belongs to the family of solute carrier proteins, and predicted to enable transmembrane transporter activity (73, 74). *FOXP4* is expressed in the proximal and distal airway epithelium and variants within this region have been linked to lung diseases (75, 76). MUC5B, on the other hand, produces a major gel-forming mucin in the lung which is important in mucociliary clearance (MCC) and host defense (77). *MUC5B* variant increases the expression of MUC5B in the lung, and therefore could provide a protective effect against SARS-CoV-2 progression (78). Furthermore, multiple other SNPs exhibited significant associations with severe COVID-19, including rs77534576 (*TAC4*), rs111837807 (*CCHCR1*), rs766826 (*ELF5)*, rs10774679 (*OAS1/OAS3/OAS2*), rs12809318 (*FBRSL1*), rs61667602 (*CRHR1*), rs2109069 (*DPP9*), rs11085727 (*TYK2*), rs1405655 (*NR1H2*), and rs13050728 (*IFNAR2*). Most of these genes have a role in the innate immune response, or lung inflammation. For instance, *TAC4* gene product has a role in blood pressure regulation, and in immune responses (72). *OAS* gene cluster, primarily *OAS3*, encodes for antiviral restriction enzyme activators that lead to degradation of viral ssRNA as a protective mechanism against viruses (79). Interestingly, the locus in OAS1/2/3 cluster, which has been associated with severe COVID-19 among individuals of European ancestry, has a protective haplotype of ∼75 kilobases (kb) derived from Neanderthals (80). This haplotype was associated with a ∼22% reduction in relative risk of becoming severely ill with COVID-19. *IFNAR2*, which encodes for interferon receptor, is critical for the antiviral host response. Mutation in the *IFNAR2* was reported to associate with critical illness in COVID-19 in a previous GWAS as well (81). *DPP9* and *TYK2*, on the other hand, are related to host-driven inflammatory lung injury, which is a main mechanism of late, life-threatening COVID-19 (81). Other genes, such as *ELF5* and *FBRSL1* have no previously reported lung trait associations, and therefore, will need further mechanistic characterization to understand their role in severe COVID-19.

In addition to severity, multiple variants were linked to susceptibility to SARS-CoV-2. A variant near *ACE2* gene (rs190509934) was significantly associated with acquiring SARS-CoV-2. On note, *ACE2* functionally interacts with *SLC6A20*, another gene that harbor a significantly associated SNP with SARS-CoV-2 susceptibility (rs73062389). Other significant SNPs were located near *NXPE3* gene on chromosome 3 (rs17412601), *PLEKHA4* on chromosome 19 (rs4801778), and *HLA-DPA1/HLA-DPB1* (rs2071351). These variants, along with the previously identified region in the *ABO* gene (at chromosome 9, rs505922), are likely modulating susceptibility to infection but not progression to a severe form (82, 83).

Besides the HGI, multiple GWA studies conducted by other consortia as well as independent research and genomics services groups identified SARS-CoV-2 related host genetic variants that influence SARS-CoV-2 outcomes, some of which were replicated in the HIG (78). It has been shown that genes related to renin-angiotensin-aldosterone system (RAAS); including the *ACE1* and *ACE2* gene polymorphisms, contribute to COVID-19 pathogenesis (84). Importantly, SARS-CoV-2 binding to the ACE2 receptor on cell surface requires cellular proteases that facilitate fusion between the virus membrane and the cell membrane, such as the TMPRSS2. Genetic polymorphisms in cellular proteases were suggested to affect SARS-CoV-2 susceptibility in various populations through *in silico* and *in vivo* studies (85, 86).

There is an accumulating evidence on the association of HLA with SARS-CoV-2 from various studies. However, many studies were unreproducible as they reported results of *in-silico* analysis, or were limited by small sample size and variability in participants' genetic ancestries. For instance, using *in-silico* analysis, it was reported that HLA-A*02:01 is associated with an increased risk of COVID-19. HLA-A*02:01 showed a relatively lower capacity to present SARS-CoV-2 antigens in comparision to other HLA class I molecules (87). In contrast, a later study that included 111 deceased COVID-19 patients and 428 volunteers reported that HLA-A*02:01, in addition to HLA-A*03:01 contributed to lower risk of severe COVID-19 (88). Another study conducted among 182 Sardinian SARS-CoV-2 patients suggested that the extended haplotype HLA-A*02:05, B*58:01, C*07:01, DRB1*03:01 has a protective effect against SARS-CoV-2 infection, in contrast to HLA-DRB1*08:01 allele which was associated with hospitalization (89). HLA-C*04:01 has been also suggested to correlate with severe clinical course of COVID-19 in a study on 435 patients from different countries (90). Additionally, a retrospective analysis on 265 Italian cohort showed that HLA-DRB1*08 was more frequent in SARS-CoV-2 infected patients, and correlated with mortality (91). Another small-size study on Italians ($n = 99$) reported that HLA-DRB1*15:01, -DQB1*06:02 and -B*27:07 were associated with severe COVID-19 (92). Despite highlighting the potential role of HLA genomics in COVID-19, these studies, as well as numerous others, necessitate validation and replication in larger cohorts. Notably, the latest findings of largest GWAS on SARS-CoV-2 by the HGI, reported multiple *HLA* related variants that associated with SARS-CoV-2 outcomes (73). Particularly, five variants (top SNP rs111837807) reached genome-wide statistical significance were located in the Coiled-Coil Alpha-Helical Rod Protein 1 (CCHCR1) gene, which is 110 kb downstream of HLA-C. These variants were associated with SARS-CoV-2 severity. Moreover, a variant within HLA-DPB1 3'UTR (rs2071351) was significantly associated with disease susceptibility (73).

A consistent feature of the SARS-CoV-2 pandemic is the male bias in disease severity (93). Remarkably, TMPRSS2 expression is regulated by the androgen receptor (AR) in non-prostatic tissues. This could be reason behind the high susceptibility of men to progress to severe COVID-19 (94). Delanghe et al. suggested

that Y-chromosome haplogroup might influence SARS-CoV-2 outcomes, considering its role in immune and inflammatory responses (95). Nevertheless, the interaction between the AR, TMPRSS2, and Y-chromosome polymorphisms and their effect on COVID-19 outcomes is still not well-addressed.

In fact, any polymorphism located in genes related directly or indirectly to the host immune response could be associated with SARS-CoV-2 outcomes. Genetic variants in genes encoding the complement component 3 (C3), Interleukin-37, and vitamin D binding protein (DBP), were also suggested as factors influencing SARS-CoV-2 outcomes (96–98).

It is worth noting that host genetics studies did not only highlight the role of genetics in the inter-individual heterogeneity in response to SARS-CoV-2, but also added additional insights on the great differences in population genetics structure. For instance, a variant that was identified close to *FOXP4* and correlated with COVID-19 severity has a frequency that is largely variable between different populations. This variant is considered rare in Europeans, with a frequency of 1% in the population, compared to East-Asian (39%) and Hispanic/Latino (18%) populations (99). These results, as well as future genetic studies, could help in identifying the factors behind the inter-population differences in response to infections.

## Immune Response to SARS-CoV-2 Vaccines

Immediately after the release of SARS-CoV-2 genetic sequence, a race for developing a vaccine has started. Over 100 SARS-CoV-2 vaccines are at different stages of clinical development (100). Most of these vaccine candidates are based on the spike (S) protein, or part of it, considering its essential role in virus entry. Multiple platforms have been utilized in the vaccine design, including using non-replicating viral vectors, inactivated whole-virus, protein subunit, messenger RNA (mRNA), and DNA-based vaccines. At present, three vaccines (Pfizer-BioNTech BNT162b2, Moderna mRNA-1273, and Janssen Ad26.CoV2.S) had already received the emergency use authorization (EUA) from the U.S. Food and Drug Administration (FDA). Six other vaccine candidates are approved under EUA in different other countries (AstraZeneca, Novavax, CureVac, Sputnik V, Sinovac, Sinopharm) (101). Additionally, Pfizer, Moderna, Janssen, and AstraZeneca vaccines have received the European Medicines Agency (EMA) approval of use in the European Union, while multiple other vaccine candidates are still under EMA review (102).

Despite the fact that vaccines play a vital role in infection control and SARS-CoV-2 is no exception, the profound differences in response to SARS-CoV-2 raise the question of whether this clinical variability will also appear in response to vaccines. Importantly, different vaccine candidates induce different immune responses. Therefore, the response to vaccination could be modulated by distinct host immunogenetic determinants that are unique to that vaccine structure.

The two SARS-CoV-2 mRNA vaccines developed by Pfizer-BioNTech and Moderna were the first to enter the race, considering the speed of cloning and synthesis. These two vaccines were also the first to receive the approval for emergency use and are currently being widely distributed and administered (103). Both vaccines are lipid nanoparticle formulated nucleoside-modified mRNAs, encoding the pre-fusion SARS-CoV-2 full-length S protein with proline substitutions and produce combined adaptive humoral and cellular immune responses (51). Vaccination with BNT162b2 (Pfizer-BioNTech) elicits potent anti-S IgG antibodies after a single dose, and neutralizing antibodies at day 29 (7 days post-boost). Additionally, an S-specific CD8+ and T helper type 1 (Th1) CD4+ T cells response was observed in 91.9 and 94.1% respectively (104). Moreover, the expression of IFNγ and IL-2 and only minimal expression of IL-4 in BNT162b2-induced CD4+ T cells confirmed a Th1 response and the absence of the potentially harmful Th2 immune response (104). Similarly, Moderna mRNA-1273 vaccine elicited and immune response after the first dose that was boosted by the second injection. High titers of binding and neutralizing anti-S antibodies post-boost, which was accompanied with a dominant Th1 CD4+, but a minimal CD8+ T-cell response (105). From the clinical trials, Pfizer-BioNTech and Moderna-mRNA-1273 reported an overall vaccine efficacy of 94.1 and 94.6% respectively (101).

With a close but lower vaccine efficacy than mRNA vaccines, AstraZeneca and Johnson/Janssen vaccines were constructed utilizing adenoviral vectors that expresses the full-length SARS-CoV-2 spike protein. Given that there is pre-existing immunity to around 70 types of human adenoviruses, AstraZeneca (AZD1222) vaccine uses a chimpanzee-derived adenovirus (ChAdOx) to circumvent the concern of pre-existing immunity. This vaccine induced the production of neutralizing antibodies in 91% and 100% of participants after prime and boost doses, respectively. Moreover, T-cell immune response was induced, peaking at 14 days post-vaccination, as measured through IFN-γ enzyme-linked immunosorbent spot assay (106). Importantly, overall vaccine efficacy in preventing COVID-19 ranged between 62 and 90% as a result of multiple factors including the diverse ethnicity of the study population (107).

Similarly, Janssen vaccine (Ad26.COV2.S) was based on a recombinant, replication deficient adenovirus (Ad26) encoding a full-length and stabilized spike protein. This vaccine elicited humoral and cellular immune responses following a single dose. Neutralizing antibodies were detected in 90 and 100% of participants at days 29 and 57, respectively. Additionally, 76–83% of participants showed CD4+T-cell responses that induced the favorable polarized (Th1 over Th2) immune response. Moreover, CD8+ T-cell responses were detected in 51–64% of participants (108). The overall efficacy of the Ad26.CoV2.S vaccine was 72% in the US; 66% in Latin America, and 57% in South Africa (101).

Other vaccine candidates, which are either in-use or in different stages of clinical trials include inactivated vaccine derived from virus propagated in culture and then chemically inactivated. The inactivated virus expresses viral proteins that are conformationally native to the wild-type virus. Sinopharm and Sinovac are examples of SARS-CoV-2 inactivated vaccines produced in China. Despite the safety concerns related to such vaccines, including the risk of antibody-dependent enhancement, it was reported that these vaccines are safe and relatively

efficient (Sinopharm: 79 and 86%—Sinovac: 78, 65, and 91.25% depending on dosing and population) (101). Nonetheless, several concerns have grown recently with regard to the real efficacy of these two vaccines. Countries where Sinovac and Sinopharm vaccines were used are still suffering from increase in COVID-19 cases, as recently reported from Mongolia, where half the people have received are vaccinated with Sinopharm (109).

Another vaccine platform that is currently used but classically has safety-related concerns is recombinant protein based vaccine. This type of vaccines has a potential risk of inducing the unfavorable Th2 biased immune response. However, this can be overcome with the use of appropriate adjuvants. Novavax vaccine (NVX-CoV2373) is an example of recombinant protein vaccine, which is composed of recombinant full-length, pre-fusion S protein with saponin-based Matrix-M adjuvant. The use of this adjuvant enhances the immune response and elicits high levels of neutralizing antibodies (110). The vaccine recorded an overall efficacy of 89.3% in UK and 60% in South Africa phase 3 clinical trials. Recently, the results of a larger clinical trial in the US and Mexico (involving almost 30,000 participants) showed an overall efficacy of 90.4% (111).

The immune response does not depend on the type of vaccine only (inactivated virus, mRNA, DNA, or protein subunit), but also on the type of adjuvant. Adjuvants are needed to activate the innate immune response through pattern recognition receptors (PRRs), which recognize pathogen-associate molecular patterns (PAMPs) (112). Depending on the type of vaccine, adjuvants can be endogenous or exogenous. Vaccines that are based on live-attenuated or killed whole virus usually contain an endogenous adjuvant that is sufficient to induce an adaptive immune response. Likewise, mRNA- and DNA-based vaccines contain an endogenous adjuvant which is the genomic material itself, yet, they require a lipid or polymer-based nanoparticles that acts as a protective vehicle to improve the vaccine uptake into cells (113). On the other hand, antigen based vaccines such as recombinant proteins require an adjuvant that acts as innate immune stimulator (114).

## Genetics and Response to SARS-CoV-2 Vaccines

Considering that SARS-CoV-2 vaccines are still new, studies on the immunogenetic determinants of vaccine efficacy are very limited. Theoretically, genetic polymorphisms in genes of the innate and adaptive immune system influence the individual response to vaccines, and SARS-CoV-2 vaccines are no exception. Actually, personalized approaches in SARS-CoV-2 vaccines are probably more important than in other vaccines, given the large inter-individual differences in response to SARS-CoV-2 infection. Analysis of host genetics factors contributing to SARS-CoV-2 clinical variability revealed a set of genetic variants that modulate response to infection. These variants could also contribute to vaccine responsiveness. For instance, a large-scale GWAS study has reported that a rare variant in the *ACE2* gene down-regulated ACE2 expression, and hence, reduces the risk of COVID-19 (115). Such variants could also modulate the response to vaccines that are based on live attenuated virus, if they depend on the interaction between ACE2 and SARS-CoV-2 spike protein. This hypothesis is not new, since genetic polymorphisms in genes coding two measles receptors, the signaling lymphocyte activation molecule (*SLAM*), and membrane cofactor protein (*CD46*), were reported to influence the immune response to live measles virus vaccination (21). These polymorphisms were hypothesized to modify measles virus binding, virus entry, or affect the level of receptor expression (116).

In addition to that, genetic mutations in genes related to pathogen sensing/recognition (e.g., TLRs), antigen presentation (e.g., HLA), and activation/maturation of lymphocytes could also affect vaccine efficacy. Multiple vaccine candidates use adjuvants as innate immune simulators, such as Novavax (protein subunit vaccine used with Matrix-M-adjuvant), Sinovac and Sinopharm vaccines (inactivated virus with aluminum hydroxide adjuvant), and BBV152 (inactivated virus with aluminum hydroxide gel adjuvant TLR7/8 agonist chemisorbed Algel) (117). These adjuvants could stimulate the activation of the pro-inflammatory NLRP3 pathway, or act as TLR7/8 agonists, bridging the innate and adaptive immune responses (118). Given the clear evidence of the genetics influencing response to vaccines to other viruses as we described above, it is of a great interest to explore whether variants in genes involved in antigen/adjuvants recognition and the subsequent immune response also contribute to SARS-CoV-2 vaccine success. Of note, rare variants in TLR3 and TLR7 have been already linked to COVID-19 in previous reports (65, 69). Therefore, they could influence response to vaccination as well.

In fact, despite the very promising data from clinical trials and real-word figures on SARS-CoV-2 vaccine efficacy, there are still a number of vaccine non-responders. Out of 52,280 hospital admissions in the UK during the second wave, 3,842 patients have received at least the first dose of a COVID-19 vaccination. This indicates that out of every 14 patients admitted to the hospital admission, one patients is at least partially vaccinated (119). Moreover, researchers reported 113 deaths among vaccinated individuals. Importantly, the majority of deaths occurred among the elderly group who were at risk of severe COVID-19. Additionally, most of the hospitalizations occurred in the 1–14 days post vaccination where immunity is not fully protective. However, there is still a number of hospitalized patients more than 21 days post-vaccination (120). This, indeed, requires further investigation to identify and understand the mechanism behind vaccine failure in this group, including the role of genetic factors.

Another critical area to explore is the effect of population genetics on SARS-CoV-2 vaccine efficacy. Notably, Black, Asian, and minority ethnic groups showed an increase in the risk of severe COVID-19 compared to other populations. Yet, despite being the most affected, these groups are relatively under-represented in vaccine trials published so far (121). Definitely, there have been great efforts to encourage the participation of these groups in vaccine clinical trials, but there is still smaller proportion of minority groups compared to other populations. For instance, out of the 552 participants in phase 2/3 Oxford–AstraZeneca trial (UK), only one participant (0.18%) was Black, and 19 (3.4%) were Asians. Moreover, the larger phase 3 interim results of the same vaccine (11,636 participants) indicated that

only 0.1–0.7% and 10.4–11.1% of participants were Black in the UK and Brazil trials, respectively. Asians, on the other hand, represented 4.3–5.7% in the UK trial, and 2.6% in Brazil trial (107). Pfizer and Moderna randomized, controlled trials also indicated the underrepresentation of these groups. While more than 30,000 participants were included in each vaccine trial, Black and Asians represented 9.3 and 4.3% in Pfizer trial, compared to 10.2 and 4.6% in Moderna trial, respectively (121–123). Using machine-learning predictions, a study suggested that SARS-CoV-2 subunit peptides may not be robustly displayed by the MHC molecules in certain populations (124). SARS-CoV-2 vaccines developed by Moderna, Pfizer, AstraZeneca, and others, may not protect individuals of non-European genetic ancestries (such as Africans or Asians) at the same level of protection as in white people (58, 124). Given the significant role of population genetic structure in shaping the response to infection and vaccination, it is important to ensure the adequate inclusion of these populations in clinical trials as well as in immunogenomics and vaccinomics studies. Furthermore, it was reported that race and ethnicity information are missing from the data reported to the CDC during the 1st month of vaccination in the US (125). Indeed, collecting ethnicity information during vaccination is essential for population stratification to evaluate the vaccine efficacy accurately.

Immunogenetic factors may influence vaccine effectiveness and could contribute to vaccine adverse events as well. This has been evidenced from studies on influenza, MMR, smallpox, and yellow fever vaccines (28, 43, 45, 46, 48). Current data indicated minor side effects of mRNA and viral vector based vaccines, such as headache, fever, fatigue, and body aches. However, studies reporting serious side effects started to emerge, including vaccine-induced immune thrombotic thrombocytopenia and neurological disorders (126, 127). This is in fact not surprising, because as large populations become vaccinated, it is possible for rare side events to appear. Additionally, while most vaccine-related side effects would be expected to appear during the first few weeks to months after vaccination, long-term effects may also occur (103). Whether these serious side effects are associated with other underlying undiagnosed conditions or are resulting from certain genetic causes, this requires further investigation. Until now, there are only two studies that investigated the genetics of reactions to SARS-CoV-2 vaccines. The first GWAS included 17,440 participants who were queried about their reactions to SARS-CoV-2 vaccination (128). Results revealed a significant association of HLA-A∗03:01 and chills, fever, fatigue, and generally feeling unwell. Of note, this association was statistically significant only for those who received the Pfizer-BioNTech vaccine, in comparison to Moderna vaccine which showed a smaller effect size. The second GWAS (in preprint) was conducted on 4,545 Japanese individuals and identified 14 associated loci with vaccine side effects (44). These loci, especially 6p21, were associated with the expression of many genes related to the immune response, including *HLA* genes, which were previously associated with SARS-CoV-2 outcomes. This study also revealed multiple associations with genes related to immunity, such as *NOTCH4* and *RPS18*. Of note, a variant in *NOTCH4* gene has been previously associated with critical illness in COVID-19 (81). These studies highlight again the importance of investigating the immunogenetic determinants of SARS-CoV-2 vaccine response in order to understand the factors shaping vaccine adverse reactions and effectiveness. Whether other host genetic variants that were associated with susceptibility or severity of SARS-CoV-2 are also effecting the response to immunization, this requires further research.

Previous reports showed the possible risk of serious vaccine adverse events in individuals with rare inborn errors of immunity (IEI), particularly with the administration of live attenuated viral vaccines. For example, live polio vaccine was linked to paralytic polio in patients with agammaglobulinaemia (129). Impaired IFN immunity has also been linked to severe illness following yellow fever or MMR vaccines in patients with IFNAR1, IFNAR2 or STAT1 and STAT2 deficiencies, respectively (130). Again, this raises the question of SARS-CoV-2 vaccine responsiveness in patients with IEI. Even if the risk of serious illness from live attenuated vaccine was reduced with the use of other vaccine platforms that have better safety (such as mRNA or protein subunit vaccines), still, these patients might not develop complete protection. In a recent study on the immunogenicity of SARS-CoV-2 vaccines on IEI patients, it was shown that vaccination on IEIs is safe, but immunogenicity is affected by specific therapies and genetic defects (131). In common variable immunodeficiency (CVID) patients, which is a condition that can be caused by genetic mutations in immune-related genes, the response to SARS-CoV-2 vaccines was different from response to infection (132). Vaccination with two doses of mRNA vaccine did not generate spike-specific memory B cells (MBCs), but atypical memory B cells (ATM) with low binding capacity to spike protein, in contrast to vaccination after natural SARS-CoV-2 infection, which generated spike-specific MBCs. Spike-specific T-cells responses were also induced in CVID patients with different rates (132). These studies highlight the importance of finding a suitable immunization strategy that ensures eliciting an adequate protection in patients with inborn errors of immunity, which could be different from strategy applied on healthy individuals. This might include the use of additional booster doses and combining different vaccines/adjuvants in order to produce broad immunity. Also, it is important to track patients with deficient humoral or cellular response to vaccine and investigate if there are any genetic errors responsible for their impaired immunity. Nonetheless, it is worth mentioning that the current use of advanced vaccine platforms and constructs, which are based on eliciting both humoral and cellular response, could help in inducing protective immunity in IEI patients, at least partially. Yet, additional studies are needed to evaluate the effectiveness of the current vaccines and estimate the durability of protection in individuals with different immunogenetic profiles.

## FUTURE PROSPECTIVE AND CONCLUSION

Current findings underline the significant role of immunogenomics in SARS-CoV-2 clinical variability. Data from research on other viruses also provided insights on the impact of immunogenomics in vaccine response. Now, with multiple SARS-CoV-2 vaccines being administered around the

world, we have to be prepared to address important questions such as 1- Are individuals with a genetic predisposition to severe COVID-19 also at risk of serious SARS-CoV-2 vaccine-related adverse events? 2- What are the factors contributing to the inter-individual and inter-population variability in vaccine response? 3- Are there variants linked to SARS-CoV-2 vaccine-induced antibody secretion as previously reported from other viruses? 4- Are there host genetic biomarkers that can be used to predict vaccine efficacy in the future? 5- Can heterologous prime boost doses offer immunological advantages in providing protection to multi-ethnic populations? While we do understand the challenges in addressing these questions, and more importantly, the difficulty in the translational implications of this area of research, we believe that in the future, we could have genetic markers identified as predictors of SARS-CoV-2 infection and vaccine response. Hopefully, these markers would guide health care providers in the process of selecting the best treatment, and probably the most suitable vaccine for an individual or a specific ethnic group.

## AUTHOR CONTRIBUTIONS

HY and MS conceived and designed the study. MS wrote the first draft of the manuscript. HA and AA proofread and revised the manuscript. All authors contributed to the article and approved the submitted version.

## FUNDING

This work was supported by the Qatar University High Impact Grant (Grant Number: QUHI-BRC-20_21-1) and Student Grant (Grant Number: QUST-1-BRC-2022-399).

## SUPPLEMENTARY MATERIAL

The Supplementary Material for this article can be found online at: https://www.frontiersin.org/articles/10.3389/fmed.2022.802312/full#supplementary-material

## REFERENCES

1. Worldometers. *COVID-19 Coronavirus Pandemic*. (2022). Available online at: https://www.worldometers.info/coronavirus/#countries (accessed February 21, 2022).
2. Poland GA, Ovsyannikova IG, Kennedy RB. Personalized vaccinology: a review. *Vaccine*. (2018) 36:5350–7. doi: 10.1016/j.vaccine.2017.07.062
3. Haralambieva IH, Ovsyannikova IG, Kennedy RB, Larrabee BR, Zimmermann MT, Grill DE, et al. Genome-wide associations of CD46 and IFI44L genetic variants with neutralizing antibody response to measles vaccine. *Hum Genet*. (2017) 136:421–35. doi: 10.1007/s00439-017-1768-9
4. Kennedy RB, Ovsyannikova IG, Haralambieva IH, Lambert ND, Pankratz VS, Poland GA. Genome-wide SNP associations with rubella-specific cytokine responses in measles-mumps-rubella vaccine recipients. *Immunogenetics*. (2014) 66:493–9. doi: 10.1007/s00251-014-0776-3
5. Nishida N, Sugiyama M, Sawai H, Nishina S, Sakai A, Ohashi J, et al. Key HLA-DRB1-DQB1 haplotypes and role of the BTNL2 gene for response to a hepatitis B vaccine. *Hepatology*. (2018) 68:848–58. doi: 10.1002/hep.29876
6. Ganczak M, Skonieczna-Zydecka K, Drozd-Dabrowska M, Adler G. Possible impact of 190G > A CCR2 and Δ32 CCR5 mutations on decrease of the HBV vaccine immunogenicity-a preliminary report. *Int J Environ Res Public Health*. (2017) 14:20166. doi: 10.3390/ijerph14020166
7. Pajewski NM, Shrestha S, Quinn CP, Parker SD, Wiener H, Aissani B, et al. A genome-wide association study of host genetic determinants of the antibody response to Anthrax Vaccine Adsorbed. *Vaccine*. (2012) 30:4778–84. doi: 10.1016/j.vaccine.2012.05.032
8. Haralambieva IH, Ovsyannikova IG, Pankratz VS, Kennedy RB, Jacobson RM, Poland GA. The genetic basis for interindividual immune response variation to measles vaccine: new understanding and new vaccine approaches. *Expert Rev Vaccines*. (2013) 12:57–70. doi: 10.1586/erv.12.134
9. Subbarao K, Mahanty S. Respiratory virus infections: understanding COVID-19. *Immunity*. (2020) 52:905–9. doi: 10.1016/j.immuni.2020.05.004
10. Vardhana SA, Wolchok JD. The many faces of the anti-COVID immune response. *J Exp Med*. (2020) 217:678. doi: 10.1084/jem.20200678
11. Zhu J, Yamane H, Paul WE. Differentiation of effector CD4 T cell populations. *Annu Rev Immunol*. (2010) 28:445–89. doi: 10.1146/annurev-immunol-030409-101212
12. Lukacs NW, Malinczak CA. Harnessing cellular immunity for vaccination against respiratory viruses. *Vaccines*. (2020) 8:40783. doi: 10.3390/vaccines8040783
13. Dörner T, Radbruch A. Antibodies and B cell memory in viral immunity. *Immunity*. (2007) 27:384–92. doi: 10.1016/j.immuni.2007.09.002
14. Pulendran B, Ahmed R. Immunological mechanisms of vaccination. *Nat Immunol*. (2011) 12:509–17. doi: 10.1038/ni.2039
15. Querec T, Bennouna S, Alkan S, Laouar Y, Gorden K, Flavell R, et al. Yellow fever vaccine YF-17D activates multiple dendritic cell subsets *via* TLR2, 7, 8, and 9 to stimulate polyvalent immunity. *J Exp Med*. (2006) 203:413–24. doi: 10.1084/jem.20051720
16. Kasturi SP, Skountzou I, Albrecht RA, Koutsonanos D, Hua T, Nakaya HI, et al. Programming the magnitude and persistence of antibody responses with innate immunity. *Nature*. (2011) 470:543–7. doi: 10.1038/nature09737
17. Dhiman N, Ovsyannikova IG, Vierkant RA, Ryan JE, Pankratz VS, Jacobson RM, et al. Associations between SNPs in toll-like receptors and related intracellular signaling molecules and immune responses to measles vaccine: preliminary results. *Vaccine*. (2008) 26:1731–6. doi: 10.1016/j.vaccine.2008.01.017
18. Pollard AJ, Bijker EM. A guide to vaccinology: from basic principles to new developments. *Nat Rev Immunol*. (2021) 21:83–100. doi: 10.1038/s41577-020-00479-7
19. Samaridou E, Heyes J, Lutwyche P. Lipid nanoparticles for nucleic acid delivery: current perspectives. *Adv Drug Deliv Rev*. (2020) 154–5:37–63. doi: 10.1016/j.addr.2020.06.002
20. Hasanpourghadi M, Novikov M, Ertl HCJ. COVID-19 vaccines based on adenovirus vectors. *Trends Biochem Sci*. (2021) 46:429–30. doi: 10.1016/j.tibs.2021.03.002
21. Poland GA, Ovsyannikova IG, Jacobson RM. Vaccine immunogenetics: bedside to bench to population. *Vaccine*. (2008) 26:6183–8. doi: 10.1016/j.vaccine.2008.06.057
22. Tan PL, Jacobson RM, Poland GA, Jacobsen SJ, Pankratz VS. Twin studies of immunogenicity–determining the genetic contribution to vaccine failure. *Vaccine*. (2001) 19:2434–9. doi: 10.1016/S0264-410X(00)00468-0
23. Höhler T, Reuss E, Evers N, Dietrich E, Rittner C, Freitag CM, et al. Differential genetic determination of immune responsiveness to hepatitis B surface antigen and to hepatitis A virus: a vaccination study in twins. *Lancet*. (2002) 360:991–5. doi: 10.1016/S0140-6736(02)11083-X
24. Newport MJ, Goetghebuer T, Weiss HA, Whittle H, Siegrist CA, Marchant A, et al. Genetic regulation of immune responses to vaccines in early life. *Genes Immun*. (2004) 5:122–9. doi: 10.1038/sj.gene.6364051
25. Chung S, Roh EY, Park B, Lee Y, Shin S, Yoon JH, et al. GWAS identifying HLA-DPB1 gene variants associated with responsiveness to hepatitis B virus vaccination in Koreans: independent association of HLA-DPB1*04:02

possessing rs1042169 G - rs9277355 C - rs9277356 A. *J Viral Hepat.* (2019) 26:1318–29. doi: 10.1007/978-981-13-0050-9
26. Pan L, Zhang L, Zhang W, Wu X, Li Y, Yan B, et al. A genome-wide association study identifies polymorphisms in the HLA-DR region associated with non-response to hepatitis B vaccination in Chinese Han populations. *Hum Mol Genet.* (2014) 23:2210–9. doi: 10.1093/hmg/ddt586
27. Png E, Thalamuthu A, Ong RT, Snippe H, Boland GJ, Seielstad M, et al. genome-wide association study of hepatitis B vaccine response in an Indonesian population reveals multiple independent risk variants in the HLA region. *Hum Mol Genet.* (2011) 20:3893–8. doi: 10.1093/hmg/ddr302
28. Feenstra B, Pasternak B, Geller F, Carstensen L, Wang T, Huang F, et al. Common variants associated with general and MMR vaccine-related febrile seizures. *Nat Genet.* (2014) 46:1274–82. doi: 10.1038/ng.3129
29. Hallberg P, Smedje H, Eriksson N, Kohnke H, Daniilidou M, Öhman I, et al. Pandemrix-induced narcolepsy is associated with genes related to immunity and neuronal survival. *EBioMedicine.* (2019) 40:595–604. doi: 10.1016/j.ebiom.2019.01.041
30. Voigt EA, Haralambieva IH, Larrabee BL, Kennedy RB, Ovsyannikova IG, Schaid DJ, et al. Polymorphisms in the wilms tumor gene are associated with interindividual variations in rubella virus-specific cellular immunity after measles-mumps-rubella II vaccination. *J Infect Dis.* (2018) 217:560–6. doi: 10.1093/infdis/jix538
31. Ovsyannikova IG, Kennedy RB, O'Byrne M, Jacobson RM, Pankratz VS, Poland GA. Genome-wide association study of antibody response to smallpox vaccine. *Vaccine.* (2012) 30:4182–9. doi: 10.1016/j.vaccine.2012.04.055
32. Kennedy RB, Ovsyannikova IG, Pankratz VS, Haralambieva IH, Vierkant RA, Poland GA. Genome-wide analysis of polymorphisms associated with cytokine responses in smallpox vaccine recipients. *Hum Genet.* (2012) 131:1403–21. doi: 10.1007/s00439-012-1174-2
33. O'Connor D, Png E, Khor CC, Snape MD, Hill AVS, van der Klis F, et al. Common genetic variations associated with the persistence of immunity following childhood immunization. *Cell Rep.* (2019) 27:3241–53.e3244. doi: 10.1016/j.celrep.2019.05.053
34. Cattaneo R. Four viruses, two bacteria, and one receptor: membrane cofactor protein (CD46) as pathogens' magnet. *J Virol.* (2004) 78:4385–8. doi: 10.1128/JVI.78.9.4385-4388.2004
35. Wiltshire SA, Leiva-Torres GA, Vidal SM. Quantitative trait locus analysis, pathway analysis, and consomic mapping show genetic variants of Tnni3k, Fpgt, or H28 control susceptibility to viral myocarditis. *J Immunol.* (2011) 186:6398–405. doi: 10.4049/jimmunol.1100159
36. Sciesielski LK, Kirschner KM, Scholz H, Persson AB. Wilms' tumor protein Wt1 regulates the Interleukin-10 (IL-10) gene. *FEBS Lett.* (2010) 584:4665–71. doi: 10.1016/j.febslet.2010.10.045
37. Naranbhai V, Carrington M. Host genetic variation and HIV disease: from mapping to mechanism. *Immunogenetics.* (2017) 69:489–98. doi: 10.1007/s00251-017-1000-z
38. Mbarek H, Ochi H, Urabe Y, Kumar V, Kubo M, Hosono N, et al. A genome-wide association study of chronic hepatitis B identified novel risk locus in a Japanese population. *Hum Mol Genet.* (2011) 20:3884–92. doi: 10.1093/hmg/ddr301
39. SeyedAlinaghi S, Mehrtak M, MohsseniPour M, Mirzapour P, Barzegary A, Habibi P, et al. Genetic susceptibility of COVID-19: a systematic review of current evidence. *Eur J Med Res.* (2021) 26:46. doi: 10.1186/s40001-021-00516-8
40. Tavasolian F, Rashidi M, Hatam GR, Jeddi M, Hosseini AZ, Mosawi SH, et al. HLA, immune response, and susceptibility to COVID-19. *Front Immunol.* (2020) 11:601886. doi: 10.3389/fimmu.2020.601886
41. Nguyen T, Liu XK, Zhang Y, Dong C. BTNL2, a butyrophilin-like molecule that functions to inhibit T cell activation. *J Immunol.* (2006) 176:7354–60. doi: 10.4049/jimmunol.176.12.7354
42. Whitaker JA, Ovsyannikova IG, Poland GA. Adversomics: a new paradigm for vaccine safety and design. *Expert Rev Vaccines.* (2015) 14:935–47. doi: 10.1586/14760584.2015.1038249
43. Bae HG, Domingo C, Tenorio A, de Ory F, Muñoz J, Weber P, et al. Immune response during adverse events after 17D-derived yellow fever vaccination in Europe. *J Infect Dis.* (2008) 197:1577–84. doi: 10.1086/587844
44. Nogawa S, Kanamori H, Tokuda K, Kawafune K, Chijiiwa M, Saito K, et al. Identification of susceptibility loci for adverse events following COVID-19 vaccination in the Japanese population: a web-based genome-wide association study. *medRxiv.* (2021) 2021:2021.11.30.21267043. doi: 10.1101/2021.11.30.21267043
45. Miller EK, Dumitrescu L, Cupp C, Dorris S, Taylor S, Sparks R, et al. Atopy history and the genomics of wheezing after influenza vaccination in children 6-59 months of age. *Vaccine.* (2011) 29:3431–7. doi: 10.1016/j.vaccine.2011.02.071
46. Reif DM, McKinney BA, Motsinger AA, Chanock SJ, Edwards KM, Rock MT, et al. Genetic basis for adverse events following smallpox vaccination. *J Infect Dis.* (2008) 198:16–22. doi: 10.1086/588670
47. Stanley SL, Frey SE, Taillon-Miller P, Guo J, Miller RD, Koboldt DC, et al. The immunogenetics of smallpox vaccination. *J Infect Dis.* (2007) 196:212–9. doi: 10.1086/518794
48. Pulendran B, Miller J, Querec TD, Akondy R, Moseley N, Laur O, et al. Case of yellow fever vaccine–associated viscerotropic disease with prolonged viremia, robust adaptive immune responses, and polymorphisms in CCR5 and RANTES genes. *J Infect Dis.* (2008) 198:500–7. doi: 10.1086/590187
49. Pöyhönen L, Bustamante J, Casanova JL, Jouanguy E, Zhang Q. Correction to: life-threatening infections due to live-attenuated vaccines: early manifestations of inborn errors of immunity. *J Clin Immunol.* (2019) 39:527. doi: 10.1007/s10875-019-00653-0
50. Azkur AK, Akdis M, Azkur D, Sokolowska M, van de Veen W, Brüggen M-C, et al. Immune response to SARS-CoV-2 and mechanisms of immunopathological changes in COVID-19. *Allergy.* 75:1564–81. doi: 10.1111/all.14364
51. Koch T, Mellinghoff SC, Shamsrizi P, Addo MM, Dahlke C. Correlates of vaccine-induced protection against SARS-CoV-2. *Vaccines.* (2021) 9:30238. doi: 10.3390/vaccines9030238
52. Xu X, Nie S, Wang Y, Long Q, Zhu H, Zhang X, et al. Dynamics of neutralizing antibody responses to SARS-CoV-2 in patients with COVID-19: an observational study. *Signal Transduct Target Ther.* (2021) 6:197. doi: 10.1038/s41392-021-00611-6
53. Zhang J, Wu Q, Liu Z, Wang Q, Wu J, Hu Y, et al. Spike-specific circulating T follicular helper cell and cross-neutralizing antibody responses in COVID-19-convalescent individuals. *Nat Microbiol.* (2021) 6:51–8. doi: 10.1038/s41564-020-00824-5
54. Le Bert N, Tan AT, Kunasegaran K, Tham CYL, Hafezi M, Chia A, et al. SARS-CoV-2-specific T cell immunity in cases of COVID-19 and SARS, and uninfected controls. *Nature.* (2020) 584:457–62. doi: 10.1038/s41586-020-2550-z
55. Cao WC, Liu W, Zhang PH, Zhang F, Richardus JH. Disappearance of antibodies to SARS-associated coronavirus after recovery. *N Engl J Med.* (2007) 357:1162–3. doi: 10.1056/NEJMc070348
56. Shah VK, Firmal P, Alam A, Ganguly D, Chattopadhyay S. Overview of immune response during SARS-CoV-2 infection: lessons from the past. *Front Immunol.* (2020) 11:1949. doi: 10.3389/fimmu.2020.01949
57. Blackwell JM, Jamieson SE, Burgner D. HLA and infectious diseases. *Clin Microbiol Rev.* (2009) 22:370–85. doi: 10.1128/CMR.00048-08
58. Valdés-Fernández BN, Duconge J, Espino AM, Ruaño G. Personalized health and the coronavirus vaccines-do individual genetics matter? *Bioessays.* (2021) 43:e2100087. doi: 10.1002/bies.202100087
59. Behzad S, Aghaghazvini L, Radmard AR, Gholamrezanezhad A. Extrapulmonary manifestations of COVID-19: radiologic and clinical overview. *Clin Imaging.* (2020) 66:35–41. doi: 10.1016/j.clinimag.2020.05.013
60. Rasmussen SA, Abul-Husn NS, Casanova JL, Daly MJ, Rehm HL, Murray MF. The intersection of genetics and COVID-19 in 2021: preview of the 2021 Rodney Howell Symposium. *Genet Med.* (2021) 23:1001–3. doi: 10.1038/s41436-021-01113-0
61. Kim KY, Kim DS. Recent advances in Kawasaki disease. *Yonsei Med J.* (2016) 57:15–21. doi: 10.3349/ymj.2016.57.1.15
62. Kabeerdoss J, Pilania RK, Karkhele R, Kumar TS, Danda D, Singh S. Severe COVID-19, multisystem inflammatory syndrome in children, and Kawasaki disease: immunological mechanisms, clinical manifestations and management. *Rheumatol Int.* (2021) 41:19–32. doi: 10.1007/s00296-020-04749-4

63. Lee EH, Kepler KL, Geevarughese A, Paneth-Pollak R, Dorsinville MS, Ngai S, et al. Race/ethnicity among children with COVID-19-associated multisystem inflammatory syndrome. *J Am Med Assoc Netw Open.* (2020) 3:e2030280. doi: 10.1001/jamanetworkopen.2020.30280
64. CDC. *Interim Clinical Guidance for Management of Patients with Confirmed Coronavirus Disease (COVID-19)*. (2020). Available online at: https://www.cdc.gov/coronavirus/2019-ncov/hcp/clinical-guidance-management-patients.html (accessed June, 2021).
65. van der Made CI, Simons A, Schuurs-Hoeijmakers J, van den Heuvel G, Mantere T, Kersten S, et al. Presence of genetic variants among young men with severe COVID-19. *J Am Med Assoc.* (2020) 324:663–73. doi: 10.1001/jama.2020.13719
66. Hu Z, Song C, Xu C, Jin G, Chen Y, Xu X, et al. Clinical characteristics of 24 asymptomatic infections with COVID-19 screened among close contacts in Nanjing, China. *Sci China Life Sci.* (2020) 63:706–11. doi: 10.1007/s11427-020-1661-4
67. covidhge.com. *The COVID Human Genetic Effort*. (2021). Available online at: https://www.covidhge.com/ (accessed June, 2021).
68. covid19hg.org. *COVID-19 Host Genetics Initiative*. Available online at: https://www.covid19hg.org/blog/ (accessed June, 2021).
69. Zhang Q, Bastard P, Liu Z, Le Pen J, Moncada-Velez M, Chen J, et al. Inborn errors of type I IFN immunity in patients with life-threatening COVID-19. *Science*. (2020) 370:abd4570. doi: 10.1126/science.abd4570
70. Bastard P, Rosen LB, Zhang Q, Michailidis E, Hoffmann HH, Zhang Y, et al. Autoantibodies against type I IFNs in patients with life-threatening COVID-19. *Science*. (2020) 370:abd4585. doi: 10.1126/science.abd4585
71. Xiao G, Wang X, Wang J, Zu L, Cheng G, Hao M, et al. CXCL16/CXCR6 chemokine signaling mediates breast cancer progression by pERK1/2-dependent mechanisms. *Oncotarget*. (2015) 6:14165–78. doi: 10.18632/oncotarget.3690
72. Marttila M, Faucon A, Vadgama N, Andrews S, Wolford B, Veerapen K. *COVID-19 HGI*. (2021). Available online at: https://www.covid19hg.org/blog/2021-03-02-freeze-5-results/ (accessed June, 2021).
73. Initiative C-HG, Ganna A. Mapping the human genetic architecture of COVID-19: an update. *medRxiv*. (2021) 2021:2021.11.08.21265944. doi: 10.1101/2021.11.08.21265944
74. Hediger MA, Romero MF, Peng JB, Rolfs A, Takanaga H, Bruford EA. The ABCs of solute carriers: physiological, pathological and therapeutic implications of human membrane transport proteinsIntroduction. *Pflugers Arch.* (2004) 447:465–8. doi: 10.1007/s00424-003-1192-y
75. Manichaikul A, Wang XQ, Sun L, Dupuis J, Borczuk AC, Nguyen JN, et al. Genome-wide association study of subclinical interstitial lung disease in MESA. *Respir Res.* (2017) 18:97. doi: 10.1186/s12931-017-0581-2
76. Lu MM Li S, Yang H, Morrisey EE. Foxp4: a novel member of the Foxp subfamily of winged-helix genes co-expressed with Foxp1 and Foxp2 in pulmonary and gut tissues. *Mech Dev.* (2002) 119(Suppl.1):S197–202. doi: 10.1016/S0925-4773(03)00116-3
77. Evans CM, Fingerlin TE, Schwarz MI, Lynch D, Kurche J, Warg L, et al. Idiopathic pulmonary fibrosis: a genetic disease that involves mucociliary dysfunction of the peripheral airways. *Physiol Rev.* (2016) 96:1567–91. doi: 10.1152/physrev.00004.2016
78. Velavan TP, Pallerla SR, Rüter J, Augustin Y, Kremsner PG, Krishna S, et al. Host genetic factors determining COVID-19 susceptibility and severity. *EBioMedicine*. (2021) 72:103629. doi: 10.1016/j.ebiom.2021.103629
79. Li Y, Banerjee S, Wang Y, Goldstein SA, Dong B, Gaughan C, et al. Activation of RNase L is dependent on OAS3 expression during infection with diverse human viruses. *Proc Natl Acad Sci USA*. (2016) 113:2241–6. doi: 10.1073/pnas.1519657113
80. Zeberg H, Pääbo S. A genomic region associated with protection against severe COVID-19 is inherited from Neandertals. *Proc Natl Acad Sci USA*. (2021) 118:pnas.2026309118. doi: 10.1073/pnas.2026309118
81. Pairo-Castineira E, Clohisey S, Klaric L, Bretherick AD, Rawlik K, Pasko D, et al. Genetic mechanisms of critical illness in COVID-19. *Nature.* (2021) 591:92–8. doi: 10.1038/s41586-020-03065-y
82. Ganna A. Mapping the human genetic architecture of COVID-19 by worldwide meta-analysis. *medRxiv*. (2021) 2021:2021.03.10.21252820. doi: 10.1101/2021.03.10.21252820
83. Ellinghaus D, Degenhardt F, Bujanda L, Buti M, Albillos A, Invernizzi P, et al. Genomewide association study of severe covid-19 with respiratory failure. *N Engl J Med.* (2020) 383:1522–34. doi: 10.1056/NEJMoa2020283
84. Calabrese C, Annunziata A, Coppola A, Pafundi PC, Guarino S, Di Spirito V, et al. ACE gene I/D polymorphism and acute pulmonary embolism in COVID-19 pneumonia: a potential predisposing role. *Front Med.* (2020) 7:631148. doi: 10.3389/fmed.2020.631148
85. Saengsiwaritt W, Jittikoon J, Chaikledkaew U, Udomsinprasert W. Genetic polymorphisms of ACE1, ACE2, and TMPRSS2 associated with COVID-19 severity: a systematic review with meta-analysis. *Rev Med Virol*. (2022) 2022:e2323. doi: 10.1002/rmv.2323
86. Al-Mulla F, Mohammad A, Al Madhoun A, Haddad D, Ali H, Eaaswarkhanth M, et al. *ACE2* and *FURIN* variants are potential predictors of SARS-CoV-2 outcome: a time to implement precision medicine against COVID-19. *Heliyon.* (2021) 7:e06133. doi: 10.1016/j.heliyon.2021.e06133
87. Tomita Y, Ikeda T, Sato R, Sakagami T. Association between HLA gene polymorphisms and mortality of COVID-19: an *in silico* analysis. *Immun Inflamm Dis.* (2020) 8:684–94. doi: 10.1002/iid3.358
88. Shkurnikov M, Nersisyan S, Jankevic T, Galatenko A, Gordeev I, Vechorko V, et al. Association of HLA class I genotypes with severity of coronavirus disease-19. *Front Immunol.* (2021) 12:641900. doi: 10.3389/fimmu.2021.641900
89. Littera R, Campagna M, Deidda S, Angioni G, Cipri S, Melis M, et al. Human leukocyte antigen complex and other immunogenetic and clinical factors influence susceptibility or protection to SARS-CoV-2 infection and severity of the disease course. The Sardinian experience. *Front Immunol.* (2020) 11:605688. doi: 10.3389/fimmu.2020.605688
90. Weiner J, Suwalski P, Holtgrewe M, Rakitko A, Thibeault C, Müller M, et al. Increased risk of severe clinical course of COVID-19 in carriers of HLA-C*04:01. *EClinicalMedicine.* (2021) 40:101099. doi: 10.1016/j.eclinm.2021.101099
91. Amoroso A, Magistroni P, Vespasiano F, Bella A, Bellino S, Puoti F, et al. HLA and AB0 polymorphisms may influence SARS-CoV-2 infection and COVID-19 severity. *Transplantation.* (2021) 105:193–200. doi: 10.1097/TP.0000000000003507
92. Novelli A, Andreani M, Biancolella M, Liberatoscioli L, Passarelli C, Colona VL, et al. HLA allele frequencies and susceptibility to COVID-19 in a group of 99 Italian patients. *HLA*. (2020) 96:610–4. doi: 10.1111/tan.14047
93. Peckham H, de Gruijter NM, Raine C, Radziszewska A, Ciurtin C, Wedderburn LR, et al. Male sex identified by global COVID-19 meta-analysis as a risk factor for death and ITU admission. *Nat Commun.* (2020) 11:6317. doi: 10.1038/s41467-020-19741-6
94. Montopoli M, Zumerle S, Vettor R, Rugge M, Zorzi M, Catapano CV, et al. Androgen-deprivation therapies for prostate cancer and risk of infection by SARS-CoV-2: a population-based study ($N = 4532$). *Ann Oncol.* (2020) 31:1040–5. doi: 10.1016/j.annonc.2020.04.479
95. Delanghe JR, De Buyzere ML, De Bruyne S, Van Criekinge W, Speeckaert MM. The potential influence of human Y-chromosome haplogroup on COVID-19 prevalence and mortality. *Ann Oncol.* (2020) 31:1582–4. doi: 10.1016/j.annonc.2020.08.2096
96. Ahmed AA, Ad'hiah AH. Interleukin-37 gene polymorphism and susceptibility to coronavirus disease 19 among Iraqi patients. *Meta Gene.* (2022) 31:100989. doi: 10.1016/j.mgene.2021.100989
97. Delanghe JR, De Buyzere ML, Speeckaert MM. C3 and ACE1 polymorphisms are more important confounders in the spread and outcome of COVID-19 in comparison with ABO polymorphism. *Eur J Prev Cardiol.* (2020) 27:1331–2. doi: 10.1177/2047487320931305
98. Shao B, Jiang S, Muyiduli X, Wang S, Mo M, Li M, et al. Vitamin D pathway gene polymorphisms influenced vitamin D level among pregnant women. *Clin Nutr*. (2018) 37:2230–7. doi: 10.1016/j.clnu.2017.10.024
99. Nasir J, Wolford B, Veerapen K. *COVID-19 HGI Results for Data Freeze 4 (October 2020)*. *Host Genetics Initiative*. (2020). Available online at: https://www.covid19hg.org/blog/2020-11-24-covid-19-hgi-results-for-data-freeze-4-october-2020/

100. WHO. *COVID-19 Vaccine Tracker and Landscape*. (2021). Available online at: https://www.who.int/publications/m/item/draft-landscape-of-covid-19-candidate-vaccines
101. Creech CB, Walker SC, Samuels RJ. SARS-CoV-2 vaccines. *J Am Med Assoc.* (2021) 325:1318–20. doi: 10.1001/jama.2021.3199
102. European Medicines Agency. *COVID-19 Vaccines: European Medicines Agency*. (2021). Available online at: https://www.ema.europa.eu/en/human-regulatory/overview/public-health-threats/coronavirus-disease-covid-19/treatments-vaccines/covid-19-vaccines (accessed June 5, 2021).
103. Connors M, Graham BS, Lane HC, Fauci AS. SARS-CoV-2 vaccines: much accomplished, much to learn. *Ann Intern Med.* (2021) 174:687–90. doi: 10.7326/M21-0111
104. Sahin U, Muik A, Vogler I, Derhovanessian E, Kranz LM, Vormehr M, et al. BNT162b2 induces SARS-CoV-2-neutralising antibodies and T cells in humans. *medRxiv*. (2020) 2020:2020.12.09.20245175. doi: 10.1101/2020.12.09.20245175
105. Jackson LA, Anderson EJ, Rouphael NG, Roberts PC, Makhene M, Coler RN, et al. An mRNA vaccine against SARS-CoV-2 - preliminary report. *N Engl J Med.* (2020) 383:1920–31. doi: 10.1056/NEJMoa2022483
106. Ramasamy MN, Minassian AM, Ewer KJ, Flaxman AL, Folegatti PM, Owens DR, et al. Safety and immunogenicity of ChAdOx1 nCoV-19 vaccine administered in a prime-boost regimen in young and old adults (COV002): a single-blind, randomised, controlled, phase 2/3 trial. *Lancet.* (2021) 396:1979–93. doi: 10.1016/S0140-6736(20)32466-1
107. Voysey M, Clemens SAC, Madhi SA, Weckx LY, Folegatti PM, Aley PK, et al. Safety and efficacy of the ChAdOx1 nCoV-19 vaccine (AZD1222) against SARS-CoV-2: an interim analysis of four randomised controlled trials in Brazil, South Africa, and the UK. *Lancet.* (2021) 397:99–111. doi: 10.1016/S0140-6736(20)32661-1
108. Sadoff J, Le Gars M, Shukarev G, Heerwegh D, Truyers C, de Groot AM, et al. Interim results of a phase 1–2a trial of Ad26COV2S covid-19 vaccine. *N Engl J Med.* (2021) 384:1824–35. doi: 10.1056/NEJMoa2034201
109. Stevenson A. *Infections Are Rising in Mongolia, Where Half the People Have Received the Sinopharm Vaccine*. New York, NY: The New York Times (2021).
110. Novavax. *Novavax COVID-19 Vaccine Demonstrates 89.3% Efficacy in UK Phase 3 Trial*. Gaithersburg (2021).
111. Howard J. *Novavax Says Covid-19 Vaccine Shows 90.4% Overall Efficacy in US/Mexico Phase 3 Trial*. (2021). Available online at: https://ktvz.com/health/2021/06/14/novavax-says-covid-19-vaccine-shows-90-4-overall-efficacy-in-us-mexico-phase-3-trial/
112. Iwasaki A, Omer SB. Why and how vaccines work. *Cell.* (2020) 183:290–5. doi: 10.1016/j.cell.2020.09.040
113. Nanomedicine and the COVID-19 vaccines. *Nat Nanotechnol.* (2020) 15:963. doi: 10.1038/s41565-020-00820-0
114. Aoshi T. Modes of action for mucosal vaccine adjuvants. *Viral Immunol.* (2017) 30:463–70. doi: 10.1089/vim.2017.0026
115. Horowitz JE, Kosmicki JA, Damask A, Sharma D, Roberts GHL, Justice AAE, et al. Genome-wide analysis in 756,646 individuals provides first genetic evidence that ACE2 expression influences COVID-19 risk and yields genetic risk scores predictive of severe disease. *medRxiv*. (2021) 2021:2020.12.14.20248176. doi: 10.1101/2020.12.14.20248176
116. Dhiman N, Jacobson RM, Poland GA. Measles virus receptors: SLAM and CD46. *Rev Med Virol.* (2004) 14:217–29. doi: 10.1002/rmv.430
117. Ella R, Vadrevu KM, Jogdand H, Prasad S, Reddy S, Sarangi V, et al. Safety and immunogenicity of an inactivated SARS-CoV-2 vaccine, BBV152: a double-blind, randomised, phase 1 trial. *Lancet Infect Dis.* (2021) 21:637–46. doi: 10.1016/S1473-3099(20)30942-7
118. He P, Zou Y, Hu Z. Advances in aluminum hydroxide-based adjuvant research and its mechanism. *Hum Vaccin Immunother.* (2015) 11:477–88. doi: 10.1080/21645515.2014.1004026
119. Egan C, Knight S, Baillie K, Harrison E, Docherty A, Semple C. *Hospitalised Vaccinated Patients During the Second Wave, Update April '21*. ISARIC4C Consortium and COVID-19 Clinical Information Network (CO-CIN) (2021). Available online at: https://assets.publishing.service.gov.uk/government/uploads/system/uploads/attachment_data/file/982499/S1208_CO-CIN_report_on_impact_of_vaccination_Apr_21.pdf
120. Mahase E. Covid-19: most people admitted to hospital after vaccination were infected before immunity could develop, research shows. *BMJ.* (2021) 373:n1127. doi: 10.1136/bmj.n1127
121. D'Souza RS, Wolfe I. COVID-19 vaccines in high-risk ethnic groups. *Lancet.* (2021) 397:1348. doi: 10.1016/S0140-6736(21)00624-3
122. Polack FP, Thomas SJ, Kitchin N, Absalon J, Gurtman A, Lockhart S, et al. Safety and efficacy of the BNT162b2 mRNA covid-19 vaccine. *N Engl J Med.* (2020) 383:2603–15. doi: 10.1056/NEJMoa2034577
123. Baden LR, El Sahly HM, Essink B, Kotloff K, Frey S, Novak R, et al. Efficacy and safety of the mRNA-1273 SARS-CoV-2 vaccine. *N Engl J Med.* (2021) 384:403–16. doi: 10.1056/NEJMoa2035389
124. Liu G, Carter B, Gifford DK. Predicted Cellular Immunity Population Coverage Gaps for SARS-CoV-2 subunit vaccines and their augmentation by compact peptide sets. *Cell Syst*. (2021) 12:102–7.e4. doi: 10.1016/j.cels.2020.11.010
125. Amy H. COVID-*19 Vaccines: Missing Race & Ethnicity Data / Single-Dose Effectiveness / J&J Recommendations*. (2021). Available online at: https://www.jwatch.org/fw117571/2021/03/02/covid-19-vaccines-missing-race-ethnicity-data-single-dose (accessed June, 2021).
126. Finsterer J, Scorza FA. SARS-CoV-2 vaccines are not free of neurological side effects. *Acta Neurol Scand.* (2021) 144:109–10. doi: 10.1111/ane.13451
127. Cines DB, Bussel JB. SARS-CoV-2 vaccine-induced immune thrombotic thrombocytopenia. *N Engl J Med*. (2021) 384:2254–6. doi: 10.1056/NEJMe2106315
128. Bolze A, Neveux I, Schiabor Barrett KM, White S, Isaksson M, Dabe S, et al. HLA-A∗03:01 is associated with increased risk of fever, chills, and stronger side effects from Pfizer-BioNTech COVID-19 vaccination. *HGG Adv*. (2022) 3:100084. doi: 10.1016/j.xhgg.2021.100084
129. Shaghaghi M, Parvaneh N, Ostad-Rahimi P, Fathi SM, Shahmahmoodi S, Abolhassani H, et al. Combined immunodeficiency presenting with vaccine-associated paralytic poliomyelitis: a case report and narrative review of literature. *Immunol Invest.* (2014) 43:292–8. doi: 10.3109/08820139.2013.859156
130. Kwok AJ, Mentzer A, Knight JC. Host genetics and infectious disease: new tools, insights and translational opportunities. *Nat Rev Genet.* (2021) 22:137–53. doi: 10.1038/s41576-020-00297-6
131. Delmonte OM, Bergerson JRE, Burbelo PD, Durkee-Shock JR, Dobbs K, Bosticardo M, et al. Antibody responses to the SARS-CoV-2 vaccine in individuals with various inborn errors of immunity. *J Allergy Clin Immunol.* (2021) 148:1192–7. doi: 10.1016/j.jaci.2021.08.016
132. Quinti I, Locatelli F, Carsetti R. The immune response to SARS-CoV-2 vaccination: insights learned from adult patients with common variable immune deficiency. *Front Immunol*. (2022) 12:815404. doi: 10.3389/fimmu.2021.815404


**Conflict of Interest:** The authors declare that the research was conducted in the absence of any commercial or financial relationships that could be construed as a potential conflict of interest.

frontiers | Frontiers in Medicine

ORIGINAL RESEARCH
published: 06 May 2022
doi: 10.3389/fmed.2022.827850

# Preliminary Study on the Combination Effect of Clindamycin and Low Dose Trimethoprim-Sulfamethoxazole on Severe *Pneumocystis* Pneumonia After Renal Transplantation

*Zhun-Yong Gu[1†], Wen-Jun Liu[1†], Dan-Lei Huang[1†], Yu-Jing Liu[2†], Hong-Yu He[1], Cheng Yang[3], Yi-Mei Liu[1], Ming Xu[3], Rui-Ming Rong[3], Du-Ming Zhu[1], Zhe Luo[1] and Min-Jie Ju[1*]*

[1] Department of Critical Care Medicine, Zhongshan Hospital, Fudan University, Shanghai, China, [2] Department of Nursing, Zhongshan Hospital, Fudan University, Shanghai, China, [3] Department of Urology Surgery, Zhongshan Hospital, Fudan University, Shanghai, China

OPEN ACCESS

**Edited by:**
Mohamed Emara,
Qatar University, Qatar

**Reviewed by:**
Yongbing Qian,
Shanghai Jiao Tong University, China
Longshan Liu,
Sun Yat-sen University, China

***Correspondence:**
Min-Jie Ju
ju.minjie@zs-hospital.sh.cn

[†] These authors have contributed equally to this work

**Specialty section:**
This article was submitted to Precision Medicine, a section of the journal Frontiers in Medicine

**Received:** 02 December 2021
**Accepted:** 11 April 2022
**Published:** 06 May 2022

**Citation:**
Gu Z-Y, Liu W-J, Huang D-L, Liu Y-J, He H-Y, Yang C, Liu Y-M, Xu M, Rong R-M, Zhu D-M, Luo Z and Ju M-J (2022) Preliminary Study on the Combination Effect of Clindamycin and Low Dose Trimethoprim-Sulfamethoxazole on Severe Pneumocystis Pneumonia After Renal Transplantation. Front. Med. 9:827850. doi: 10.3389/fmed.2022.827850

**Objective:** Evaluate the effect of the combination of clindamycin with low-dose trimethoprim-sulfamethoxazole (TMP/SMX) regimen on sever *Pneumocystis* pneumonia (PCP) after renal transplantation.

**Method:** 20 severe PCP patients after renal transplantation were included in this historical-control, retrospective study. A 10 patients were treated with the standard dose of TMP/SMX (T group), the other 10 patients were treated with the combination of clindamycin and low dose TMP/SMX (CT group).

**Results:** Although there was no significant difference in the hospital survival between the two groups, the CT protocol improved the PaO2/FiO2 ratio more significantly and rapidly after the 6th ICU day (1.51 vs. 0.38, $P = 0.014$). CT protocol also ameliorated the pulmonary infiltration and the lactate dehydrogenase level more effectively. Moreover, the CT protocol reduced the incidence of pneumomediastinum (0 vs. 50%, $P = 0.008$), the length of hospital staying (26.5 vs. 39.0 days, $P = 0.011$) and ICU staying (12.5 vs. 22.5 days, $P = 0.008$). Furthermore, more thrombocytopenia (9/10 vs. 3/10, $P = 0.020$) was emerged in the T group than in the CT group. The total adverse reaction rate was much lower in the CT group than in the T group (8/80 vs. 27/80, $P < 0.001$). Consequently, the dosage of TMP/SMX was reduced in 8 patients, while only 2 patients in the CT group received TMP/SMX decrement ($P = 0.023$).

**Conclusion:** The current study proposed that clindamycin combined with low-dose TMP/SMX was more effective and safer the than single use of TMP/SMX for severe PCP patients after renal transplantation (NCT 04328688).

**Keywords: clindamycin, trimethoprim-sulfamethoxazole, *Pneumocystis* pneumonia, renal transplantation, combination**

## INTRODUCTION

*Pneumocystis* pneumonia (PCP) is a severe disease with high morbidity and mortality, which almost exclusively affects immunocompromised patients (1–4), including solid organ transplant (SOT). SOT was one of the most frequent underlying diseases among non-HIV-PCP patients (3). For SOT patients, the overall incidence of PCP varies from 5 to 15% (5, 6), which increases along with the increasing numbers of transplantations. The incidence is also influenced by the type of the transplanted organ and the immunosuppressive regimen (7). Non-HIV-PCP will progress more rapidly than HIV-PCP, predominantly in hypoxemia (5, 8, 9). Consequently, studies have proposed that the mortality of non-HIV-PCP is as high as 30 – 60% (3, 10, 11), which is significantly higher than that of HIV-PCP (5). How to effectively treat severe PCP after SOT has become an urgent problem to be solved.

At present, trimethoprim-sulfamethoxazole (TMP/SMX) is still recommended as the first-line treatment for PCP after SOT (12, 13), and the standard dose is 15–20 mg/kg/d TMP combined with 75–100 mg/kg/d SMX. However, these dosages are resulted from some small, observational studies during 1970s and 1980s (14–16), without randomized control. Hence, the optimal dose of TMP/SMX for PCP after SOT remains ambiguous. Furthermore, the standard dosages are more likely to cause side effects (bone marrow depression, hyperkalemia and nephrotoxicity, et al.) due to the large dose and poor compliance with medication (17). To reduce the adverse reactions of TMP/SMX and improve the adherence to medication, the prevention strategies of PCP after SOT were referred, including the escalating protocol, the half dose protocol and the single tablet chemoprophylaxis protocol (18–20). As a result, the medium dose (10 mg/kg/d TMP) (21), decreasing dose (22, 23) and low dose strategy (4–10 mg/kg/d TMP) (17) are used to treat SOT-PCP. However, the effect after dose modification remains controversial (14, 24, 25). Moreover, increasing numbers of studies have indicated that mutations in dihydropteroate synthase genes may be associated with the emergence of TMP/ SMX resistant strains (26, 27), especially for patients who taken sulfa as prophylaxis after SOT. Therefore, it is of clinical importance to find a treatment that can both improve the efficacy and reduce the adverse effects on the base of low dose TMP/SMX.

In the TMP/SMX failed PCP cases, pentamidine, atovaquone, dapsone and clindamycin-primaquine can be used as the second-line alternatives, both for HIV-PCP (28) and non-HIV-PCP patients (12, 29). However, no agent has been shown to have better outcomes than TMP/SMX. In severe infections, intravenous pentamidine probably remains the preferred second-line agent after TMP/SMX. However, pentamidine therapy can be complicated by numerous toxicities including pancreatitis, hypo- and hyperglycemia, bone marrow suppression, renal failure, and electrolyte disturbances. Consequently, more and more studies suggest that clindamycin-based alternatives play an increasing role in treating of SOT-PCP, especially for patients who are refractory to TMP/SMX or pentamidine or both (30–33). Clindamycin is a lincosamide agent that inhibits protein synthesis at the chain elongation step by interfering with transpeptidation of the 50S ribosomal subunit. Therefore, the objective of this study is to investigate the safety and efficacy of the preemption clindamycin with low-dose TMP/SMX regimen (CT regimen) for severe PCP after renal transplantation.

## MATERIALS AND METHODS

### Study Design and Population

We performed a historical-control, retrospective study of PCP patients after renal transplantation, during September 2017 to February 2020. All the patients were admitted with a confirmation of *Pneumocystis* in the blood sample and/or broncho-alveolar lavage (BAL) fluid by "Next-generation" sequencing (NGS) technology (27) and the typical signs listed in the including criteria: (1) Patients were admitted into ICU for distress of respiratory (P/F ratio $<$ 250 mmHg); (2) age $>$18 years; (3) presented with the symptoms of fever; and (4) tachypnea (respiratory rate $>$25 breaths/min), and dry cough et al., with diffuse interstitial processes on chest radiograph, but without significant sputum production (34). Pregnant women or terminal stage patients (patients with advanced cancer or severe insufficiency of organ function). All the patients were transferred to ICU immediately after they were admitted. All patients provided informed consent, and this study was approved by the Ethics Committee of Zhongshan Hospital, Fudan University (No. B2019-267R).

In the first stage of the study (September 1st, 2017 to December 31th, 2018), a total of 12 PCP patients were admitted to our department for hypoxemia. Two patients were excluded, one for renal failure the other one for end stage of carcinoma. Finally, ten patients were included in the study; they were initially treated with the standard dose of TMP/SMX (T group, 15 mg/kg/d TMP). The second stage was from January 1st, 2019 to February 6th, 2020. A total of 11 PCP patients were admitted, while one was excluded for heart failure. Consequently, ten patients were included and treated with the combination of clindamycin and low initial dose of TMP/SMX (CT group, 8 mg/kg/d TMP) (**Figure 1**). The TMP/SMX-based regimens were initiated from the ICU ward. In both groups, the dosage of TMP/SMX would be modified according to the baseline renal function, white blood cell or platelets count, the clinical effect and the side effect. Clindamycin was initiated at the dosage of was 600 – 900 mg IV or po q6 – 8 h and stopped until the P/F ratio was higher than 300 mmHg and/or the pulmonary infiltration was alleviated.

### Other Interventions Besides Trimethoprim-Sulfamethoxazole and Clindamycin

Upon admission, immunosuppressants were stopped in all patients. According to the protocol from our team, the patients were initially administered with methylprednisolone at 2.0–2.5 mg/kg/day once every 12 h. This dosage was continued until oxygenation improved, followed by gradual tapering (via a 20 mg reduction every 2–3 days) (35). Empirical antibiotic therapy included moxifloxacin, meropenem, and ganciclovir.

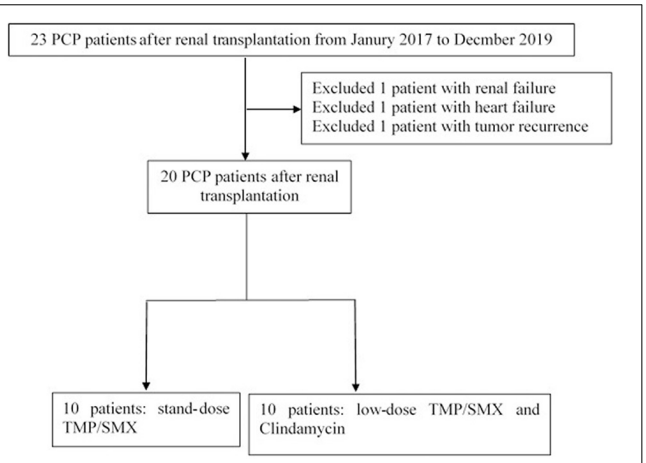


**FIGURE 1 |** Patient-selection flow chart.

If fungal infection was suspected, antifungal therapy was initiated. The dosages of all drugs were adjusted based on the allograft function. The heart rate (HR), blood pressure (BP), respiratory rate (RR), and arterial oxygen saturation ($SaO_2$) were continuously monitored in all patients. In addition, lung CT scan was performed once every 5–7 days, meanwhile, bedside lung and heart ultrasound was performed twice a day to manifest the pulmonary infiltration, heart function and mediastinal emphysema.

## Protocol for Oxygen Therapy

High-flow Nasal Cannula (HFNC) was considered the first-line treatment if the P/F ratio was under 250 mmHg while using a conventional face mask at a maximum concentration (36). Initially, HFNC was settled with a flow rate of 40–60 L/min and the humidification temperature 31°C. $FiO_2$ was modified to maintain a $SaO_2 > 92\%$. Whenever HFNC could not keep the target $SaO_2$, non-invasive ventilation (NIV) or invasive mechanical ventilation (IMV) would be considered.

## Study Outcomes

The primary endpoint was the hospital survival. The secondary endpoints including the length of hospital staying ($LOS_{HOS}$), length of ICU staying ($LOS_{ICU}$), the time for P/F ratio to 300 mmHg, need for mechanical ventilation (invasive or non-invasive) or extra corporeal membrane oxygenation (ECMO), need for renal replacement therapy (RRT), changes of renal function, pneumomediastinum and superinfection rate.

## Statistical Analysis

Normally distributed data were expressed as mean ± SD and compared with the use of unpaired *t* test. Non-normal data was reported as median (interquartile range) and compared with the use of Mann-Whitney *U* test. Differences between categoric variables, expressed as n (%) were assessed with the use of chi-square or Fisher exact test when necessary. A two-tailed *P* value of $< 0.05$ was considered to indicate statistical significance. The results were analyzed with the use of SPSS statistical software (version 17.0; SPSS, Chicago, IL, United States).

# RESULTS

## Baseline Characteristics of the Study Population

The mean age was 48.5 and 40.0 years in the T group and the CT group, respectively ($P = 0.719$). There were 8 and 7 male patients in T group and CT group, respectively ($P = 0.628$). The Body Mass Index (BMI) was similar between the T and CT group (21.1 vs. 20.5 kg/m$^2$, $P = 0.481$). There was no significant difference in the comorbidities and coinfection between the T and CT group (**Table 1**). The PSI score between the T and CT group was similar (80 vs. 80, $P = 0.6$). Other clinical characteristics between the CT and the T group on admission, including the APACHE II score (17.5 vs. 14.0, $P = 0.176$), SOFA score (6 vs. 4, $P = 0.127$), the P/F ratio (148.5 vs. 146.0 mmHg, $P = 0.677$), lactate dehydrogenase (LDH, 456.7 vs. 437.2 U/L, $P = 0.804$), C-reactive protein (CRP, 74.9 vs. 67.6 mg/L, $P = 0.774$), procalcitonin (PCT, 0.9 vs. 0.2 ng/mL, $P = 0.178$), total bilirubin (5.9 vs. 9.8 μmol/L, $P = 0.300$), creatinine (223.3 vs. 144.5 μmol/L, $P = 0.205$), platelet (PLT, 219.5 vs. 230.6 × 10$^9$/L, $P = 0.832$), hemoglobin (94.4 vs. 103.5 g/dL, $P = 0.242$), leukocyte count (8.1 vs. 10.0 × 10$^9$/L, $P = 0.417$), lymphocyte count (0.44 vs. 0.36 × 10$^9$/L, $P = 0.378$), $CD4^+/CD8^+$ ratio (1.2 vs. 1.4, $P = 0.964$), globulin (21.8 vs. 19.2 g/L, $P = 0.239$), kalium (4.2 vs. 4.2 mmol/L, $P = 0.901$) and 1,3 – β – D glucan (207.0 vs. 265.0 pg/mL, $P = 0.887$) were all balanced distributed. Nine patients in the CT group and 8 in the T group received HFNC on ICU admission ($P = 0.556$). More patients were administrated with vasopressor in the CT group than in the T group (30 vs. 10% $P = 0.290$).

## Outcomes

### Survival and Length of Staying

There were 8 surviving discharge records in the T group, while all the patients survived in the CT group (mortality, 20 vs. 0%, $P = 0.168$). Meanwhile, compared to the T group, CT group had a shorter staying of hospital (26.5 vs. 39.0 days, $P = 0.011$), ICU (12.5 vs. 22.5 days, $P = 0.008$) and less hospital cost (183,694.5 vs. 255,712.0 CNY, $P = 0.505$) (**Table 2**).

### Need for Mechanical Ventilation

During the ICU staying, the length of HFNC application was similar between CT group and T group (168.0 vs. 156.0 h, $P = 0.616$). The non-invasive ventilation (NIV) rate was similar in CT group and in T group (20 vs. 30%, $P = 0.865$), but the invasive ventilation (IMV) rate was relatively lower in CT group than in T group (0 vs. 30%, $P = 0.211$). One patient adopted ECMO in T group, while none of CT group needed. The pneumomediastinum incidence was much higher in the T group than in the CT group (50 vs. 0%, $P = 0.033$) (**Table 2**).

### Oxygenation and Pulmonary Infiltration Improvement

A P/F ratio higher than 300 mmHg was fulfilled in a shorter time in the CT group than in the T group (5.5 vs. 11.0 days, $P = 0.068$)

(**Table 2** and **Figure 2**). On the other hand, the improvement of P/F ratio $[{}^{(P/F_n - P/F_0)}/_{P/F_0}]$ in the CT group was much more significantly than in the T group after the 6th day after ICU admission (1.51 vs. 0.38, $P = 0.014$) (**Figure 3**).

Pulmonary tomography scan also indicated that the CT protocol could alleviate the pulmonary infiltration more effectively and quickly than the T protocol, as shown in **Supplementary Figure 1**.

## Other Outcomes

The daily fluctuation of the infection markers, hepatic function, renal function and the hematological system from the different therapies were displayed in **Supplementary Figure 2**. Compared to the T group, CT group was associated with more significant improvement of LDH $[{}^{(LDH_0 - LDH_n)}/_{LDH_0}]$ (0.461 vs. 0.009, $P = 0.023$) (**Supplementary Figure 1**).

There was no difference in the need for renal replacement therapy (10 vs. 0%, $P = 0.343$), renal allograft survival (90 vs. 80%, $P = 1$), $^{\Delta}$eGFR (−19.8 vs. 7.15%, $P = 0.400$), transfusion of platelets (30 vs. 40%, $P = 0.660$) or red blood cell (30 vs. 60%, $P = 0.196$) between the CT group and T group (**Table 2**).

## Adverse Reaction

The adverse reactions of TMP/SMX include rash, anorexia, leucopenia, anemia, thrombocytopenia, hepatic injure, renal injure and hyperkalemia. As for Common Terminology Criteria for Adverse Events 5.0 (CTCAE) $\geq$ 3 grade adverse reactions, there was no rash, anorexia, renal injure or hyperkalemia in either T group or CT group (**Table 3**). There was no difference in the occurrence of leucopenia (7/10 vs. 2/10, $P = 0.07$), anemia (6/10 vs. 1/10, $P = 0.057$) or hepatic injure (5/10 vs. 2/10, $P = 0.350$) between the T group than in the CT group. While, more thrombocytopenia (9/10 vs. 3/10, $P = 0.020$) was emerged in the T group than in the CT group. A total of 27 adverse reactions occurred in the T group, while only 8 in the CT group

**TABLE 1 |** Baseline characteristics of 20 PCP patients after renal transplantation.

| | T group | CT group | *P* |
|---|---|---|---|
| Age (years) | 48.5 | 40.0 | 0.719# |
| Male (%) | 8 (80%) | 7 (10%) | 0.628# |
| Body Mass Index (kg/m$^2$) | 21.1 | 20.5 | 0.481# |
| Time from transplantation to PCP onset (days) | 234.5 | 313.0 | 0.161# |
| Comorbidity (n) | | | |
| Hypertension (n) | 2 (20%) | 2 (20%) | 1.000* |
| Smoking (n) | 1 (10%) | 2 (20%) | 0.556* |
| Diabetes (n) | 2 (20%) | 2 (20%) | 1.000* |
| Coronary artery disease (n) | 2 (20%) | 3 (30%) | 0.628* |
| Chronic bronchitis (n) | 1 (10%) | 2 (20%) | 0.556* |
| Coinfection (n) | 4 (40%) | 3 (30%) | 0.660* |
| Bacteria (n) | 1 (10%) | 0 (0%) | 0.343* |
| Fungus (n) | 2 (20%) | 2 (20%) | 1.000* |
| Virus (n) | 1 (10%) | 1 (10%) | 1.000* |
| **On admission** | | | |
| PSI score | 80.0 | 80.0 | 0.600# |
| APACHE II score | 14.0 | 17.5 | 0.161# |
| SOFA score | 4.0 | 6.0 | 0.127# |
| $PaO_2/FiO_2$ ratio | 146.0 | 148.5 | 0.176# |
| Vasopressor (%) | 1 (10%) | 3 (30%) | 0.290* |
| HFNC (%) | 8 (80%) | 9 (90%) | 0.556* |
| Lactate dehydrogenase (U/L) | 437.2 | 456.7 | 0.804# |
| C-reactive protein (mg/L) | 67.6 | 74.9 | 0.774# |
| Procalcitonin (μg/L) | 0.2 | 0.9 | 0.178# |
| Creatinine (μmol/L) | 144.5 | 223.3 | 0.205# |
| eGFR (ml/min/1.73 m$^2$) | 72.0 | 42.6 | 0.216# |
| Total Bilirubin (mg/dL) | 9.8 | 5.9 | 0.300# |
| Platelet count ( × 10$^9$/L) | 230.6 | 219.5 | 0.832# |
| Hemoglobin (g/dL) | 103.5 | 94.4 | 0.242# |
| Leukocyte count ( × 10$^9$/L) | 10.0 | 8.1 | 0.417# |
| Lymphocyte count ( × 10$^9$/L) | 0.36 | 0.44 | 0.378# |
| $CD4^+/CD8^+$ ratio | 1.4 | 1.2 | 0.964# |
| Globulin (g/L) | 19.2 | 21.8 | 0.239# |
| Kalium (mmol/L) | 4.2 | 4.2 | 0.901# |
| 1,3 – β – D glucan (pg/mL) | 265.0 | 207.0 | 0.887# |

#*Mann-Whitney U and Wilcoxon tests; *Fisher exact tests.*

**TABLE 2 |** Outcomes of 20 PCP patients after renal transplantation.

| | T group | CT group | *P* |
|---|---|---|---|
| Hospital mortality (%) | 2 (20%) | 0 (0%) | 0.168* |
| Length of hospital staying (days) | 39.0 | 26.5 | 0.011# |
| Length of ICU staying (days) | 22.5 | 12.5 | 0.008# |
| HFNC (h) | 156.0 | 168.0 | 0.616# |
| Mechanical ventilation (%) | 4 (40%) | 2 (20%) | 0.356* |
| Non-invasive positive-pressure ventilation (NIV, %) | 3 (30%) | 2 (20%) | 0.628* |
| NIV (h) | 17.0 | 106.8 | 0.567# |
| Invasive mechanical ventilation (IMV, %) | 3 (30%) | 0 (0%) | 0.211* |
| IMV (h) | 240.0 | 0.0 | 0.185# |
| Extra corporeal membrane oxygenation (%) | 1 (10%) | 0 (0%) | 0.343* |
| Extra corporeal membrane oxygenation (d) | 6.0 | 0.0 | 0.343# |
| Time for P/F to 300 mmHg (h) | 11.0 | 5.5 | 0.068# |
| Renal replacement therapy (n) | 0 (0%) | 1 (10%) | 0.343* |
| Changes of renal function, $^{\Delta}$eGFR (%) | 7.15 | −19.8 | 0.400# |
| Renal allograft survival (%) | 8 (80%) | 9 (90%) | 1* |
| Pneumomediastinum (%) | 5 (50%) | 0 (0%) | 0.008* |
| Hospital Cost (¥) | 255712.0 | 183694.5 | 0.505# |
| Average TMP/SMX dosage (mg/d) | 146.0 | 227.4 | 0.094# |
| Decrement of TMP/SMX dosage | 8 (80%) | 2 (20%) | 0.023* |
| Transfusion of platelets (%) | 4 (40%) | 3 (30%) | 0.660* |
| Transfusion of Red blood cell (%) | 6 (60%) | 3 (30%) | 0.196* |

#*Mann-Whitney U and Wilcoxon tests; *Fisher exact tests.* $^{\Delta}eGFR = (eGFR_0 - eGFR_n)/eGFR_0$.

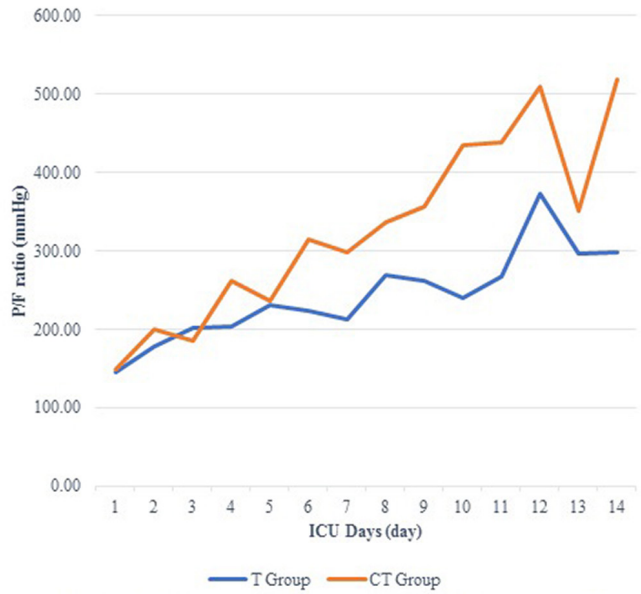


| ICU days | 1 | 2 | 3 | 4 | 5 | **6** | 7 | 8 | 9 | 10 | 11 | **12** | 13 | 14 |
|---|---|---|---|---|---|---|---|---|---|---|---|---|---|---|
| **T Group ($n$ = 10)** | 146 | 178.87 | 201 | 203.5 | 230.3 | 222.83 | 213.5 | 269.29 | 262.5 | 240 | 266.67 | **372** | 297.25 | 298.33 |
| **CT Group ($n$ = 10)** | 148.5 | 200.5 | 185 | 261 | 236.5 | **314** | 297.5 | 337 | 356.44 | 435 | 439 | 510 | 350.47 | 519 |
| **P** | 0.176 | 0.418 | 0.187 | 0.344 | 0.27 | 0.215 | 0.04 | 0.103 | 0.039 | 0.023 | 0.011 | 0.035 | 0.318 | 0.159 |

**FIGURE 2 |** Daily P/F ratio of PCP patients after renal transplantation. For patients in the CT group, the P/F ratio had been elevated to more than 300 mmHg in the 6th ICU day. On the other hand, the P/F ratio of patients from T group could not be higher than 300 mmHg before the 12th ICU day.

**TABLE 3 |** Present of estimated adverse events from TMP/SMX during the treatment among the groups.

| | T Group ($n$ = 10) | CT Group ($n$ = 10) | $P$ |
|---|---|---|---|
| Rash (times) | 0 | 0 | 1.000 |
| Anorexia (times) | 0 | 0 | 1.000 |
| Leucopenia (times) | 7 | 2 | 0.07* |
| Anemia (times) | 6 | 1 | 0.057* |
| Thrombocytopenia | 9 | 3 | 0.020* |
| Hepatic injure (times) | 5 | 2 | 0.350* |
| Renal injure (times) | 0 | 0 | 1.000 |
| Hyperkalemia (times) | 0 | 0 | 1.000 |
| Total AE (times) | 27 | 8 | < 0.001# |

# $\chi^2$ tests; * Fisher exact tests.

(27/80 vs. 8/80, $P$ < 0.001). In the T group, the dosage of TMP/SMX was reduced in 8 patients, while only 2 patients in the CT group received TMP/SMX decrement ($P$ = 0.023) (**Table 2**). The comparison of the daily dose indicated an escalating dose of TMP/SMX in CT group and a decrease dose of TMP/SMX in T group (**Supplementary Figure 3**).

## DISCUSSION

In the present study, we found that in comparison to standard dose TMP/SMX, clindamycin combined with low-dose TMP/SMX significantly improved the oxygenation of severe PCP patients after renal transplantation (P/F variability 1.51 vs. 0.38, $P$ = 0.014). The CT protocol was also associated with a shorter length of ICU (12.5 vs. 22.5 days, $P$ = 0.008) and hospital staying (26.5 vs. 39.0 days, $P$ = 0.011) compared with the T group. Meanwhile, the combined drug administration did not increase the occurrence rates of hepatic or renal toxicity, but rather reduced the severe adverse reactions of TMP/SMX (27/80 vs. 8/80, $P$ < 0.001) and eventually improve the compliance.

*Pneumocystis* pneumonia patients, especially the non-HIV-PCP patients were usually associated with poor outcome (17, 24, 28). In the present study, the hospital mortality of severe PCP in standard dose TMP/SMX was 20% which was similar to the previous report (24). In comparison, all the patients in CT group were discharged. In the current study, the $LOS_{ICU}$ of PCP patients of the T group was 22.5 days, which was similar to the previous study (37). When the combination protocol was applied, the $LOS_{ICU}$ significantly reduced from 22.5 to 12.5 days ($P$ = 0.008) and $LOS_{HOS}$ reduced from 39.0 to 26.5 days ($P$ = 0.011). Moreover, the CT protocol could alleviate the pulmonary infiltration more effectively and quickly than the T protocol. Therefore, we proposed that the combination of clindamycin and low-dose TMP/SMX could improve the outcome of severe PCP after renal transplantation.

The clinical benefit of CT protocol may be due to the following mechanisms. First, CT protocol can improve patients' oxygenation in a better and quicker way. We found that although the initial P/F ratio was similar between the CT group and the T group, patients in the CT group spent only 5.5 days to achieve

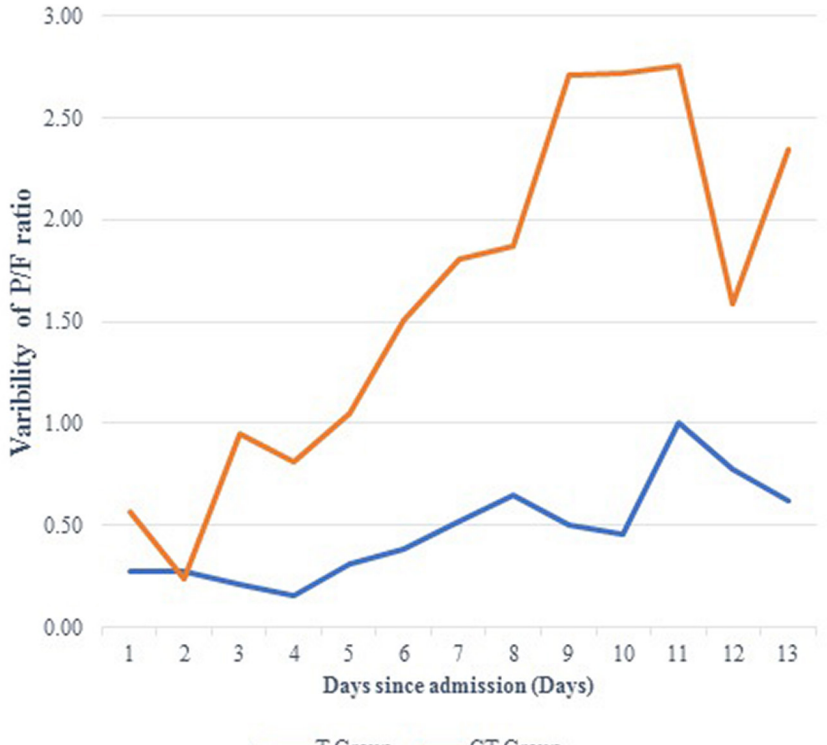


| Days since admission | 1 | 2 | 3 | 4 | 5 | **6** | 7 | 8 | 9 | 10 | 11 | 12 | 13 |
|---|---|---|---|---|---|---|---|---|---|---|---|---|---|
| T Group ($n = 10$) | 0.28 | 0.27 | 0.21 | 0.16 | 0.31 | **0.38** | 0.52 | 0.65 | 0.51 | 0.46 | 1.01 | 0.78 | 0.62 |
| CT Group ($n = 10$) | 0.56 | 0.24 | 0.95 | 0.81 | 1.05 | **1.51** | 1.81 | 1.87 | 2.71 | 2.72 | 2.75 | 1.59 | 2.35 |
| P | 0.102 | 0.757 | 0.06 | 0.05 | 0.05 | **0.014** | 0.02 | 0.01 | 0.01 | 0.009 | 0.01 | 0.239 | 0.106 |

**FIGURE 3 |** Comparison of the improvement of P/F ratio between CT group and T group. After the 6th ICU day, the improvement of P/F ratio was more significantly in the CT group than in the T group.

the P/F ratio > 300 mmHg, while patients in the T group need 11 days. Moreover, after the 6th ICU day, patients in the CT group displayed a more significant P/F ratio improvement then patients in the T group (1.51 vs. 0.38, $P = 0.014$). In line with the more effective oxygenation improvement, the ratio of IMV was accordingly lower in the CT group than in the T group (30 vs. 0%). Mechanical ventilation had confirmed as the independent predictor of increased mortality for HIV-PCP patients (38, 39).

Second, pneumothorax or pneumomediastinum is also associated with worse outcomes of PCP, with one study citing an increase in mortality up to 50% (40). We found that half of the T group got pneumomediastinum while no one of the CT group got it. We propose that the higher IMV rate in the T group might lead to higher incidence of spontaneous pneumothorax or pneumomediastinum because IMV could increase the pressure of the alveoli that can result in alveolar rupture (41). Pneumothorax or pneumomediastinum may be also a result of severe inflammation and fibrosis from PCP (42). We found that CT group was associated with significant improvement in LDH ($P = 0.023$, **Supplementary Figure 1**). Several studies have reported that elevated serum LDH levels were associated with the severity of several pulmonary disorders (43–45). Our team had previously demonstrated that elevated LDH was associated with 90-day mortality in renal transplant recipients with severe CAP (46). Elevated serum LDH levels were mainly due to the impaired pulmonary parenchymal cells or local inflammatory cells, such as alveolar macrophages and polymorphonuclear neutrophils (47). Therefore, the improvement in pulmonary injury and reduced the pneumothorax or pneumomediastinum probability were referred to a significant reduction of LDH by CT protocol.

Although it had been known that TMP/SMX treated PCP by interfering folate metabolism in pneumocystis (48), there are few studies about how did clindamycin treat PCP. Up to now, clindamycin was known to have the following therapeutic mechanisms: (1) Inhibit the protein synthesis in a parasite-specific organelle (the apicoplast) (49), which was related to the mitochondrial function and the lifecycle; (2) Reduce the protein and nucleic acid synthesis in *Plasmodium falciparum* (50). We proposed that the different effects from TMP/SMX and clindamycin could create a 1+1 > 2 effect in PCP treatment. We are also preparing to explore to the underlying mechanisms of the CT protocol.

There was a lower initial TMP/SMX dose in the CT group than in the T group (**Supplementary Figure 3**), while it was finally found that there was a relatively higher mean daily dose of TMP/SMX in CT group than in the T group (227.4 vs. 146.0 mg TMP, $P = 0.094$). There existed the following reasons. First of all, in the current study, patients were more fragile to the standard or high dose of TMP/SMX for their poor eGFR from the renal allograft. Second, clindamycin could facilitate patients recover from PCP together with the recovery of renal function through the pathway different from TMP/SMX. Therefore, we proposed that for severe PCP after renal transplantation, the higher initial dose of TMP/SMX was an important risk factor for severe adverse reactions of TMP/SMX (27/80 vs. 8/80, $P < 0.001$) and clindamycin could help to create a suitable state when patients could tolerant an escalating dose of TMP/SMX. In addition, our results indicated that for severe PCP after renal transplantation, the higher total TMP/SMX dose was more important than the higher initial dose for a good outcome.

This study is the first one that provide preliminary evidence to support the combination of clindamycin and low-dose TMP/SMX for severe PCP patients after renal transplantation especially when they were intolerant to the standard dose of TMP/SMX for the poor renal function. However, several limitations exist. First, this is not a random design, but a single-centered retrospective observation study. Second, the cohort volume is small. Finally, the underlying mechanisms for CT protocol to treat PCP is not explored in the current study. We are looking forward to carry out a multicenter RCT trial and the *in vivo* or *in vitro* study to reinforce the current results.

## CONCLUSION

The current study proposed that clindamycin combined with low-dose TMP/SMX was more effective and safer than single use of TMP/SMX for severe PCP patients after renal transplantation.

## DATA AVAILABILITY STATEMENT

The original contributions presented in the study are included in the article/**Supplementary Material**, further inquiries can be directed to the corresponding author.

## ETHICS STATEMENT

The studies involving human participants were reviewed and approved by the Ethics Committee of Zhongshan Hospital, Fudan University. The patients/participants provided their written informed consent to participate in this study.

## AUTHOR CONTRIBUTIONS

M-JJ, Z-YG, D-LH, W-JL, and Y-JL involved the study design and manuscript preparation. Z-YG, D-LH, Y-ML, and H-YH involved in the data collection and data analysis. M-JJ and CY involved in the statistical design. MX, R-MR, D-MZ, and ZL involved in the manuscript preparation. All authors read and approved the final manuscript.

## FUNDING

This work was supported by the Clinical Research Plan of SHDC (grant number SHDC2020CR4067) and the Shanghai Science and Technology Commission (grant numbers 20S31905300 and 20Y11900900).

## SUPPLEMENTARY MATERIAL

The Supplementary Material for this article can be found online at: https://www.frontiersin.org/articles/10.3389/fmed.2022.827850/full#supplementary-material

## REFERENCES

1. Bollee G, Sarfati C, Thiery G, Bergeron A, de Miranda S, Menotti J, et al. Clinical picture of *Pneumocystis jiroveci* pneumonia in cancer patients. *Chest.* (2007) 132:1305–10.
2. Roblot F, Godet C, Le Moal G, Garo B, Faouzi Souala M, Dary M, et al. Analysis of underlying diseases and prognosis factors associated with *Pneumocystis* carinii pneumonia in immunocompromised HIV-negative patients. *Eur J Clin Microbiol Infect Dis.* (2002) 21:523–31. doi: 10.1007/s10096-002-0758-5
3. Yale SH, Limper AH. *Pneumocystis* carinii pneumonia in patients without acquired immunodeficiency syndrome: associated illness and prior corticosteroid therapy. *Mayo Clin Proc.* (1996) 71:5–13. doi: 10.4065/71.1.5
4. Zahar JR, Robin M, Azoulay E, Fieux F, Nitenberg G, Schlemmer B. *Pneumocystis* carinii pneumonia in critically ill patients with malignancy: a descriptive study. *Clin Infect Dis.* (2002) 35:929–34. doi: 10.1086/342338
5. Roux A, Canet E, Valade S, Gangneux-Robert F, Hamane S, Lafabrie A, et al. *Pneumocystis jirovecii* pneumonia in patients with or without AIDS, France. *Emerg Infect Dis.* (2014) 20:1490–7.
6. Sepkowitz KA. Opportunistic infections in patients with and patients without acquired immunodeficiency syndrome. *Clin Infect Dis.* (2002) 34:1098–107. doi: 10.1086/339548
7. Martin SI, Fishman JA. *Pneumocystis* pneumonia in solid organ transplantation. *Am J Transplant.* (2013) 13 (Suppl. 4):272–9.
8. Nuesch R, Bellini C, Zimmerli W. *Pneumocystis* carinii pneumonia in human immunodeficiency virus (HIV)-positive and HIV-negative immunocompromised patients. *Clin Infect Dis.* (1999) 29:1519–23. doi: 10.1086/313534
9. Rego de Figueiredo I, Vieira Alves R, Drummond Borges D, Torres M, Lourenco F, Antunes AM, et al. Pneumocystosis pneumonia: a comparison study between HIV and non-HIV immunocompromised patients. *Pulmonology.* (2019) 25:271–4. doi: 10.1016/j.pulmoe.2019.04.003
10. Thomas CF Jr., Limper AH. *Pneumocystis* pneumonia. *N Engl J Med.* (2004) 350:2487–98.
11. Ward MM, Donald F. *Pneumocystis carinii* pneumonia in patients with connective tissue diseases: the role of hospital experience in diagnosis and mortality. *Arthritis Rheum.* (1999) 42:780–9. doi: 10.1002/1529-0131(199904)42:4<780::AID-ANR23>3.0.CO;2-M
12. Martin SI, Fishman JA. *Pneumocystis* pneumonia in solid organ transplant recipients. *Am J Transplant.* (2009) 9 (Suppl. 4):S227–33.
13. Tasaka S, Tokuda H. *Pneumocystis jirovecii* pneumonia in non-HIV-infected patients in the era of novel immunosuppressive therapies. *Kansenshogaku Zasshi.* (2014) 88(6 Suppl. 11):26–39.

14. Hughes WT, Feldman S, Sanyal SK. Treatment of *Pneumocystis* carinii pneumonitis with trimethoprim-sulfamethoxazole. *Can Med Assoc J.* (1975) 112:47–50.
15. Lau WK, Young LS. Trimethoprim-sulfamethoxazole treatment of *Pneumocystis* carinii pneumonia in adults. *N Engl J Med.* (1976) 295:716–8.
16. Winston DJ, Lau WK, Gale RP, Young LS. Trimethoprim-sulfamethoxazole for the treatment of *Pneumocystis* carinii pneumonia. *Ann Intern Med.* (1980) 92:762–9.
17. Nakashima K, Aoshima M, Nakashita T, Hara M, Otsuki A, Noma S, et al. Low-dose trimethoprim-sulfamethoxazole treatment for *Pneumocystis* pneumonia in non-human immunodeficiency virus-infected immunocompromised patients: A single-center retrospective observational cohort study. *J Microbiol Immunol Infect.* (2018) 51:810–20. doi: 10.1016/j.jmii.2017.07.007
18. Abe Y, Fujibayashi K, Nishizaki Y, Yanagisawa N, Nojiri S, Nakano S, et al. Conventional-dose versus half-dose Sulfamethoxazole-trimethoprim for the Prophylaxis of *Pneumocystis* pneumonia in patients with systemic rheumatic disease: a non-blind, randomized controlled trial. *Acta Med Okayama.* (2019) 73:85–9. doi: 10.18926/AMO/56464
19. Takenaka K, Komiya Y, Ota M, Yamazaki H, Nagasaka K. A dose-escalation regimen of trimethoprim-sulfamethoxazole is tolerable for prophylaxis against *Pneumocystis jiroveci* pneumonia in rheumatic diseases. *Mod Rheumatol.* (2013) 23:752–8. doi: 10.1007/s10165-012-0730-x
20. Utsunomiya M, Dobashi H, Odani T, Saito K, Yokogawa N, Nagasaka K, et al. Optimal regimens of sulfamethoxazole-trimethoprim for chemoprophylaxis of *Pneumocystis* pneumonia in patients with systemic rheumatic diseases: results from a non-blinded, randomized controlled trial. *Arthritis Res Ther.* (2017) 19:7. doi: 10.1186/s13075-016-1206-8
21. Thomas M, Rupali P, Woodhouse A, Ellis-Pegler R. Good outcome with trimethoprim 10 mg/kg/day-sulfamethoxazole 50 mg/kg/day for *Pneumocystis jirovecii* pneumonia in HIV infected patients. *Scand J Infect Dis.* (2009) 41:862–8. doi: 10.3109/00365540903214256
22. Eeftinck Schattenkerk JK, Lange JM, van Steenwijk RP, Danner SA. Can the course of high dose cotrimoxazole for *Pneumocystis* carinii pneumonia in AIDS be shorter? A possible solution to the problem of cotrimoxazole toxicity. *J Intern Med.* (1990) 227:359–62. doi: 10.1111/j.1365-2796.1990.tb00172.x
23. Creemers-Schild D, Kroon FP, Kuijper EJ, de Boer MG. Treatment of *Pneumocystis* pneumonia with intermediate-dose and step-down to low-dose trimethoprim-sulfamethoxazole: lessons from an observational cohort study. *Infection.* (2016) 44:291–9. doi: 10.1007/s15010-015-0851-1
24. Kosaka M, Ushiki A, Ikuyama Y, Hirai K, Matsuo A, Hachiya T, et al. A four-center retrospective study of the efficacy and toxicity of low-dose trimethoprim-sulfamethoxazole for the treatment of *Pneumocystis* pneumonia in patients without HIV infection. *Antimicrob Agents Chemother.* (2017) 61:e1173–17. doi: 10.1128/AAC.01173-17
25. Schmidt JJ, Lueck C, Ziesing S, Stoll M, Haller H, Gottlieb J, et al. Clinical course, treatment and outcome of *Pneumocystis* pneumonia in immunocompromised adults: a retrospective analysis over 17 years. *Crit Care.* (2018) 22:307. doi: 10.1186/s13054-018-2221-8
26. Long Y, Zhang C, Su L, Que C. *Pneumocystis jirovecii* dihydropteroate synthase gene mutations in a group of HIV-negative immunocompromised patients with Pneumocystis pneumonia. *Exp Ther Med.* (2014) 8:1825–30. doi: 10.3892/etm.2014.2002
27. Montesinos I, Delforge ML, Ajjaham F, Brancart F, Hites M, Jacobs F, et al. Evaluation of a new commercial real-time PCR assay for diagnosis of *Pneumocystis jirovecii* pneumonia and identification of dihydropteroate synthase (DHPS) mutations. *Diagn Microbiol Infect Dis.* (2017) 87:32–6. doi: 10.1016/j.diagmicrobio.2016.10.005
28. Roux A, Gonzalez F, Roux M, Mehrad M, Menotti J, Zahar JR, et al. Update on pulmonary *Pneumocystis jirovecii* infection in non-HIV patients. *Med Mal Infect.* (2014) 44:185–98.
29. Fishman JA, Gans H. *Pneumocystis jiroveci* in solid organ transplantation: guidelines from the American society of transplantation infectious diseases community of practice. *Clin Transplan.* (2019) 33:e13587. doi: 10.1111/ctr.13587
30. Benfield T, Atzori C, Miller RF, Helweg-Larsen J. Second-line salvage treatment of AIDS-associated Pneumocystis jirovecii pneumonia: a case series and systematic review. *J Acquir Immune Defic Syndr.* (2008) 48:63–7. doi: 10.1097/QAI.0b013e31816de84d
31. Nickel P, Schurmann M, Albrecht H, Schindler R, Budde K, Westhoff T, et al. Clindamycin-primaquine for pneumocystis jiroveci pneumonia in renal transplant patients. *Infection.* (2014) 42:981–9. doi: 10.1007/s15010-014-0660-y
32. Li H, Huang H, He H. Successful treatment of severe *Pneumocystis* pneumonia in an immunosuppressed patient using caspofungin combined with clindamycin: a case report and literature review. *BMC Pulm Med.* (2016) 16:144. doi: 10.1186/s12890-016-0307-0
33. Smego RA Jr., Nagar S, Maloba B, Popara M. A meta-analysis of salvage therapy for *Pneumocystis* carinii pneumonia. *Arch Intern Med.* (2001) 161:1529–33.
34. Fujii T, Nakamura T, Iwamoto A. *Pneumocystis* pneumonia in patients with HIV infection: clinical manifestations, laboratory findings, and radiological features. *J Infect Chemother.* (2007) 13:1–7. doi: 10.1007/s10156-006-0484-5
35. Tu GW, Ju MJ, Han Y, He HY, Rong RM, Xu M, et al. Moderate-dose glucocorticoids as salvage therapy for severe pneumonia in renal transplant recipients: a single-center feasibility study. *Ren Fail.* (2014) 36:202–9. doi: 10.3109/0886022X.2013.846771
36. Tu G, He H, Yin K, Ju M, Zheng Y, Zhu D, et al. High-flow nasal cannula versus noninvasive ventilation for treatment of acute hypoxemic respiratory failure in renal transplant recipients. *Transplant Proc.* (2017) 49:1325–30. doi: 10.1016/j.transproceed.2017.03.088
37. Iriart X, Bouar ML, Kamar N, Berry A. *Pneumocystis* pneumonia in solid-organ transplant recipients. *J Fungi (Basel).* (2015) 1:293–331.
38. Radhi S, Alexander T, Ukwu M, Saleh S, Morris A. Outcome of HIV-associated *Pneumocystis* pneumonia in hospitalized patients from 2000 through 2003. *BMC Infect Dis.* (2008) 8:118. doi: 10.1186/1471-2334-8-118
39. Morris A, Wachter RM, Luce J, Turner J, Huang L. Improved survival with highly active antiretroviral therapy in HIV-infected patients with severe *Pneumocystis* carinii pneumonia. *AIDS.* (2003) 17:73–80. doi: 10.1097/00002030-200301030-00010
40. Ingram RJ, Call S, Andrade A, White C, Wheeler D. Management and outcome of pneumothoraces in patients infected with human immunodeficiency virus. *Clin Infect Dis.* (1996) 23:624–7. doi: 10.1093/clinids/23.3.624
41. Ali HS, Hassan IF, George S. Extra corporeal membrane oxygenation to facilitate lung protective ventilation and prevent ventilator-induced lung injury in severe *Pneumocystis* pneumonia with pneumomediastinum: a case report and short literature review. *BMC Pulm Med.* (2016) 16:52. doi: 10.1186/s12890-016-0214-4
42. Yee D, Fu D, Hui C, Dharmadhikari N, Carino G. A rare case of 4 Ps: bilateral pneumothoraces and pneumomediastinum in *Pneumocystis* pneumonia. *R I Med J (2013).* (2020) 103:52–4.
43. Sun J, Su J, Xie Y, Yin MT, Huang Y, Xu L, et al. Plasma IL-6/IL-10 Ratio and IL-8, LDH, and HBDH level predict the severity and the risk of death in AIDS patients with *Pneumocystis* pneumonia. *J Immunol Res.* (2016) 2016:1583951. doi: 10.1155/2016/1583951
44. Lu A, Wang C, Zhang X, Wang L, Qian L. Lactate dehydrogenase as a biomarker for prediction of refractory mycoplasma pneumoniae pneumonia in children. *Respir Care.* (2015) 60:1469–75. doi: 10.4187/respcare.03920
45. Terpstra ML, Aman J, van Nieuw Amerongen GP, Groeneveld AB. Plasma biomarkers for acute respiratory distress syndrome: a systematic review and meta-analysis*. *Crit Care Med.* (2014) 42:691–700. doi: 10.1097/01.ccm.0000435669.60811.24
46. Su Y, Ju MJ, Ma JF, Tu GW, He HY, Gu ZY, et al. Lactate dehydrogenase as a prognostic marker of renal transplant recipients with severe community-acquired pneumonia: a 10-year retrospective study. *Ann Transl Med.* (2019) 7:660. doi: 10.21037/atm.2019.10.75
47. Drent M, Cobben NA, Henderson RF, Wouters EF, van Dieijen-Visser M. Usefulness of lactate dehydrogenase and its isoenzymes as indicators of lung damage or inflammation. *Eur Respir J.* (1996) 9:1736–42. doi: 10.1183/09031936.96.09081736

48. Lane BR, Ast JC, Hossler PA, Mindell DP, Bartlett MS, Smith JW, et al. Dihydropteroate synthase polymorphisms in *Pneumocystis* carinii. *J Infect Dis.* (1997) 175:482–5.
49. Fichera ME, Roos DS. A plastid organelle as a drug target in apicomplexan parasites. *Nature.* (1997) 390:407–9.
50. Seaberg LS, Parquette AR, Gluzman IY, Phillips GW Jr., Brodasky TF, Krogstad DJ. Clindamycin activity against chloroquine-resistant Plasmodium falciparum. *J Infect Dis.* (1984) 150:904–11. doi: 10.1093/infdis/150.6.904

**Conflict of Interest:** The authors declare that the research was conducted in the absence of any commercial or financial relationships that could be construed as a potential conflict of interest.

**Publisher's Note:** All claims expressed in this article are solely those of the authors and do not necessarily represent those of their affiliated organizations, or those of the publisher, the editors and the reviewers. Any product that may be evaluated in this article, or claim that may be made by its manufacturer, is not guaranteed or endorsed by the publisher.

frontiers | Frontiers in Medicine

CASE REPORT
published: 15 June 2022
doi: 10.3389/fmed.2022.905350

# Next-Generation Sequencing Technology Combined With Multiplex Polymerase Chain Reaction as a Powerful Detection and Semiquantitative Method for Herpes Simplex Virus Type 1 in Adult Encephalitis: A Case Report

*Weibi Chen, Yingfeng Wu and Yan Zhang**

*Xuanwu Hospital, Capital Medical University, Beijing, China*

OPEN ACCESS

***Edited by:***
*Sondes Haddad-Boubaker, Pasteur Institute of Tunis, Tunisia*

***Reviewed by:***
*Kaouther Ayouni, Pasteur Institute of Tunis, Tunisia*
*Marwa Arbi, Pasteur Institute of Tunis, Tunisia*

***Correspondence:**
*Yan Zhang*
*zhangylq@sina.com*

***Specialty section:***
*This article was submitted to Precision Medicine, a section of the journal Frontiers in Medicine*

***Received:*** *27 March 2022*
***Accepted:*** *23 May 2022*
***Published:*** *15 June 2022*

***Citation:***
*Chen W, Wu Y and Zhang Y (2022) Next-Generation Sequencing Technology Combined With Multiplex Polymerase Chain Reaction as a Powerful Detection and Semiquantitative Method for Herpes Simplex Virus Type 1 in Adult Encephalitis: A Case Report. Front. Med. 9:905350. doi: 10.3389/fmed.2022.905350*

**Background:** Traditional testing for specific microbes or categories of central nervous system (CNS) infectious diseases is often limited in sensitivity and timeliness. However, failure to initiate a timely etiological diagnosis and corresponding treatment in patients with neurologic infections contribute to poor outcomes.

**Case Summary:** A 58 year-old male presented acutely with fever, abnormal mental behavior, seizures and decreased consciousness. Brain magnetic resonance imaging (MRI) showed an abnormal FLAIR/T2 signal mainly in the left thalamus, temporal lobe, insular lobe, and bilateral hippocampus. To identify the pathogen, the cerebrospinal fluid (CSF) sample of the patient was used for metagenomic next-generation sequencing (mNGS) analysis and multiplex polymerase chain reaction (mPCR). The results showed 188 herpes simplex virus (HSV-1)-specific sequences. After acyclovir and foscarnet sodium treatment, the ratio of HSV-1/internal reference reads decreased from 813/493 to 695/1961, which coincided with clinical remission.

**Conclusion:** This study indicates that mNGS combined with mPCR may be an effective method for etiological diagnostic and dynamic clinical surveillance for HSV-1 encephalitis.

**Keywords: encephalitis, herpes simplex virus type 1, metagenomic next-generation sequencing, multiplex PCR, sequencing**

## INTRODUCTION

Encephalitis is defined as the presence of an inflammatory process of the brain in association with clinical evidence of neurologic dysfunction. As an important cause of morbidity, mortality, and permanent neurological sequelae, encephalitis remains a worldwide health problem. Of the pathogens reported to cause encephalitis, the majority are viruses (1). Viral agents include primary neurotropic viruses such as arboviruses, herpesviruses, and rabies virus, as well as other

nervous system pathogens such as enteroviruses, measles, respiratory viruses, etc., causing disease in the central nervous system (CNS) and elsewhere in the body. However, the pathogens for encephalitis cases are not identified in approximately 50% of patients (1, 2). Fever, headache, altered mental status, seizures, and/or focal neurologic signs, are common but non-specific symptoms of encephalitis, that overlap with those of different viral encephalitis, non-viral infectious entities or inflammatory encephalitis of non-infectious origin (3). These symptoms do not reliably identify the underlying etiology. In addition, metabolic or toxic encephalopathy, can also mimic viral encephalitis. Since empirical treatment may be ineffective or even harmful, accurate information about etiological agents and individualized management of a patient who presents with encephalitis are required to ensure good outcomes.

Traditional diagnostic techniques (e.g., virus culture, hemagglutination inhibition assay, enzyme immunoassay, and direct fluorescent antibody detection) were once the mainstays for pathogen detection, but the sensitivity and timeliness are limited for viral pathogens. Advances in molecular technology have now allowed its use as a clinical diagnostic tool. Metagenomic next-generation sequencing (mNGS) provides an unbiased analysis method, that can theoretically identify viruses, bacteria, parasites, fungi, and other pathogens by sequencing the total RNA or DNA in the samples of patients with known sequences (4–7). Previous studies have reported that mNGS of cerebrospinal fluid (CSF) obtained from patients with CNS infectious diseases can effectively identify different pathogens (5, 8), but none of these studies indicated mNGS as a semiquantitative method in clinical application.

Here, we report a case of herpes simplex encephalitis (HSE). In the case, mNGS analysis and multiplex PCR (mPCR) were used to identify the herpes simplex virus (HSV-1) and served a semiquantitative method to determine the pathogenic load.

## CASE DESCRIPTION

A 58-year-old male, with a history of hypertension, was admitted because of fever, abnormal mental behavior, epileptic seizures, and decreased consciousness. In the morning before admission, he was found to be slow to respond with a mild fever of 37.6°C. Blood examinations showed a peripheral blood leukocyte count of 15,860/$mm^3$ (lymphocytes: 12.1%); C-reactive protein level of 25.4 mg/L; and normal procalcitonin level. Brain magnetic resonance imaging (MRI) revealed an abnormal signal of T2-weighted images and fluid-attenuated inversion recovery images (T2/FLAIR) in the left thalamus, temporal lobe, insular lobe and bilateral hippocampus (**Figure 1**). During that day, he had frequent seizures and gradually felt increasingly sleepy. Four days before admission, the patient experienced anorexia and abdominal distension with no anal discharge. A computed tomography (CT) scan showed luminal distension in the proximal part of the intestine and accumulation of luminal contents. Physical examination on admission revealed stupor with a positive meningeal irritation sign, moist rales in both lungs, abdominal distension and hyperactive bowel sounds (at least 10 times/min). Further diagnostic work-up was performed. Lumbar puncture was performed on the second day after admission, which showed elevated intracranial pressure of 260 $mmH_2O$. Cerebrospinal fluid (CSF) analysis revealed inflammatory changes with pleocytosis of 24 leukocytes/μl (96% monocytes) and normal biochemistry with a glucose level of 55.62 mg/dl and a protein level of 33 mg/dl. CSF culture was also performed for pathogen detection, which did not reveal any pathogens. An electroencephalogram (EEG) performed on admission showed lateralized periodic discharges (LPDs) on the left (**Figure 2A**). The presumptive diagnosis of viral encephalitis was made. However, serological tests for infectious agents, including herpes simplex virus (HSV-1, 2), varicella zoster virus (VZV), cytomegalovirus (CMV), Epstein–Barr virus (EBV), and human herpes virus (HHV6, 7, 8), were all negative. The CSF sample was then sent for mNGS analysis and mPCR to identify the pathogen, which was approved by the Ethics Committee of Xuanwu Hospital, Capital Medical University [No. (2020) 104]. Written informed consent was provided by the patient. The mPCR procedure was performed as described below.

### Nucleic Acid Extraction

The CSF samples were centrifuged at 13,000 rpm for 10 min and ground on a grinding mill (Tiss-24, Jingxin, Shanghai, China) at 60 Hz for 10 min. The ground samples were then used for DNA/RNA extraction and purification (Zymo BIOMICS DNA/RNA Miniprep Kit, R2002) according to the manufacturer's instructions.

### Construction of the Sequencing Library

The extracted nucleic acids were used to construct the pathogen-targeted high-throughput sequencing library. The library was built by using a Pathogeno One High-Throughput Sequencing Library Construction kit (Shanghai Pathogeno Medical Technology Co., Ltd., China, SJ0005). A group of nucleic acid standards with known concentrations were added to the amplification system. In this process, two rounds of PCR were conducted. The sample nucleic acid and cDNA were used as templates, and a total of 524 microorganism-specific primers were chosen for multiple PCR amplification to enrich the target pathogen sequences, which contain bacteria (294), viruses (79), fungi (65), parasites (38), spirochetes (7), and others (41). Following the amplification step, PCR products were purified by beads and then amplified using primers with sequencing adapters and different barcodes. After purification of the final amplified products by agarose gel electrophoresis, quality inspection, and quantification were performed using a Qubit4.0 fluorometer. Normally, the library fragment size was approximately 400 bp, and the library concentration was at least 1 ng/μ l.

### High-Throughput Sequencing

The concentration of the mixed library was requantified and then diluted to a final concentration of 4 nM. Next, 5 μl of the mixed library was added with 5 μl of freshly prepared NaOH (0.2 M). After vortexing and centrifuging at 280 g for 1 min, the library was placed at room temperature for 5 min. The denatured library was sequenced on a MiSeq system (Illumina, Inc., San Diego, CA,

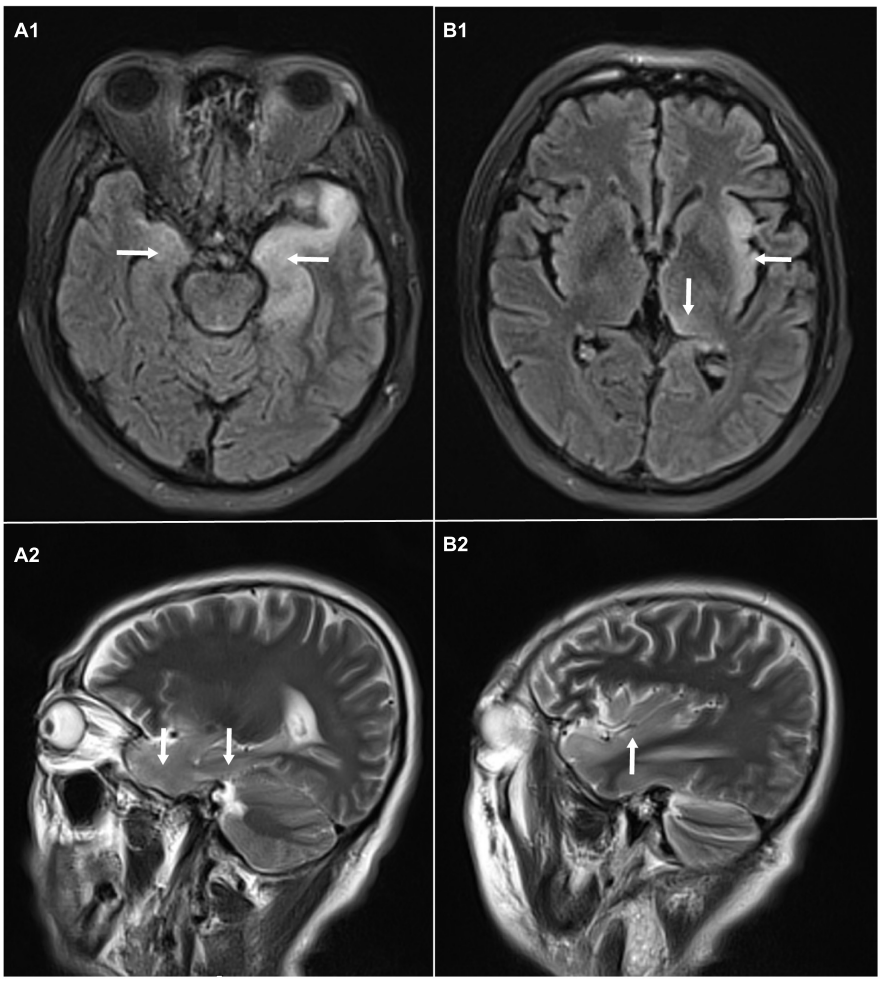


**FIGURE 1 |** Brain magnetic resonance imaging: abnormal signal of T2-weighted images and fluid-attenuated inversion recovery images (T2/FLAIR) in the left thalamus, temporal lobe, insular lobe and bilateral hippocampus. **(A1)** Axial MRI showed high signals on FLAIR in the left temporal lobe and bilateral hippocampus. **(A2)** Sagittal MRI showed high signals on T2 in the temporal lobe and hippocampus. **(B1)** Axial MRI showed high signals on FLAIR in left thalamus, and insular lobe. **(B2)** Sagittal MRI showed high signals on T2 in left insular lobe.

United States) using a MiSeq reagent kit v2 (average 0.05 million reads per library, with sequencing read length = PE60). FastQ files were generated by MiSeq Reporter software.

## Data Analysis

The raw data were first identified by the linker, the reads with a paired-end length > 60 bp were retained, and then low-quality filtering was performed to retain reads with Q30 > 50% as high-quality data. The paired-ended aligned reads were compared with the pathogen database to confirm the number of sequences (reads) in each sample. Through the statistical analysis of the read number after sequencing, we can obtain the ratio between the read number of the specific amplification target and the read number of these standards, and then calculated the approximate content of the specific amplification target.

The CSF sequencing results returned 3 days later, showing that the number of HSV-1-specific sequences was 188, with a ratio of HSV-1/internal reference reads of 813/493. On admission, empirical antiviral treatment (acyclovir: 10 mg/kg intravenously every 8 h) and antiseizure medications (intramuscular injection of phenobarbital 0.2 g followed by phenobarbital (90 mg) orally every 8 h and levetiracetam (1,500 mg) orally every 12 h were given to the patient. However, he remained unconscious 7 days after admission, when the plasma concentration of phenobarbital was 28.49 μg/ml. An EEG was then performed again, which indicated that periodic discharge had disappeared, and only a small amount of epileptic discharges could be seen, as shown in **Figure 2B**. In case of the possibility of acyclovir resistance, foscarnet sodium (50 mg/kg) was also given intravenously twice per day. Fourteen days after admission, the patient recovered from unconsciousness. A repeated CSF examination was performed, which showed a fewer inflammatory changes with pleocytosis of 12 leukocytes/μl (100% monocytes), a glucose level of 66 mg/dl, and a protein level of 42 mg/dl. The mNGS test of the CSF sample showed a ratio of HSV-1/internal reference reads of 695/1961. Compared with the

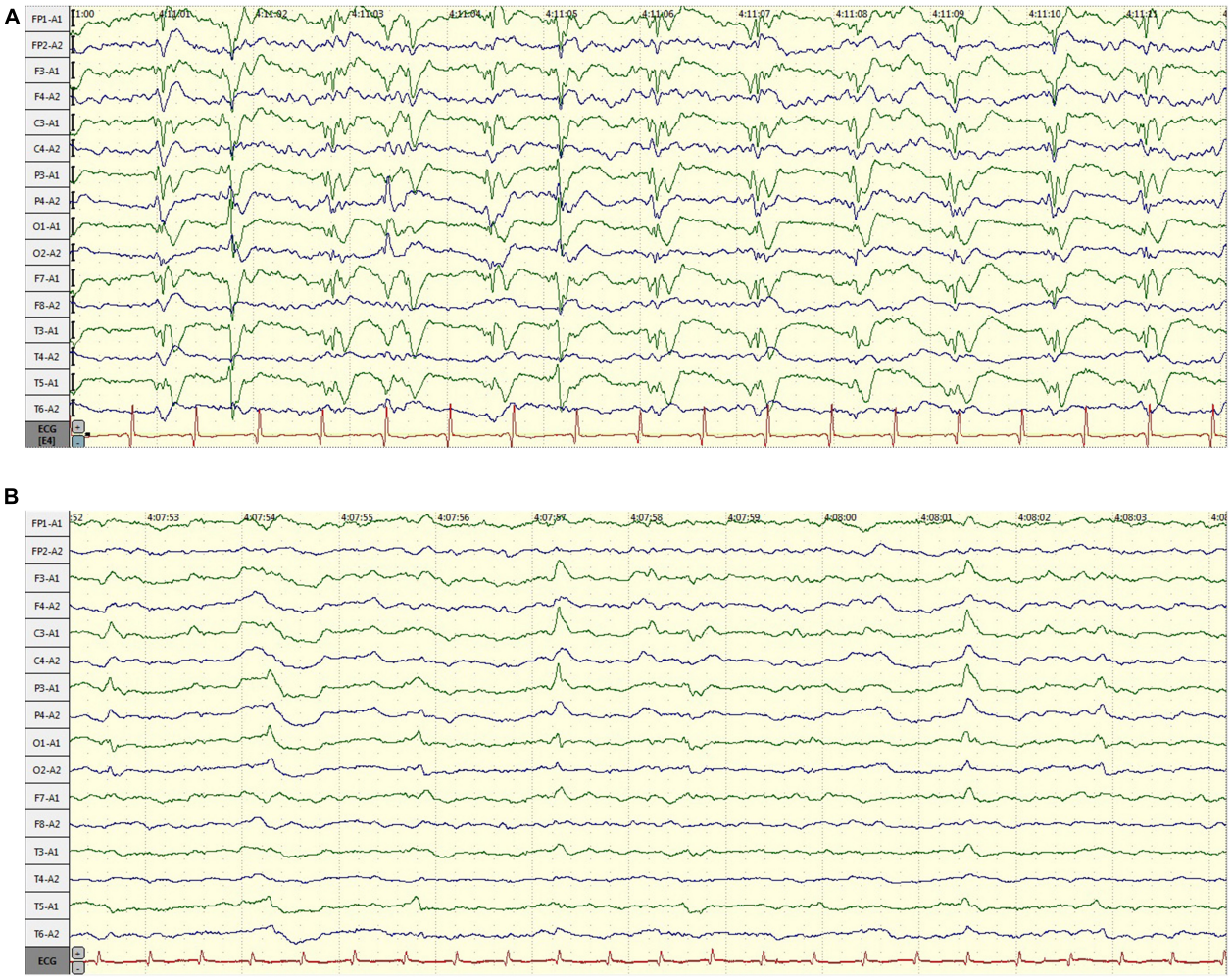


**FIGURE 2 |** The changes of electroencephalogram (EEG) over time. **(A)** EEG performed on admission: lateralized periodic discharges (PDs) on the left; **(B)** EEG performed 7 days after admission: PDs had disappeared.

first mNGS analysis, the relative pathogenic load was reduced five times, which coincided with clinical remission. In addition, tests for anti-HSV IgM and IgG in serum as well as anti-HSV IgG in CSF were positive. Since the virus load determined *via* mNGS did not drop to zero, antiviral therapy (intravenous drip of acyclovir and foscarnet sodium) was continued for another 2 weeks. A summary of the timeline is presented in **Figure 3**.

The follow-up results at 6 months after discharge were as follows: self-care, no epilepsy or emotional abnormalities, mild cognitive impairment, and normal character orientation. The patient could communicate with people, but he often forgot some words and some people's names.

## DISCUSSION

In this case, we used mNGS and mPCR to identify the pathogen in the CSF of the patient, and we found that the specific sequences mapped to HSV-1 genomic regions and that the relative pathogenic load was reduced five times, which coincided with the improvement in clinical symptoms.

CNS infectious diseases are caused by different pathogens. The detection of a wide range of pathogens is essential to maximize the diagnostic rate for patients with CNS infectious diseases (9). However, the causative pathogens for encephalitis cannot be identified in some cases (1, 2), in part due to a lack of standardized diagnostic approaches, while the traditional microbiological tests (culture, smear, and immunoassay) chosen are often pathogen specific. Specific etiology diagnosis is important to guide the corresponding therapy and avoid unnecessary or even potential harm to patients (10). Under these circumstances, mNGS as a broad-spectrum pathogen analysis method, has revolutionized the field of infectious diseases, especially given the limited CSF samples. In recent years, mNGS has been successfully used to identify viral (11–15), bacterial (16–18), Ureaplasma parvum (19), fungal (20), toxoplasmic (21), and tuberculous (8) pathogens in CNS infections. A previous multicenter study in


**FIGURE 3 |** Timeline of the clinical history.

the United States reported that mNGS could detect pathogens (13 of 58) that were not detected by conventional methods (5). Compared with that of traditional clinical diagnosis, mNGS techniques also dramatically reduced the diagnostic period to less than 3 days, as seen in this study.

Currently, there are no reliable criteria or standard analysis methods to accurately discriminate between insignificant contaminants and true infectious organisms, or to define a positive mNGS result without the need for a confirmatory test. Based on a prospective multicenter study, Xing et al. proposed that different CNS infectious diseases were associated with different positive diagnostic criteria due to variations in lifestyles and genomic sequences (8). The pathogen HSV-1 identified in this study is consistent with the clinical manifestations of herpes simplex encephalitis, and the improvement in clinical symptoms after corresponding antiviral treatment verified the accuracy of the etiological diagnosis. Recently, some criteria have been proposed, such as mapping of at least three sequencing reads to

three different genomic regions of a virus genome or the absence of virus sequencing reads in negative controls (5, 22).

In this study, the level of pathogens reads relative to the internal reference in the two CSF samples of the patient was calculated by using mNGS combined with mPCR. Intriguingly, the decrease in the relative level of HSV-1 coincided with the improvement in clinical symptoms. Using an internal reference as a benchmark, the relative level of the virus can be accurately detected and objectively interpreted even if the level of the virus is low. Therefore, compared with the traditional qualitative detection of mNGS, our semiquantitative detection method offers a better sensitivity for pathogen identification and pathogenic load determination.

According to the guidelines, empirical antibiotics are commonly initiated in patients with suspected encephalitis, pending the results of diagnostic studies. Early administration of acyclovir for 14–21 days was recommended by the Infectious Diseases Society of America (23). With the application of antiviral drugs, the mortality of HSE has decreased (24). However, acyclovir-resistant herpes encephalitis and relapse of HSV encephalitis after completion of acyclovir therapy have been reported (25). In this patient, in the case of acyclovir resistance, foscarnet sodium was also given. Although significant clinical improvement was observed in the patient after 2 weeks of antiviral therapy, the viral load in the CSF had not yet decreased to zero, antiviral drugs were therefore continued for another 2 weeks to prevent relapse, which is a much longer course than recommended. At the follow-up 6 months after discharge, the patient's condition was relatively good and satisfactory.

## CONCLUSION

This study proves that mNGS combined with mPCR may be an effective method for etiological diagnosis and dynamic clinical surveillance for HSV-1 encephalitis.

## ETHICS STATEMENT

Written informed consent was obtained from the patient for the publication of this case report and any potentially identifiable images or data included in this article.

## AUTHOR CONTRIBUTIONS

WC designed, administrated the study, analyzed the data, and drafted the manuscript. YW provided the resources and participated within the analysis. YZ provided the resources, supervised the study, and reviewed the manuscript. All authors contributed to the article and approved the submitted version.

## FUNDING

This work was supported by the National Key Research and Development Program of China (2020YFC2005403) and the Research Foundation of China Association Against Epilepsy (grant no. CJ-B-2021-18).

## REFERENCES

1. Glaser CA, Honarmand S, Anderson LJ, Schnurr DP, Forghani B, Cossen CK, et al. Beyond viruses: clinical profiles and etiologies associated with encephalitis. *Clin Infect Dis.* (2006) 43:1565–77. doi: 10.1086/509330
2. Vora NM, Holman RC, Mehal JM, Steiner CA, Blanton J, Sejvar J. Burden of encephalitis-associated hospitalizations in the United States, 1998-2010. *Neurology.* (2014) 82:443–51. doi: 10.1212/WNL.0000000000000086
3. Venkatesan A, Tunkel AR, Bloch KC, Lauring AS, Sejvar J, Bitnun A, et al. Case definitions, diagnostic algorithms, and priorities in encephalitis: consensus statement of the international encephalitis consortium. *Clin Infect Dis.* (2013) 57:1114–28. doi: 10.1093/cid/cit458
4. Gardy JL, Loman NJ. Towards a genomics-informed, real-time, global pathogen surveillance system. *Nat Rev Genet* (2018) 19:9–20.
5. Wilson MR, Sample HA, Zorn KC, Arevalo S, Yu G, Neuhaus J, et al. Clinical metagenomic sequencing for diagnosis of meningitis and encephalitis. *N Engl J Med.* (2019) 380:2327–40. doi: 10.1056/NEJMoa1803396
6. Ramachandran PS, Wilson MR. Metagenomics for neurological infections - expanding our imagination. *Nat Rev Neurol.* (2020) 16:547–56. doi: 10.1038/s41582-020-0374-y
7. Gu W, Deng XD, Lee M, Sucu YD, Arevalo S, Stryke D, et al. Rapid pathogen detection by metagenomic next-generation sequencing of infected body fluids. *Nat Med.* (2021) 27:115–24. doi: 10.1038/s41591-020-1105-z
8. Xing XW, Zhang JT, Ma YB, He MW, Yao GE, Wang W, et al. Metagenomic next-generation sequencing for diagnosis of infectious encephalitis and meningitis: a large, prospective case series of 213 patients. *Front Cell Infect Microbiol.* (2020) 10:88. doi: 10.3389/fcimb.2020.00088
9. Hong NTT, Anh NT, Mai NTH, Nghia HDT, Nhu LNT, Thanh TT, et al. Performance of metagenomic next-generation sequencing for the diagnosis of viral meningoencephalitis in a resource-limited setting. *Open Forum Infect Dis.* (2020) 7:ofaa046. doi: 10.1093/ofid/ofaa046
10. Polage CR, Cohen SH. State-of-the-art microbiologic testing for community-acquired meningitis and encephalitis. *J Clin Microbiol.* (2016) 54:1197–202. doi: 10.1128/JCM.00289-16
11. Guan H, Shen A, Lv X, Yang X, Ren H, Zhao Y, et al. Detection of virus in CSF from the cases with meningoencephalitis by next-generation sequencing. *J Neurovirol.* (2016) 22:240–5. doi: 10.1007/s13365-015-0390-7
12. Olson CA, Dominguez SR, Miller S, Chiu CY, Messacar K. Gastroenteritis, hepatitis, encephalopathy, and human herpesvirus 6 detection in an immunocompetent child: benefits and risks of syndromic multiplex molecular panel testing. *J Pediatr.* (2019) 212:228–31. doi: 10.1016/j.jpeds.2019.04.058
13. Cao J, Zhu XQ. Acute viral encephalitis associated with human parvovirus B19 infection: unexpectedly diagnosed by metagenomic next-generation sequencing. *J Neurovirol.* (2020) 26:980–3. doi: 10.1007/s13365-020-00885-6
14. Liu LL, Guo LY, Dong J, Huang WH, Zhao L, Liu B, et al. Next-generation sequencing technology as a powerful detection and semi-quantitative method for herpes simplex virus type 1 in pediatric encephalitis. *J Neurovirol.* (2020) 26:273–6. doi: 10.1007/s13365-019-00803-5
15. Nilsson A, Edner N, Albert J, Ternhag A. Fatal encephalitis associated with coronavirus OC43 in an immunocompromised child. *Infect Dis (Lond).* (2020) 52:419–22. doi: 10.1080/23744235.2020.1729403
16. Culbreath K, Melanson S, Gale J, Baker J, Li F, Saebo O, et al. Validation and retrospective clinical evaluation of a quantitative 16s rrna gene metagenomic sequencing assay for bacterial pathogen detection in body fluids. *J Mol Diagn.* (2019) 21:913–23. doi: 10.1016/j.jmoldx.2019.05.002
17. Dai Y, Chen L, Chang W, Lu H, Cui P, Ma X. Culture-negative streptococcus suis infection diagnosed by metagenomic next-generation sequencing. *Front Public Health.* (2019) 7:379. doi: 10.3389/fpubh.2019.00379
18. Zhang X, Wu Z, Wang K. Diagnosis of *Streptococcus suis* meningoencephalitis with metagenomic next-generation sequencing of the cerebrospinal fluid: a case report with literature review. *BMC Infect Dis.* (2020) 20:884. doi: 10.1186/s12879-020-05621-3

19. Wang Q, Wang K, Zhang Y, Lu C, Yan Y, Huang X, et al. Neonatal Ureaplasma parvum meningitis: a case report and literature review. *Transl Pediatr.* (2020) 9:174–9.
20. Wylie KM, Blanco-Guzman M, Wylie TN, Lawrence SJ, Ghobadi A, DiPersio JF, et al. High-throughput sequencing of cerebrospinal fluid for diagnosis of chronic Propionibacterium acnes meningitis in an allogeneic stem cell transplant recipient. *Transpl Infect Dis.* (2016) 18:227–33. doi: 10.1111/tid.12512
21. Hu Z, Weng X, Xu C, Lin Y, Cheng C, Wei H, et al. Metagenomic next-generation sequencing as a diagnostic tool for toxoplasmic encephalitis. *Ann Clin Microbiol Antimicrob* (2018) 17:45. doi: 10.1186/s12941-018-0298-1
22. Miller S, Naccache SN, Samayoa E, Messacar K, Arevalo S, Federman S, et al. Laboratory validation of a clinical metagenomic sequencing assay for pathogen detection in cerebrospinal fluid. *Genome Res.* (2019) 29:831–42. doi: 10.1101/gr.238170.118
23. Tunkel AR, Glaser CA, Bloch KC, Sejvar JJ, Marra CM, Roos KL, et al. The management of encephalitis: clinical practice guidelines by the infectious diseases society of America. *Clin Infect Dis.* (2008) 47:303–27.
24. Mailles A, De Broucker T, Costanzo P, Martinez-Almoyna L, Vaillant V, Stahl JP, et al. Long-term outcome of patients presenting with acute infectious encephalitis of various causes in France. *Clin Infect Dis.* (2012) 54:1455–64. doi: 10.1093/cid/cis226
25. Inagaki T, Satoh M, Fujii H, Yamada S, Shibamura M, Yoshikawa T, et al. Acyclovir sensitivity and neurovirulence of herpes simplex virus type 1 with amino acid substitutions in the viral thymidine kinase gene, which were detected in the patients with intractable herpes simplex encephalitis previously reported. *Jpn J Infect Dis.* (2018) 71:343–9. doi: 10.7883/yoken.JJID.2018.176

**Conflict of Interest:** The authors declare that the research was conducted in the absence of any commercial or financial relationships that could be construed as a potential conflict of interest.

**Publisher's Note:** All claims expressed in this article are solely those of the authors and do not necessarily represent those of their affiliated organizations, or those of the publisher, the editors and the reviewers. Any product that may be evaluated in this article, or claim that may be made by its manufacturer, is not guaranteed or endorsed by the publisher.

frontiers | Frontiers in Medicine

ORIGINAL RESEARCH
published: 20 June 2022
doi: 10.3389/fmed.2022.910098

# Association Between the *LZTFL1* rs11385942 Polymorphism and COVID-19 Severity in Colombian Population

*Mariana Angulo-Aguado[1†], David Corredor-Orlandelli[1†], Juan Camilo Carrillo-Martínez[1], Mónica Gonzalez-Cornejo[1], Eliana Pineda-Mateus[1], Carolina Rojas[1], Paula Triana-Fonseca[2], Nora Constanza Contreras Bravo[1], Adrien Morel[1], Katherine Parra Abaunza[3], Carlos M. Restrepo[1], Dora Janeth Fonseca-Mendoza[1*‡] and Oscar Ortega-Recalde[1*‡]*

[1] Center for Research in Genetics and Genomics – CIGGUR, GENIUROS Research Group, School of Medicine and Health Sciences, Universidad Del Rosario, Bogotá, Colombia, [2] Department of Molecular Diagnosis, Genética Molecular de Colombia SAS, Bogotá, Colombia, [3] Hospital Universitario Mayor – Méderi – Universidad del Rosario, Bogotá, Colombia

OPEN ACCESS

**Edited by:**
Renan Pedra de Souza, Universidade Federal de Minas Gerais, Brazil

**Reviewed by:**
Átila Duque Rossi, Federal University of Rio de Janeiro, Brazil
Barbara Eleni Rosato, University of Naples Federico II, Italy

***Correspondence:**
Oscar Ortega-Recalde
oscarj.ortega@urosario.edu.co
Dora Janeth Fonseca-Mendoza
dora.fonseca@urosario.edu.co

†These authors share first authorship
‡These authors share last authorship

**Specialty section:**
This article was submitted to Precision Medicine, a section of the journal Frontiers in Medicine

**Received:** 31 March 2022
**Accepted:** 26 May 2022
**Published:** 20 June 2022

**Citation:**
Angulo-Aguado M, Corredor-Orlandelli D, Carrillo-Martínez JC, Gonzalez-Cornejo M, Pineda-Mateus E, Rojas C, Triana-Fonseca P, Contreras Bravo NC, Morel A, Parra Abaunza K, Restrepo CM, Fonseca-Mendoza DJ and Ortega-Recalde O (2022) Association Between the LZTFL1 rs11385942 Polymorphism and COVID-19 Severity in Colombian Population. Front. Med. 9:910098. doi: 10.3389/fmed.2022.910098

Genetic and non-genetic factors are responsible for the high interindividual variability in the response to SARS-CoV-2. Although numerous genetic polymorphisms have been identified as risk factors for severe COVID-19, these remain understudied in Latin-American populations. This study evaluated the association of non-genetic factors and three polymorphisms: *ACE* rs4646994, *ACE2* rs2285666, and *LZTFL1* rs11385942, with COVID severity and long-term symptoms by using a case-control design. The control group was composed of asymptomatic/mild cases ($n = 61$) recruited from a private laboratory, while the case group was composed of severe/critical patients ($n = 63$) hospitalized in the Hospital Universitario Mayor-Méderi, both institutions located in Bogotá, Colombia. Clinical follow up and exhaustive revision of medical records allowed us to assess non-genetic factors. Genotypification of the polymorphism of interest was performed by amplicon size analysis and Sanger sequencing. In agreement with previous reports, we found a statistically significant association between age, male sex, and comorbidities, such as hypertension and type 2 diabetes mellitus (T2DM), and worst outcomes. We identified the polymorphism *LZTFL1* rs11385942 as an important risk factor for hospitalization ($p < 0.01$; OR = 5.73; 95% CI = 1.2–26.5, under the allelic test). Furthermore, long-term symptoms were common among the studied population and associated with disease severity. No association between the polymorphisms examined and long-term symptoms was found. Comparison of allelic frequencies with other populations revealed significant differences for the three polymorphisms investigated. Finally, we used the statistically significant genetic and non-genetic variables to develop a predictive logistic regression model, which was implemented in a Shiny web application. Model discrimination was assessed using the area under the receiver operating characteristic curve (AUC = 0.86; 95% confidence interval 0.79–0.93). These results suggest that *LZTFL1* rs11385942 may be a potential biomarker for COVID-19 severity in addition to conventional non-genetic risk factors.

A better understanding of the impact of these genetic risk factors may be useful to prioritize high-risk individuals and decrease the morbimortality caused by SARS-CoV2 and future pandemics.

**Keywords: *LZTFL1*, *ACE*, *ACE2*, host genetics, infection severity, COVID-19**

## INTRODUCTION

SARS-CoV-2 (Severe acute respiratory syndrome coronavirus 2) is a novel coronavirus, first identified in China in late December 2019 (1). The disease caused by this virus, named COVID-19, rapidly spread across the globe being declared a pandemic by the WHO in March 2021 (2). Up to the first week of March 2022, more than 450 million confirmed cases and 6 million deaths were reported worldwide, from which ∼6 million confirmed cases and 139.000 deaths occurred in Colombia (3, 4). The clinical course and severity of COVID-19 disease are highly variable among individuals, ranging from asymptomatic cases to severe respiratory failure and death (5).

Different clinical risk factors, including aging, male sex and comorbidities such as cardiovascular disease, hypertension, diabetes mellitus, chronic obstructive pulmonary lung disease, immunosuppression and obesity have been linked to more severe courses of COVID-19 (6, 7). Importantly, numerous studies have shown that host genetic factors also play a critical role in SARS-CoV-2 disease progression and severity (8–10). Early works suggested a potential role of genes related to the renin-angiotensin-aldosterone system (RAAS) (*ACE1* and *ACE2*), the ABO blood group system and the human leukocyte antigen (HLA) (11–13). The RAAS pathway is a physiological system that plays an important role in the homeostatic control of blood pressure and body water-electrolyte balance (14). Angiotensin I converting enzyme and angiotensin converting enzyme 2, coded by the genes *ACE* and *ACE2*, respectively, are critical regulators of this pathway and may also contribute to multiple organ injuries in COVID-19. In lung vascular endothelium, ACE catalyzes Angiotensin I conversion into Angiotensin II, an active peptide that promotes vasoconstriction, inflammation and thrombosis (15). Conversely, ACE2 converts Angiotensin II into angiotensin-(1–7), molecules that counteract the effects of Angiotensin II, including vasodilatation and vascular protection (16). Polymorphisms that increase *ACE* expression have been associated with more severe COVID-19 infections. The *ACE* insertion(Ins)/deletion(Del) polymorphism (rs4646994) is of particular interest as the resulting decrease in ACE activity has been linked to a protective effect in Ins allele carriers (17). Moreover, ACE2 has a dual role as the SARS-CoV-2 receptor, allowing virus internalization, and as RAAS regulator, catalyzing angiotensin II degradation (16, 18). Whole exome studies (WES) have identified more than 30 variants in the *ACE2* gene, potentially interfering with protein structure, stabilization and expression, and contributing to the high interindividual variability and susceptibility to COVID-19 (19). Among these variants, NM_001371415.1:c.439+4G>A (rs2285666) polymorphism is related to an increase of 50% of ACE2 expression, compared to wild-type G/G genotype carriers, and decreases the risk of severe SARS-CoV2 infection (20). In addition, two large genome-wide association studies, oriented to find genetic susceptibly locus, identified an association signal at chromosome 3p21.31 (rs11385942 and rs10490770) as the one with the most significant association with respiratory failure and mechanical ventilation requirement amongst severe COVID-19 patients (21, 22). This locus contains several genes related to cell signaling and solute transportation, including *CCR9*, *CXCR6*, *LZTFL1*, and *SLC6A20*. *LZTFL1* gene, the most promising candidate, codifies for a protein involved in the primary cilia function and the immunological synapse between T-cells and antigen-presenting cells (23).

Despite their relevance, genetic host factors related to COVID-19 severity remain understudied in Latin-American populations, limiting their potential use as predictive biomarkers and the development of predictive models. Furthermore, the study of these factors is particularly relevant considering that Latin-American countries have been severely affected by the COVID-19 pandemic. In this study, we performed an ambispective case-control analysis to evaluate the association between non-genetic factors and genetic factors, including the polymorphisms rs4646994 (*ACE*), rs2285666 (*ACE2*), and rs11385942 (*LZTFL1*), and COVID-19 severity and long-term symptoms in Colombian population. The results of this study support a positive association between the *LZTFL1* rs11385942 locus variant and an increased risk of severe SARS-CoV-2 infection. Furthermore, we developed a predictive model integrating non-genetic and genetic factors, potentially useful to identify high-risk individuals and prioritize prevention and mitigation efforts.

## METHODS

### Study Population and Sampling

This study enrolled 145 patients between 18 and 60 years with confirmed diagnosis of COVID-19 by positive RT-PCR (reverse transcriptase polymerase chain reaction), antigens or antibodies (IgG and/or IgM for SARS-CoV-2) tests. The control group consisted of 71 patients who were classified as asymptomatic or mild COVID-19, group non-hospitalized. The case group was composed of 74 patients with severe or critical disease, group hospitalized. Subcategorization of the case group was made with patients critically ill who required intensive care unit (ICU), group hospitalized-ICU. Clinical severity was determined according to national guidelines for COVID-19 by the Colombian Health Ministry (24). Cases were recruited among hospitalized patients at the Hospital Universitario Mayor-Méderi (Bogotá, Colombia). Controls were enrolled from a private laboratory (Genética Molecular de Colombia, Bogotá, Colombia). Cases and controls were invited to participate in this

study and those who accepted signed an informed consent and underwent buccal swap or peripheral blood sampling. Patients were enrolled between December 2020–July 2021 and all subjects were unvaccinated at the time of recruitment.

The sample size was calculated with a $p$ (sample proportion) of 7% according to the minimum allele frequency (MAF) for the allele with the reported lowest frequency, in our case the polymorphism rs11385942, a confidence level of 95% ($\alpha = 0.05$, $z = 1.96$), a margin of error ($e$) of 5%, and a population size $N = 8{,}000{,}000$ for Bogotá city. Using the formula $n = Nz^2 * p(1\text{-}p)/\alpha^2(N\text{-}1)+z^2 * p(1\text{-}p)$, implemented in the OpenEpi web-tool, we estimated that the minimum sample size was 101 (25). This value was approximated to 145 individuals considering possible clinical follow up lost. Given this is the first study to assess allele frequency for the polymorphisms of interest in Colombian population, MAF were obtained from the GnomAD database for Latino-American individuals (26). This study followed the guidelines of the Declaration of Helsinki and all experimental procedures were approved by the Ethics Committee of Universidad del Rosario (DVO005 1543-CV1334).

## Clinical Data Collection and Follow Up

Data collection and clinical follow up were conducted through phone calls at least 21 days after the diagnosis. Data was obtained through a standardized format that included the following clinical and demographical information: sex, age, blood type, medical history, comorbidities, drugs use, symptoms, long-term symptoms, and any change in disease severity. Furthermore, we performed an exhaustive revision of clinical records of hospitalized patients to validate the information collected previously and verify the clinical classification and severity criteria according to the clinical guidelines mentioned before. One hundred and twenty four patients, 61 cases and 63 controls, completed the clinical follow up and continued in the study.

## DNA Extraction and Genotyping

Total genomic DNA was obtained from buccal swab or blood samples using either the Quick-DNA™ Miniprep Plus Kit (Zymo Research) or the Buccal Swab DNA Kit (Promega). The buccal swab samples were collected in a cotton swab and the blood samples were collected in EDTA tubes, 5 mL for patient. Genomic DNA was quantified using a nanodrop spectrophotometer. All samples were aliquoted and stored at 4°C until analysis. Polymerase chain reaction (PCR) was used to amplify and genotype three polymorphisms of interest: *ACE* 289bp ALU Ins/Del (rs4646994), *ACE2* c.439+4G>A (rs2285666), and *LZTFL1* c.323+621dup (rs11385942). Primers were designed using PrimerBlast (27). Primers sequences and PCR conditions are listed in **Supplementary Table 1**. For *ACE* rs4646994 genotyping, PCR products were run on a 1% agarose gel stained by ethidium bromide and amplicon sizes were used to determine individual genotypes. Fragments obtained were 191 bp for the Del allele and 480 bp for the Ins allele. For *ACE2* rs2285666 and *LZTL1* rs11385942, PCR products were purified and sequenced through Sanger method. Sequences were analyzed with the software Geneious Prime v2021.2 (Biomatters) (28). Genotypes were assigned in batches of 20 samples by two independent researchers. In case the results were in disagreement, a third researcher reassessed the results and a final consensus was achieved. These researchers were blind to the case-control status of the individuals. Genotypification was attempted in 125 individuals, being successful in 124 (99.2%).

## Statistical Analysis and Predictive Model

A bivariate analysis was performed between clinical and demographic variables with the severe COVID-19 outcome (non-hospitalized vs. hospitalized, including UCI and non-UCI patients) or the presence of long-term COVID-19 symptoms using the $\chi^2$, Mann-Whitney and OR statistics. All the analyses were conducted using this case-control definition unless otherwise stated. Significant thresholds were set as $p < 0.05$, and a 95% confidence interval for the OR. Long-term COVID-19 symptoms were defined as persistent symptoms beyond 3 weeks from initial symptoms onset (29). An extended analysis of long-term symptoms was performed grouping symptoms into the following categories: (1) frequent (fatigue, headache, attention deficit, alopecia, dyspnea), (2) organ system affected (neurological, psychiatric, osteomuscular, respiratory, and cardiovascular), and (3) others including the ones with low sample and literature prevalence (dysphagia, otorhinolaryngological, ophthalmological and cutaneous manifestations) according to Lopez-Leon et al. (30).

Population genetic statistics, including allelic frequencies, genotypic frequencies and Hardy–Weinberg equilibrium (HWE), were calculated using the SNPStats software (31). The deviation of the HWE was established using a $\chi^2$ goodness-of-fit test with 1° of freedom (df) except for the SNP in *ACE2* rs2285666 located in the X chromosome, for which HWE was determined using the R package "HWadmiX" (32). Allelic frequencies obtained from the study were compared to other populations using the $\chi^2$ and Fisher's exact test statistics (21, 26, 33–46). $p$-values <0.05 were considered statistically significant.

The bivariate association analysis between genetic polymorphisms and severity outcome or the presence of long-term symptoms was performed with the PLINK software (47). Different genetic models, including allelic, genotypic, dominant and recessive, were assessed with the Cochran-Armitage trend, genotypic (2df), dominant gene action (1df), and recessive gene (1df) tests. In addition, a subgroup analysis between control (non-hospitalized) and ICU-hospitalized patients ($n = 26$) was conducted under the allelic model. The clinical and genetic variables with a significant correlation were used to build a multivariate logistic regression model in order to develop a predictive risk model for severe disease. Different combinations of variables were tested to construct the models, and these were compared using the Akaike Information Criterion (AIC) and the Coefficient of Discrimination D (Tjur's R2) parameters. This last method, Tjur's R2, is used for binomial logistic models and a value approaching 1 indicates that there is a clear separation between the predicted values for the response outcomes (48). For the model construction we evaluated and handled the potentially cofounding and interacting variables. We assessed the variation inflation factor (VIF) to protect our model to be inflated by multicollinearity, all the variables included had

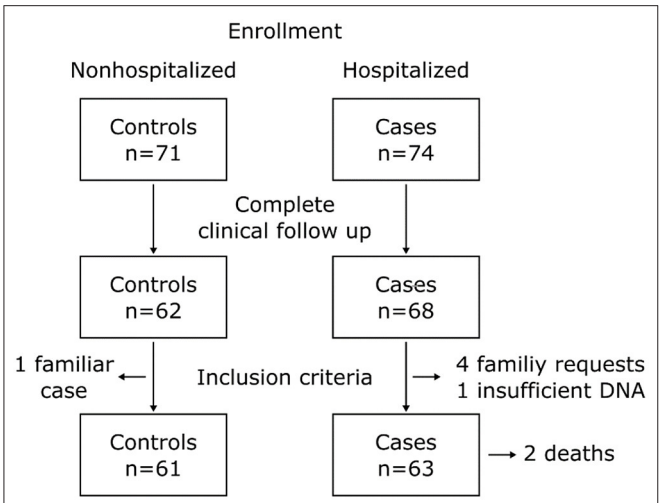


**FIGURE 1 |** Flowchart of the study participants.

a VIF value of 1. Model comparison was assessed by calculating the area under the receiver operating characteristic curve (AUC), direct comparison between the scores obtained from the models, integrated discrimination improvement (IDI) and cross-validation parameters, including concordance, sensitivity, specificity, and net benefit at different cutoff probabilities. Concordance was defined as the correctly estimated outcomes using several cutoff values for the predicted affection probability. The IDI score and cross-validation parameters were calculated with the R packages PredictABEL and rmda, respectively (49, 50). Finally, an open-source and online application was developed for users to easily access and test the model. The predictive model was constructed using R v4.1.2 and the online application was built using the Shiny package for R (51).

# RESULTS

## Clinical and Demographic Data

In total 145 patients, 71 controls and 74 cases were enrolled in the study. Nine patients from the control group and six patients from the cases group were excluded from the study by loss to follow up. One control was excluded due to familial relationship, one case was excluded by insufficient DNA and four cases were excluded due to direct request from the family. The final number of patients included was 61 controls and 63 cases. Two patients from the cases group died due to COVID-19 complications; nevertheless, clinical follow up was completed with help of relatives. A summary of the study participants is presented in **Figure 1**. For the control group, 29.5% ($n = 18$) diagnoses were made by RT-PCR, 63.9% ($n = 39$) by antigen test, and 6.6% ($n = 4$) by antibodies. The sampling methods for this group were 67.2% ($n = 41$) by buccal swabs and 32.8% ($n = 20$) from peripheral blood. For the case group, 98.4% ($n = 62$) diagnoses were made by RT-PCR and 1.6% ($n = 1$) by antigen test and 100% samples were taken from peripheral blood.

Demographic and clinical characteristics of our study population are summarized in **Table 1**. The mean age for the control group was 36.6 ± 10.8 years and that for the case group was 47.3 ± 9.53 years. Men accounted 42.6% ($n = 26$) of controls and 65% ($n = 41$) of the case group. Among the most common comorbidities in our study population were type 2 diabetes mellitus (T2DM) 11.3% ($n = 14$), hypertension 16.1% ($n = 20$) and obesity 21.8% ($n = 27$). Most patients (56.5%, $n = 70$) presented no comorbidities, 27.4 ($n = 34$) patients had 1 comorbidity and 16.1% ($n = 20$) had two or more comorbidities. The different signs and symptoms observed in the patients are presented in **Table 2**. Respiratory symptoms were the most common, these included dyspnea 55.6% ($n = 69$) and cough 64.5% ($n = 80$), followed by systemic symptoms, including fever 52.4% ($n = 65$), fatigue 81.5% ($n = 101$) and osteomuscular pain 70.2% ($n = 87$). Long-term symptoms were frequent (57.3%, $n = 71$), these included common symptoms (39.5%, $n = 49$), respiratory (15.3%, $n = 19$), osteomuscular (8.9%, $n = 11$), neurologic (22.6%, $n = 28$) and psychiatric (19.4%, $n = 24$). Demographic and clinical characteristics in patients with and without long-term COVID-19 symptoms are presented in **Table 3**.

## Clinical Association Analysis

Our study revealed a significant statistical correlation between SARS CoV-2 severity and multiple clinical variables reported previously, including age ($p < 0.01$), male sex ($p = 0.01$; OR = 2.51; 95% CI = 1.21–5.18), hypertension ($p < 0.01$; OR = 7.14; 95% CI = 1.97–25.88) and T2DM ($P < 0.01$; OR = 15.6; 95% CI = 1.97–123.42). Interestingly, other clinical variables, including blood group, cardiovascular, pulmonary, and other systemic diseases, such as cancer and obesity, were non-statistically significant in our sample ($p > 0.05$). Additionally, presence of no comorbidities was a protective factor ($p < 0.01$; OR = 0.17; 95% CI = 0.08–0.38) and presence of two or more comorbidities conferred an increased risk of severe disease ($p < 0.01$; OR = 11.8; 95% CI = 2.6–53.5). Symptoms who exhibited significant association with severe disease were mainly respiratory, systemic, and neurological, and included dyspnea ($p < 0.01$, OR = 29.54; 95% CI = 10.91–80.01), cough ($p < 0.01$; OR = 4.69; 95% IC=2.1–10.49) and fever ($p < 0.01$; OR = 4.41; 95% CI = 2.08–9.38) and mental status disturbance ($p = 0.04$; OR = 2.63; 95% CI = 1–6.93). In contrast, anosmia ($p < 0.01$; OR = 0.2; 95% CI = 0.09–0.42), ageusia ($p < 0.01$; OR = 0.30; 95% CI = 0.14–0.63), and headache ($p = 0.02$ OR = 0.42; 95% CI = 0.2–0.9) were more frequent in patients with mild disease (**Table 2**).

Presence of long-term symptoms was associated with disease severity ($p < 0.01$; OR = 3.37; 95% CI = 1.6–7.1). 42.6% patients in the control group developed these symptoms, in contrast to the 71.4% in the case group. Categories significantly different were common long-term symptoms ($p < 0.01$; OR = 6.91; 95% CI = 3.03–15.77), psychiatric ($p < 0.01$; OR = 34.5; 95% CI = 4.48–265.78) and respiratory ($p = 0.01$; OR = 4.45; 95% CI = 1.39–14.32), whereas cardiovascular long-term symptoms were present only in cases ($p < 0.01$). Multiple acute symptoms were associated with long-term symptoms, such as presence of fatigue

**TABLE 1 |** Demographic and clinical characteristics of the study population.

| Variable | Controls ($n = 61$) | Cases ($n = 63$) | *p*-value | CI95% | OR |
|---|---|---|---|---|---|
| Age | 36.6 (±10.8) | 47.3 (±9.53) | <0.01* | | |
| Male sex | 26 (42.6%) | 41 (65.0%) | 0.01* | 1.21–5.18 | 2.51 |
| **Blood group** | | | | | |
| O | 38 (62.3%) | 42 (66.7%) | 0.61 | 0.58–2.53 | 1.21 |
| A | 20 (32.8%) | 12 (19.0%) | 0.08 | 0.21–1.10 | 0.48 |
| B | 2 (3.3%) | 2 (3.2%) | 1 | 0.13–7.09 | 0.97 |
| AB | 1 (1.6%) | 0 (0%) | 0.98 | – | – |
| **Comorbidities** | | | | | |
| Arrhythmia | 0 (0%) | 1 (1.58%) | 1 | – | – |
| Asthma | 2 (3.27%) | 1 (1.58%) | 0.97 | 0.04–5.39 | 0.48 |
| Autoimmune disease | 0 (0%) | 2 (3.17%) | 0.49 | – | |
| Cancer | 1 (1.63%) | 3 (4.76%) | 0.63 | 0.30–29.66 | 3.00 |
| Chronic kidney disease | 5 (8.2%) | 1 (1.58%) | 0.22 | 0.59–45.63 | 5.17 |
| COPD | 0 (0%) | 2 (3.2%) | 0.49 | – | – |
| Coronary disease | 0 (0%) | 2 (3.2%) | 0.49 | – | – |
| T2DM | 1 (1.63%) | 13 (20.6%) | <0.01* | 1.97–123.42 | 15.6 |
| Hypertension | 3 (4.91%) | 17 (26.9%) | <0.01* | 1.97–25.88 | 7.14 |
| HIV/Immunodeficiency | 0 (0%) | 2 (3.2%) | 0.49 | – | – |
| Obesity | 9 (14.7%) | 18 (28.5%) | 0.09 | 0.95–5.65 | 2.31 |
| No comorbidities | 47 (77%) | 23 (36.5%) | <0.01* | 0.08–0.38 | 0.17 |
| One comorbidity | 12(19.7%) | 22 (34.9%) | 0.05 | 0.97–4.96 | 2.19 |
| Two or more Comorbidities | 2 (3.27%) | 18 (28.5%) | <0.01* | 2.60–53.50 | 11.80 |
| Chronic use of steroids | 1 (1.63%) | 1 (1.58%) | 1 | 0.06–15.83 | 0.97 |
| Smoking history | 28 (45.9%) | 18 (28.5%) | 0.05 | 0.23–1.02 | 0.48 |

**Statistical significant, p-value < 0.05; COPD, Chronic obstructive pulmonary disease.*

($p < 0.01$; OR = 5.12; 95% CI = 1.85–14.13), osteomuscular pain (0.04; OR = 2.26; 95% CI = 1.03–4.94), dyspnea ($p < 0.01$; OR = 4.96; 95% CI = 2.30–10.69), ageusia ($p = 0.01$; OR = 2.53; 95% CI = 1.22–5.27) and brain fog ($p = 0.02$; OR = 3.26; 95% CI 1.12–9.46).

## Genetic Variants and Association Analysis

The *ACE* rs4646994 genotypic distribution in the total sample was 0.35 (43/124), 0.45 (56/124) and 0.2 (25/124) for Ins/Ins, Ins/Del and Del/Del, respectively. The allele frequency for the Del allele was 0.43 (106/248). For *ACE2* rs2285666, an X-linked SNP, the distribution was 0.5 (29/58), 0.4 (23/58) and 0.1 (6/58) for G/G and G/A and A/A genotypes, respectively, and 0.53 (35/66) and 0.47 (31/66) for G and A genotypes in hemizygous individuals, respectively. The allele frequency for the allele A was 0.36 (66/180). Finally, for *LZTFL1* rs11385942, the distribution was 0.9 (111/124) and 0.1 (13/124) for the genotypes WT/WT and WT/Ins, respectively. We did not observe homozygous individuals for the allele Ins. The allele frequency for this allele was 0.05 (13/235). Genotypic and allelic frequencies are presented in **Table 4**. All genotypes were found to be in HWE (*ACE* rs4646994 $p = 0.46$, *ACE2* rs2285666 $p = 0.25$ and *LZTFL1* rs11385942 $p = 1$). Genotype frequencies by clinical subgroups (controls, cases hospitalized no ICU and cases hospitalized in ICU) are presented in **Supplementary Table 2**.

Bivariate analysis between the genetic polymorphisms and COVID-19 severity revealed a statistically significant association between the *LZTFL1* rs11385942 polymorphism with severe COVID-19 and severe COVID-19 requiring hospitalization in ICU ($p = 0.01$; OR = 5.73; 95% CI = 1.24–26.46 and $p = 0.02$; OR = 6.12; 95% CI = 1.14–32.63, respectively, under the allelic genetic model). No association was found between the *ACE* rs4646994 and *ACE2* rs2285666 polymorphisms, and COVID-19 severity under any of the models tested (**Table 5**). Nevertheless, an association between *ACE* rs4646994 Del and neurological long-term symptoms (e.g., ageusia, anosmia, and vertigo) was identified under the Cochran-Armitage test ($p < 0.01$; OR = 0.32; 95% CI = 0.16–0.63).

## Population Genetic Analysis

Next, we compared the allelic frequencies obtained in this study with those of other datasets including populations of European, Asian, African, North American, and Latin-American ancestries (**Supplementary Table 3**). We found significant statistical differences for the three systems assessed. For *ACE* rs46469949, East Asia allelic frequencies were the only population with no statistical differences. For *ACE2* the rs2285666 allelic frequency found in our study was similar to those reported in Mexican

**TABLE 2 |** COVID-19 symptoms in the studied population.

| Variable | Controls ($n = 61$) | Cases ($n = 63$) | *p*-value | CI 95% | OR |
|---|---|---|---|---|---|
| **Acute symptoms** | | | | | |
| Ageusia | 40 (65.5%) | 23 (36.5%) | <0.01* | 0.14–0.63 | 0.30 |
| Anosmia | 42 (68.8%) | 19 (30.1%) | <0.01* | 0.09–0.42 | 0.20 |
| Cough | 29 (47.5%) | 51 (80.9%) | <0.01* | 2.10–10.49 | 4.69 |
| Diarrhoea | 11 (18%) | 20 (31.7%) | 0.07 | 0.91–4.90 | 2.11 |
| Dyspnea | 13 (21.3%) | 56 (88.8%) | <0.01* | 10.91–80.01 | 29.54 |
| Fatigue | 42 (68.8%) | 59 (93.6%) | <0.01* | 2.12–21.04 | 6.67 |
| Fever > 38°C | 21 (34.4%) | 44 (69.8%) | <0.01* | 2.08–9.38 | 4.41 |
| Haemoptysis | 2 (3.2%) | 6 (9.52%) | 0.29 | 0.60–16.03 | 3.11 |
| Headache | 44 (72.1%) | 33 (52.3%) | 0.02* | 0.20–0.90 | 0.42 |
| Mental status disturbance | 7 (11.4%) | 16 (25.3%) | 0.04* | 1.00–6.93 | 2.63 |
| Odynophagia | 29 (47.5%) | 29 (46%) | 0.86 | 0.46–1.91 | 0.94 |
| Osteomuscular pain | 39 (63.9%) | 48 (76.1%) | 0.13 | 0.83–3.94 | 1.81 |
| Rhinorrhea | 33 (54%) | 24 (38%) | 0.07 | 0.26–1.07 | 0.52 |
| **Long-term symptoms** | | | | | |
| Presence | 26 (42.6%) | 45 (71.4%) | <0.01* | 1.60–7.09 | 3.37 |
| Common | 11 (18%) | 38 (60.3%) | <0.01* | 3.03–15.77 | 6.91 |
| Cardiovascular | 0 (0%) | 8 (12.6%) | 0.01* | – | – |
| Neurologic | 16 (26.2%) | 12 (19%) | 0.33 | 0.28–1.55 | 0.66 |
| Osteomuscular | 4 (6.55%) | 7 (11.1%) | 0.56 | 0.49–6.42 | 1.78 |
| Psychiatric | 1 (1.63%) | 23 (36.5%) | <0.01* | 4.48–265.78 | 34.50 |
| Respiratory | 4 (6.55%) | 15 (23.8%) | 0.01* | 1.39–14.32 | 4.45 |
| Other long-term symptoms | 0 (0%) | 2 (3.2%) | 0.49 | | |

**Statistical significant, p-value < 0.05.*

and American populations. Finally, for *LZTFL1* rs11385942, the comparison was made against COVID-19 patients obtained from a previous study. We found significant differences with Italian controls but not with Italian cases or Spanish population (**Table 6**).

## Predictive Model and App Development

Genetic and non-genetic significant variables obtained from the previous analyses were entered into a logistic regression model. Different combinations of variables were tested, and the models obtained were compared by Akaike's Information Criterion (AIC) and Coefficient of Discrimination D (Tjur's R2). The best model had the lowest AIC and highest Tjur's R2 values. This model incorporated sex, age, number of comorbidities and the polymorphism *LZTFL1* rs11385942. The resulting predicting score that includes these variables was:

$$Adjusted\ score = \frac{1}{1 + e^{-(-2.88+(0.077*age)+0.81(male)+(0.99*comorb)+1.44(WT/Alt))}} \quad (1)$$

Where the adjusted score is a number between 0 and 1, "*age*" the age in years, "*male*" male sex, "*comorb*" represents the number of comorbidities and "*WT/Alt*" the risk allele for the *LZTFL1* rs11385942 polymorphism.

Score distribution using this model for cases and controls is presented in **Figures 2A,B**. The model achieved good discrimination power (AUC = 0.857; 95% confidence interval 0.79–0.93) (**Figure 2C**) (**Supplementary Table 4**). Comparison between the clinical (Age + Sex + Comorbidities) and complete models (Age + Sex + Comorbidities + risk allele) showed a slight increase in the AUC, 0.846 vs. 0.857, respectively. Model comparison was assessed by three additional methods. First, direct comparison between the scores obtained from the clinical and complete model showed a high correlation, nevertheless, for several individuals, the risk scores changed noticeably when the risk allele is included in the model (**Figure 2D**). Next, we compared the models using the IDI score (52). This method is defined as the difference in the discrimination slopes between two models, the discrimination slopes are calculated as the difference of predicted probabilities for events and non-events (53). We obtained a positive IDI score (0.026; confidence interval 95% 0.001–0.051, *p*-value: 0.039) supporting a significant improvement for the complete model. Third, we calculated cross-validation parameters including concordance, sensitivity, specificity and net benefit for different probability cutoffs (54). Net benefit is a decision analytic measure, which puts benefits and harms on the same scale

**TABLE 3 |** Demographic and clinical characteristics in patients with and without long-term COVID-19 symptoms.

| Variables | Patient with no long-term symptoms ($n = 53$) | Patients with long term symptoms ($n = 71$) | *p*-value | CI 95% | OR |
|---|---|---|---|---|---|
| Hospitalized | 18 (34%) | 45 (63.4) | 0.00 | 1.60–7.10 | 3.37 |
| Age | 40 (±12.1) | 43.5 (±10.8) | 0.095 | | |
| Male sex | 32 (60.3%) | 35 (49.2%) | 0.22 | 0.31–3.22 | 0.64 |
| **Blood group** | | | | | |
| O | 30 (56.6%) | 50 (70.4%) | 0.11 | 0.87–3.84 | 1.83 |
| A | 15 (28.3%) | 17 (23.9%) | 0.58 | 0.36–1.79 | 0.80 |
| B | 1 (1.88%) | 3 (4.22%) | 0.82 | 0.23–22.69 | 2.29 |
| AB | 0 (0%) | 1 (1.40%) | 1 | – | – |
| **Comorbidities** | | | | | |
| Coronary disease | 0 (0%) | 2 (2.81%) | 0.60 | – | – |
| Arrhythmias | 0 (0%) | 1 (1.40%) | 1 | – | – |
| Hypertension | 8 (15.0%) | 12 (16.9%) | 0.98 | 0.43–3.03 | 1.14 |
| COPD | 0 (0%) | 2 (2.81%) | 0.60 | – | – |
| Asthma | 1 (1.88%) | 2 (2.81%) | 0.97 | 0.04–5.39 | 0.48 |
| T2DM | 6 (11.3%) | 8 (11.26%) | 1 | 0.32–3.06 | 0.99 |
| Chronic kidney disease | 4 (7.54%) | 2 (2.81%) | 0.42 | 0.06–2.02 | 0.36 |
| Cancer | 1 (1.88%) | 3 (4.22%) | 0.82 | 0.23–22.69 | 2.29 |
| Obesity | 10 (18.8%) | 17 (23.9%) | 0.49 | 0.56–3.26 | 1.35 |
| HIV/Immunodeficiency | 1 (1.88%) | 1 (1.40%) | 1 | 0.05–12.15 | 0.74 |
| Autoimmune disease | 0 (0%) | 2 (2.81%) | 0.60 | – | – |
| No comorbidities | 34 (64.1%) | 36 (50.7%) | 0.13 | 0.28–1.19 | 0.57 |
| One comorbidity | 13(24.5%) | 21(29.6%) | 0.53 | 0.58–2.90 | 1.29 |
| Two or more comorbidities | 6 (11.3%) | 14 (19.7%) | 0.31 | 0.69–5.40 | 1.92 |
| Chronic use of steroids | 0 (0%) | 2 (2.81%) | 0.60 | – | – |
| Smoking history | 14 (26.4%) | 32 (45.0%) | 0.05 | 1.03–4.81 | 2.23 |
| **Acute symptoms** | | | | | |
| Ageusia | 20 (37.7%) | 43 (60.5%) | 0.01* | 1.22–5.27 | 2.53 |
| Anosmia | 21 (39.6%) | 40 (56.3%) | 0.07 | 0.95–4.05 | 1.97 |
| Cough | 31 (58.4%) | 49 (69.0%) | 0.23 | 0.75–3.32 | 1.58 |
| Diarrhoea | 10 (18.8%) | 21 (29.5%) | 0.17 | 0.77–4.25 | 1.81 |
| Dyspnoea | 18 (33.9%) | 51 (71.8%) | <0.01* | 2.30–10.69 | 4.96 |
| Fatigue | 36 (67.9%) | 65 (91%) | <0.01* | 1.85–14.13 | 5.12 |
| Fever > 38°C | 21 (39.6%) | 44 (61.9%) | 0.01* | 1.20–5.15 | 2.48 |
| Haemoptysis | 1 (1.88%) | 7 (9.8%) | 0.15 | 0.68–47.72 | 5.69 |
| Headache | 30 (56.6%) | 47 (66.1%) | 0.28 | 0.72–3.12 | 1.50 |
| Odynophagia | 23 (43.3%) | 35 (49.2%) | 0.51 | 0.62–2.59 | 1.27 |
| Osteomuscular Pain | 32 (60.3%) | 55 (77.4%) | 0.04* | 1.03–4.94 | 2.26 |
| Rhinorrhea | 20 (37.7%) | 37 (52.1%) | 0.11 | 0.87–3.71 | 1.80 |
| Brain fog | 5 (9.43%) | 18 (25.3%) | 0.02* | 1.12–9.46 | 3.26 |

**Statistical significant, p-value < 0.05; COPD Chronic obstructive pulmonary disease.*

to be compared (55). The results of this analysis showed that the concordance and net benefit were better for most of the probability cutoffs tested (**Supplementary Table 5**). This improvement was particularly noticeable at probabilities between 0.3 and 0.4.

Finally, the complete model was used to design a web-based application using the R package Shiny. The application is open-access and is accessible through a shinyApp server (https://oscarortega.shinyapps.io/COVID19_UR_Shiny/). The source code of the shiny app is publicly available on Github at https://github.com/OscarOrt/COVID_19_risk.

## DISCUSSION

During the last 2 years, the COVID-19 pandemic has caused vast disruptions in almost any sphere of human activity. Despite

**TABLE 4 |** Allelic and genotypic frequencies for cases and controls.

| Gen | SNP | Allele frequency controls | | Allele frequency cases | | Genotype controls | | | Genotype cases | | | HWE |
|---|---|---|---|---|---|---|---|---|---|---|---|---|
| | | WT | Alt | WT | Alt | WT/WT | WT/Alt | Alt/Alt | WT/WT | WT/Alt | Alt/Alt | |
| *ACE* | rs4646994 | 0.6 | 0.4 | 0.55 | 0.45 | 0.39 | 0.41 | 0.2 | 0.3 | 0.49 | 0.21 | 0.46 |
| *ACE2* | rs2285666 | 0.63 | 0.37 | 0.65 | 0.35 | 0.47 ♀ | 0.39 ♀ | 0.14 ♀ | 0.55 ♀ | 0.41 ♀ | 0.04 ♀ | 0.25 |
| | | | | | | 0.52 ♂ | – | 0.48 ♂ | 0.54 ♂ | – | 0.46 ♂ | |
| *LZTFL1* | rs11385942 | 0.98 | 0.02 | 0.91 | 0.09 | 0.97 | 0.03 | 0 | 0.83 | 0.17 | 0 | 1 |

*ACE WT allele (Ins), ACE2 WT allele (G), LZTFL WT allele (no dup); Alt, alternative; WT, Wild Type; ♀ Genotype frequencies in females; ♂ Genotype frequences in males (hemizygous).*

**TABLE 5 |** Genetic association analysis for severe COVID-19.

| SNP | Model | Genotypes/alleles in cases | Genotypes/alleles in controls | χ2 | df | *p*-value | OR | IC 95% |
|---|---|---|---|---|---|---|---|---|
| ACE rs4646994 | Genotypic (2 df) test | 13/31/19 | 12/25/24 | 1.23 | 2 | 0.54 | – | – |
| | Cochran-Armitage trend test | 57/69 | 49/73 | 0.60 | 1 | 0.43 | – | – |
| | Allelic | 57/69 | 49/73 | 0.65 | 1 | 0.41 | 1.23 | 0.74–2.03 |
| | Dominant | 44/19 | 37/24 | 1.15 | 1 | 0.28 | – | – |
| | Recessive | 13/50 | 12/49 | 0.01 | 1 | 0.89 | – | – |
| ACE2 rs2285666 | Genotypic (2 df) test | 1/9/12 | 5/14/17 | – | – | – | – | – |
| | Cochran-Armitage trend test | 11/33 | 24/48 | 0.85 | 1 | 0.35 | – | – |
| | Allelic | 11/33 | 24/48 | 0.90 | 1 | 0.34 | 0.92 | 0.50–1.69 |
| | Dominant | 10/12 | 19/17 | – | – | – | – | – |
| | Recessive | 1/21 | 5/31 | – | – | – | – | – |
| LZTFL1 | Genotypic (2 df) test | 0/11/52 | 0/2/59 | – | – | – | – | – |
| rs11385942 | Cochran-Armitage trend test | 11/115 | 2/120 | 6.64 | 1 | <0.01* | – | – |
| | Allelic | 11/115 | 2/120 | 6.27 | 1 | 0.01* | 5.73 | 1.24–26.46 |
| | Dominant | 11/52 | 2/59 | – | – | – | – | – |
| | Recessive | 0/63 | 0/61 | – | – | – | – | – |

**Statistical significant, p-value < 0.05; df degrees of freedom; Genotypic (2 df) test: Alt/Alt vs. WT/Alt vs. WT/WT; Cochran-Armitage trend test: Alt vs. WT; Allelic: Alt vs. WT; Dominant: Alt/Alt + WT/Alt vs. WT/WT; Recessive: Alt/Alt vs. WT/Alt + WT/WT; ACE WT allele (Ins), ACE2 WT allele (G), LZTFL WT allele (no dup); Alt, alternative; WT, Wild Type.*

**TABLE 6 |** Population case-control analysis of allele frequencies.

| SNP | Region | Total case alleles | Cases WT alleles/AF | Cases Alt alleles/AF | *p*-value cases | Total controls alleles | Controls WT alleles/AF | Controls Alt alleles/AF | *p*-value controls | Source |
|---|---|---|---|---|---|---|---|---|---|---|
| *LZTFL1* rs11385942 | Present study | 126 | 115/0.91 | 11/0.09 | | 122 | 120/0.98 | 20/0.02 | | |
| | Italy | 1,670 | 1,436/0.86 | 234/0.14 | 0.12 | 2,510 | 2,284/0.91 | 226/0.09 | <0.01* | (21) |
| | Spain | 1,550 | 1,410/0.91 | 140/0.09 | 0.96 | 1,900 | 1,805/0.95 | 9/0.05 | 0.14 | (21) |

**Statistical significant, p-value < 0.05; AF, Allele frequency; Alt, alternative; WT, Wild Type.*

the growing knowledge about the biology and clinical features of this disease, many aspects of its physiopathology and clinical progression remain to be understood. Of particular interest in this process are host risk factors that could contribute to severe courses of COVID-19 and presence of long-term symptoms. These factors include non-genetic and genetic variables. In this study, we aimed to characterize the impact of these variables on COVID-19 outcomes in a sample of Colombian population. We identified several risk factors including the polymorphism *LZTFL1* rs11385942 and incorporated these variables into a predictive model. To the best of our knowledge, this is the first study to evaluate the association between genetic risk factors and

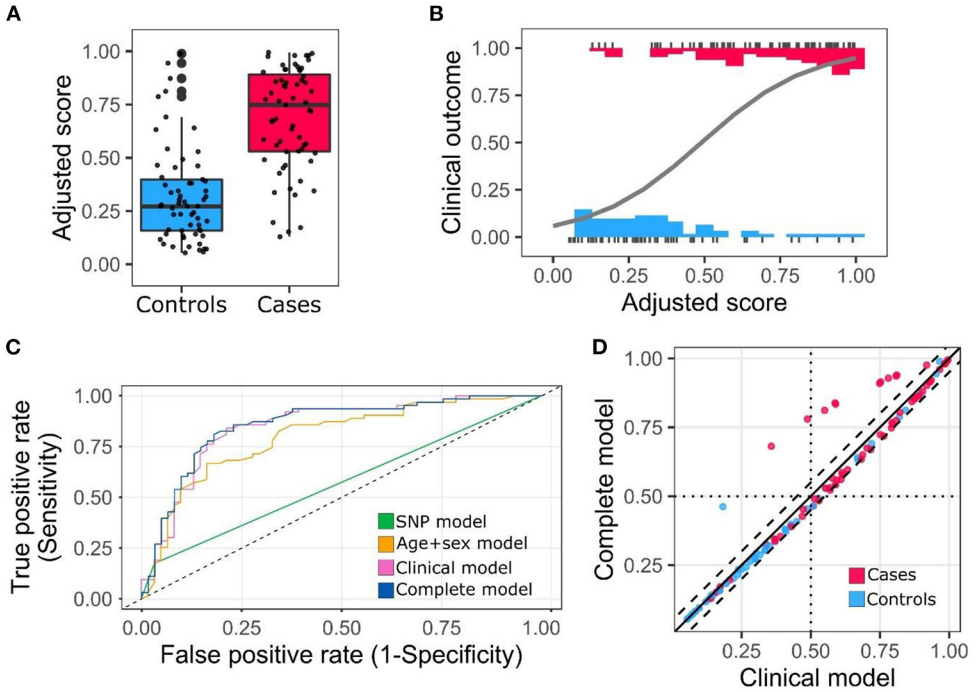


**FIGURE 2 |** Adjusted score distribution for cases and controls and ROC curve. **(A)** Box plot of the adjusted scores categorized by cases and controls. **(B)** Distribution and regression model for adjusted scores. Clinical outcome 0 corresponds to non-hospitalization and 1 to hospitalization. **(C)** Receiver operating characteristic (ROC) curve. **(D)** Score comparison clinical model vs. complete model. Dashed lines cutoff value ±0.05.

COVID-19 severity in a Latin-American population using a case-control design and illustrates the importance of host genetics in SARS-CoV-2 clinical outcomes.

Several non-genetic factors have been associated with poor COVID-19 prognosis, including age, male sex and comorbidities (56). In agreement with such reports, we found a significant association between age, male sex, hypertension and T2DM. Both hypertension and T2DM had been previously identified as independent risk factors for increased morbimortality in COVID-19 patients (57–61). The mechanism by which hypertension is a risk factor has been attributed to hyperactivation of the RAAS pathway, which increases the inflammatory response, cytokine storm, myocardial remodeling, acute lung injury, and endothelial damage (62). Similarly, it has been proposed that T2DM contributes to thromboembolic complications and organ damage through glucotoxicity, oxidative stress, and increased cytokine production (63). Interestingly, hyperglycemia in non-diabetic patients had a negative impact on patient outcomes (64), highlighting the importance of adequate metabolic control in the management of these patients. Other comorbidities analyzed did not show a statistically significant association individually, probably because the sample size was not large enough to detect such associations. Nonetheless, when grouped, the presence of two or more comorbidities conferred an increased risk of severe COVID-19, an effect possibly explained by the additive effect of risk factors to determine the clinical progression of the disease. The second point worth mentioning about clinical features in the studied population was the prevalence of acute symptoms. Among the most common symptoms reported in the literature are generalized weakness, dry cough, headache, dyspnea, and myalgias (65). In our sample, respiratory and systemic symptoms, including dyspnea, cough, fever and fatigue, were associated with severe disease, whereas flu-like symptoms, such as ageusia, anosmia and headache, were more frequent in patients with a mild form of the disease. Other studies, that included, populations have reported similar findings (66, 67). Lower respiratory tract symptoms are often related to severe COVID19, as they are a manifestation of underlying lung compromise.

Another element included in our analysis was the incidence of long-term COVID-19 symptoms, a phenomenon also reported in other viral infections including Spanish Flu SARS CoV-1 and MERS (68). Our findings are consistent with global literature, in which the most common long-term symptoms were fatigue (50–72.8%), joints pain (31.4%), headache (28.9%), chest pain (20–28.9%), dyspnea (28.2%) and palpitations (9%) (68–70). Remarkably, growing evidence suggests that psychiatric illness is an important COVID-19 sequel, affecting particularly specific populations such as Hispanic and African patients (71, 72). Psychiatric long-term symptoms were highly prevalent in hospitalized patients in our study (36.5%). Despite our study being limited by the absence of a standardized mental health scale for patient follow up, our data support these observations

(73). The mechanistic basis for these symptoms is attributed to the ability of the virus to infect the central nervous system via the blood-brain barrier and the olfactory bulb, affecting thereafter neurons on the hypothalamus, cortex and brainstem, which could explain many of the neuropsychiatric manifestations (71, 74). On the other hand, the absence of association between comorbidities and long-term symptoms has been also observed in the literature (75). Demographic variables such as sex are of much debate, as there is contradictory evidence of higher rates of long-term symptoms in female individuals (76). Finally, several acute symptoms associated with long-term compromise found in this study have been previously reported in the literature and include fatigue, dyspnea and osteomuscular pain and myalgias (77).

Regarding our genetic findings, our study identified the *LZFTL1* rs11385942 as a significant genetic factor associated with disease severity, conferring risk for severe/critical clinical outcomes. This polymorphism is located in the 3p21.31 locus, a region previously described as an important risk factor for severe respiratory disease in several studies (21, 78). There are six candidate genes in this locus potentially involved in the disease progression presumably by viral entry or clearance and immunological response, these are *SLC6A20*, *LZTFL1*, *CCR9*, *FYCO1*, *CXCR6*, and *XCR1* (78). The rs11385942 polymorphism is located at intron 5 of *LZFTL1* and recent studies have assessed its functional significance in SARS-CoV-2 infection, suggesting a regulatory role. A CRISPRi analysis using lung epithelial cell lines showed that *LZTFL1* expression is severely affected by this polymorphism (79). LZTFL1 (leucine zipper transcription factor like 1) protein is highly expressed in lung cells and regulates airway cilia and epithelial-mesenchymal transition, a developmental process critical for the innate immune and inflammatory response. Remarkably, the rs11385942 polymorphism has been associated with higher levels of C5a and soluble terminal complement complex C5b-9 (SC5b-9) plasma levels during SARS-CoV-2 infection, suggesting that enhanced immune system and complement activation might be important pathways in the deleterious effect of this variant (80). Moreover, it has been described that complement activation and membrane attack complex (MAC) formation leads to upregulation of pro-inflammatory proteins and inflammasomes causing severe lung injury and, in parallel, endothelial cells death, platelet activation and induction of the coagulation cascade leading to thrombus formation, well-known physiopathological findings in severe COVID-19 (81, 82). The results of another recent study suggest that rs11385942 is in genetic linkage with the polymorphism rs17713054G>A, the gain-of-function risk A allele upregulates the expression of *LZTFL1* by generating a CCAAT/enhancer binding protein beta motif (23). Despite other molecular mechanisms cannot be discarded, this evidence supports *LZTFL1* as a candidate effector and provides further support to our findings. Additional studies have found supporting evidence for this association (79, 83). In line with these observations, genotypification of the risk allele in this gene could be useful as a molecular predictive biomarker for COVID-19 severe/critical clinical outcomes.

Since the beginning of the pandemic, numerous studies have explored the role of host genetic variability in COVID-19 severity and susceptibility. These studies have included genome-wide association studies (GWAS), which have identified multiple reproducible associations (21, 22, 84–86). Given the underrepresentation of Latin American population in these initiatives, our study allowed us to reproduce the association of the 3p21.32 locus in an ethnically different cohort and suggests that the variation in this region modulates the disease outcome (21). Importantly, detailed exploration of "expanded" phenotypes, other than clinical severity, including symptomatic/paucisymptomatic and Exposed_Positive/Exposed_Negative phenotypes have identified a much larger proportion of protective minor alleles (85). These results suggest that using additional phenotype definitions can identify protective associations. Our patients classified as asymptomatic-mild/severe-critical are more likely enriched for risk alleles conferred by loci such as those analyzed in our study.

It is important to highlight that case-control association studies are potentially influenced by population stratification due to undetected population substructure produced by differences in ancestry generating spurious associations (87). To avoid confounding due to population stratification, analysis using ancestry markers (AIMs) are useful to estimate variability between cases and controls (88). Although our study did not carry out this evaluation, we estimate that sampled population shares a similar gene pool without the influence of factors such as geographic isolation or non-random mating. Additionally, the individuals analyzed come from the Colombian Andean region, a geographical area where high inter-individual variation has not been identified (89), which supports the ethnic similarity of the cases and controls included. Here, LZFTL1 rs11385942 was identified as a significant genetic factor associated with severe COVID-19 ($p = 0.01$; OR = 5.73; 95% CI = 1.24–26.46) supporting an important genetic effect. Previously, it has been suggested a need for approaches such as family-based designs or genomic control when the identified genetic effects are very small (OR < 1.20) (90). Finally, although stratification may be less of a concern than originally anticipated and the evidence against a large effect of population stratification, hidden or otherwise, it is important to consider it in false positive or negative association arising from differences in local ancestry (87, 88, 91).

Two polymorphisms analyzed in our study, *ACE* rs4646994 and *ACE2* rs2285666, are important regulators of the RAAS pathway, a physiological system implicated in COVID-19 susceptibility and severity (92). Despite we did not find evidence of association between these polymorphisms and COVID-19 severity, numerous studies support a biological basis for such relationship (92–94). The *ACE2* rs2285666 T allele is associated with a significant increase in ACE2 expression (95). Interestingly, association studies of this polymorphism with COVID-19 severity have had contradictory results and similar findings to ours have been reported by several authors (43, 96, 97). Among these, next-generation sequencing analysis in patients hospitalized for COVID-19 indicated no association between *ACE2* variants and COVID-19 severity (97). Such discrepancies might be explained by population-specific differences, the

additive role of other genes interacting with risk alleles or other mechanisms not assessed such as epigenetic modifiers (98–100). Concerning *ACE* rs4646994 the Del allele has been associated with increased ACE expression, higher enzyme activity and elevated production of angiotensin II (101). Despite *ACE* Del/Del genotype and Del allele have been associated with increased COVID-19 patient severity (101–103), our results failed to replicate these findings in the Colombian population. In agreement with our results, other studies have reported no association between *ACE* rs4646994 and COVID-19 severity (43, 96). Collectively, current evidence contains conflicting results about the role of this polymorphism in SARS-CoV-2 infections. The reasons for these discrepancies are unclear and similar to the *ACE2* rs2285666 polymorphism require further exploration. Interestingly, a recent meta-analysis evaluating several polymorphisms related to COVID-19 outcomes found a significant association between the polymorphism ACE rs4646994 and COVID-19 severity (104). Results of individual association studies must be considered carefully and discrepancies in the findings may be the result of underpowered sample sizes, therefore replicates and more robust studies should be considered to validate these associations. On the other hand, we identified *ACE* rs4646994 Del allele as a protective factor for neurological long-term symptoms, we hypothesize this could be related to an increased catalytic activity resulting in vasoconstriction that counterbalances the intracerebral vasodilation and brain edema due to the anaerobic metabolism in cerebral cells in response to SARS-CoV-2 induced hypoxia (105, 106). Whereas, interesting, this hypothesis requires experimental and clinical validation.

Comparison of allelic frequencies obtained in our study with other populations revealed important differences. For *ACE* rs4646994, Asia was the only region with a similar allele frequency to our studied population (40). This may reflect the ancestral origin of Native American population in Colombia or the admixture between an ancestral population with a higher frequency and Europeans, where allele frequencies are considerably lower (107, 108). For the *ACE2* polymorphism, the allelic frequency was similar to Mexican population, probably due to a common ancestry and admixture history (44). For the variant *LZTFL1* rs11385942, no differences were found with Spanish, European and African populations. Remarkably, Zeberg and Pääbo (109) described that the 3p21.31 region, the locus where the variant is located, was inherited from Neanderthals. The mixture of native Americans and Europeans probably modified the ancestral genetic pool leading to the current allele frequencies. Additionally, it has been proposed that differences in allelic frequencies for the 3p21.31 risk haplotype are produced by natural selection in response to pathogens (109).

Another important determinant of COVID-19 severity is viral genetics (10). It has been identified that specific SARS-CoV-2 variants are associated with differences in severity and mortality, for example, the alpha and gamma variants are related to increased hospitalization, ICU admission and mortality risk (110–112). While our study did not assess variant differences in cases and controls, genomic surveillance studies conducted during the sample collection period (December 2020–July 2021) in Bogotá, showed that the predominant variants were B.1.621 (Mu) 57.3% (469/819), P.1 (Gamma) 14% (114/819) and B.1.1.7 (alpha) 2.8% (23/819) (113). The most common variant found in this interval of time, Mu, was classified as a variant being monitored (VBM) by the Centers for Disease Control and Prevention (CDC U.S.) without reported major effects on infectivity, transmissibility or severity (114). The coexistence of several variants during this period constitutes a source of variation and might reflect a more complex dynamics of host-pathogen interactions.

Our clinical and genetic association analysis allowed us to identify several risk factors related to disease severity. These factors were incorporated into a predictive risk model using a multivariate logistic regression including demographic, clinical, and genetic traits. To date, ∼50 prediction models and scoring systems, have been published (115). These models are useful tools to facilitate decision-making in healthcare services and rely mostly on clinical features such as age, sex, number of comorbidities, hypertension, T2DM, chronic obstructive lung disease, cancer, cardiovascular disease. However, it is noteworthy that COVID-19 severity is influenced by viral and host genetic factors (10). Recent models, which like ours incorporate a multifactorial approach (genetic and non-genetic factors), included several single nucleotide variants (SNVs) (116). These models have achieved good results in discriminating COVID-19 severity groups and highlighted the role of integrated approaches to predict clinical outcomes. Furthermore, other models aiming to predict adverse outcomes are based on detailed clinical features during diagnosis, admission and hospitalization have been developed, nevertheless, its accessibility and clinical implementation have been limited (117, 118). We propose our model as a useful tool to estimate *a priori* severe or critical illness risk. Notably, despite the minor increase in the AUC when the clinical and complete models were compared, detailed analysis of the discrimination performance and cross-validation parameters suggest that the incorporation of the risk allele improves the risk prediction model. Further studies involving larger sample sizes might be useful to validate these findings. Likewise, the implementation of our model into a web application might facilitate its usage by healthcare providers in limited-resource settings during the current SARS-CoV-2 pandemics and future health emergencies caused by similar pathogens.

In summary, our study explores the relation between non-genetic and genetic factors, with COVID-19 outcomes in Colombian population, demonstrating a positive association between the *LZTFL1* rs11385942 polymorphism and severe disease. By establishing such association, we point up the importance of genetic host factors in SARS-CoV-2 infection. In addition, our work identified previously known non-genetic factors and developed a predictive model which was implemented in a web application, providing a useful tool for risk prediction. Integrative approaches, like ours, may be helpful to better understand COVID-19 clinical progression, refine healthcare efforts and reduce the morbimortality of patients with this disease.

## Study Limitations

Our study has potential limitations. First, the sample size was calculated in order to have 80% statistical power based on previous association reports for the variant with the lower allele frequency (*LZTF1* rs11385942.), nevertheless, it could have been limited to detect potential small effect sizes for the rs4646994 and rs228566 SNPs in our population. Second, some clinical variables assessed in the clinical follow-up interview were self-reported. Even though most of this information was confirmed in the clinical record, this could have been a potential source of bias. Third, we did not match the case-control groups by age or sex for the statistical analysis. Considering these variables are known risk factors, we aimed to assess their impact on COVID-19 outcome. Fourth, as previously mentioned, analysis of potential population stratification was not performed. In addition, COVID-19 severity is a multifactorial trait and other important variables, including environmental factors, SARS-CoV-2 variants, and additional host genetic polymorphisms, described as risk or protective factors were not evaluated. Assessment of such variables in future studies could help to improve discriminative models and medical risk assessment. Finally, we should highlight that our proposed risk model constitutes a proof-of-concept of the feasibility of this integrative approach and further studies with larger sample sizes and independent replications are required to validate the model.

## DATA AVAILABILITY STATEMENT

The original contributions presented in the study are included in the article/**Supplementary Material**, further inquiries can be directed to the corresponding author/s.

## ETHICS STATEMENT

The studies involving human participants were reviewed and approved by Ethics Committee of Universidad del Rosario (DVO005 1543-CV1334). The patients/participants provided their written informed consent to participate in this study.

## AUTHOR CONTRIBUTIONS

MA-A, DC-O, MG-C, EP-M, CR, DF-M, and OO-R contributed to conception and design of the study. MA-A, PT-F, NC, AM, DF-M, and OO-R performed DNA extraction and genetic analysis. MA-A, DC-O, JC-M, EP-M, CR, PT-F, KP, DF-M, and OO-R collected clinical data and organized the database. MA-A, JC-M, PT-F, and OO-R performed the statistical analysis. MA-A, DC-O, JC-M, PT-F, AM, DF-M, and OO-R wrote sections of the manuscript. All authors contributed to manuscript revision, read, and approved the submitted version.

## FUNDING

This project was supported by the Universidad del Rosario (Grant IV-TSE026).

## SUPPLEMENTARY MATERIAL

The Supplementary Material for this article can be found online at: https://www.frontiersin.org/articles/10.3389/fmed.2022.910098/full#supplementary-material

## REFERENCES

1. Zhu N, Zhang D, Wang W, Li X, Yang B, Song J, et al. A novel coronavirus from patients with pneumonia in China, 2019. *N Engl J Med.* (2020) 382:727–33. doi: 10.1056/NEJMoa2001017
2. Hu B, Guo H, Zhou P, Shi Z-L. Characteristics of SARS-CoV-2 and COVID-19. *Nat Rev Microbiol.* (2021) 19:141–54. doi: 10.1038/s41579-020-00459-7
3. Center for Systems Science and Engineering (CSSE) by the Johns Hopkins University (JHU). *COVID-19 Dashboard.* (2022). Available online at: https://coronavirus.jhu.edu/map.html
4. Ministerio de Salud y Protección Social C. *Situación Actual Coronavirus (COVID-19) Colombia.* (2022). Available online at: https://www.minsalud.gov.co/salud/publica/PET/Paginas/Covid-19_copia.aspx
5. Verity R, Okell LC, Dorigatti I, Winskill P, Whittaker C, Imai N, et al. Estimates of the severity of coronavirus disease 2019: a model-based analysis. *Lancet Infect Dis.* (2020) 20:669–77. doi: 10.1016/S1473-3099(20)30243-7
6. Deng G, Yin M, Chen X, Zeng F. Clinical determinants for fatality of 44,672 patients with COVID-19. *Crit Care.* (2020) 24:179. doi: 10.1186/s13054-020-02902-w
7. Williamson EJ, Walker AJ, Bhaskaran K, Bacon S, Bates C, Morton CE, et al. Factors associated with COVID-19-related death using OpenSAFELY. *Nature.* (2020) 584:430–36. doi: 10.1038/s41586-020-2521-4
8. Velavan TP, Pallerla SR, Rüter J, Augustin Y, Kremsner PG, Krishna S, et al. Host genetic factors determining COVID-19 susceptibility and severity. *eBioMedicine.* (2021) 72:103629. doi: 10.1016/j.ebiom.2021.103629
9. Fricke-Galindo I, Falfán-Valencia R. Genetics insight for COVID-19 susceptibility and severity: a review. *Front Immunol.* (2021) 12:622176. doi: 10.3389/fimmu.2021.622176
10. Ovsyannikova IG, Haralambieva IH, Crooke SN, Poland GA, Kennedy RB. The role of host genetics in the immune response to SARS-CoV-2 and COVID-19 susceptibility and severity. *Immunol Rev.* (2020) 296:205–19. doi: 10.1111/imr.12897
11. Kachuri L, Francis SS, Morrison ML, Wendt GA, Bossé Y, Cavazos TB, et al. The landscape of host genetic factors involved in immune response to common viral infections. *Genome Med.* (2020) 12:93. doi: 10.1186/s13073-020-00790-x
12. Gemmati D, Bramanti B, Serino ML, Secchiero P, Zauli G, Tisato V. COVID-19 and individual genetic susceptibility/receptivity: role of ACE1/ACE2 genes, immunity, inflammation and coagulation. Might the double X-chromosome in females be protective against SARS-CoV-2 compared to the single X-chromosome in males? *Int J Mol Sci.* (2020) 21:3474. doi: 10.3390/ijms21103474
13. Wang F, Huang S, Gao R, Zhou Y, Lai C, Li ZZ, et al. Initial whole-genome sequencing and analysis of the host genetic contribution to COVID-19 severity and susceptibility. *Cell Discov.* (2020) 6:83. doi: 10.1038/s41421-020-00231-4
14. Gelen V, Kükürt A, Sengül E. "Role of the Renin-Angiotensin-Aldosterone System in Various Disease Processes: An Overview". *Renin-Angiotensin Aldosterone System*. London: IntechOpen (2021). doi: 10.5772/intechopen.97354
15. Saad H, Jabotian K, Sakr C, Mahfouz R, Akl IB, Zgheib NK. The role of angiotensin converting enzyme 1 insertion/deletion genetic polymorphism in the risk and severity of COVID-19 infection. *Front Med.* (2021) 8:798571. doi: 10.3389/fmed.2021.798571
16. Ni W, Yang X, Yang D, Bao J, Li R, Xiao Y, et al. Role of angiotensin-converting enzyme 2 (ACE2) in COVID-19. *Crit Care.* (2020) 24:422. doi: 10.1186/s13054-020-03120-0

17. Hatami N, Ahi S, Sadeghinikoo A, Foroughian M, Javdani F, Kalani N, et al. Worldwide ACE (I/D) polymorphism may affect COVID-19 recovery rate: an ecological meta-regression. *Endocrine.* (2020) 68:479–84. doi: 10.1007/s12020-020-02381-7
18. Hoffmann M, Kleine-Weber H, Schroeder S, Krüger N, Herrler T, Erichsen S, et al. SARS-CoV-2 cell entry depends on ACE2 and TMPRSS2 and is blocked by a clinically proven protease inhibitor. *Cell.* (2020) 181:271–80.e8. doi: 10.1016/j.cell.2020.02.052
19. Benetti E, Tita R, Spiga O, Ciolfi A, Birolo G, Bruselles A, et al. ACE2 gene variants may underlie interindividual variability and susceptibility to COVID-19 in the Italian population. *Eur J Hum Genet.* (2020) 28:1602–14. doi: 10.1038/s41431-020-0691-z
20. Srivastava A, Bandopadhyay A, Das D, Pandey RK, Singh V, Khanam N, et al. Genetic association of ACE2 rs2285666 polymorphism with COVID-19 spatial distribution in India. *Front Genet.* (2020) 11:564741. doi: 10.3389/fgene.2020.564741
21. Ellinghaus D, Degenhardt F, Bujanda L, Buti M, Albillos A, Invernizzi P, et al. Genomewide association study of severe Covid-19 with respiratory failure. *N Engl J Med.* (2020) 383:1522–34. doi: 10.1056/NEJMoa2020283
22. COVID-19 Host Genetics Initiative. Mapping the human genetic architecture of COVID-19. *Nature.* (2021) 600:472–7. doi: 10.1038/s41586-021-03767-x
23. Downes DJ, Cross AR, Hua P, Roberts N, Schwessinger R, Cutler AJ, et al. Identification of LZTFL1 as a candidate effector gene at a COVID-19 risk locus. *Nat Genet.* (2021) 53:1606–15. doi: 10.1038/s41588-021-00955-3
24. Ministerio de Salud y Protección Social de Colombia. *Lineamientos Para el Manejo Clínico de Pacientes con Infección por Nuevo Coronavirus COVID-19.* (2020). Available online at: https://www.minsalud.gov.co/Ministerio/Institucional/Procesos y procedimientos/PSSS03.pdf
25. Dean AG. *OpenEpi: Open Source Epidemiologic Statistics for Public Health.* (2007). Available online at: http://www.OpenEpi.com; http://ci.nii.ac.jp/naid/10025863040/en/ (accessed March 10, 2022).
26. Karczewski KJ, Francioli LC, Tiao G, Cummings BB, Alföldi J, Wang Q, et al. The mutational constraint spectrum quantified from variation in 141,456 humans. *Nature.* (2020) 581:434–43. doi: 10.1530/ey.17.14.3
27. Ye J, Coulouris G, Zaretskaya I, Cutcutache I, Rozen S, Madden TL. Primer-BLAST: a tool to design target-specific primers for polymerase chain reaction. *BMC Bioinformatics.* (2012) 13:134. doi: 10.1186/1471-2105-13-134
28. Kearse M, Moir R, Wilson A, Stones-Havas S, Cheung M, Sturrock S, et al. Geneious Basic: an integrated and extendable desktop software platform for the organization and analysis of sequence data. *Bioinformatics.* (2012) 28:1647–9. doi: 10.1093/bioinformatics/bts199
29. Raveendran AV, Jayadevan R, Sashidharan S. Long COVID: an overview. *Diabetes Metab Syndr Clin Res Rev.* (2021) 15:869–75. doi: 10.1016/j.dsx.2021.04.007
30. Lopez-Leon S, Wegman-Ostrosky T, Perelman C, Sepulveda R, Rebolledo PA, Cuapio A, et al. More than 50 long-term effects of COVID-19: a systematic review and meta-analysis. *Sci Rep.* (2021) 11:16144. doi: 10.1038/s41598-021-95565-8
31. Solé X, Guinó E, Valls J, Iniesta R, Moreno V. SNPStats: a web tool for the analysis of association studies. *Bioinformatics.* (2006) 22:1928–9. doi: 10.1093/bioinformatics/btl268
32. Backenroth D, Carmi S. A test for deviations from expected genotype frequencies on the X chromosome for sex-biased admixed populations. *Heredity.* (2019) 123:470–78. doi: 10.1038/s41437-019-0233-z
33. Al-Harbi EM, Farid EM, Gumaa KA, Singh J. Genotypes and allele frequencies of angiotensin-converting enzyme (ACE) insertion/deletion polymorphism among Bahraini population with type 2 diabetes mellitus and related diseases. *Mol Cell Biochem.* (2012) 362:219–23. doi: 10.1007/s11010-011-1146-1
34. Salem A, Batzer MA. High frequency of the D allele of the angiotensin-converting enzyme gene in Arabic populations. *BMC Res Notes.* (2009) 2:99. doi: 10.1186/1756-0500-2-99
35. Comas D, Calafell F, Benchemsi N, Helal A, Lefranc G, Stoneking M, et al. Alu insertion polymorphisms in NW Africa and the Iberian Peninsula: evidence for a strong genetic boundary through the Gibraltar Straits. *Hum Genet.* (2000) 107:312–319. doi: 10.1007/s004390000370
36. Barley J, Blackwood A, Carter ND, Crews DE, Cruickshank JK, Jeffery S, et al. Angiotensin converting enzyme insertion/deletion polymorphism: association with ethnic origin. *J Hypertens.* (1994) 12:955–7.
37. Rutledge DR, Browe CS, Ross EA. Frequencies of the angiotensinogen gene and angiotensin I converting enzyme (ACE) gene polymorphisms in African Americans. *Biochem Mol Biol Int.* (1994) 34:1271–5.
38. Lee E. Population genetics of the angiotensin-converting enzyme in Chinese. *Br J Clin Pharmacol.* (1994) 37:212–14. doi: 10.1111/j.1365-2125.1994.tb04264.x
39. Saab YB, Gard PR, Overall ADJ. The geographic distribution of the ACE II genotype: a novel finding. *Genet Res.* (2007) 89:259–67. doi: 10.1017/S0016672307009019
40. Sarangarajan R, Winn R, Kiebish MA, Bountra C, Granger E, Narain NR. Ethnic prevalence of angiotensin-converting enzyme deletion (D) polymorphism and COVID-19 risk: rationale for use of angiotensin-converting enzyme inhibitors/angiotensin receptor blockers. *J Racial Ethn Heal Disparities.* (2021) 8:973–80. doi: 10.1007/s40615-020-00853-0
41. Strafella C, Caputo V, Termine A, Barati S, Gambardella S, Borgiani P, et al. Analysis of ACE2 genetic variability among populations highlights a possible link with COVID-19-related neurological complications. *Genes.* (2020) 11:741. doi: 10.3390/genes11070741
42. Clarke L, Zheng-Bradley X, Smith R, Kulesha E, Xiao C, Toneva I, et al. The 1000 genomes project: data management and community access. *Nat Methods.* (2012) 9:459–62. doi: 10.1038/nmeth.1974
43. Gómez J, Albaiceta GM, García-Clemente M, López-Larrea C, Amado-Rodríguez L, Lopez-Alonso I, et al. Angiotensin-converting enzymes (ACE, ACE2) gene variants and COVID-19 outcome. *Gene.* (2020) 762:145102. doi: 10.1016/j.gene.2020.145102
44. Lozano-Gonzalez K, Padilla-Rodríguez E, Texis T, Gutiérrez MN, Rodríguez-Dorantes M, Cuevas-Córdoba B, et al. Allele frequency of ACE2 intron variants and its association with blood pressure. *DNA Cell Biol.* (2020) 39:2095–101. doi: 10.1089/dna.2020.5804
45. Phan L, Jin Y, Zhang H, Qiang W, Shekhtman E, Shao D, et al. *ALFA: Allele Frequency Aggregator.* National Center *for* Biotechnology Information, US National Library *of* Medicine (2020).
46. Balanovsky O, Petrushenko V, Mirzaev K, Abdullaev S, Gorin I, Chernevskiy D, et al. Variation of genomic sites associated with severe Covid-19 across populations: global and national patterns. *Pharmgenomics Pers Med.* (2021) 14:1391–402. doi: 10.2147/PGPM.S320609
47. Purcell S, Neale B, Todd-Brown K, Thomas L, Ferreira MAR, Bender D, et al. PLINK: a tool set for whole-genome association and population-based linkage analyses. *Am J Hum Genet.* (2007) 81:559–75. doi: 10.1086/519795
48. Tjur T. Coefficients of determination in logistic regression models—a new proposal: the coefficient of discrimination. *Am Stat.* (2009) 63:366–72. doi: 10.1198/tast.2009.08210
49. Kundu S, Aulchenko YS, van Duijn CM, Janssens ACJW. PredictABEL: an R package for the assessment of risk prediction models. *Eur J Epidemiol.* (2011) 26:261–4. doi: 10.1007/s10654-011-9567-4
50. Brown M. *Package 'rmda'* (2018). Available online at: https://cran.r-project.org/web/packages/rmda/rmda.pdf (accessed May 25, 2022).
51. R Core Team. *R: A Language and Environment for Statistical Computing* (2020).
52. Pencina MJ, D'Agostino RB, D'Agostino RB, Vasan RS. Evaluating the added predictive ability of a new marker: from area under the ROC curve to reclassification and beyond. *Stat Med.* (2008) 27:157–72. doi: 10.1002/sim.2929
53. Pencina MJ, D'Agostino RB, Demler OV. Novel metrics for evaluating improvement in discrimination: net reclassification and integrated discrimination improvement for normal variables and nested models. *Stat Med.* (2012) 31:101–13. doi: 10.1002/sim.4348
54. Kesselmeier M, Legrand C, Peil B, Kabisch M, Fischer C, Hamann U, et al. Practical investigation of the performance of robust logistic regression to predict the genetic risk of hypertension. *BMC Proc.* (2014) 8:S65. doi: 10.1186/1753-6561-8-S1-S65
55. Zhang Z, Rousson V, Lee W-C, Ferdynus C, Chen M, Qian X, et al. Decision curve analysis: a technical note. *Ann Transl Med.* (2018) 6:308. doi: 10.21037/atm.2018.07.02

56. Zheng Z, Peng F, Xu B, Zhao J, Liu H, Peng J, et al. Risk factors of critical & mortal COVID-19 cases: a systematic literature review and meta-analysis. *J Infect.* (2020) 81:e16–25. doi: 10.1016/j.jinf.2020.04.021
57. Mancia G, Rea F, Ludergnani M, Apolone G, Corrao G. Renin–Angiotensin–Aldosterone System Blockers and the Risk of Covid-19. *N Engl J Med.* (2020) 382:2431–40. doi: 10.1056/NEJMoa2006923
58. Liang X, Shi L, Wang Y, Xiao W, Duan G, Yang H, et al. The association of hypertension with the severity and mortality of COVID-19 patients: evidence based on adjusted effect estimates. *J Infect.* (2020) 81:e44–7. doi: 10.1016/j.jinf.2020.06.060
59. Gao C, Cai Y, Zhang K, Zhou L, Zhang Y, Zhang X, et al. Association of hypertension and antihypertensive treatment with COVID-19 mortality: a retrospective observational study. *Eur Heart J.* (2020) 41:2058–66. doi: 10.1093/eurheartj/ehaa433
60. Holman N, Knighton P, Kar P, O'Keefe J, Curley M, Weaver A, et al. Risk factors for COVID-19-related mortality in people with type 1 and type 2 diabetes in England: a population-based cohort study. *Lancet Diabetes Endocrinol.* (2020) 8:823–33. doi: 10.1016/S2213-8587(20)30271-0
61. Yang J, Zheng Y, Gou X, Pu K, Chen Z, Guo Q, et al. Prevalence of comorbidities and its effects in patients infected with SARS-CoV-2: a systematic review and meta-analysis. *Int J Infect Dis.* (2020) 94:91–5. doi: 10.1016/j.ijid.2020.03.017
62. Paz Ocaranza M, Riquelme JA, García L, Jalil JE, Chiong M, Santos RAS, et al. Counter-regulatory renin–angiotensin system in cardiovascular disease. *Nat Rev Cardiol.* (2020) 17:116–29. doi: 10.1038/s41569-019-0244-8
63. Tang N, Li D, Wang X, Sun Z. Abnormal coagulation parameters are associated with poor prognosis in patients with novel coronavirus pneumonia. *J Thromb Haemost.* (2020) 18:844–7. doi: 10.1111/jth.14768
64. Wang S, Ma P, Zhang S, Song S, Wang Z, Ma Y, et al. Fasting blood glucose at admission is an independent predictor for 28-day mortality in patients with COVID-19 without previous diagnosis of diabetes: a multi-centre retrospective study. *Diabetologia.* (2020) 63:2102–11. doi: 10.1007/s00125-020-05209-1
65. Guan W, Ni Z, Hu Y, Liang W, Ou C, He J, et al. Clinical characteristics of coronavirus disease 2019 in China. *N Engl J Med.* (2020) 382:1708–20. doi: 10.1056/NEJMoa2002032
66. Iroungou BA, Mangouka LG, Bivigou-Mboumba B, Moussavou-Boundzanga P, Obame-Nkoghe J, Nzigou Boucka F, et al. Demographic and clinical characteristics associated with severity, clinical outcomes, and mortality of COVID-19 infection in gabon. *JAMA Netw Open.* (2021) 4:e2124190. doi: 10.1001/jamanetworkopen.2021.24190
67. Mehta OP, Bhandari P, Raut A, Kacimi SEO, Huy NT. Coronavirus disease (COVID-19): comprehensive review of clinical presentation. *Front Public Heal.* (2021) 8:582932. doi: 10.3389/fpubh.2020.582932
68. Islam MF, Cotler J, Jason LA. Post-viral fatigue and COVID-19: lessons from past epidemics. *Fatigue Biomed Heal Behav.* (2020) 8:61–9. doi: 10.1080/21641846.2020.1778227
69. Carod Artal FJ. Síndrome post-COVID-19: epidemiología, criterios diagnósticos y mecanismos patogénicos implicados. *Rev Neurol.* (2021) 72:384. doi: 10.33588/rn.7211.2021230
70. Kamal M, Abo Omirah M, Hussein A, Saeed H. Assessment and characterisation of post-COVID-19 manifestations. *Int J Clin Pract.* (2021) 75:e13746. doi: 10.1111/ijcp.13746
71. Nakamura ZM, Nash RP, Laughon SL, Rosenstein DL. Neuropsychiatric complications of COVID-19. *Curr Psychiatry Rep.* (2021) 23:25. doi: 10.1007/s11920-021-01237-9
72. Czeisler MÉ, Wiley JF, Facer-Childs ER, Robbins R, Weaver MD, Barger LK, et al. Mental health, substance use, and suicidal ideation during a prolonged COVID-19-related lockdown in a region with low SARS-CoV-2 prevalence. *J Psychiatr Res.* (2021) 140:533–44. doi: 10.1016/j.jpsychires.2021.05.080
73. Parker C, Shalev D, Hsu I, Shenoy A, Cheung S, Nash S, et al. Depression, anxiety, and acute stress disorder among patients hospitalized with COVID-19: a prospective cohort study. *J Acad Consult Psychiatry.* (2021) 62:211–19. doi: 10.1016/j.psym.2020.10.001
74. Moldofsky H, Patcai J. Chronic widespread musculoskeletal pain, fatigue, depression and disordered sleep in chronic post-SARS syndrome; a case-controlled study. *BMC Neurol.* (2011) 11:37. doi: 10.1186/1471-2377-11-37
75. Moreno-Pérez O, Merino E, Leon-Ramirez J-M, Andres M, Ramos JM, Arenas-Jiménez J, et al. Post-acute COVID-19 syndrome. Incidence and risk factors: a Mediterranean cohort study. *J Infect.* (2021) 82:378–83. doi: 10.1016/j.jinf.2021.01.004
76. Yong SJ. Long COVID or post-COVID-19 syndrome: putative pathophysiology, risk factors, and treatments. *Infect Dis.* (2021) 53:737–54. doi: 10.1080/23744235.2021.1924397
77. Sudre CH, Murray B, Varsavsky T, Graham MS, Penfold RS, Bowyer RC, et al. Attributes and predictors of long COVID. *Nat Med.* (2021) 27:626–31. doi: 10.1038/s41591-021-01292-y
78. Pairo-Castineira E, Clohisey S, Klaric L, Bretherick AD, Rawlik K, Pasko D, et al. Genetic mechanisms of critical illness in Covid-19. *Nature.* (2020) 591:92–8. doi: 10.1101/2020.09.24.20200048
79. Fink-Baldauf IM, Stuart WD, Brewington JJ, Guo M, Maeda Y. CRISPRi links COVID-19 GWAS loci to LZTFL1 and RAVER1. *eBioMedicine.* (2022) 75:103806. doi: 10.1016/j.ebiom.2021.103806
80. Valenti L, Griffini S, Lamorte G, Grovetti E, Uceda Renteria SC, Malvestiti F, et al. Chromosome 3 cluster rs11385942 variant links complement activation with severe COVID-19. *J Autoimmun.* (2021) 117:102595. doi: 10.1016/j.jaut.2021.102595
81. Xie CB, Jane-Wit D, Pober JS. Complement membrane attack complex. *Am J Pathol.* (2020) 190:1138–50. doi: 10.1016/j.ajpath.2020.02.006
82. Malas MB, Naazie IN, Elsayed N, Mathlouthi A, Marmor R, Clary B. Thromboembolism risk of COVID-19 is high and associated with a higher risk of mortality: a systematic review and meta-analysis. *EClinicalMedicine.* (2020) 29–30:100639. doi: 10.1016/j.eclinm.2020.100639
83. Nakanishi T, Pigazzini S, Degenhardt F, Cordioli M, Butler-Laporte G, Maya-Miles D, et al. Age-dependent impact of the major common genetic risk factor for COVID-19 on severity and mortality. *J Clin Invest.* (2021) 131:e152386. doi: 10.1101/2021.03.07.21252875
84. Horowitz JE, Kosmicki JA, Damask A, Sharma D, Roberts GHL, Justice AE, et al., Yadav A, Leader JB, et al. Genome-wide analysis provides genetic evidence that ACE2 influences COVID-19 risk and yields risk scores associated with severe disease. *Nat Genet.* (2022) 54:382–92. doi: 10.1038/s41588-021-01006-7
85. Roberts GHL, Partha R, Rhead B, Knight SC, Park DS, Coignet M V., et al. Expanded COVID-19 phenotype definitions reveal distinct patterns of genetic association and protective effects. *Nat Genet.* (2022) 54:374–81. doi: 10.1038/s41588-022-01042-x
86. Shelton JF, Shastri AJ, Ye C, Weldon CH, Filshtein-Sonmez T, Coker D, et al. Trans-ancestry analysis reveals genetic and nongenetic associations with COVID-19 susceptibility and severity. *Nat Genet.* (2021) 53:801–8. doi: 10.1038/s41588-021-00854-7
87. Freedman ML, Reich D, Penney KL, McDonald GJ, Mignault AA, Patterson N, et al. Assessing the impact of population stratification on genetic association studies. *Nat Genet.* (2004) 36:388–93. doi: 10.1038/ng1333
88. Hellwege JN, Keaton JM, Giri A, Gao X, Velez Edwards DR, Edwards TL. Population stratification in genetic association studies. *Curr Protoc Hum Genet.* (2017) 95:1.22.1–1.22.23. doi: 10.1002/cphg.48
89. Ossa H, Aquino J, Pereira R, Ibarra A, Ossa RH, Pérez LA, et al. Outlining the ancestry landscape of colombian admixed populations. *PLoS ONE.* (2016) 11:e0164414. doi: 10.1371/journal.pone.0164414
90. Little J, Higgins JP., Ioannidis JP., Moher D, Gagnon F, von Elm E, et al. STrengthening the REporting of Genetic Association Studies (STREGA)— an extension of the STROBE statement. *PLoS Med.* (2009) 6:e1000022. doi: 10.1371/journal.pmed.1000022
91. Ioannidis JPA, Ntzani EE, Trikalinos TA. "Racial" differences in genetic effects for complex diseases. *Nat Genet.* (2004) 36:1312–18. doi: 10.1038/ng1474
92. Saengsiwaritt W, Jittikoon J, Chaikledkaew U, Udomsinprasert W. Genetic polymorphisms of ACE1, ACE2, and TMPRSS2 associated with COVID-19 severity: a systematic review with meta-analysis. *Rev Med Virol.* (2022) e2323. doi: 10.1002/rmv.2323
93. Coto E, Avanzas P, Gómez J. The renin-angiotensin-aldosterone system and coronavirus disease 2019. *Eur Cardiol.* (2021) 16:e07. doi: 10.15420/ecr.2020.30
94. Zipeto D, Palmeira J da F, Argañaraz GA, Argañaraz ER. ACE2/ADAM17/TMPRSS2 interplay may be the

main risk factor for COVID-19. *Front Immunol.* (2020) 11:576745. doi: 10.3389/fimmu.2020.576745
95. Khayat AS, de Assumpção PP, Meireles Khayat BC, Thomaz Araújo TM, Batista-Gomes JA, Imbiriba LC, et al. ACE2 polymorphisms as potential players in COVID-19 outcome. *PLoS ONE.* (2020) 15:e0243887. doi: 10.1371/journal.pone.0243887
96. Karakaş Çelik S, Çakmak Genç G, Pişkin N, Açikgöz B, Altinsoy B, Kurucu Işsiz B, Dursun A. Polymorphisms of ACE (I/D) and ACE2 receptor gene (Rs2106809, Rs2285666) are not related to the clinical course of COVID-19: a case study. *J Med Virol.* (2021) 93:5947–52. doi: 10.1002/jmv.27160
97. Novelli A, Biancolella M, Borgiani P, Cocciadiferro D, Colona VL, D'Apice MR, et al. Analysis of ACE2 genetic variants in 131 Italian SARS-CoV-2-positive patients. *Hum Genomics.* (2020) 14:29. doi: 10.1186/s40246-020-00279-z
98. Li Y, Li H, Zhou L. EZH2-mediated H3K27me3 inhibits ACE2 expression. *Biochem Biophys Res Commun.* (2020) 526:947–52. doi: 10.1016/j.bbrc.2020.04.010
99. Lambert DW, Clarke NE, Hooper NM, Turner AJ. Calmodulin interacts with angiotensin-converting enzyme-2 (ACE2) and inhibits shedding of its ectodomain. *FEBS Lett.* (2008) 582:385–90. doi: 10.1016/j.febslet.2007.11.085
100. Saponaro F, Rutigliano G, Sestito S, Bandini L, Storti B, Bizzarri R, et al. ACE2 in the era of SARS-CoV-2: controversies and novel perspectives. *Front Mol Biosci.* (2020) 7:588618. doi: 10.3389/fmolb.2020.588618
101. Mir MM, Mir R, Alghamdi MAA, Alsayed BA, Wani JI, Alharthi MH, et al. Strong association of angiotensin converting enzyme-2 gene insertion/deletion polymorphism with susceptibility to SARS-CoV-2, hypertension, coronary artery disease and COVID-19 disease mortality. *J Pers Med.* (2021) 11:1098. doi: 10.3390/jpm11111098
102. Gunal O, Sezer O, Ustun GU, Ozturk CE, Sen A, Yigit S, et al. Angiotensin-converting enzyme-1 gene insertion/deletion polymorphism may be associated with COVID-19 clinical severity: a prospective cohort study. *Ann Saudi Med.* (2021) 41:141–146. doi: 10.5144/0256-4947.2021.141
103. Verma S, Abbas M, Verma S, Khan FH, Raza ST, Siddiqi Z, et al. Impact of I/D polymorphism of angiotensin-converting enzyme 1 (ACE1) gene on the severity of COVID-19 patients. *Infect Genet Evol.* (2021) 91:104801. doi: 10.1016/j.meegid.2021.104801
104. de Araújo JLF, Menezes D, de Aguiar RS, de Souza RP. IFITM3, FURIN, ACE1, and TNF-α genetic association with COVID-19 outcomes: systematic review and meta-analysis. *Front Genet.* (2022) 13:775246. doi: 10.3389/fgene.2022.775246
105. Soltani Zangbar H, Gorji A, Ghadiri T. A review on the neurological manifestations of COVID-19 infection: a mechanistic view. *Mol Neurobiol.* (2021) 58:536–49. doi: 10.1007/s12035-020-02149-0
106. Purwaningroom DL, Saifurrohman M, Widodo N, Putri JF, Lukitasari M. Alteration of splicing pattern on angiotensin converting enzyme gene due to the insertion of ALU elements. *Int J Comput Biol.* (2015) 4:53. doi: 10.34040/IJCB.4.2.2015.61
107. Silva WA, Bonatto SL, Holanda AJ, Ribeiro-Dos-Santos AK, Paixão BM, Goldman GH, et al. Mitochondrial genome diversity of Native Americans supports a single early entry of founder populations into America. *Am J Hum Genet.* (2002) 71:187–92. doi: 10.1086/341358
108. Rishishwar L, Conley AB, Wigington CH, Wang L, Valderrama-Aguirre A, Jordan IK. Ancestry, admixture and fitness in Colombian genomes. *Sci Rep.* (2015) 5:12376. doi: 10.1038/srep12376
109. Zeberg H, Pääbo S. The major genetic risk factor for severe COVID-19 is inherited from Neanderthals. *Nature.* (2020) 587:610–12. doi: 10.1038/s41586-020-2818-3
110. Funk T, Pharris A, Spiteri G, Bundle N, Melidou A, Carr M, et al. Characteristics of SARS-CoV-2 variants of concern B.1.1.7, B.1.351 or P.1: data from seven EU/EEA countries, weeks 38/2020 to 10/2021. *Eurosurveillance.* (2021) 26:2100348. doi: 10.2807/1560-7917.ES.2021.26.16.2100348
111. Volz E, Mishra S, Chand M, Barrett JC, Johnson R, Geidelberg L, et al. Assessing transmissibility of SARS-CoV-2 lineage B.1.1.7 in England. *Nature.* (2021) 593:266–9. doi: 10.1038/s41586-021-03470-x
112. Faria NR, Mellan TA, Whittaker C, Claro IM, Candido D da S, Mishra S, et al. Genomics and epidemiology of the P.1 SARS-CoV-2 lineage in Manaus, Brazil. *Science.* (2021) 372:815–21. doi: 10.1126/science.abh2644
113. Instituto Nacional de Salud Colombia. *COVID-19 en Colombia.* (2021). Available online at: https://www.ins.gov.co/Noticias/Paginas/coronavirus-casos.aspx (accessed February 1, 2021).
114. Centers for Disease Control and Prevention (U.S.). *SARS-CoV-2 Variant Classifications and Definitions.* (2022). Available online at: https://www.cdc.gov/coronavirus/2019-ncov/variants/variant-classifications.html
115. Chen Y, Zhou X, Yan H, Huang H, Li S, Jiang Z, et al. CANPT score: a tool to predict severe COVID-19 on admission. *Front Med.* (2021) 8:608107. doi: 10.3389/fmed.2021.608107
116. Dite GS, Murphy NM, Allman R. An integrated clinical and genetic model for predicting risk of severe COVID-19: a population-based case-control study. *PLoS ONE.* (2021) 16:e0247205. doi: 10.1371/journal.pone.0247205
117. Jimenez-Solem E, Petersen TS, Hansen C, Hansen C, Lioma C, Igel C, et al. Developing and validating COVID-19 adverse outcome risk prediction models from a bi-national European cohort of 5594 patients. *Sci Rep.* (2021) 11:3246. doi: 10.1038/s41598-021-81844-x
118. Gao Y, Cai G-Y, Fang W, Li H-Y, Wang S-Y, Chen L, et al. Machine learning based early warning system enables accurate mortality risk prediction for COVID-19. *Nat Commun.* (2020) 11:5033. doi: 10.1038/s41467-020-18684-2

**Conflict of Interest:** The authors declare that the research was conducted in the absence of any commercial or financial relationships that could be construed as a potential conflict of interest.

**Publisher's Note:** All claims expressed in this article are solely those of the authors and do not necessarily represent those of their affiliated organizations, or those of the publisher, the editors and the reviewers. Any product that may be evaluated in this article, or claim that may be made by its manufacturer, is not guaranteed or endorsed by the publisher.

frontiers | Frontiers in Molecular Biosciences

ORIGINAL RESEARCH
published: 22 July 2022
doi: 10.3389/fmolb.2022.846996

# Decreased Interfacial Dynamics Caused by the N501Y Mutation in the SARS-CoV-2 S1 Spike:ACE2 Complex

*Wesam S. Ahmed*[1†], *Angelin M. Philip*[2†] *and Kabir H. Biswas*[1*†]

[1]*Division of Biological and Biomedical Sciences, College of Health and Life Sciences, Hamad Bin Khalifa University, Qatar Foundation, Doha, Qatar,* [2]*Division of Genomics and Translational Biomedicine, College of Health and Life Sciences, Hamad Bin Khalifa University, Qatar Foundation, Doha, Qatar*

OPEN ACCESS

**Edited by:**
*Alessandra Magistrato, Consiglio Nazionale delle Ricerche (CNR), Italy*

**Reviewed by:**
*Antonella Di Pizio, Technical University of Munich, Germany*
*Angelo Spinello, University of Palermo, Italy*
*Federico Iacovelli, University of Rome Tor Vergata, Italy*

***Correspondence:**
*Kabir H. Biswas*
*kbiswas@hbku.edu.qa*

**†ORCID:**
*Wesam S Ahmed*
*orcid.org/0000-0002-3441-2631*
*Angelin M Philip*
*orcid.org/0000-0001-7222-4669*
*Kabir H Biswas*
*orcid.org/0000-0001-9194-4127*

**Specialty section:**
*This article was submitted to Biological Modeling and Simulation, a section of the journal Frontiers in Molecular Biosciences*

**Received:** *06 January 2022*
**Accepted:** *28 April 2022*
**Published:** *22 July 2022*

**Citation:**
*Ahmed WS, Philip AM and Biswas KH (2022) Decreased Interfacial Dynamics Caused by the N501Y Mutation in the SARS-CoV-2 S1 Spike: ACE2 Complex. Front. Mol. Biosci. 9:846996. doi: 10.3389/fmolb.2022.846996*

Coronavirus Disease of 2019 (COVID-19) caused by Severe Acute Respiratory Syndrome Coronavirus 2 (SARS-CoV-2) has resulted in a massive health crisis across the globe, with some genetic variants gaining enhanced infectivity and competitive fitness, and thus significantly aggravating the global health concern. In this regard, the recent SARS-CoV-2 alpha, beta, and gamma variants (B.1.1.7, B.1.351, and P.1 lineages, respectively) are of great significance in that they contain several mutations that increase their transmission rates as evident from clinical reports. By the end of March 2021, these variants were accounting for about two-thirds of SARS-CoV-2 variants circulating worldwide. Specifically, the N501Y mutation in the S1 spike receptor binding domain (S1-RBD) of these variants have been reported to increase its affinity for ACE2, although the basis for this is not entirely clear yet. Here, we dissect the mechanism underlying the increased binding affinity of the N501Y mutant for ACE2 using molecular dynamics (MD) simulations of the available ACE2-S1-RBD complex structure (6M0J) and show a prolonged and stable interfacial interaction of the N501Y mutant S1-RBD with ACE2 compared to the wild type S1-RBD. Additionally, we find that the N501Y mutant S1-RBD displays altered dynamics that likely aids in its enhanced interaction with ACE2. By elucidating a mechanistic basis for the increased affinity of the N501Y mutant S1-RBD for ACE2, we believe that the results presented here will aid in developing therapeutic strategies against SARS-CoV-2 including designing of therapeutic agents targeting the ACE2-S1-RBD interaction.

**Keywords: ACE2, COVID-19, molecular dynamics simulation, SARS-CoV-2, S1 spike protein, N501Y mutant**

## INTRODUCTION

Severe acute respiratory syndrome coronavirus 2 (SARS-CoV-2) is a positive-sense, single stranded, enveloped RNA virus that belongs to the Coronaviridae family and is the causative agent of the coronavirus disease 2019 (COVID-19). (Wu et al., 2020) As of October 2021, more than 245 million confirmed cases have been reported worldwide, with more than five million deaths (https://covid19.who.int/). In general, coronaviruses express four structural proteins: nucleocapsid (N) protein that encapsulates the genomic material; membrane (M) protein that promotes the membrane curvature to bind to the N protein; envelope (E) protein which ensures virus assembly and release; and envelope-anchored spike (S) glycoprotein that protrudes from the viral surface and facilitates viral attachment and entry into host cells. (V'kovski, 2021; Hussein et al., 2020; Shang et al., 2020) The

latter is cleaved during viral entry into two subunits, namely S1 and S2. (Samavati and Uhal, 2020) Viral attachment to host cells occurs through binding of its receptor binding domain (RBD) - which is part of the S1 subunit – to the host cell membrane-localized angiotensin converting enzyme 2 (ACE2) receptor. It is important to note that the affinity of SARS-CoV-2 S1-RBD for ACE2 was reported to be 10 times higher than that of SARS-CoV, providing a biochemical basis for the increased infection efficiency of SARS-CoV-2 compared to SARS-CoV. (Andersen et al., 2020) In this regard, computational studies have revealed an expanded network of hydrogen bond (H-bond) and hydrophobic interactions formed at the interface of ACE2-S1-RBD complex in SARS-CoV-2. (Spinello et al., 2020; Wang et al., 2020) Given these, the ACE2-S1-RBD interaction has become an attractive target for developing inhibitors of viral entry into host cell. (Andersen et al., 2020; Choudhary et al., 2020; Shang, 2020; Walls, 2020; Wrapp et al., 2020) For instance, the human recombinant soluble ACE2 protein has been utilized for reducing SARS-CoV-2 binding to the cellular ACE2 receptor leading to reduced injury to multiple organs, including the lungs, kidneys, and heart. (Zoufaly et al., 2020) Similarly, monoclonal antibodies such as 18F3 and 7B11 have been developed to neutralize SARS-CoV-2 infection by blocking epitopes on the S1-RBD. (Tai et al., 2020)

On top of the increased affinity of SARS-CoV-2 S1-RBD to ACE2 compared to SARS-CoV, new genetic variants with increased infectivity and virulence, likely arising under increased immunological pressure in patients suffering from COVID-19 or convalescent plasma therapy (Avanzato et al., 2020; Choi et al., 2020), have further complicated our efforts towards thwarting the pandemic. One of the key examples of such variants is the S1-RBD D614G mutant that has outcompeted the Wuhan-Hu-1. (Hou et al., 2020; Plante, 2021; Volz, 2021; Zhang et al., 2020) A comparative study conducted by Hou *et al* observed that this variant is superior in infecting the epithelial cells and replicates in higher number than the ancestral virus. The structural analysis showed that the S1-RBD containing the D614G mutation is more flexible and explores the open conformation more than the wild type (WT) protein, thus, leading to an increased affinity for ACE2. (Hou et al., 2020; Yurkovetskiy et al., 2020; Mansbach, 2021) Subsequently, a new phylogenetic group of SARS-CoV-2 (lineage B.1.1.7) was identified in the COVID-19 Genomics United Kingdom Consortium dataset with greater than 50% of the cases belonging to this new cluster (alpha variant) that has an estimated 50–70% increased transmissibility, as per epidemiological and virological investigations. (Rambaut et al., 2020; Santos and Passos, 2021) Indeed, reports of the presence of this variant has emerged from other countries as well. Sequence analysis indicates the presence of a total of 17 mutations spanning the ORF1ab, spike, and the N protein in the genome of this variant. (Santos and Passos, 2021) Majority of these mutations (8 out of the total 17), however, are present in the spike protein. These include deletion mutations (ΔH69, ΔV70 and ΔY144) and missense mutations (N501Y, A570D, P681H, T716I, S982A and D1118H). Of these, the N501Y substitution strikes out as one of the most interesting mutations due to its presence at the ACE2-S1-RBD interaction interface (Lan et al., 2020), raising the possibility of an altered interaction between the two proteins. In fact, deep mutational analysis of S1-RBD (Procko, 2020; Narayanan and Procko, 2021), in combination with the yeast-surface-display platform, has revealed an increased affinity of the N501Y mutant S1-RBD to ACE2 (apparent $K_d$ of $3.9 \times 10^{-11}$ M for the WT vs $2.2 \times 10^{-11}$ M for the N501Y mutant). (Starr et al., 2020) Furthermore, some computational studies suggest higher binding affinity for the N501Y S1-RBD mutant to ACE2 as a result of increased coordinated hydrophobic interactions between Y501 of S1-RBD and Y41 and K353 of ACE2. (Luan et al., 2021; Spinello et al., 2021) In addition, a recent study demonstrated the $EC_{50}$ of the mutant S1-RBD possessing a total of nine mutations (I358F, V445K, N460K, I468T, T470M, S477N, E484K, Q498R, N501Y) was nearly 17 times lower than that of the WT S1-RBD. (Zahradník, 2021)

The emergence of the B.1.1.7 alpha lineage has coincided with two independents viral evolutions, the B.1.351 (beta) and P.1 (gamma) lineages of SARS-CoV-2, all of which share the N501Y mutation in S1-RBD. The emergence of these lineages elicited new concerns regarding the evolutionary capacity of the virus. (Liu, 2021a; Tian, 2021a; Martin et al., 2021) Since December 2021, these variants have been collectively referred to as variants of concern (VOC) by the World Health Organization (WHO). By the end of March 2021, these lineages were accounting for about two-thirds of the circulating variants worldwide (Huang et al., 2021). The currently ongoing convergent evolution of N501Y lineage has led viruses to broaden the fitness landscape. (Martin et al., 2021) Structural biological studies of the SARS-CoV-2 S1-RBD proposes that N501Y mutation may increase its affinity for ACE2 binding (Starr et al., 2020; Ostrov, 2021) and that the open conformation of the N501Y mutant spike protein (Teruel et al., 2021) is associated with more efficient viral entry, transmission and infection (Leung et al., 2021). N501Y and deletion of codons 69–70 have shown a consistent fitness advantage for replication in the upper airway in the hamster model, with higher shedding in nasal secretions, as well as in primary human airway epithelial cells. (Liu, 2021a) Additionally, S-proteins of the three N501Y S1-RBD VOCs (B.1.1.7, B.1.351, and P.1 lineages) possess increased infectivity in cells expressing mouse ACE2 (Li et al., 2021). Hence, it is conceivable that mice are susceptible to the newly emerging, high frequency N501Y mutation. (Huang et al., 2021; Justo Arevalo et al., 2021) Further, this serves as an evidence for the constantly evolving SARS-CoV-2 with more contagious mutations spreading rapidly with the possibility of increasing host range. (Liu, 2021b; Chen et al., 2021; Liu et al., 2021)

The N501Y substitution alone had a phenotype similar to that of the combined eight mutations (Δ69-70, Δ145, N501Y, A570D, P681H, T716I, S982A, D1118H), suggesting that it is the major spike determinant driving increased transmission of the United Kingdom variant. Surface plasmon resonance (SPR) experiments on immobilized WT and mutant S1-RBDs (N501Y and triple mutant N501Y, K417N, E484K) demonstrated a 10-fold increased affinity to ACE2 receptor. Further, the impact of K417N and E484K was verified by

single point mutations which clearly suggested a minimal impact on ACE2 binding. These highlights the vital role of N501Y in increasing the binding affinity to ACE2, thereby decelerating rate of dissociation from the ACE2 receptor in comparison to the WT. (Tian, 2021a; Istifli et al., 2021; Villoutreix et al., 2021) Computational studies by Socher et al., showed increased contact at 501 when tyrosine is present. (Socher et al, 2021) Additional studies have shown high number of contacts formed by residues F486, Y489, T500 and Y505 with ACE2 receptor. (Wan et al., 2020) Recently, the spread of a new SARS-CoV-2 spike N501Y variant harboring a set of amino acid substitutions including L18F, L452R, N501Y, A653V, H655Y, D796Y, G1219V ± Q677H in western European countries including Turkey, Nigeria, and especially France, suggests the continuous emergence of a new 501Y lineages. (Colson, 2021)

In the current study, we performed multiple all atom, explicit solvent MD simulations to gain insights into the mechanism underlying the increased affinity of the N501Y mutant S1-RBD for ACE2. Simulations of the WT and the N501Y mutant S1-RBD in complex with ACE2 showed a prolonged and stable interaction between the Y501 residue with the neighbouring Y41 and K353 residues in ACE2 in the mutant complex as compared to the N501 residue in the WT complex. Importantly, these simulations also revealed a localized decreased dynamics for interfacial residues in the mutant as compared to the WT complex that led to changes in interfacial interactions of these residues, although these were most noticeable for residues near the N501Y S1-RBD mutation site.

# MATERIALS AND METHODS

## ACE2-S1-RBD Structure Preparation

The three-dimensional structure of ACE2-S1-RBD complex spanning residues S19 to D615 of human ACE2 and T333 to G526 of SARS-CoV-2 S1 glycoprotein was obtained from the RCSB PDB database as a PDB file (PDB ID: 6M0J). (Lan et al., 2020) PyMOL (The PyMOL Molecular Graphics System, Version 2.0.0, Schrödinger, LLC; pymol. org) was used to visualize the three-dimensional structure and to generate the N501Y mutant structure using the Mutagenesis tool available in PyMOL. WT and mutant PDB structure files were exported after removing ions and solvent molecules.

## ACE2-S1-RBD Molecular Dynamics Simulations

Molecular dynamics simulations were performed using NAMD version 2.13 software (Phillips et al., 2005) and CHARMM36 force field (Best et al., 2012), as described previously (Altamash et al., 2021). The simulation system consisting of the biomolecular complex formed by the ACE2-S1-RBD was generated from the previously prepared PDB files using the QwikMD Toolkit (Ribeiro et al., 2016) available as a plugin in the Visual Molecular Dynamics (VMD) (Humphrey et al., 1996) software V1.9.3. Briefly, the proteins were solvated using TIP3P (transferable intermolecular potential with three points) (Jorgensen et al., 1983) cubic water box and charges were neutralized using 0.15 M NaCl final concentration in explicit solvent with Periodic Boundary Conditions applied. The biomolecular simulation systems consisted of ~453,000 atoms. Energy minimization was first performed for 1,000 timesteps, followed by a thermalization step where the system was slowly heated for 0.25 ns using a temperature ramp where the temperature was raised from 60 to 310 K at 1 K increment. Temperature and pressure were then maintained at 310 K using Langevin temperature control and at 1.0 atm using Nose-Hoover Langevin piston control, respectively, and a 1 ns constrained equilibration step was then performed where protein backbone atoms where constrained using harmonic potential. Finally, two independent 100 ns runs were performed for both the WT and the N501Y mutant ACE2-S1-RBD complex. A 2 fs time step of integration was chosen for all simulation where short-range non-bonded interactions were handled at 12 Å cut-off with 10 Å switching distance, while Particle-mesh Ewald (PME) scheme was used to handle long-range electrostatic interactions at 1 Å PME grid spacing. Trajectory frames were saved every 10,000 steps.

## ACE2-S1-RBD Molecular Dynamics Simulation Trajectory Analysis

Analysis of the trajectories was performed using the available tools in the VMD software. (Humphrey et al., 1996) Independent root-mean-square deviation (RMSD) calculations of backbone Cα atoms of ACE2 and S1-RBD proteins were performed using the "RMSD trajectory Tool" in VMD. (Humphrey et al., 1996) Root-mean-square fluctuations (RMSF) measurements were performed for Cα atoms of each protein. The representative composite timestep snapshot images were prepared by saving the trajectory coordinates as PDB file format every 10 ns and then combining a total of 11 frames to form the composite images. Representative trajectory movies of the 100 ns simulations were prepared from 500 trajectory snapshots (5 snapshots/ns) generated using VMD Movie Maker Tool (Humphrey et al., 1996) and compiled using Fiji distribution of ImageJ software (Schindelin et al., 2012) at a frame rate of 60 fps.

Energy calculations were performed using "NAMD Energy" analysis tool available as part of VMD. Binding free energy changes were estimated through molecular mechanics Poisson-Boltzmann surface area (MM-PBSA) method (Kollman et al., 2000) using the CaFE 1.0 tool (Liu and Hou, 2016) and VMD (Humphrey et al., 1996). Center-of-mass distances between paired selections were determined using VMD. (Humphrey et al., 1996) Dynamic Cross-Correlation (DCC) analysis was performed using the DCC algorithm from MD-TASK software suite (Brown et al., 2017) for analyzing molecular dynamics trajectories (https://mdmtaskweb.rubi.ru.ac.za/) as well as by using Bio3D R package (Grant et al., 2006; Skjærven et al., 2014). DCC calculations were based on the position of Cα atoms obtained after aligning trajectory frames on the Cα atoms of the original complex structure. Average DCC figures were prepared using MATLAB and results were represented as heat maps that indicate the range of correlations from +1 (high

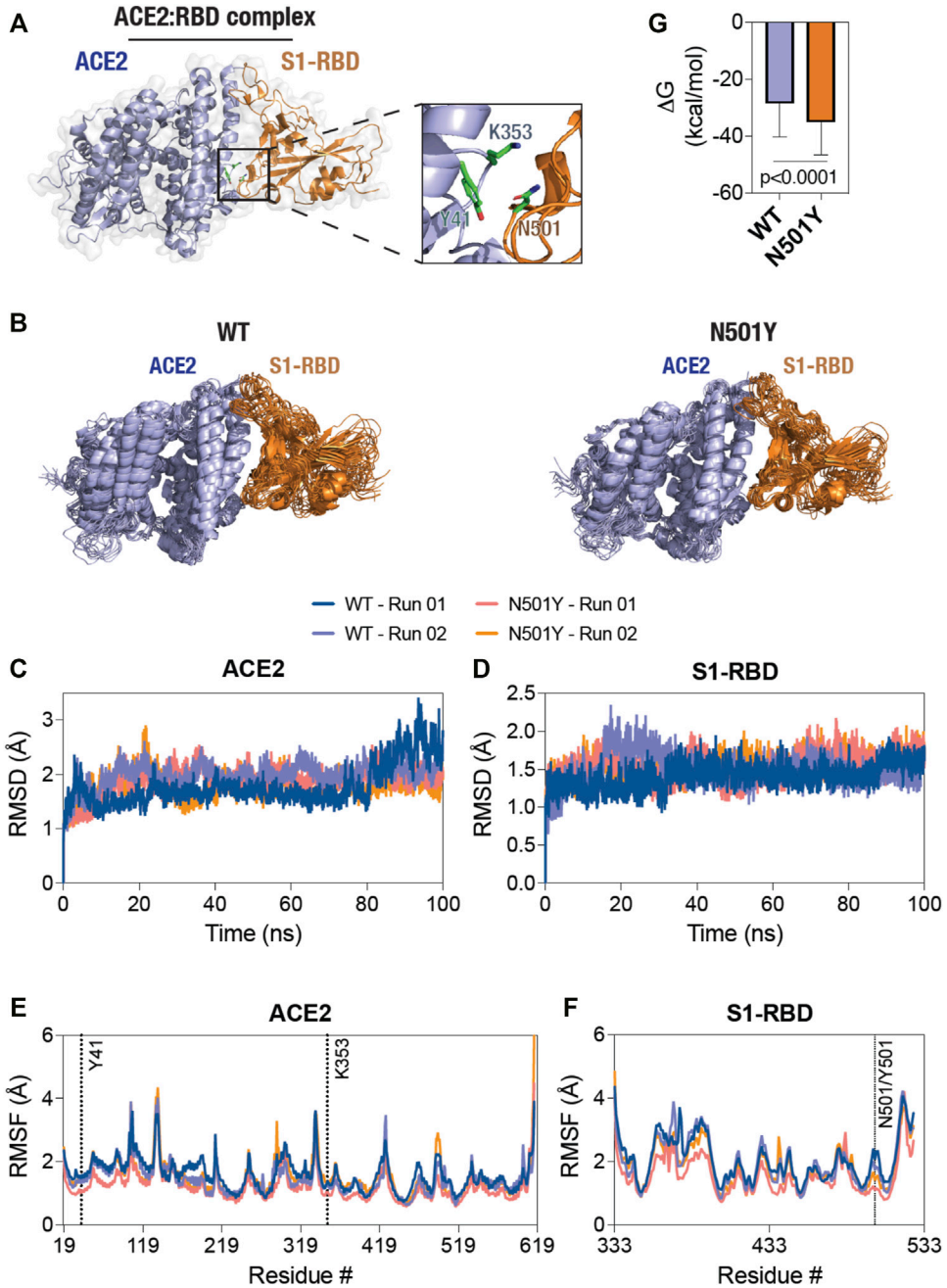


**FIGURE 1 |** Decreased structural dynamics of the N501Y mutant S1-RBD in complex with ACE2. **(A)** Cartoon representation of the ACE2-S1-RBD structure (PDB: 6M0J (Lan et al., 2020) showing the relative positioning of residues Y41 and K353 in ACE2 (light blue) and residue N501 in S1-RBD (orange). **(B)** Cartoon representation of the WT (left panel) and the N501Y mutant (right panel) ACE2-S1-RBD complex showing structural evolution of the complex over time in a 100 ns all-atom, explicit solvent MD simulation. Composite images were prepared using 11 consecutive frames from up to 100 ns simulations with each frame being 10 ns apart. **(C, D)** Graph showing backbone (Cα) root-mean-square deviation (RMSD) values of ACE2 **(C)** and S1-RBD **(D)** obtained from the simulation of the WT and N501Y mutant ACE2-S1-RBD complexes. **(E,F)** Graph showing backbone (Cα) root-mean-square fluctuation (RMSF) values of ACE2 **(E)** and S1-RBD **(F)** obtained from up to 100 ns simulations of the WT and N501Y mutant ACE2-S1-RBD complexes. **(G)** Graph showing binding free energy changes (ΔG, kcal/mol) obtained from the last 50 ns of MD simulation using the MM-PBSA method (mean ± S.D.).

correlation) to 0 (no correlation) to −1 (high anti-correlation). H-bond analysis between ACE2 and S1-RBD was performed at a cut-off distance of 3.5 Å and a cut-off A-D-H angle of 20° using the "Hydrogen Bonds" analysis extension in VMD (Brielle and Arkin, 2020; Mallik et al., 2021). Interfacial residues were determined from the available ACE2-S1-RBD complex (PDB ID: 6m0j) at a cut-off distance of 5 Å using PyMOL. Standard deviations of the inter-residue distances obtained over the course

of the simulation were then normalized with their respective average distances and plotted as a ratio of N501Y mutant to WT ACE2-S1-RBD complexes.

## Data Analysis and Figure Preparation

GraphPad Prism (version nine for macOS, GraphPad Software, La Jolla California United States ; www.graphpad.com), in combination with Microsoft Excel, were used for data analysis and graph preparation. Figures were assembled using Adobe Illustrator.

# RESULTS AND DISCUSSION

In order to understand the mechanism underlying the enhanced affinity of the N501Y mutant over the WT S1-RBD for ACE2, we initiated MD simulations with the available ACE2-S1-RBD complex structure (PDB ID: 6M0J) (Lan et al., 2020). A closer inspection of the ACE2-S1-RBD interface indicated that residues Y41 and K353 of ACE2 are in close proximity to the N501 residue of S1-RBD (**Figure 1A**). In fact, N501 has been reported to participate in H-bond interaction (at 3.7 Å distance) with Y41 residue of ACE2, indicating its potential role in the ACE2-S1-RBD interaction. (Lan et al., 2020) We hypothesized that this interaction at the residue-level is altered by the N501Y mutation in S1-RBD. We also hypothesized that other pair-wise interactions at the interface may be altered by the same mutation. To test these hypotheses, we initiated multiple, all-atom MD simulations in explicit solvent with the WT and the N501Y mutant ACE2-S1-RBD complex structure and analyzed the trajectories obtained for general structural dynamics and specific interactions. Further, we performed the simulations in duplicates to test the consistency of the results and for statistical support.

These MD simulations revealed a generally decreased dynamics of the N501Y mutant ACE2-S1-RBD complex compared to the WT complex as seen from the composite image of the complexes obtained from the simulation trajectories (**Figure 1B**). (Biswas, 2018; Biswas and Visweswariah, 2017; Biswas, 2017; Biswas et al., 2015; Fiskerstrand et al., 2012; Biswas and Visweswariah, 2011; Biswas et al., 2008) However, RMSD analysis of backbone atoms of the proteins ACE2 and S1-RBD individually, taken over the entire course of simulation, did not show any clearly discernable trend for structural evolution of amino acid residues in the complex (**Figures 1C, D**). This suggests that any alteration in the biochemical interaction between the two proteins likely arises due to changes in the dynamics of specific, individual residues in the proteins. Indeed, RMSF analysis of individual amino acid residues in the proteins showed several distinct changes, with a general decrease in the N501Y mutant complex (**Figure 1E**). Specifically, in ACE2, residue positions S106 until S128 and L176 until M190 of ACE2 showed a reduced RMSF values in the N501Y mutant complex. RMSF analysis of S1-RBD showed a reduced structural fluctuation of Y501 in the mutant complex compared to N501 in the WT complex (**Figure 1F**), indicating a more stable interaction with adjacent, interfacial residues in ACE2. Importantly, residue positions sequentially (Y495 until Q506) and physically (D442 until N448) adjacent to Y501 also showed reduced dynamic fluctuations, indicating a local stabilizing effect of the mutation. Additionally, residue positions from R357 until N370, F377 until T393, G404 until I434, and S459 until R466, showed reduced RMSF values in the mutant complex (**Figure 1F**). The latter is suggestive of the possibility of an allosteric effect of the N501Y S1-RBD mutation on the mutant ACE2-S1-RBD complex as compared the WT complex. (Biswas et al., 2008; Biswas and Visweswariah, 2011; Fiskerstrand et al., 2012; Biswas et al., 2015; Biswas, 2017; Biswas and Visweswariah, 2017; Biswas, 2018) Overall, binding free energy changes estimated using MM-PBSA method (Kollman et al., 2000) revealed higher binding energy in the mutant complex compared to the WT (**Figure 1G**).

Following these analyses, we determined the residue-residue distances based on the center-of-mass between position 501 in S1-RBD and key residues, Y41 and K353, in ACE2 of the ACE2-S1-RBD complexes, as they evolve during the span of the simulations (**Figure 2A**). First, N501 residue in the WT complex showed a substantially higher structural fluctuations in comparison to Y501 in the mutant complex (**Figure 2A**; left panel, Supporting Movies 1 and 2). This was not the case for N501Y S1-RBD mutant, in which Y501 sustained its contact at the ACE2-S1-RBD interface over the entire simulation time (**Figure 2A**; right panel, Supporting Movies 3 and 4). Indeed, the inter-residue distance analysis revealed a dramatic increase in the distance between Y41 and K353 in ACE2 and N501 in S1-RBD after about 30 ns in the first simulation run, while a smaller, more fluctuating, increases at different times were seen in the second run (**Figures 2B, D**). This is in contrast to the distances measured for the same pair of ACE2 residues with Y501 in the mutant complex (~7 and ~4.5 Å, respectively) (**Figures 2B, D**). These data suggests that Y501 residue of N501Y mutant S1-RBD forms more stable interactions at the interface with Y41 and K353 residues of ACE2 compared to the WT. To determine if the N501Y mutation impacts interaction at the opposite end of the ACE2-S1-RBD interface, we monitored the inter-residue distances between the H-bond-forming Q24 residue of ACE2 and N487 of S1-RBD and the closely juxtaposed (but not in H-bond interaction) T27 residue in ACE2 and Y489 in S1-RBD (Lan et al., 2020). In contrast to the observations made with the Y41-N501 and K353-N501 pairs, these pairs did not show substantial difference in fluctuations of their relative positioning (**Figures 2D, E**) compared to the mutant complex, suggesting that the effect of the N501Y mutation on the ACE2 and S1-RBD interface may be local in the timescale we have explored here.

We then attempted to determine if there are any correlated confirmational dynamics of the complex in the WT and the N501Y mutant using dynamic cross-correlation (DCC) analysis. Application of a minimum cut-off of 0.8 to positive and negative DCC values obtained from individual MD runs showed a generally greater correlated motions (both positive as well as negative) in the WT ACE2-S1-RBD complex compared to the N501Y mutant complex. However, DCC analysis did not reveal any dynamically correlated motions between N501 of S1-RBD or any other interfacial residues located near this position

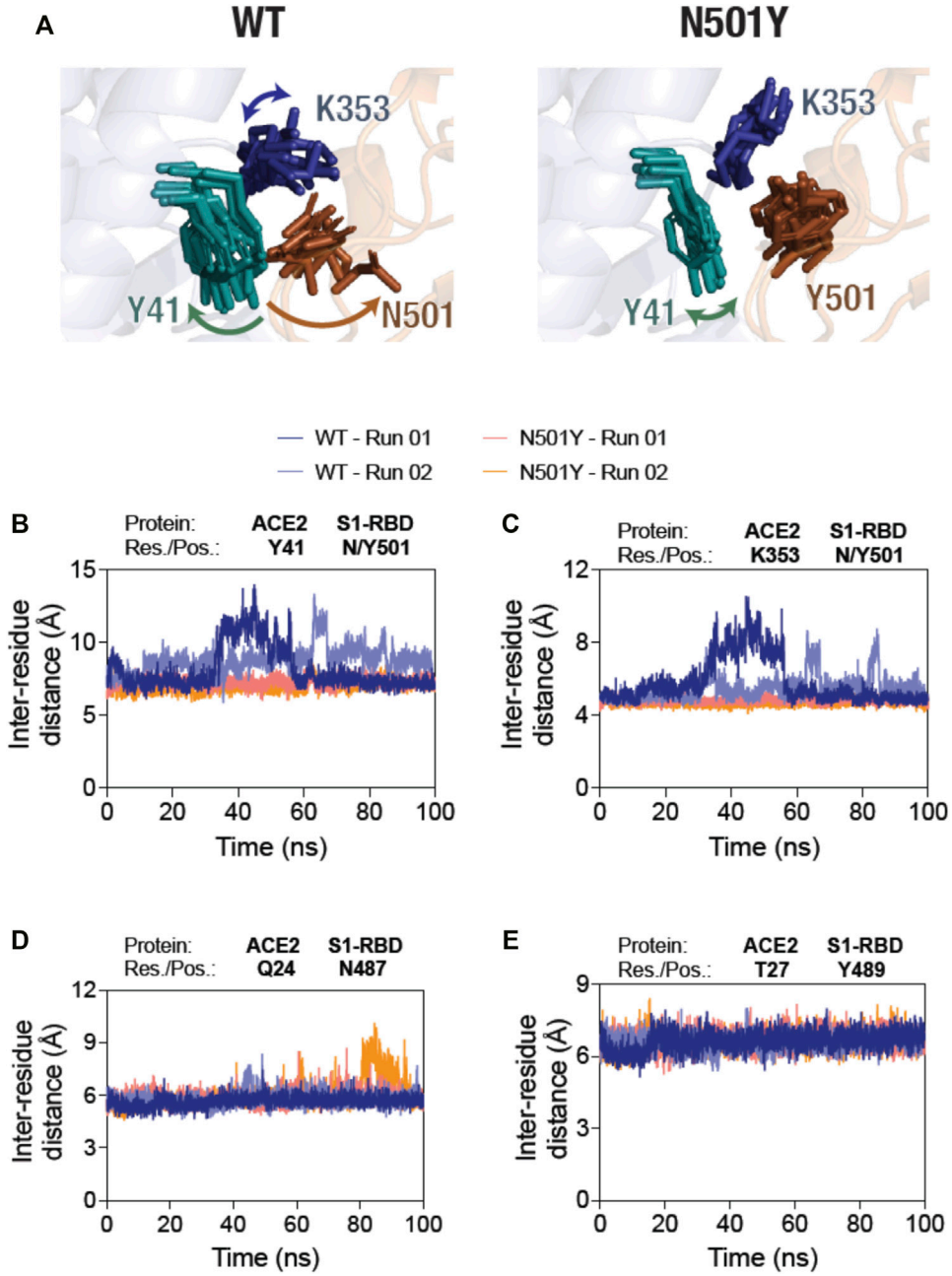


**FIGURE 2 |** Sustained interaction of S1-RBD Y501 residue (N501Y mutant) with ACE2. **(A)** Temporal evolution of residues Y41 and K353 in ACE2 and either the N501 in the WT S1-RBD (left panel) or the Y501 in the N501Y mutant S1-RBD (right panel) in the MD simulation. A total of 11 frames obtained from up to 100 s simulations, each 10 ns apart, were compiled together. Note the increased fluctuation of the N501 residue in the WT S1-RBD. **(B–E)** Graph showing inter-residue distances between the center of masses of residue Y41 in ACE2 and N501 in the WT and Y501 in the N501Y mutant S1-RBD **(B)**, K353 in ACE2 and N501 in the WT and Y501 in the N501Y mutant S1-RBD **(C)**, Q24 in ACE2 and N487 in either the WT or the N501Y mutant S1-RBD **(D)**, and T27 in ACE2 and Y489 in either the WT or the N501Y mutant S1-RBD **(E)**. Note the increased inter-residue distance fluctuations between the residues Y41 and K353 in ACE2 and N501 in S1-RBD in the WT ACE2-S1-RBD complex compared to the N501Y mutant complex **(B,C)**.

and residues in ACE2 in the WT complex. Although, in the S1-RBD mutant complex, high dynamical cross-correlations were observed between residues Y501 and G502 of S1-RBD on one side and ACE2 interfacial residues, namely K353, and G354, on the other side (**Figure 3A**). Interestingly, application of the cut-off to the negative DCC values revealed a higher anti-correlated motions between the two chains in the WT complex compared to the mutant complex (**Figure 3A**). Moreover, by averaging the DCC values for the two runs, our results revealed higher dynamical cross-correlated motions between cluster of interfacial residues

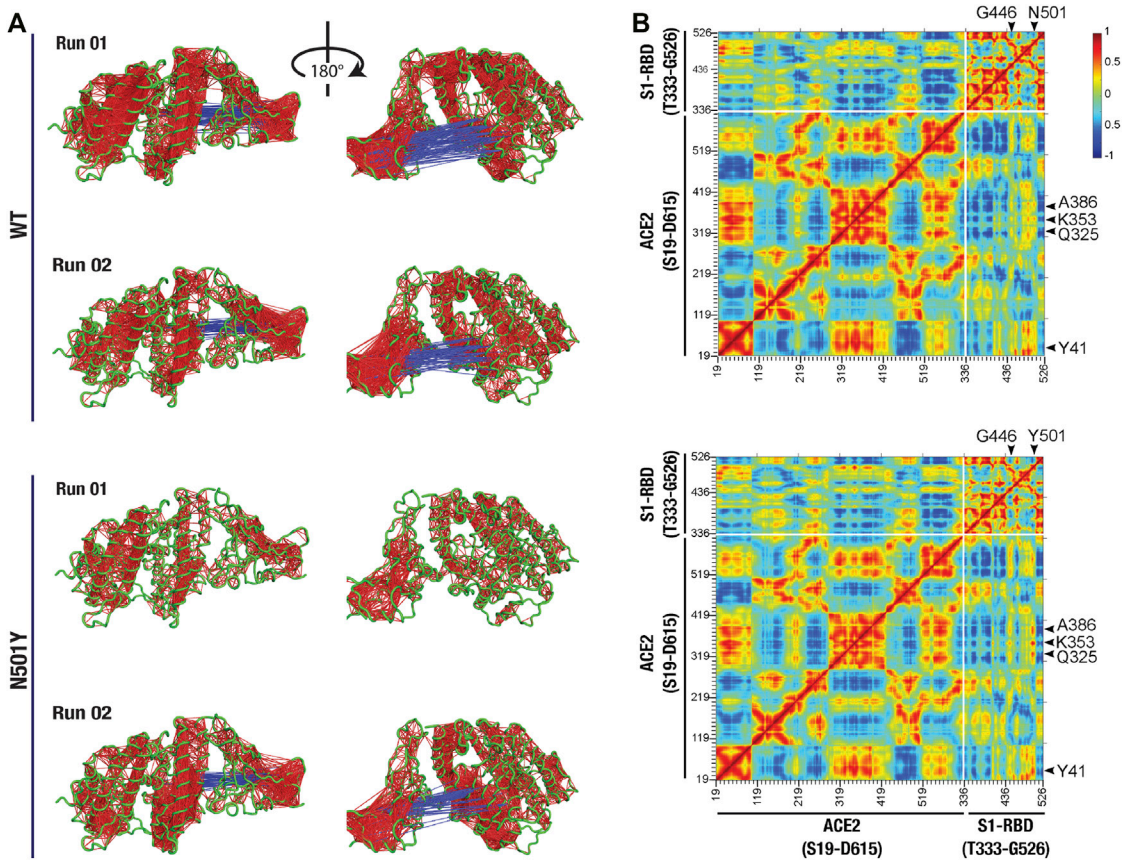


**FIGURE 3 |** Altered dynamical cross-correlated motions in the ACE2-S1-RBD N501Y mutant complex. **(A)** Cartoon representation of ACE2-S1-RBD WT (top two panels) and N501Y mutant (bottom two panels) complex showing DCC values (cut-off, ±0.8). Note the positively correlated motions observed between Y501 and G502 on S1-RBD and residues K353 and G354 on ACE2 in the mutant complex but not in the WT complex, while less dynamically anti-correlated motions were observed in the mutant complex compared to the WT complex. **(B)** Heat map showing average DCC values from two independent 100 ns MD simulations of the WT (top panel) and the N501Y mutant (bottom panel) ACE2-S1-RBD complex (cut-off, ±0.8). Note the higher dynamically cross-correlated motions between residues at the interface in the N501Y mutant complex. Also note the global decrease in the anti-correlated motions in the mutant complex.

sequentially adjacent to the mutation site in the N501Y mutant S1-RBD (residues G496, Q498, T500, Y501, G502, V503, Y505) on one side and ACE2 interfacial clustered positions (S19, Q24, T27, F28, D30, K31, H34, E35, E37, D38, Y41, Q42, L45) (Q325, G326, N330), and (A386, R393) on the other side, compared to the WT ACE2-S1-RBD complex (**Figure 3B**). Similar observations were made for the DCC values between all the aforementioned ACE2 clustered positions and S1-RBD clustered residues (V445, G446, and Y449) that are physically adjacent to the mutation site as they are located on the same end of the interface as the N/Y501 clustered position mentioned earlier. Additionally, the average DCC analysis revealed a global decrease in the significantly dynamic anti-correlated motions in the mutant compared to the WT complex (**Figure 3B**). These results provide insight on the effect of the N501Y mutation on the dynamics of interfacial residues adjacent, either in protein sequence or in terms of physical location, to the mutation site and the distant effect of the mutation on the dynamics of non-interfacial residues manifested as a decrease in the anti-correlated inter-chain motions in the mutant complex.

In order to better understand how the two proteins interact at the interface and how this interaction compares in the WT and mutant complexes, we next performed interfacial H-bond occupancy analysis using a 3.5 Å cut-off distance and 20° cut-off angle. By applying a cut-off trajectory occupancy time of 5%, we were able to identify 19 unique H-bonds that form at the interface during the span of the simulation time by either the main chain or side chain of residues (**Figure 4A**). Interestingly, this analysis revealed that position 501 of S1-RBD is capable of H-bond formation with residues Y41 of ACE2 in the WT complex but not in the mutant complex. In fact, Y501 in the S1-RBD mutant complex did not form any substantial H-bonds with residues in ACE2. This indicates that Y501 residue in the mutant S1-RBD does not contribute to significant H-bond formation at the interface, but rather may be involved in forming other types of noncovalent interactions. In fact, by calculating interaction energy between this position and interfacial residues in ACE2, we found that this position forms additional, and more sustained, van der Waals interactions at the interface (**Supplementary Figure S1**). Recent reports suggest that this position is involved in π-π and π-cation interactions (Tian,

**A**

| Residue Pairs | WT | | N501Y | | Mean Diff. |
|---|---|---|---|---|---|
| ACE2 \| S1-RBD | Run 01 | Run 02 | Run 01 | Run 02 | |
| D355-Side \| T500-Side | 2.76 | 14.08 | 50.43 | 37.7 | 35.645 |
| K353-Main \| G502-Main | 36.07 | 48.71 | 66.27 | 68.44 | 24.965 |
| H34-Side \| Y453-Side | 0.82 | 3.37 | 0.1 | 28.68 | 12.295 |
| Q24-Side \| A475-Main | 2.8 | 4.32 | 8.28 | 11.1 | 6.13 |
| K31-Side \| E484-Side | 1.48 | 6.48 | 13.76 | 5.44 | 5.62 |
| Y41-Side \| T500-Side | 4.48 | 9.15 | 6.78 | 14.4 | 3.775 |
| E35-Side \| Q493-Side | 45.55 | 23.85 | 37.49 | 39.26 | 3.675 |
| K31-Side \| Q493-Side | 5.68 | 5.67 | 3.62 | 5.1 | -1.315 |
| D30-Side \| K417-Side | 37.75 | 37.62 | 22.42 | 49.48 | -1.735 |
| Y41-Side \| N501-Side | 6.4 | 0.04 | 0 | 0 | -3.22 |
| S19-Main \| A475-Main | 4.32 | 7.01 | 1.46 | 2.74 | -3.565 |
| K353-Side \| G496-Main | 0.88 | 7.45 | 0 | 0 | -4.165 |
| Y41-Side \| Q498-Side | 2.26 | 7.9 | 0.98 | 0.34 | -4.42 |
| Q42-Side \| Q498-Side | 16.34 | 8 | 12.42 | 1.98 | -4.97 |
| Y83-Side \| N487-Side | 42.09 | 46.49 | 41.57 | 35.08 | -5.965 |
| E37-Side \| Y505-Side | 27.67 | 4.32 | 15.12 | 4.04 | -6.415 |
| K353-Side \| Q498-Side | 11.38 | 6.18 | 0 | 0 | -8.78 |
| S19-Side \| A475-Main | 24.02 | 20.76 | 9.34 | 17.12 | -9.16 |
| D38-Side \| Y449-Side | 5.56 | 15.27 | 2 | 0.06 | -9.385 |

*N501 = Y501 in the N501Y mutant S1-RBD

**B**

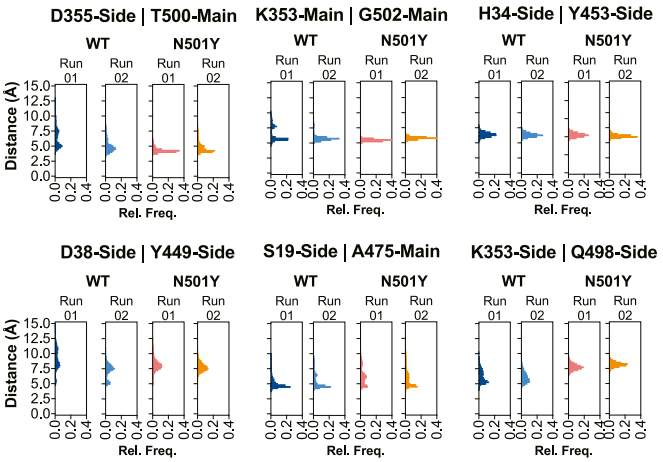


**FIGURE 4 |** Altered H-bonding between ACE2-S1-RBD interfacial residues. **(A)** Table showing H-bonds formed at the interface by applying a cut-off of 3.5 Å distance, 20° angle, and ≥5% occupancy time. Numbers represent the % occupancy time of the H-bond during the total simulation time. **(B)** Histograms representing distance measurements between H-bond forming pairs that showed the highest alterations in H-bond formation at the interface. Mean Diff, Mean difference, i.e., difference between H-bond mean percent occupancy time of the WT and mutant complexes. Blue and red colors indicate increase and decrease in occupancy time, respectively, in the mutant complex.

2021a; Ostrov, 2021). All these results are in contrast with previous reports suggesting enhanced H-bond formation by Y501 in the mutant complex (Ali et al., 2021; Tian, 2021b; Santos and Passos, 2021) driving the enhanced binding affinity of N501Y S1-RBD mutant to ACE2 (Khan, 2021; Leung et al., 2021; Zhao et al., 2021). More importantly, by calculating the difference between mean % occupancy time, we were able to determine changes in the % occupancy time between H-bonds formed in WT and mutant complexes. Interestingly, residues immediately adjacent to the 501 position in S1-RBD (T500 and G502) had the highest change in the H-bond occupancy (+35.6% and +25%, respectively), further indicating that the local effect of the mutation on the interface (**Figure 4A**). Distribution analysis of distances between H-bonding residue pairs that showed the highest increase and decrease in H-bond formation over the courses of the simulations revealed that the distance between these pairs generally increased and decreased, respectively, in the mutant complex (**Figure 4B**). More importantly, distance measurements revealed that in both cases (increased and decreased H-bond mean occupancy time) distance fluctuations between H-bond forming residue pairs decreased in the mutant complex compared to the WT complex (**Supplementary Figure S2**). Additionally, analysis of distance between interfacial residues that contribute to substantial H-bond interaction at the interface, but have a mean occupancy time not changing with the mutation (namely ACE2-D30-sidechain:S1-RBD-K417-sidechain, and ACE2-E35-sidechain:S1-RBD-Q493-sidechain), revealed that these residues are not located near the mutation site and display no marked differences in distance fluctuations between the WT and mutant complexes (**Supplementary Figure S3**), suggesting the stabilizing effect of the mutation as a key driving factor that alters H-bond interactions at the interface. The same can be concluded from calculating the distance between close-by interfacial residues at the far opposite end of the interface as was described above (**Figures 2E, F**).

To further confirm the effect of N501Y mutation on the interface, we calculated pair-wise residue distances between residues that form the ACE2-S1-RBD interface. Using a cut-off distance of 5 Å, we were able to identify 25 interfacial residues in ACE2 and 22 in S1-RBD providing a total of 550 interfacial residue pairs (**Figure 5A**). The mean and standard deviation of 5,000 distance measurements (obtained from 5,000 trajectory frames) for each pair were then calculated. Standard deviations were then normalized with the mean distances for each interfacial residue pair (averaged over the two MD simulation runs) and the ratio of standard deviations obtained for the N501Y mutant and WT complexes were plotted as heatmap (**Figure 5B**). A value greater than 1.0 of the ratios indicate a higher pair-wise distance fluctuation, and thus, a destabilizing effect in the mutant complex compared to the WT, while a value lesser than 1.0 indicates a decreased distance fluctuation, and thus, a stabilizing effect. This analysis revealed a general stabilizing effect of the mutation on the interfacial residues with ratios ranging from 0.21 (minimum; corresponding to K353:N501 residue pairs) to 2.64 (maximum; corresponding to Q24:F486 residue pairs) with a mean of 0.86. Interestingly, the stabilizing effect was more prominent on residues that are adjacent to the mutation site either in sequence (T500, G502 and V503) or in physical proximity (V445 and G446), which further supports the idea of a stabilizing effect of the mutation on residues at the interface, including the mutated N501 residue (**Figures 5B,C**). Interestingly, this distance fluctuation analysis showed a maximum number of residues pairs involving T500 residue in the N501Y mutant S1-RBD, even more than residue pairs involving Y501 residue itself (**Figure 5B**). These results are in agreement with recent reports, both computational (Jawad et al., 2021; Socher, 2021; Villoutreix et al., 2021) as well as experimental (Liu, 2021a; Tian, 2021a; Huang et al., 2021; Li et al., 2021; Niu et al., 2021), showing an increased affinity of the N501Y mutant S1-RBD for ACE2 receptor.

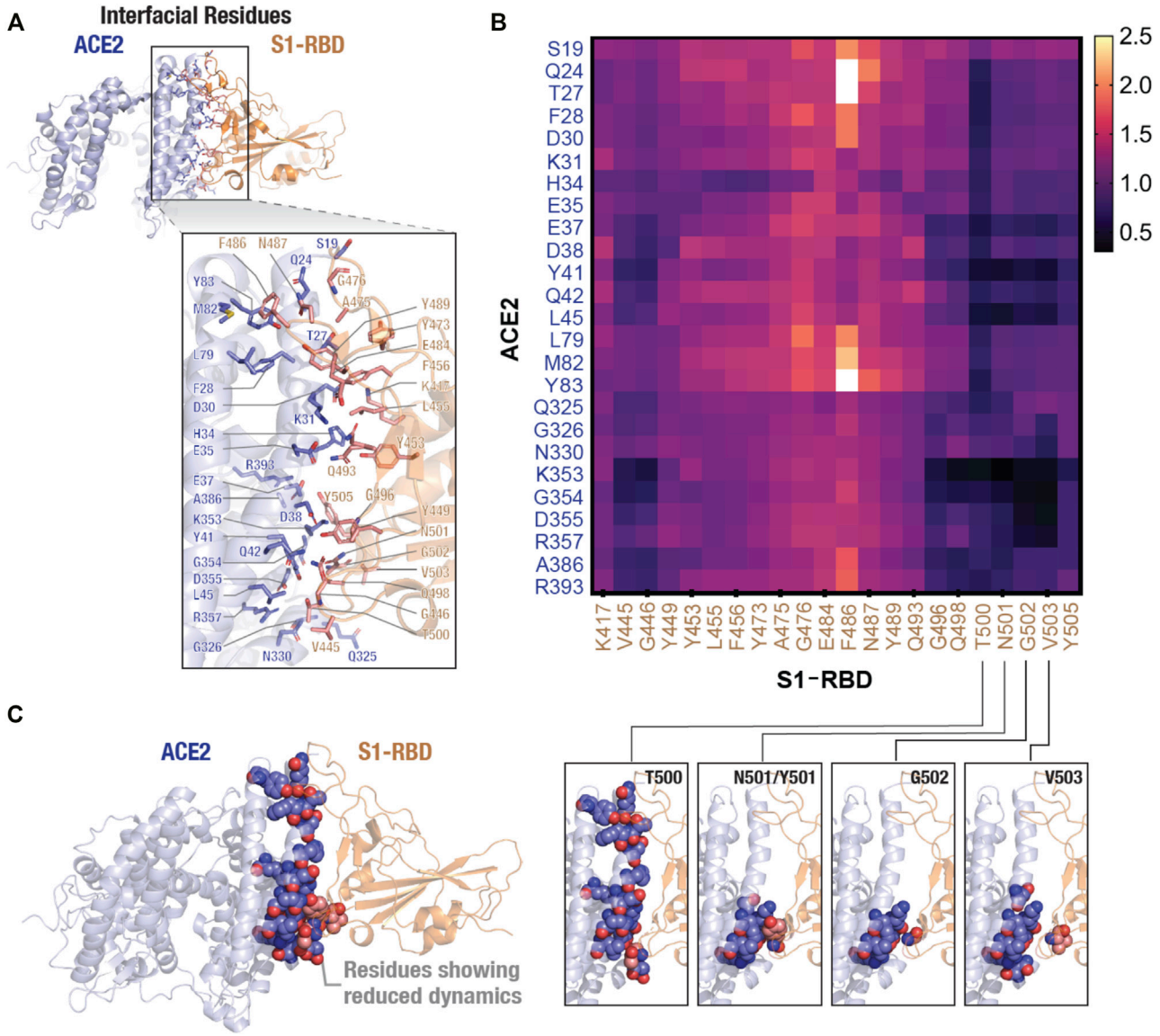


**FIGURE 5 |** Stabilizing effect of the N501Y mutation on ACE2-S1-RBD interfacial interaction. **(A)** Cartoon representation showing interfacial residues determined from the available ACE2-S1-RBD complex (PDB ID: 6m0j) at a cut-off distance of 5Å. A total of 25 residues (blue) and 22 residues (orange) were identified at the interface in ACE2 and S1-RBD, respectively. **(B)** Heatmap representing ratio of inter-residue distance fluctuations (standard deviation normalized to average distances) in the N501Y and WT ACE2-S1-RBD complexes. Note the decrease in the dynamics of Y501 and residues neighboring the mutation site, indicating a stabilizing effect of the mutation. **(C)** Schematic showing reduced dynamics of interfacial residues in the N501Y mutant. ACE2 (blue) and S1-RBD (orange) complex showing interfacial residues with reduced dynamics in the N501Y mutant in comparison to the WT interface.

After our work had become publicly available as a preprint in January 2020 (Ahmed et al., 2021), several studies reported characterization of the N501Y mutation, either alone or in combination with other SARS-CoV-2 spike mutations that exist in the VOC. For instance, Gobeil et al. (2021), using cryo-electron microscopy experiments, showed that all three VOC that contain the N501Y mutation (B.1.1.7, B.1.351, and P.1) have an increased propensity for the open-state of the spike protein, which is required for ACE2 binding, and, consequentially, an increased binding affinity for ACE2 (Gobeil, 2021). Teruel et al. (2021), using coarse-grained normal mode analysis of a large number mutants, demonstrated that the N501Y mutation alone markedly increases the SARS-CoV-2 spike open-state occupancy by increasing the flexibility of the closed-state and decreasing the flexibility of the open-state (Teruel et al., 2021) in a manner similar to that of the D614G mutation (Benton et al., 2021; Zhang et al., 2021). In fact, a computational study published in early 2020 suggested N501 residue as being compatible with, but not ideal for, human ACE2 binding (Wan et al., 2020). In addition to these, some MD simulation studies reported an enhanced binding affinity of N501Y mutant S1-RBD for ACE2 (Jawad et al., 2021; Luan et al., 2021; Spinello et al., 2021), with the possibility of a local conformational change caused by the N501Y

mutation (Socher, 2021). However, such a conformational change was not observed in another MD simulation study performed with the ACE2-S1-RBD complex of the N501Y containing B.1.1.7 and B.1.531 SARS-CoV-2 variant spike protein (Villoutreix et al., 2021). In agreement with our findings, Jawad et al. (2021) (Jawad et al., 2021) showed that the N501 residue does not form substantial H-bond interaction with ACE2 residues, and that the N501Y S1-RBD mutation significantly enhances ACE2 binding by altering amino acid interactions with ACE2 at the interface. Thus, altered interfacial residue dynamics allowing for a sustained ACE2-S1-RBD interaction, likely driving the increased transmissibility of the B.1.1.7 variant, reported here appear to be consistent across multiple studies.

## CONCLUSION

To conclude, the MD simulations performed here with the ACE2-S1-RBD complex provide an unambiguous mechanistic insight into the increased binding affinity of the N501Y mutant S1-RBD for ACE2. Specifically, our computational work shows that the mutation of N501 residue into tyrosine (Y) results in a stable interaction with the Y41 and K353 residues in ACE2. This is positively impacted by the altered dynamics of the S1-RBD upon N501Y mutation, which is more noticeable on residues adjacent to mutation site, and extends to include certain nonadjacent residues, although the reason behind it is not entirely clear and will likely require further investigation. The N501Y S1-RBD mutation, classified as a high-frequency temporal dynamics mutation (Justo Arevalo et al., 2021), has gained tremendous interest from the scientific community given its presence in three of the SARS-CoV-2 VOC that by march accounted for more than two-thirds of the circulating variants world-wide (Huang et al., 2021). A number of studies corroborating our conclusions have appeared, which suggest the essential role of N501Y S1-RBD mutation in the transmissibility of SARS-CoV-2 variants that carry this mutation by forming a high affinity and more stable interaction at the ACE2-S1-RBD interface, possibly by altering interfacial dynamics as is evident from our study. We believe that the results outlined here will be helpful in efforts towards thwarting this new wave of COVID-19 by enabling discovery of potent inhibitors of ACE2-S1-RBD interaction (Andersen et al., 2020; Choudhary et al., 2020; Shang, 2020; Walls, 2020; Wrapp et al., 2020) or the development of high affinity ACE2 variants for use as decoys (Chan et al., 2020; Glasgow et al., 2020; Chan et al., 2021; Jing and Procko, 2021).

## DATA AVAILABILITY STATEMENT

The original contributions presented in the study are included in the article/**Supplementary Material,** further inquiries can be directed to the corresponding author.

## AUTHOR CONTRIBUTIONS

KB conceived the experiments. WA, AP, and KB performed experiments, analyzed data, prepared figures, and wrote the manuscript. All authors reviewed and approved the manuscript.

## FUNDING

This work is supported by an internal funding from the College of Health and Life Sciences, Hamad Bin Khalifa University, a member of the Qatar Foundation. WA and AP. are supported by scholarship from the College of Health and Life Sciences, Hamad Bin Khalifa University, a member of the Qatar Foundation. Some of the computational research work reported in the manuscript were performed using high-performance computer resources and services provided by the Research Computing group in Texas A and M University at Qatar. Research Computing is funded by the Qatar Foundation for Education, Science and Community Development (http://www.qf.org.qa). Open Access funding provided by the Qatar National Library.

## SUPPLEMENTARY MATERIAL

The Supplementary Material for this article can be found online at: https://www.frontiersin.org/articles/10.3389/fmolb.2022.846996/full#supplementary-material

## REFERENCES

Ahmed, W. S., Phillip, A. M., and Biswas, K. H. (2021). *Stable Interaction of the UK B. 1.1. 7 Lineage SARS-CoV-2 S1 Spike N501Y Mutant with ACE2 Revealed by Molecular Dynamics Simulation*. bioRxiv. (NY: Cold Spring Harbor). doi:10.1101/2021.01.07.425307

Ali, F., Kasry, A., and Amin, M. (2021). The New SARS-CoV-2 Strain Shows a Stronger Binding Affinity to ACE2 Due to N501Y Mutant. *Med. Drug Discov.* 10, 100086 doi:10.1016/j.medidd.2021.100086

Altamash, T., Ahmed, W., Rasool, S., and Biswas, K. H. (2021). Intracellular Ionic Strength Sensing Using NanoLuc. *Int. J. Mol. Sci.* 22 (2), E677. doi:10.3390/ijms22020677

Andersen, K. G., Rambaut, A., Lipkin, W. I., Holmes, E. C., and Garry, R. F. (2020). The Proximal Origin of SARS-CoV-2. *Nat. Med.* 26, 450–452. doi:10.1038/s41591-020-0820-9

Avanzato, V. A., Matson, M. J., Seifert, S. N., Pryce, R., Williamson, B. N., Anzick, S. L., et al. (2020). Case Study: Prolonged Infectious SARS-CoV-2 Shedding from an Asymptomatic Immunocompromised Individual with Cancer. *Cell* 183 (7), 1901–1912. doi:10.1016/j.cell.2020.10.049

Benton, D. J., Wrobel, A. G., Roustan, C., Borg, A., Xu, P., Martin, S. R., et al. (2021). The Effect of the D614G Substitution on the Structure of the Spike Glycoprotein of SARS-CoV-2. *Proc. Natl. Acad. Sci. U. S. A.* 118 (9), e2022586118. doi:10.1073/pnas.2022586118

Best, R. B., Zhu, X., Shim, J., Lopes, P. E. M., Mittal, J., Feig, M., et al. (2012). Optimization of the Additive CHARMM All-Atom Protein Force Field Targeting Improved Sampling of the Backbone ϕ, ψ and Side-Chain χ1 and χ2 Dihedral Angles. *J. Chem. Theory Comput.* 8 (9), 3257–3273. doi:10.1021/ct300400x

Biswas, K. H. (2017). Allosteric Regulation of Proteins. *Reson* 22 (1), 37–50. doi:10.1007/s12045-017-0431-z

Biswas, K. H., Badireddy, S., Rajendran, A., Anand, G. S., and Visweswariah, S. S. (2015). Cyclic Nucleotide Binding and Structural Changes in the Isolated GAF Domain ofAnabaenaadenylyl Cyclase, CyaB2. *PeerJ* 3, e882. doi:10.7717/peerj.882

Biswas, K. H. (2018). Regulation of α-catenin Conformation at Cadherin Adhesions. *Jbse* 13 (4), 17–00699. doi:10.1299/jbse.17-00699

Biswas, K. H., Sopory, S., and Visweswariah, S. S. (2008). The GAF Domain of the cGMP-Binding, cGMP-specific Phosphodiesterase (PDE5) Is a Sensor and a Sink for cGMP. *Biochemistry* 47 (11), 3534–3543. doi:10.1021/bi702025w

Biswas, K. H., and Visweswariah, S. S. (2011). Distinct Allostery Induced in the Cyclic GMP-Binding, Cyclic GMP-specific Phosphodiesterase (PDE5) by Cyclic GMP, Sildenafil, and Metal Ions. *J. Biol. Chem.* 286 (10), 8545–8554. doi:10.1074/jbc.m110.193185

Biswas, K. H., and Visweswariah, S. S. (2017). Buffer NaCl Concentration Regulates Renilla Luciferase Activity and Ligand-Induced Conformational Changes in the BRET-Based PDE5 Sensor. *Matters* 3, 5. doi:10.19185/matters.201702000015

Brielle, E. S., and Arkin, I. T. (2020). Quantitative Analysis of Multiplex H-Bonds. *J. Am. Chem. Soc.* 142 (33), 14150–14157. doi:10.1021/jacs.0c04357

Brown, D. K., Penkler, D. L., Sheik Amamuddy, O., Ross, C., Atilgan, A. R., Atilgan, C., et al. (2017). MD-TASK: a Software Suite for Analyzing Molecular Dynamics Trajectories. *Bioinformatics* 33 (17), 2768–2771. doi:10.1093/bioinformatics/btx349

Chan, K. K., Tan, T. J. C., Narayanan, K. K., and Procko, E. (2021). An Engineered Decoy Receptor for SARS-CoV-2 Broadly Binds Protein S Sequence Variants. *Sci. Adv.* 7 (8), eabf1738. doi:10.1126/sciadv.abf1738

Chan, K. K., Dorosky, D., Sharma, P., Abbasi, S. A., Dye, J. M., Kranz, D. M., et al. (2020). Engineering Human ACE2 to Optimize Binding to the Spike Protein of SARS Coronavirus 2. *Science* 369 (6508), 1261–1265. doi:10.1126/science.abc0870

Chen, C., Boorla, V. S., Banerjee, D., Chowdhury, R., Cavener, V. S., Nissly, R. H., et al. (2021). Computational Prediction of the Effect of Amino Acid Changes on the Binding Affinity between SARS-CoV-2 Spike RBD and Human ACE2. *Proc. Natl. Acad. Sci. U. S. A.* 118 (42), e2106480118. doi:10.1073/pnas.2106480118

Choi, B., Choudhary, M. C., Regan, J., Sparks, J. A., Padera, R. F., Qiu, X., et al. (2020). Persistence and Evolution of SARS-CoV-2 in an Immunocompromised Host. *N. Engl. J. Med.* 383 (23), 2291–2293. doi:10.1056/nejmc2031364

Choudhary, S., Malik, Y. S., and Tomar, S. (2020). Identification of SARS-CoV-2 Cell Entry Inhibitors by Drug Repurposing Using In Silico Structure-Based Virtual Screening Approach. *Front. Immunol.* 11, 1664. doi:10.3389/fimmu.2020.01664

Colson, P. (2021). Spreading of a New SARS-CoV-2 N501Y Spike Variant in a New Lineage. *Clin. Microbiol. Infect.* 27 (9), 1352.e1–1352.e5. doi:10.1016/j.cmi.2021.05.006

Fiskerstrand, T., Arshad, N., Haukanes, B. I., Tronstad, R. R., Pham, K. D.-C., Johansson, S., et al. (2012). Familial Diarrhea Syndrome Caused by an ActivatingGUCY2CMutation. *N. Engl. J. Med.* 366 (17), 1586–1595. doi:10.1056/nejmoa1110132

Glasgow, A., Glasgow, J., Limonta, D., Solomon, P., Lui, I., Zhang, Y., et al. (2020). Engineered ACE2 Receptor Traps Potently Neutralize SARS-CoV-2. *Proc. Natl. Acad. Sci. U.S.A.* 117 (45), 28046–28055. doi:10.1073/pnas.2016093117

Gobeil, S. M., Janowska, K., McDowell, S., Mansouri, K., Parks, R., Stalls, V., et al. (2021). Effect of Natural Mutations of SARS-CoV-2 on Spike Structure, Conformation and Antigenicity. *Science* 373 (6555), eabi6226. doi:10.1126/science.abi6226

Grant, B. J., Rodrigues, A. P. C., ElSawy, K. M., McCammon, J. A., and Caves, L. S. D. (2006). Bio3d: An R Package for the Comparative Analysis of Protein Structures. *Bioinformatics* 22 (21), 2695–2696. doi:10.1093/bioinformatics/btl461

Hou, Y. J., Chiba, S., Halfmann, P., Ehre, C., Kuroda, M., Dinnon, K. H., et al. (2020). SARS-CoV-2 D614G Variant Exhibits Efficient Replication *Ex Vivo* and Transmission *In Vivo*. *Science* 370 (6523), 1464–1468. doi:10.1126/science.abe8499

Huang, H., Zhu, Y., Niu, Z., Zhou, L., and Sun, Q. (2021). SARS-CoV-2 N501Y Variants of Concern and Their Potential Transmission by Mouse. *Cell Death Differ.* 28 (10), 2840–2842. doi:10.1038/s41418-021-00846-4

Humphrey, W., Dalke, A., and Schulten, K. (1996). VMD: Visual Molecular Dynamics. *J. Mol. Graph.* 14 (1), 33–38. doi:10.1016/0263-7855(96)00018-5

Hussein, H. A., Hassan, R., Chino, M., and Febbraio, F. (2020). Point-of-Care Diagnostics of COVID-19: From Current Work to Future Perspectives. *Sensors (Basel, Switzerland)* 20 (15), 4289. doi:10.3390/s20154289

Istifli, E. S., Netz, P. A., Sihoglu Tepe, A., Sarikurkcu, C., and Tepe, B. (2021). Understanding the Molecular Interaction of SARS-CoV-2 Spike Mutants with ACE2 (Angiotensin Converting Enzyme 2). *J. Biomol. Struct. Dyn.*, 1–12. doi:10.1080/07391102.2021.1975569

Jawad, B., Adhikari, P., Podgornik, R., and Ching, W.-Y. (2021). Key Interacting Residues between RBD of SARS-CoV-2 and ACE2 Receptor: Combination of Molecular Dynamics Simulation and Density Functional Calculation. *J. Chem. Inf. Model.* 61 (9), 4425–4441. doi:10.1021/acs.jcim.1c00560

Jing, W., and Procko, E. (2021). ACE2-based Decoy Receptors for SARS Coronavirus 2. *Proteins* 89 (9), 1065–1078. doi:10.1002/prot.26140

Jorgensen, W. L., Chandrasekhar, J., Madura, J. D., Impey, R. W., and Klein, M. L. (1983). Comparison of Simple Potential Functions for Simulating Liquid Water. *J. Chem. Phys.* 79 (2), 926–935. doi:10.1063/1.445869

Justo Arevalo, S., Zapata Sifuentes, D., J. Huallpa, C., Landa Bianchi, G., Castillo Chávez, A., Garavito-Salini Casas, R., et al. (2021). Dynamics of SARS-CoV-2 Mutations Reveals Regional-Specificity and Similar Trends of N501 and High-Frequency Mutation N501Y in Different Levels of Control Measures. *Sci. Rep.* 11 (1), 17755. doi:10.1038/s41598-021-97267-7

Khan, A., Zia, T., Suleman, M., Khan, T., Ali, S. S., and Abbasi, A. A., et al. (2021). Higher Infectivity of the SARS-CoV-2 New Variants Is Associated with K417N/T, E484K, and N501Y Mutants: An Insight from Structural Data. *J. Cell. physiology* 236 (10), 7045–7057. doi:10.1002/jcp.30367

Kollman, P. A., Massova, I., Reyes, C., Kuhn, B., Huo, S., Chong, L., et al. (2000). Calculating Structures and Free Energies of Complex Molecules: Combining Molecular Mechanics and Continuum Models. *Acc. Chem. Res.* 33 (12), 889–897. doi:10.1021/ar000033j

Lan, J., Ge, J., Yu, J., Shan, S., Zhou, H., Fan, S., et al. (2020). Structure of the SARS-CoV-2 Spike Receptor-Binding Domain Bound to the ACE2 Receptor. *Nature* 581 (7807), 215–220. doi:10.1038/s41586-020-2180-5

Leung, K., Shum, M. H., Leung, G. M., Lam, T. T., and Wu, J. T. (2021). Early Transmissibility Assessment of the N501Y Mutant Strains of SARS-CoV-2 in the United Kingdom, October to November 2020. *Euro Surveill.* 26 (1), 2002106. doi:10.2807/1560-7917.es.2020.26.1.2002106

Li, Q., Nie, J., Wu, J., Zhang, L., Ding, R., Wang, H., et al. (2021). SARS-CoV-2 501Y.V2 Variants Lack Higher Infectivity but Do Have Immune Escape. *Cell* 184 (9), 2362–2371. doi:10.1016/j.cell.2021.02.042

Liu, H., and Hou, T. (2016). CaFE: a Tool for Binding Affinity Prediction Using End-point Free Energy Methods. *Bioinformatics* 32 (14), 2216–2218. doi:10.1093/bioinformatics/btw215

Liu, K., Tan, S., Niu, S., Wang, J., Wu, L., Sun, H., et al. (2021a). Cross-species recognition of SARS-CoV-2 to bat ACE2. Proceedings of the National Academy of Sciences of the United States of America 118 (1), e2020216118. doi:10.1073/pnas.2020216118

Liu, Y., Hu, G., Wang, Y., Ren, W., Zhao, X., Ji, F., et al. (2021b). Functional and Genetic Analysis of Viral Receptor ACE2 Orthologs Reveals a Broad Potential Host Range of SARS-CoV-2. *Proceedings of the National Academy of Sciences of the United States of America* 118 (12), e2025373118. doi:10.1073/pnas.2025373118

Liu, Y. (2021). *The N501Y Spike Substitution Enhances SARS-CoV-2 Transmission*. bioRxiv, 2021.

Luan, B., Wang, H., and Huynh, T. (2021). Enhanced Binding of the N501Y-Mutated SARS-CoV-2 Spike Protein to the Human ACE2 Receptor: Insights from Molecular Dynamics Simulations. *FEBS Lett.* 595 (10), 1454–1461. doi:10.1002/1873-3468.14076

Mallik, S., Prasad, R., Das, K., and Sen, P. (2021). Alcohol Functionality in the Fatty Acid Backbone of Sphingomyelin Guides the Inhibition of Blood Coagulation. *RSC Adv.* 11 (6), 3390–3398. doi:10.1039/d0ra09218e

Mansbach, R. A., Chakraborty, S., Nguyen, K., Montefiori, D. C., Korber, B., Gnanakaran, S., et al. (2021). The SARS-CoV-2 Spike Variant D614G Favors an Open Conformational State. *Sci. Adv* 7 (16), eabf3671. doi:10.1126/sciadv.abf3671

Martin, D. P., Weaver, S., Tegally, H., San, J. E., Shank, S. D., Wilkinson, E., et al. (2021). The Emergence and Ongoing Convergent Evolution of the SARS-CoV-2 N501Y Lineages. *Cell* 184 (20), 5189–5200. doi:10.1016/j.cell.2021.09.003

Narayanan, K. K., and Procko, E. (2021). Deep Mutational Scanning of Viral Glycoproteins and Their Host Receptors. *Front. Mol. Biosci.* 8, 636660. doi:10.3389/fmolb.2021.636660

Niu, Z., Zhang, Z., Gao, X., Du, P., Lu, J., Yan, B., et al. (2021). N501Y Mutation Imparts Cross-Species Transmission of SARS-CoV-2 to Mice by Enhancing Receptor Binding. *Sig Transduct. Target Ther.* 6 (1), 284. doi:10.1038/s41392-021-00704-2

Ostrov, D. A. (2021). Structural Consequences of Variation in SARS-CoV-2 B.1.1.7. *J. Cell Immunol.* 3 (2), 103–108. doi:10.33696/immunology.3.085

Phillips, J. C., Braun, R., Wang, W., Gumbart, J., Tajkhorshid, E., Villa, E., et al. (2005). Scalable Molecular Dynamics with NAMD. *J. Comput. Chem.* 26 (16), 1781–1802. doi:10.1002/jcc.20289

Plante, J. A., Liu, Y., Liu, J., Xia, H., Johnson, B. A., Lokugamage, K. G., et al. (2021). Spike Mutation D614G Alters SARS-CoV-2 Fitness. *Nature* 592 (7852), 116–121. doi:10.1038/s41586-020-2895-3

Procko, E. (2020). Deep Mutagenesis in the Study of COVID-19: a Technical Overview for the Proteomics Community. *Expert Rev. Proteomics* 17 (9), 633–638. doi:10.1080/14789450.2020.1833721

Rambaut, A., Loman, N., Pybus, O., Barclay, W., Barrett, J., Carabelli, A., et al.on behalf of COVID-19 Genomics Consortium UK (CoG-UK) (2020). *Preliminary Genomic Characterisation of an Emergent SARS-CoV-2 Lineage in the UK Defined by a Novel Set of Spike Mutations*. Edinburgh: Virological.org.

Ribeiro, J. V., Bernardi, R. C., Rudack, T., Stone, J. E., Phillips, J. C., Freddolino, P. L., et al. (2016). QwikMD - Integrative Molecular Dynamics Toolkit for Novices and Experts. *Sci. Rep.* 6, 26536. doi:10.1038/srep26536

Samavati, L., and Uhal, B. D. (2020). ACE2, Much More Than Just a Receptor for SARS-COV-2. *Front. Cell Infect. Microbiol.* 10, 317. doi:10.3389/fcimb.2020.00317

Santos, J. C., and Passos, G. A. (2021). *The High Infectivity of SARS-CoV-2 B.1.1.7 Is Associated with Increased Interaction Force between Spike-ACE2 Caused by the Viral N501Y Mutation*. bioRxiv. (NY: Cold Spring Harbor). doi:10.1101/2020.12.29.424708

Schindelin, J., Arganda-Carreras, I., Frise, E., Kaynig, V., Longair, M., Pietzsch, T., et al. (2012). Fiji: an Open-Source Platform for Biological-Image Analysis. *Nat. Methods* 9 (7), 676–682. doi:10.1038/nmeth.2019

Shang, J., Ye, G., Shi, K., Wan, Y., Luo, C., Aihara, H., et al. (2020). Structural Basis of Receptor Recognition by SARS-CoV-2. *Nature* 581 (7807), 221–224. doi:10.1038/s41586-020-2179-y

Shang, J., Wan, Y., Luo, C., Ye, G., Geng, Q., Auerbach, A., et al. (2020). Cell Entry Mechanisms of SARS-CoV-2. *Proc. Natl. Acad. Sci. U.S.A.* 117 (21), 11727–11734. doi:10.1073/pnas.2003138117

Skjærven, L., Yao, X. Q., Scarabelli, G., and Grant, B. J. (2014). Integrating Protein Structural Dynamics and Evolutionary Analysis with Bio3D. *BMC Bioinforma.* 15 (1), 399. doi:10.1186/s12859-014-0399-6

Socher, E., Conrad, M., Heger, L., Paulsen, F., Sticht, H., Zunke, F., et al. (2021). Computational Decomposition Reveals Reshaping of the SARS-CoV-2-ACE2 Interface Among Viral Variants Expressing the N501Y Mutation. *J. Cell Biochem.* 122 (12), 1863–1872. doi:10.1002/jcb.30142

Spinello, A., Saltalamacchia, A., Borišek, J., and Magistrato, A. (2021). Allosteric Cross-Talk Among Spike's Receptor-Binding Domain Mutations of the SARS-CoV-2 South African Variant Triggers an Effective Hijacking of Human Cell Receptor. *J. Phys. Chem. Lett.* 12 (25), 5987–5993. doi:10.1021/acs.jpclett.1c01415

Spinello, A., Saltalamacchia, A., and Magistrato, A. (2020). Is the Rigidity of SARS-CoV-2 Spike Receptor-Binding Motif the Hallmark for its Enhanced Infectivity? Insights from All-Atom Simulations. *J. Phys. Chem. Lett.* 11 (12), 4785–4790. doi:10.1021/acs.jpclett.0c01148

Starr, T. N., Greaney, A. J., Hilton, S. K., Ellis, D., Crawford, K. H. D., Dingens, A. S., et al. (2020). Deep Mutational Scanning of SARS-CoV-2 Receptor Binding Domain Reveals Constraints on Folding and ACE2 Binding. *Cell* 182 (5), 1295–1310. doi:10.1016/j.cell.2020.08.012

Tai, W., Zhang, X., He, Y., Jiang, S., and Du, L. (2020). Identification of SARS-CoV RBD-Targeting Monoclonal Antibodies with Cross-Reactive or Neutralizing Activity against SARS-CoV-2. *Antivir. Res.* 179, 104820. doi:10.1016/j.antiviral.2020.104820

Teruel, N., Mailhot, O., and Najmanovich, R. J. (2021). Modelling Conformational State Dynamics and its Role on Infection for SARS-CoV-2 Spike Protein Variants. *PLoS Comput. Biol.* 17 (8), e1009286. doi:10.1371/journal.pcbi.1009286

Tian, F. (2021a). *Mutation N501Y in RBD of Spike Protein Strengthens the Interaction between COVID-19 and its Receptor ACE2*. bioRxiv. (NY: Cold Spring Harbor).

Tian, F., Tong, B., Sun, L., Shi, S., Zheng, B., Wang, Z., et al. (2021b). *N501Y Mutation of Spike Protein in SARS-CoV-2 Strengthens its Binding to Receptor ACE2*. Elife, 10, e69091. doi:10.7554/eLife.69091

Villoutreix, B. O., Calvez, V., Marcelin, A. G., and Khatib, A. M. (2021). In Silico Investigation of the New UK (B.1.1.7) and South African (501Y.V2) SARS-CoV-2 Variants with a Focus at the ACE2-Spike RBD Interface. *Int. J. Mol. Sci.* 22 (4), 1695. doi:10.3390/ijms22041695

V'kovski, P., Kratzel, A., Steiner, S., Stalder, H., and Thiel, V. (2021). Coronavirus Biology and Replication: Implications for SARS-CoV-2. *Nat. Rev. Microbiol.* 19 (3), 155–170. doi:10.1038/s41579-020-00468-6

Volz, E., Hill, V., McCrone, J. T., Price, A., Jorgensen, D., O'Toole, Á., et al. (2020). Evaluating the Effects of SARS-CoV-2 Spike Mutation D614G on Transmissibility and Pathogenicity. *Cell* 184 (1), 64–75.e11. doi:10.1016/j.cell.2020.11.020

Walls, A. C., Park, Y. J., Tortorici, M. A., Wall, A., McGuire, A. T., Veesler, D., et al. (2020). Structure, Function, and Antigenicity of the SARS-CoV-2 Spike Glycoprotein. *Cell* 183 (6), 1735. doi:10.1016/j.cell.2020.11.032

Wan, Y., Shang, J., Graham, R., Baric, R. S., and Li, F. (2020). Receptor Recognition by the Novel Coronavirus from Wuhan: an Analysis Based on Decade-Long Structural Studies of SARS Coronavirus. *J. Virol.* 94 (7), e00127–20. doi:10.1128/JVI.00127-20

Wang, Y., Liu, M., and Gao, J. (2020). Enhanced Receptor Binding of SARS-CoV-2 through Networks of Hydrogen-Bonding and Hydrophobic Interactions. *Proc. Natl. Acad. Sci. U.S.A.* 117 (25), 13967–13974. doi:10.1073/pnas.2008209117

Wrapp, D., Wang, N., Corbett, K. S., Goldsmith, J. A., Hsieh, C.-L., Abiona, O., et al. (2020). Cryo-EM Structure of the 2019-nCoV Spike in the Prefusion Conformation. *Science* 367 (6483), 1260–1263. doi:10.1126/science.abb2507

Wu, F., Zhao, S., Yu, B., Chen, Y.-M., Wang, W., Song, Z.-G., et al. (2020). A New Coronavirus Associated with Human Respiratory Disease in China. *Nature* 579 (7798), 265–269. doi:10.1038/s41586-020-2008-3

Yurkovetskiy, L., Wang, X., Pascal, K. E., Tomkins-Tinch, C., Nyalile, T. P., Wang, Y., et al. (2020). Structural and Functional Analysis of the D614G SARS-CoV-2 Spike Protein Variant. *Cell* 183 (3), 739–751. doi:10.1016/j.cell.2020.09.032

Zahradník, J. (2021). *SARS-CoV-2 RBD* in Vitro *Evolution Follows Contagious Mutation Spread, yet Generates an Able Infection*. bioRxiv. (NY: Cold Spring Harbor), 2021.

Zhang, J., Cai, Y., Xiao, T., Lu, J., Peng, H., Sterling, S. M., et al. (2021). Structural Impact on SARS-CoV-2 Spike Protein by D614G Substitution. *Science* 372 (6541), 525–530. doi:10.1126/science.abf2303

Zhang, L., Jackson, C. B., Mou, H., Ojha, A., Peng, H., Quinlan, B. D., et al. (2020). SARS-CoV-2 Spike-Protein D614G Mutation Increases Virion Spike Density and Infectivity. *Nat. Commun.* 11 (1), 6013. doi:10.1038/s41467-020-19808-4

Zhao, S., Lou, J., Cao, L., Zheng, H., Chong, M. K. C., Chen, Z., et al. (2021). Quantifying the Transmission Advantage Associated with N501Y Substitution of SARS-CoV-2 in the UK: an Early Data-Driven Analysis. *J. Travel Med.* 28 (2), taab011. doi:10.1093/jtm/taab011

Zoufaly, A., Poglitsch, M., Aberle, J. H., Hoepler, W., Seitz, T., Traugott, M., et al. (2020). Human Recombinant Soluble ACE2 in Severe COVID-19. *Lancet Respir. Med.* 8 (11), 1154–1158. doi:10.1016/s2213-2600(20)30418-5

**Conflict of Interest:** The authors declare that the research was conducted in the absence of any commercial or financial relationships that could be construed as a potential conflict of interest.

frontiers | Frontiers in Medicine

TYPE Case Report
PUBLISHED 11 January 2023
DOI 10.3389/fmed.2022.879971



OPEN ACCESS

EDITED BY
Mohamed Emara,
Qatar University, Qatar

REVIEWED BY
Luís Carlos Lopes-Júnior,
Federal University of Espirito Santo, Brazil
Deborah Duricka,
Neuroversion Inc., United States

*CORRESPONDENCE
Laura V. Schaefer
✉ lschaefe@uni-potsdam.de

SPECIALTY SECTION
This article was submitted to Precision Medicine, a section of the journal Frontiers in Medicine

RECEIVED 25 March 2022
ACCEPTED 22 December 2022
PUBLISHED 11 January 2023

CITATION
Schaefer LV and Bittmann FN (2023) Case report: Individualized pulsed electromagnetic field therapy in a Long COVID patient using the Adaptive Force as biomarker. *Front. Med.* 9:879971. doi: 10.3389/fmed.2022.879971



# Case report: Individualized pulsed electromagnetic field therapy in a Long COVID patient using the Adaptive Force as biomarker

Laura V. Schaefer[1,2]* and Frank N. Bittmann[1,2]

[1]Regulative Physiology and Prevention, Department of Sports and Health Sciences, University Potsdam, Potsdam, Germany, [2]Practice of Integrative Medicine Bittmann, Potsdam, Germany

The increasing prevalence of Long COVID is an imminent public health disaster, and established approaches have not provided adequate diagnostics or treatments. Recently, anesthetic blockade of the stellate ganglion was reported to improve Long COVID symptoms in a small case series, purportedly by "rebooting" the autonomic nervous system. Here, we present a novel diagnostic approach based on the Adaptive Force (AF), and report sustained positive outcome for one severely affected Long COVID patient using individualized pulsed electromagnetic field (PEMF) at the area C7/T1. AF reflects the capacity of the neuromuscular system to adapt adequately to external forces in an isometric holding manner. In case, maximal isometric AF ($AFiso_{max}$) is exceeded, the muscle merges into eccentric muscle action. Thereby, the force usually increases further until maximal AF (AFmax) is reached. In case adaptation is optimal, $AFiso_{max}$ is ∼99–100% of AFmax. This holding capacity ($AFiso_{max}$) was found to be vulnerable to disruption by unpleasant stimulus and, hence, was regarded as functional parameter. AF was assessed by an objectified manual muscle test using a handheld device. Prior to treatment, $AFiso_{max}$ was considerably lower than AFmax for hip flexors (62 $N$ = ∼28% AFmax) and elbow flexors (71 $N$ = ∼44% AFmax); i.e., maximal holding capacity was significantly reduced, indicating dysfunctional motor control. We tested PEMF at C7/T1, identified a frequency that improved neuromuscular function, and applied it for ∼15 min. Immediately post-treatment, $AFiso_{max}$ increased to ∼210 $N$ (∼100% AFmax) at hip and 184 $N$ (∼100% AFmax) at elbow. Subjective Long COVID symptoms resolved the following day. At 4 weeks post-treatment, maximal holding capacity was still on a similarly high level as for immediately post-treatment (∼100% AFmax) and patient was symptom-free. At 6 months the patient's Long COVID symptoms have not returned. This case report suggests (1) AF could be a promising diagnostic for post-infectious illness, (2) AF can be used to test effective treatments for post-infectious illness, and (3) individualized PEMF may resolve post-infectious symptoms.

KEYWORDS

**individualized pulsed electromagnetic field, Adaptive Force, muscular holding capacity, case report, Long COVID, post-COVID syndrome, muscle weakness, fatigue**

## 1. Introduction

"Long COVID" receives increasing attention due to the high number of affected persons during SARS-CoV-2 pandemic. Six month post-infection 57% of COVID-19 survivors show one or more sequelae, after 1 year still half of them present at least one symptom (1, 2), regardless of infection severity (3). Long COVID shows similarities to myalgic encephalomyelitis/chronic fatigue syndrome (ME/CFS) (4–9), which is known since decades and can arise after viral infections (7–12). For post-infectious syndromes a dysfunction of the autonomous nervous system (ANS) was discussed to be the cause or at least a component (4, 7–9). The underlying mechanisms, the causality and the influence of pre-existing health conditions are not sufficiently known (1, 13). Innovative diagnostics and efficient causal therapies are urgently needed (14, 15).

Recently, Liu and Duricka reported sustained positive clinical outcomes for two Long COVID patients after stellate ganglion block (SGB), i.e., injecting local anesthetics near the stellate ganglion (4). Based on the rapid resolution of symptoms the authors concluded the "system needs to 'reboot' to produce functional recovery" (4). The positive effect of SGB was suggested to be based on "sympathectomy," which "produces its beneficial effects… by attenuating chronic sympathetic hyper responsiveness, improving cerebral and regional blood flow, and recalibrating the autonomic nervous system toward pre-COVID homeostasis" or "rebalancing the interaction between the nervous and immune system" (4).

Despite of delaying broad acceptance as valid treatment (4), therapeutic local anesthesia to sympathetic ganglia is supposed to be a promising approach for relieving severe conditions (16–20). It is applied since decades to treat several conditions, e.g., acute/chronic pain, functional disorders, dysautonomia, and chronic inflammation (16, 21). SGB, e.g., reduced the symptoms in patients with posttraumatic stress disorders (22, 23), may modulate the immune response (24), or stabilized ventricular rhythm (25). The local injection is claimed to be safe (4, 21), however, it is invasive and involves some risks (21, 26).

Another approach to influence the ANS is the use of weak, low-frequency pulsatile electromagnetic fields (PEMF) (27). Animal studies support the hypothesis that PEMF can be useful in therapy (27–30), e.g., in cardiac diseases (27, 30, 31). In humans, PEMF could normalize dysautonomia in children (32, 33) and was found to be effective to treat neuropathic/postsurgical pain and edema as well as several other indications (34–37). PEMF acupuncture of BL15 (bladder meridian and paravertebral T5) was found to activate the parasympathetic nervous system (38). Moreover, PEMF showed positive effects in cancer treatment (39). It modulated the physiology and electrochemistry of cancer cells and had immunomodulatory and systematic effects (39–41). PEMF was suggested to be a "suitable therapeutic approach with neuroimmunomodulatory, anti-inflammatory, anti-hyperglycemic, anti-hyperalgesic, and anti-allodynic actions" (35). Despite of those findings, development of PEMF therapy is slow due to the lack of scientifical evidence-based knowledge (36). Furthermore, the application parameters of PEMF were claimed to be "quite diverse, with no clear rationale for why particular parameters are chosen" (35).

Based on the above-mentioned knowledge and own clinical experience, we hypothesize (1) individualized PEMF in the sense of non-invasive neural therapy can be useful for treatment of dysautonomia in Long COVID; (2) the appropriate and helpful application parameters of PEMF can be tested by Adaptive Force (AF); (3) The AF can serve as biomarker (diagnostic/follow-up).

The AF characterizes the holding capacity of the neuromuscular system, which can be assessed, e.g., by a manual muscle test (MMT) objectified by a handheld device (42–44). During MMT, the tester applies a smoothly increasing force on the patient's limb in direction of muscle lengthening up to a considerably high force level. In case, the patient can adapt the muscle tension maintaining the isometric position during the entire force increase, the MMT is rated as "stable" and the maximal AF (AFmax) is reached under isometric conditions [AFmax = maximal isometric AF ($AFiso_{max}$)]. An "unstable" adaptation is characterized by yielding of the limb during force increase. The patient is not able to adapt adequately. $AFiso_{max}$ is considerably low and AFmax is reached during eccentric muscle action (43–45).

Healthy persons usually show stable adaptation ($\frac{AFiso_{max}}{AFmax} \geq$ 99%) (43–45). Based on own practical experience, patients with, e.g., post-infectious syndromes show unstable adaptation. Common measurements of maximal strength (e.g., hand grip force) usually do not show a significant difference between patients and controls (46, 47). Two studies revealed a significantly reduced force in ME/CFS (48, 49). However, one did not describe sex effects. Females were overrepresented in ME/CFS group (96 vs. 62% in controls) (49), which might explain the lower strength. The findings are inconclusive and highlight that common maximal strength assessments might not be appropriate to investigate motor function in post-infectious states. We hypothesize $AFiso_{max}$ might be a decisive motor function to investigate and uncover clear differences between patients and controls. Moreover, $AFiso_{max}$ can react immediately to positive and negative inputs (43–45). A proposed neurophysiological explanation was given previously (42–45). Hence, the AF might be a useful biomarker to investigate patients and to determine helpful treatments, such as the individual PEMF.

This case report presents the positive clinical outcome for one Long COVID patient after a single treatment with individualized PEMF using the AF as biomarker.

## 2. Patient information

A 24-year-old female (168 cm, 65 kg; student since 2016; student assistant since 2020) presented herself in our practice of integrative medicine in August 2021. She reported a non-critical course of COVID-19 infection in December 2020 which lasted 2–3 weeks with symptoms as fever, loss of smell/taste, muscle pain and headache.

Afterwards she felt quite good for ∼8 weeks. In March 2021 a state of Long COVID arose with severe symptoms as pronounced fatigue, fast exhaustion, post-exertional "crashs," weakness, concentration problems, loss of speaking abilities, headache, muscle pain/cramps, sensitivity to stimuli (light/noise) and loss of smell. Less pronounced were nausea, nerve tingling, visual disturbances, memory, and sleeping problems and heavy perspiration. She was not able to proceed her Bachelor thesis, work as assistant or participate in social life. She appeared to be emotionally strong with good family bonding, although she naturally perceived her condition as very burdensome, especially because of the prospect of the clinicians she had to be patient, wait and pace herself.

She had a borreliosis infection in 2016. No other pre-existing health issues were reported (infections/hormonal/digestive/psychological). She always was sportive but sometimes not able to climb stairs in the current condition.

She already received exercise and physiotherapy, reflective breathing massage, tried supplements/vitamins and melatonin pills for sleeping problems. None of them led to a considerable condition improvement. Pacing herself resulted in a state in which she partly could resume work/studies. However, as soon as she went beyond her (low) limits (physically/cognitive/emotionally), a crash resulted (recovery: few days).

## 3. Clinical findings

The intensity of common Long COVID symptoms was inquired on a numerical scale [0-no to 10-very strong; according to Liu and Duricka (4)] retrospectively for pre-COVID baseline, during Long COVID (post-COVID) as well as 1-day, 4-weeks, and ∼6-month post-treatment (Figure 1). Fatigue, memory/concentration issues, headache, muscle pain, loss of smell/taste, depression/anxiety, dizziness, and post-exertion malaise were rated by ≥ 9 post-COVID.

For physical examination, the AF of nine different muscles/muscle groups was assessed on both sides by the MMT [hip flexors/adductors/abductors/extensors, foot dorsiflexors, pectoralis major (sternal and clavicular part), deltoid, and elbow flexors]. For left elbow/hip flexors, the AF was objectified (see below, Figure 2). All tested muscles showed a clearly unstable behavior in MMTs pre-treatment.

## 4. Timeline

Figure 3.

## 5. Diagnostic assessment

Diagnostic challenges for Long COVID appear because diagnosis is currently based on exclusion (15, 50). The patient provided documentation of a received extensive diagnostic assessment from a medical clinic (diagnosis: Long COVID). All other possible causes were excluded therein.

Besides the symptom intensity at five timepoints (Figure 1), the AF of left elbow and hip flexors was objectified by a handheld device which records reaction force ($N$) between tester and patient as well as limb position [angular velocity (°/s)]. It consists of strain gauges (co. Sourcing map, model: a14071900ux0076, precision: 1.0 ± 0.1%, sensitivity: 0.3 mV/V) and kinematic sensor technology (Bosch BNO055, 9-axis absolute orientation sensor, sensitivity: ± 1%) (42–45). Data were AD converted, buffered (sampling rate: 180 Hz) and sent (Bluetooth 5.0) to a tablet with measuring software (sticky notes). Data processing and evaluation were performed according to Schaefer et al. (43–45) in NI DIAdem 20.0 (National Instruments, Austin, TX, USA). Signals were interpolated (1 kHz) and filtered (Butterworth, filter degree 5, cut-off frequency 20 Hz). For visualization (Figure 2) the angular velocity was additionally filtered (degree: 3, cut-off: 10 Hz) to smoothen the oscillations (note: this leads to slightly different results between visual inspection in Figure 2 and results given below).

The following parameters were extracted: (1) AFmax (N): peak value of the whole trial. This can be reached either during isometric or eccentric muscle action. (2) $AFiso_{max}$ (N): the maximal isometric AF refers to the highest force under isometric conditions. This was defined as the force at the moment in which the gyrometer signal increased above zero, indicating a yielding of the limb (breaking point). In case the gyrometer signal oscillated ∼0 during the entire trial, $AF_{max} = AFiso_{max}$. (3) Slope: the slope of force rise before $AFiso_{max}$ of all trials was calculated by the difference quotient to control the increase. Reference points (time, force) were 70% and 100% of averaged $AFiso_{max}$ of all as unstable assessed MMTs. The decadic logarithm was taken from values [lg($N$/s)] since force rise is exponential. Arithmetic means (M) and standard deviations (SD) of each parameter were calculated of the three trials for each muscle and timepoint (Table 1).

Figure 2 shows the signals of the three trials of left elbow/hip flexors at each timepoint (pre, post, and end), Table 1 shows the respective values. The entry MMTs were clearly unstable, indicated by low $AFiso_{max} \approx$ ∼71 N (elbow) and ∼62 N (hip). The muscle started to lengthen at ∼44 ± 25% of AFmax (elbow) and ∼28 ± 6% (hip). The slope was slightly smoother for pre

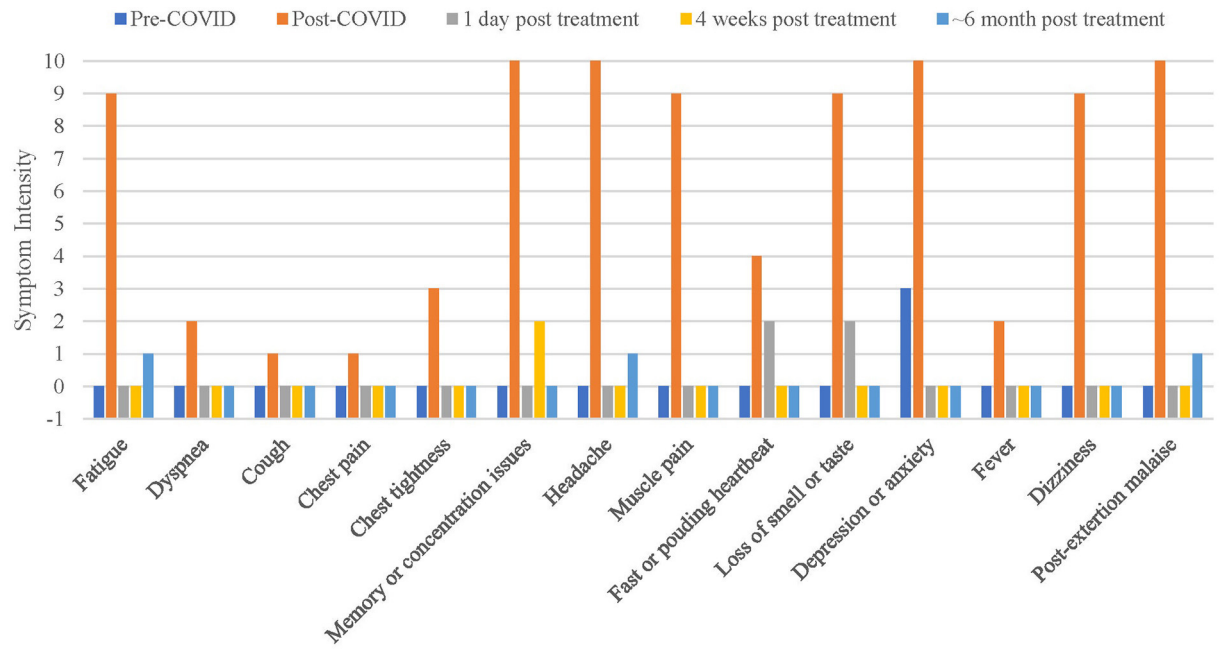


FIGURE 1
Intensity of Long COVID symptoms over time. Data was collected retrospectively for pre-COVID. Y-axis was set to −1 to visualize a score of zero [visualization was chosen following Liu and Duricka (4)].

vs. post vs. end (Table 1). Thus, the conditions for adaptation should have been even better in pre-tests.

After initial AF assessment, we tested the individual supportive PEMF frequency. For that, we placed the coil anteriorly centered to the area of stellate ganglion (C7/T1) and performed the MMT repeatedly whereby before each test we adjusted the frequency. As soon as the muscle showed stability, we used this frequency for treatment. The stabilized holding capacity indicates that exactly this configuration is supportive for the patient's system. Hence, the motor output leads us to the helpful PEMF frequency by instantaneously gaining stability. The PEMF has a reach of ∼20 cm and, therefore, it had no special lateral effect.

Immediately after PEMF application (see below), all muscles were clearly stable in MMT. Results of AF values are given (Figure 2C, Table 1). The first trial of elbow flexors was not fully stable, indicated by a deviation of gyrometer signal above zero. However, the breaking point ($AFiso_{max}$) was on a high force (174 N ≈ 99% of AFmax). All other trials post-treatment showed full stability with high AFmax reached during isometric conditions [M ± SD: $\frac{AFiso_{max}}{AFmax}$ = 99.6 ± 0.7% (elbow); 100 ± 0% (hip)]. The isometric holding capacity was immediately increased by 2.6 (elbow) and 3.4-fold (hip) force compared to pre-treatment. The patient was able to maintain the isometric position of muscles during the entire force increase in contrast to pre-state. Those results support the manually assessed motor function as immediate reaction to the individual PEMF therapy.

## 6. Therapeutic intervention

Individualized PEMF therapy using bioMATRIX driver (Roland Pechan GmbH & Co.KG; sinusoidal signal, 100–1,000 Hz, max. 3 mT) was applied *via* coil to the area of C7/T1 assuming that it affects the stellate ganglion in order to "reboot" the ANS in the sense of a non-invasive neural therapy. The individual PEMF frequency of 550 Hz (flux density 1 mT) was tested by the AF and was applied for ∼15 min. Established PEMF devices work with up to 10 mT (51). Only one treatment was performed since the condition improved immediately.

## 7. Follow-up and outcomes

The symptoms intensity improved immediately 1-day post-treatment and sustained until now (6-month post-treatment; Figure 1). The day after treatment she gave feedback (e-mail; translated): "I woke up this morning for the first time since months without a feeling of hangover. I don't have headache; my head feels broad and open (…). An incredible feeling. I don't have any nausea, I feel as 1,000 kg burden were removed from my body. I feel totally easy and energetic. I had no problems to fall asleep yesterday and slept through without melatonin pills. This morning I got out of bed without any difficulties, directly felt like doing Yoga and went for a bicycle trip." She also felt like having "drunk 10 cups

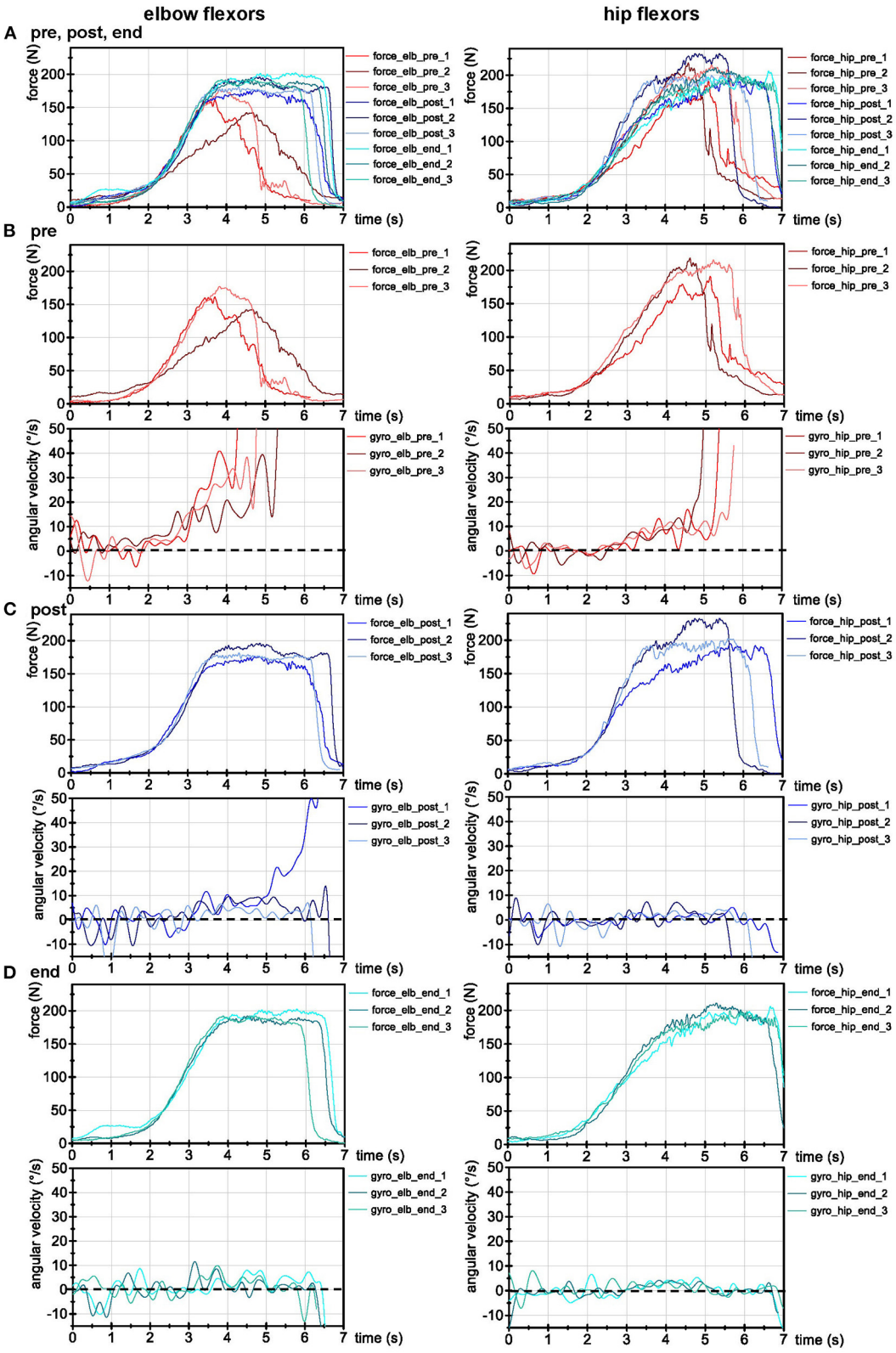


FIGURE 2
AF recordings of left elbow and hip flexors. **(A)** Force (N) of all trials before (pre), directly after (post) and 4 weeks after treatment (end). **(B)** Force (N) and angular velocity (°/s) of AF recordings pre-treatment, **(C)** directly post-treatment, and **(D)** 4-weeks post-treatment (end). All signals were filtered (butterworth; force: filter degree 5, cut-off frequency: 20 Hz; angular velocity: filter degree: 10, cut-off: 3 Hz). Dotted lines indicate zero for angular velocity.

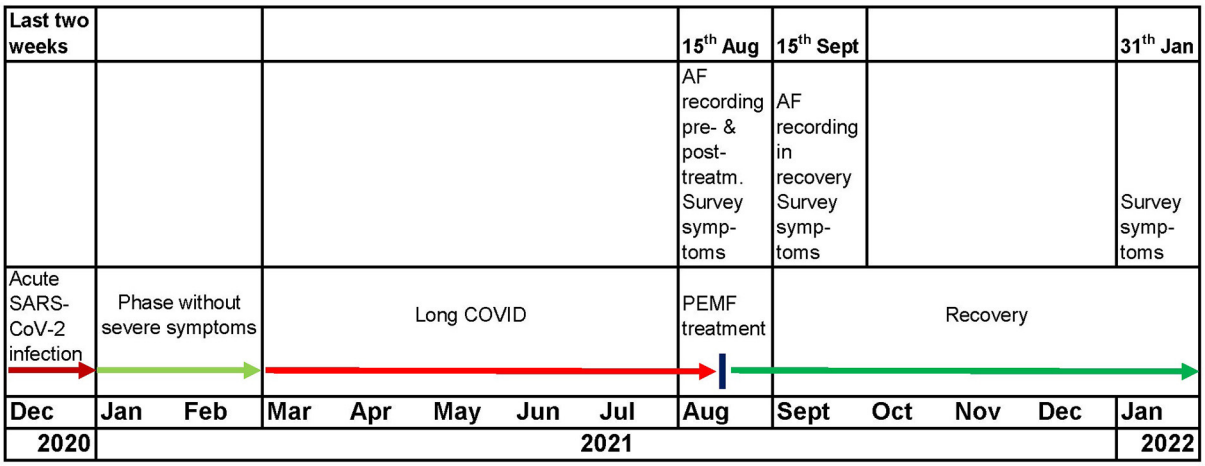


FIGURE 3
Timeline from acute SARS-CoV-infection over the ~6-month Long COVID period until the individualized PEMF treatment resulting into sustained recovery (~6-month post-treatment).

**TABLE 1** Results of Adaptive Force (AF) of left elbow and hip flexors.

| | $AFiso_{max}$ (*N*) | | | AFmax (*N*) | | | $\frac{AFiso_{max}}{AFmax}$ (%) | | | Slope [lg(*N*/s)] | | |
|---|---|---|---|---|---|---|---|---|---|---|---|---|
| | Pre | Post | End | Pre | Post | End | Pre | Post | End | Pre | Post | End |
| | Elbow flexors | | | | | | | | | | | |
| 1 | 111.45 | 174.24 | 202.34 | 161.45 | 176.29 | 202.34 | 0.69 | 0.99 | 1.00 | 1.89 | 1.96 | 1.90 |
| 2 | 28.50 | 196.23 | 192.39 | 142.64 | 196.23 | 192.39 | 0.20 | 1.00 | 1.00 | 1.68 | 1.85 | 1.94 |
| 3 | 73.50 | 181.62 | 192.43 | 177.16 | 181.62 | 192.43 | 0.41 | 1.00 | 1.00 | 2.01 | 1.95 | 1.99 |
| M | 71.15 | 184.03 | 195.72 | 160.42 | 184.71 | 195.72 | 0.44 | 1.00 | 1.00 | 1.86 | 1.92 | 1.95 |
| SD | 41.52 | 11.19 | 5.73 | 17.28 | 10.33 | 5.73 | 0.25 | 0.01 | 0.00 | 0.17 | 0.06 | 0.05 |
| CV | 0.58 | 0.06 | 0.03 | 0.11 | 0.06 | 0.03 | 0.57 | 0.01 | 0.00 | 0.09 | 0.03 | 0.02 |
| | Hip flexors | | | | | | | | | | | |
| 1 | - | 194.70 | 206.05 | 190.83 | 194.70 | 206.05 | - | 1.00 | 1.00 | 1.59 | 1.98 | 1.91 |
| 2 | 71.33 | 232.72 | 211.09 | 218.49 | 232.72 | 211.09 | 0.33 | 1.00 | 1.00 | 1.66 | 1.87 | 1.86 |
| 3 | 51.76 | 202.60 | 199.68 | 215.53 | 202.60 | 199.68 | 0.24 | 1.00 | 1.00 | 1.81 | 2.08 | 1.69 |
| M | 61.54 | 210.01 | 205.61 | 208.28 | 210.01 | 205.61 | 0.28 | 1.00 | 1.00 | 1.69 | 1.98 | 1.82 |
| SD | 13.84 | 20.06 | 5.72 | 15.19 | 20.06 | 5.72 | 0.06 | 0.00 | 0.00 | 0.11 | 0.11 | 0.12 |
| CV | 0.22 | 0.10 | 0.03 | 0.07 | 0.10 | 0.03 | 0.22 | 0.00 | 0.00 | 0.07 | 0.06 | 0.06 |

Single values of each trial, the arithmetic means (M), standard deviations (SD), and coefficients of variation (CV) of the maximal isometric AF ($AFiso_{max}$), the maximal AF (AFmax), their ratio (%), and of the slope of force rise [lg(N/s)] are given for each timepoint (pre: before treatment, post: directly after treatment, end: 4-weeks after treatment).

of coffee. I don't know where to go with my energy. It almost feels uncomfortable since my body is so twitchy." It appears that the treatment led to sympathetic hyper activation. However, this adverse unanticipated reaction dissolved the next day.

Two weeks post-treatment she reported she still feels physically and mentally healthy. She was able to exercise as intensive as before COVID-infection (85 km bicycle trip without problems), she had no concentration issues and meetings with several persons were no problem anymore. "I am grateful and happy to have my life back."

At follow-up appointment 4-weeks post-treatment, she felt well and healthy (Figure 1). All above-mentioned muscles showed stability in MMT, supported by AF recordings (Figure 2D, Table 1). The patient was able to stabilize the muscles in isometric holding conditions despite of the external increase

until a considerably high $AFiso_{max}$ = AFmax = 195.7 ± 5.7 N (elbow) and 205.6 ± 5.7 N (hip).

Approximately 6-weeks post-treatment she received a lymph drainage (head and shoulder girdle) independent of our intervention and reported of headache, fatigue, concentration problems and sensitivity to stimuli afterwards for 3 days. She had another appointment in our practice ∼1 week later. The muscles were still stable in entry MMTs. They became unstable after lymph drainage performed in our practice indicating that it irritated her system. By applying an individually newly tested PEMF frequency (590 Hz) the muscles were stabilized again. After the next lymph drainage independent of our intervention, she perceived headache for 1 hour but felt well afterwards. Approximately 10-weeks post-treatment she reported "I feel currently wonderful". The sustainability was underpinned by the last assessment (January 2022; Figure 1). She reported, she is physically completely on the level before COVID, "if not better." However, after emotional stress fatigue sometimes returns, but not in the previous extent.

## 8. Discussion

This case report suggests that low-frequency PEMF to the area of stellate ganglion with individually tested frequency using the AF might be an effective therapy in Long COVID patients. Since Liu and Duricka found a similar outcome after SGB (4), we assume that PEMF to the area C7/T1 affect the stellate ganglion. Based on our case and their suggestion that "cervical sympathetic chain activity can be blocked with local anesthetic, allowing the regional autonomic nervous system to 'reboot"' (4), we propose the same effect might be gained by individualized PEMF therapy. A rationale for the mechanisms behind the hypothesis rebooting the ANS was given by Liu and Duricka (4).

The benefit of PEMF is that it is non-invasive, the patient does not feel anything of the intervention (see below) and no side effects are known (36, 39, 52). However, a successful treatment will not be that easy in every Long COVID patient. Some will have more severe pre-existing health issues which might hinder the positive outcome of a single treatment. From our current experience, three main factors in Long COVID occur: dysautonomia, pre-existing, and/or current mental stress and previous infections affecting the lymphatic system, which might lead to lymphatic entrapments post-COVID. Based on psychoneuroimmunology it is known that those factors interact (53). This is underpinned by the present case, since the patient relapsed after lymph drainage but could be switched back by one re-treatment. The switching between both states as immediate responses to disturbing or helping interventions speaks for a regulative character of Long COVID condition, at least in part. This would explain the instant reversibility observed in some cases. It is suggested that the complex psychoneuroimmunological network might still be vulnerable after "rebooting" the ANS. Lymphatic and mental stress might impede an immediate positive outcome or lead to a relapse. Consequently, such conditions must be treated, too. However, the ANS dysfunction—presumably triggered by SARS-CoV-2 infection—could benefit from individualized PEMF therapy determined by the holding capacity ($AFiso_{max}$) of the neuromuscular system.

$AFiso_{max}$ was suggested to be especially sensitive regarding interfering inputs entering the complex motor control processes. At least the thalamus, cerebellum, inferior olivary nucleus, red nucleus, basal ganglia, cingulate cortex, and the sensorimotor cortex are involved in processing adaptive motor control (54–95). Due to the strong interconnections between those areas (73, 84) and since they also process other inputs (e.g., emotions/nociception) (63, 65, 68, 69, 73, 96–99), it was proposed that the motor output in the sense of $AFiso_{max}$ can be modified by different stimuli—positive and negative ones. The pro-inflammatory cytokine/chemokine profile (100), organ damage, lymphatic stress and/or the dysautonomia in Long COVID might impair that motor function. In case this is based on malfunction, it can be resolved immediately by applying the helpful therapy, e.g., individualized PEMF. The instantaneous improvement of $AFiso_{max}$ by 2.6 and 3.4-fold by applying the individualized PEMF frequency clearly demonstrated this. This effect cannot be reached by training. It must be the result of a functional readjustment of the patient's system. In contrast to maximal forces (as AFmax or MVIC), which can be reached also in dysfunctional state [as found here or in other studies (46, 47)], the holding capacity might uncover the dysfunction. In case the patient must adapt in an isometric holding manner to an increasing external force, the maximal force cannot be demanded under isometric conditions anymore. The adjustment of tension under stable muscle length fails and the limb gives way on significantly low forces. The $AFiso_{max}$ improved though immediately by applying the helpful PEMF. As was postulated by Mert (35), there is no rationale which PEMF parameters should be applied. So, why not "ask" the patient's system? The holding capacity seems to lead the way to the individual helpful parameters. Applying any frequency would not have this positive effect. Therefore, it is necessary to test the PEMF frequency individually by adequate biomarkers, as the neuromuscular holding capacity.

## 9. Conclusion

In conclusion, we suggest (1) to include pre-existing health issues of Long COVID individuals, especially concerning mental stress and previous infections and to examine the lymphatic system regarding flow restrictions. (2) The AF provides a valuable biomarker which can be used as functional diagnostic parameter for patients in post-infectious states, to determine the individual appropriate cause-related therapy and to monitor follow-up, since it seems to correlate with the patient's condition. (3) Soft, low-frequency PEMF with an individually tested

frequency for each patient at the actual timepoint seems to be useful to "reboot" the dysfunctional ANS and might be an alternative non-invasive neural therapy. Further research is needed to verify and pursue this approach.

## Data availability statement

The original contributions presented in the study are included in the article/supplementary material, further inquiries can be directed to the corresponding author.

## Ethics statement

Ethical review and approval was not required for the study on human participants in accordance with the local legislation and institutional requirements. The patients/participants provided their written informed consent to participate in this study. The patient gave written informed consent to publish her case.

## Author contributions

FB performed the measurements. LS analyzed the data and wrote the manuscript. All authors planned and designed the treatment process and measurements of the patient. All authors critically revised the manuscript and approved it for publication.

## Funding

The publication of this article was funded by the Deutsche Forschungsgemeinschaft (DFG, German Research Foundation) - Project number 491466077.

## Conflict of interest

The authors declare that the research was conducted in the absence of any commercial or financial relationships that could be construed as a potential conflict of interest.

## Publisher's note



## References

1. Taquet M, Dercon Q, Luciano S, Geddes JR, Husain M, Harrison PJ. Incidence, co-occurrence, and evolution of long-COVID features: A 6-month retrospective cohort study of 273,618 survivors of COVID-19. *PLoS Med.* (2021) 18:e1003773. doi: 10.1371/journal.pmed.1003773

2. Huang L, Yao Q, Gu X, Wang Q, Ren L, Wang Y, et al. 1-year outcomes in hospital survivors with COVID-19: A longitudinal cohort study. *Lancet.* (2021) 398:747–58. doi: 10.1016/S0140-6736(21)01755-4

3. Solve ME/CFS Initiative. *Long Covid Alliance (LCA)*. (2021). Available online at: https://solvecfs.org/long-covid-alliance/

4. Liu LD, Duricka DL. Stellate ganglion block reduces symptoms of Long COVID: A case series. *J Neuroimmunol.* (2022) 362:577784. doi: 10.1016/j.jneuroim.2021.577784

5. Jason LA, Islam M, Conroy K, Cotler J, Torres C, Johnson M, et al. COVID-19 symptoms over time: comparing long-haulers to ME/CFS. *Fatigue Biomed Health Behav.* (2021) 9:59–68. doi: 10.1080/21641846.2021.1922140

6. Mantovani E, Mariotto S, Gabbiani D, Dorelli G, Bozzetti S, Federico A, et al. Chronic fatigue syndrome: An emerging sequela in COVID-19 survivors? *J Neurovirol.* (2021) 27:631–7. doi: 10.1007/s13365-021-01002-x

7. Wirth KJ, Scheibenbogen C, Paul F. An attempt to explain the neurological symptoms of Myalgic Encephalomyelitis/Chronic Fatigue Syndrome. *J Transl Med.* (2021) 19:471. doi: 10.1186/s12967-021-03143-3

8. Petracek LS, Suskauer SJ, Vickers RF, Patel NR, Violand RL, Swope RL, et al. Adolescent and young adult ME/CFS after confirmed or probable COVID-19. *Front Med.* (2021) 8:668944. doi: 10.3389/fmed.2021.668944

9. Wirth KJ, Scheibenbogen C. Pathophysiology of skeletal muscle disturbances in myalgic encephalomyelitis/chronic fatigue syndrome (ME/CFS). *J Transl Med.* (2021) 19:162. doi: 10.1186/s12967-021-02833-2

10. Hickie I, Davenport T, Wakefield D, Vollmer-Conna U, Cameron R, Vernon SD, et al. Post-infective and chronic fatigue syndromes precipitated by viral and non-viral pathogens: Prospective cohort study. *Br Med J.* (2006) 333:575. doi: 10.1136/bmj.38933.585764.AE

11. Shikova E, Reshkova V, Kumanova A, Raleva S, Alexandrova D, Capo N, et al. Cytomegalovirus, Epstein-Barr virus, and human herpesvirus-6 infections in patients with myalgic encephalomyelitis/chronic fatigue syndrome. *J Med Virol.* (2020) 92:3682–8. doi: 10.1002/jmv.25744

12. Estévez-López F, Mudie K, Wang-Steverding X, Bakken IJ, Ivanovs A, Castro-Marrero J, et al. Systematic review of the epidemiological burden of myalgic encephalomyelitis/chronic fatigue syndrome across Europe: Current evidence and EUROMENE research recommendations for epidemiology. *J Clin Med.* (2020) 9:1557. doi: 10.3390/jcm9051557

13. Morris G, Maes M, Berk M, Puri BK. Myalgic encephalomyelitis or chronic fatigue syndrome: how could the illness develop? *Metab Brain Dis.* (2019) 34:385–415. doi: 10.1007/s11011-019-0388-6

14. Augustin M, Schommers P, Stecher M, Dewald F, Gieselmann L, Gruell H, et al. Post-COVID syndrome in non-hospitalised patients with COVID-19: a longitudinal prospective cohort study. *Lancet Reg Health Eur.* (2021) 6:100122. doi: 10.1016/j.lanepe.2021.100122

15. Sisó-Almirall A, Brito-Zerón P, Ferrín LC, Kostov B, Moreno AM, Mestres J, et al. Long COVID-19: Proposed primary care clinical guidelines for diagnosis and disease management. *Int J Environ Res Public Health.* (2021) 18:4350. doi: 10.3390/ijerph18084350

16. Weinschenk S. Neural therapy—A review of the therapeutic use of local anesthetics. *Acupunct Relat Ther.* (2012) 1:5–9. doi: 10.1016/j.arthe.2012.12.004

17. Mak AKY, Hu Z, Zhang JX, Xiao Z, Lee TMC. Neural correlates of regulation of positive and negative emotions: An fMRI study. *Neurosci Lett.* (2009) 457:101–6. doi: 10.1016/j.neulet.2009.03.094

18. Pfister M, Fischer L. Die Behandlung des komplexen regionalen Schmerzsyndroms der oberen Extremität mit wiederholter Lokalanästhesie des Ganglion stellatum. *Praxis.* (2009) 98:247–57. doi: 10.1024/1661-8157.98.5.247

19. van Eijs F, Stanton-Hicks M, Van Zundert J, Faber CG, Lubenow TR, Mekhail N, et al. 16. Complex Regional Pain Syndrome: 16 CRPS. *Pain Pract.* (2011) 11:70–87. doi: 10.1111/j.1533-2500.2010.00388.x

20. Hey M, Wilson I, Johnson MI. Stellate ganglion blockade (SGB) for refractory index finger pain – A case report. *Ann Phys Rehabil Med.* (2011) 54:181–8. doi: 10.1016/j.rehab.2011.03.001

21. Narouze S. Ultrasound-guided stellate ganglion block: Safety and efficacy. *Curr Pain Headache Rep.* (2014) 18:424. doi: 10.1007/s11916-014-0424-5

22. Lipov E, Navaie M, Stedje-Larsen ET, Burkhardt K, Smith JC, Sharghi LH, et al. A novel application of stellate ganglion block: Preliminary observations for the treatment of post-traumatic stress disorder. *Mil Med.* (2012) 177:125–7. doi: 10.7205/MILMED-D-11-00328

23. Mulvaney SW, Lynch JH, Hickey MJ, Rahman-Rawlins T, Schroeder M, Kane S, et al. Stellate ganglion block used to treat symptoms associated with combat-related post-traumatic stress disorder: A case series of 166 patients. *Mil Med.* (2014) 179:1133–40. doi: 10.7205/MILMED-D-14-00151

24. Yokoyama M, Nakatsuka H, Itano Y, Hirakawa M. Stellate ganglion block modifies the distribution of lymphocyte subsets and natural-killer cell activity. *Anesthesiology.* (2000) 92:109–109. doi: 10.1097/00000542-200001000-00021

25. Tian Y, Wittwer ED, Kapa S, McLeod CJ, Xiao P, Noseworthy PA, et al. Effective use of percutaneous stellate ganglion blockade in patients with electrical storm. *Circ Arrhythm Electrophysiol.* (2019) 12:7118. doi: 10.1161/CIRCEP.118.007118

26. Brobyn TL. Neural therapy: An overlooked game changer for patients suffering chronic pain? *J Pain Relief.* (2015) 4:184. doi: 10.4172/2167-0846.1000184

27. Wang S, Zhou X, Huang B, Wang Z, Zhou L, Wang M, et al. Noninvasive low-frequency electromagnetic stimulation of the left stellate ganglion reduces myocardial infarction-induced ventricular arrhythmia. *Sci Rep.* (2016) 6:30783. doi: 10.1038/srep30783

28. Krayukhina K, Yu A, Lobkaeva EP, Devyatkova NS. Effect of low-frequency pulsatile AC magnetic field on the state of the autonomic nervous system in rats. *Biophysics.* (2010) 55:637–41. doi: 10.1134/S0006350910040226

29. Kholodov K, Yu A. *The Effect of Electromagnetic and Magnetic Fields on the Central Nervous System. NASA Technical Translation, TTF-465*. Washington, DC: National Aeronautics and Space Administration (1967).

30. Scherlag BJ, Yamanashi WS, Hou Y, Jacobson JI, Jackman WM, Lazzara R. Magnetism and cardiac arrhythmias. *Cardiol Rev.* (2004) 12:85–96. doi: 10.1097/01.crd.0000094029.10223.2f

31. Yu L, Dyer JW, Scherlag BJ, Stavrakis S, Sha Y, Sheng X, et al. The use of low-level electromagnetic fields to suppress atrial fibrillation. *Heart Rhythm.* (2015) 12:809–17. doi: 10.1016/j.hrthm.2014.12.022

32. Bolotova NV, Raigorodsky YM, Dronova EG, Posokhova NV. The use of magnetic sympathocor-rection for the treatment of vegetative disorders in the children with obesity. *Russ J Physiother Balneology Rehabil.* (2013) 12:30–4. Available online at: https://rjpbr.com/1681-3456/article/view/41416

33. Yermishev OV. The levels of functional-vegetative homeostasis as criteria for magnetotherapy efficacy. *Int J Med Med Res.* (2018) 2018:8902. doi: 10.11603/ijmmr.2413-6077.2018.1.8902

34. Shupak NM, Prato FS, Thomas AW. Therapeutic uses of pulsed magnetic-field exposure: A review. *URSI Radio Sci Bull.* (2003) 307:9–32. doi: 10.23919/URSIRSB.2003.7909506

35. Mert T. Pulsed magnetic field treatment as antineuropathic pain therapy. *Rev Neurosci.* (2017) 28:751–8. doi: 10.1515/revneuro-2017-0003

36. Strauch B, Herman C, Dabb R, Ignarro LJ, Pilla AA. Evidence-based use of pulsed electromagnetic field therapy in clinical plastic surgery. *Aesthet Surg J.* (2009) 29:135–43. doi: 10.1016/j.asj.2009.02.001

37. Nelson FR, Zvirbulis R, Pilla AA. Non-invasive electromagnetic field therapy produces rapid and substantial pain reduction in early knee osteoarthritis: A randomized double-blind pilot study. *Rheumatol Int.* (2013) 33:2169–73. doi: 10.1007/s00296-012-2366-8

38. Lee JW, Kim JY, Hyun JH, Lee YH. Analysis of HRV and body temperature variation for manual acupuncture and PEMF (Pulsed Electro-Magnetic Field) acupuncture stimulation. *Acupunct Electrother Res.* (2021) 47:91–9. doi: 10.3727/036012921X16287835103390

39. Vadalà M, Morales-Medina JC, Vallelunga A, Palmieri B, Laurino C, Iannitti T. Mechanisms and therapeutic effectiveness of pulsed electromagnetic field therapy in oncology. *Cancer Med.* (2016) 5:3128–39. doi: 10.1002/cam4.861

40. Yamaguchi S, Ogiue-Ikeda M, Sekino M, Ueno S. Effects of pulsed magnetic stimulation on tumor development and immune functions in mice. *Bioelectromagnetics.* (2006) 27:64–72. doi: 10.1002/bem.20177

41. Barbault A, Costa FP, Bottger B, Munden RF, Bomholt F, Kuster N, et al. Amplitude-modulated electromagnetic fields for the treatment of cancer: Discovery of tumor-specific frequencies and assessment of a novel therapeutic approach. *J Exp Clin Cancer Res.* (2009) 28:51. doi: 10.1186/1756-9966-28-51

42. Bittmann FN, Dech S, Aehle M, Schaefer LV. Manual muscle testing—Force profiles and their reproducibility. *Diagnostics.* (2020) 10:996. doi: 10.3390/diagnostics10120996

43. Schaefer LV, Dech S, Bittmann FN. Adaptive Force and emotionally related imaginations – preliminary results suggest a reduction of the maximal holding capacity as reaction to disgusting food imagination. *Heliyon.* (2021) 7:e07827. doi: 10.1016/j.heliyon.2021.e07827

44. Schaefer LV, Dech S, Aehle M, Bittmann FN. Disgusting odours affect the characteristics of the Adaptive Force in contrast to neutral and pleasant odours. *Sci Rep.* (2021) 11:16410. doi: 10.1038/s41598-021-95759-0

45. Schaefer LV, Dech S, Wolff LL, Bittmann FN. Emotional imagery influences the adaptive force in young women: Unpleasant imagery reduces instantaneously the muscular holding capacity. *Brain Sci.* (2022) 12:1318. doi: 10.3390/brainsci12101318

46. Lloyd AR, Hales JP, Gandevia SC. Muscle strength, endurance and recovery in the post-infection fatigue syndrome. *J Neurol Neurosurg Psychiatry.* (1988) 51:1316–22. doi: 10.1136/jnnp.51.10.1316

47. Rutherford OM, White PD. Human quadriceps strength and fatiguability in patients with post viral fatigue. *J Neurol Neurosurg Psychiatry.* (1991) 54:961–4. doi: 10.1136/jnnp.54.11.961

48. Jäkel B, Kedor C, Grabowski P, Wittke K, Thiel S, Scherbakov N, et al. Hand grip strength and fatigability: Correlation with clinical parameters and diagnostic suitability in ME/CFS. *J Transl Med.* (2021) 19:159. doi: 10.1186/s12967-021-02774-w

49. Meeus M, Ickmans K, Struyf F, Kos D, Lambrecht L, Willekens B, et al. What is in a name? Comparing diagnostic criteria for chronic fatigue syndrome with or without fibromyalgia. *Clin Rheumatol.* (2016) 35:191–203. doi: 10.1007/s10067-014-2793-x

50. NICE. *COVID-19 Rapid Guideline: Managing the Long-Term Effects of COVID-19*. (2022). p. 106. Available online at: https://www.nice.org.uk/guidance/ng188/resources/covid19-rapid-guideline-managing-the-longterm-effects-of-covid19-pdf-51035515742.

51. Quittan M. Magnetfeldtherapie—klinische Wirksamkeiten. *Trauma Berufskrankh.* (2004) 6:4. doi: 10.1007/s10039-003-0758-4

52. Hedén P, Pilla AA. Effects of pulsed electromagnetic fields on postoperative pain: A double-blind randomized pilot study in breast augmentation patients. *Aesthetic Plast Surg.* (2008) 32:660–6. doi: 10.1007/s00266-008-9169-z

53. Wright AGC, Aslinger EN, Bellamy B, Edershile EA, Woods WC. Psychoneuroimmunology of stress and mental health. In: KL Harkness, EP Hayden, editors, *The Oxford Handbook of Stress and Mental Health*. Oxford: Oxford University Press (2020). p. 26–44. doi: 10.1093/oxfordhb/9780190681777.013.2

54. Pflüger HJ, Sillar K. Motor control. In: *Neurosciences - From Molecule to Behavior: A University Textbook*. Berlin/?Heidelberg?: Springer. (2013). p. 479–524. doi: 10.1007/978-3-642-10769-6_23

55. Huggenberger S, Moser N, Schröder H, Cozzi B, Granato A, Merighi A. *Neuroanatomie des Menschen: mit 202 größtenteils farbigen Abbildungen*. Berlin/?Heidelberg?: Springer (2019). doi: 10.1007/978-3-662-56461-5

56. Albus JS. A theory of cerebellar function. *Math Biosci.* (1971) 10:25–61. doi: 10.1016/0025-5564(71)90051-4

57. Ashe J, Bushara K. The olivo-cerebellar system as a neural clock. In: H Merchant, V de Lafuente, editors, *Neurobiology of Interval Timing*. vol. 829. New York, NY: Springer. (2014). p. 155–65. doi: 10.1007/978-1-4939-1782-2_9

58. Lawrenson C, Bares M, Kamondi A, Kovács A, Lumb B, Apps R, et al. The mystery of the cerebellum: Clues from experimental and clinical observations. *Cerebellum Ataxias.* (2018) 5:8. doi: 10.1186/s40673-018-0087-9

59. Shadmehr R, Smith MA, Krakauer JW. Error correction, sensory prediction, and adaptation in motor control. *Annu Rev Neurosci.* (2010) 33:89–108. doi: 10.1146/annurev-neuro-060909-153135

60. Ivry RB. Exploring the role of the cerebellum in sensory anticipation and timing: Commentary on Tesche and Karhu. *Hum Brain Mapp*. (2000) 9:115–8. doi: 10.1002/(SICI)1097-0193(200003)9:3<115::AID-HBM1>3.0.CO;2-5

61. Bengtsson F, Ekerot CF, Jörntell H. *In vivo* analysis of inhibitory synaptic inputs and rebounds in deep cerebellar nuclear neurons. *PLoS ONE*. (2011) 6:e18822. doi: 10.1371/journal.pone.0018822

62. Lang EJ, Apps R, Bengtsson F, Cerminara NL, De Zeeuw CI, Ebner TJ, et al. The roles of the olivocerebellar pathway in motor learning and motor control. A consensus paper. *Cerebellum*. (2017) 16:230–52. doi: 10.1007/s12311-016-0787-8

63. Groenewegen HJ. The basal ganglia and motor control. *Neural Plast*. (2003) 10:107–20. doi: 10.1155/NP.2003.107

64. Jörntell H. Cerebellar physiology: Links between microcircuitry properties and sensorimotor functions: Cerebellar physiology. *J Physiol*. (2017) 595:11–27. doi: 10.1113/JP272769

65. Vogt BA, Finch DM, Olson CR. Functional heterogeneity in cingulate cortex: The anterior executive and posterior evaluative regions. *Cereb Cortex*. (1992) 2:435–43. doi: 10.1093/cercor/2.6.435-a

66. Rosenbaum DA. *Human Motor Control*. Amsterdam: Elsevier (2010).

67. Galizia CG. *Neurosciences—From Molecule to Behavior: A University Textbook*. Berlin Heidelberg: Springer (2013).

68. Rothwell JC. *Control of Human Voluntary Movement*. Gaithersburg, MD: Aspen Publishers (1987). doi: 10.1007/978-1-4684-7688-0

69. Doya K. Complementary roles of basal ganglia and cerebellum in learning and motor control. *Curr Opin Neurobiol*. (2000) 10:732–9. doi: 10.1016/S0959-4388(00)00153-7

70. Wu T, Hallett M. The cerebellum in Parkinson's disease. *Brain*. (2013) 136:696–709. doi: 10.1093/brain/aws360

71. Caligiore D, Pezzulo G, Baldassarre G, Bostan AC, Strick PL, Doya K, et al. Consensus paper: Towards a systems-level view of cerebellar function: The interplay between cerebellum, basal ganglia, and cortex. *Cerebellum*. (2017) 16:203–29. doi: 10.1007/s12311-016-0763-3

72. Pelzer EA, Hintzen A, Goldau M, von Cramon DY, Timmermann L, Tittgemeyer M. Cerebellar networks with basal ganglia: Feasibility for tracking cerebello-pallidal and subthalamo-cerebellar projections in the human brain. *Eur J Neurosci*. (2013) 38:3106–14. doi: 10.1111/ejn.12314

73. Morecraft RJ, Tanjii J. Cingulofrontal interactions and the cingulate motor areas. In: Vogt BA, editor, *Cingulate Neurobiology and Disease*. Oxford; New York, NY: Oxford University Press (2009) pp. 113–144.

74. Gerfen CR, Wilson CJ. The basal ganglia. In: Swanson LW, Bjorklund A, Hokfelt T, editors. *Handbook of Chemical Neuroanatomy*, Vol. 12. Amsterdam: Elsevier (1996). p. 371–468. doi: 10.1016/S0924-8196(96)80004-2

75. Wise SP, Murray EA, Gerfen CR. The frontal cortex-basal ganglia system in primates. *Crit Rev Neurobiol*. (1996) 10:317–56. doi: 10.1615/CritRevNeurobiol.v10.i3-4.30

76. O'Halloran CJ, Kinsella GJ, Storey E. The cerebellum and neuropsychological functioning: A critical review. *J Clin Exp Neuropsychol*. (2012) 34:35–56. doi: 10.1080/13803395.2011.614599

77. Schlerf JE, Galea JM, Bastian AJ, Celnik PA. Dynamic modulation of cerebellar excitability for abrupt, but not gradual, visuomotor adaptation. *J Neurosci*. (2012) 32:11610–7. doi: 10.1523/JNEUROSCI.1609-12.2012

78. Jueptner M, Ottinger S, Fellows SJ, Adamschewski J, Flerich L, Müller SP, et al. The relevance of sensory input for the cerebellar control of movements. *Neuroimage*. (1997) 5:41–8. doi: 10.1006/nimg.1996.0249

79. Welsh JP, Lang EJ, Suglhara I, Llinás R. Dynamic organization of motor control within the olivocerebellar system. *Nature*. (1995) 374:453–7. doi: 10.1038/374453a0

80. Vitek JL, Ashe J, DeLong MR, Alexander GE. Physiologic properties and somatotopic organization of the primate motor thalamus. *J Neurophysiol*. (1994) 71:1498–513. doi: 10.1152/jn.1994.71.4.1498

81. Sherman S. Thalamus. *Scholarpedia*. (2006) 1:1583. doi: 10.4249/scholarpedia.1583

82. Haber SN, Calzavara R. The cortico-basal ganglia integrative network: The role of the thalamus. *Brain Res Bull*. (2009) 78:69–74. doi: 10.1016/j.brainresbull.2008.09.013

83. Sommer MA. The role of the thalamus in motor control. *Curr Opin Neurobiol*. (2003) 13:663–70. doi: 10.1016/j.conb.2003.10.014

84. Vogt BA, Nimchinsky EA, Vogt LJ, Hof PR. Human cingulate cortex: Surface features, flat maps, and cytoarchitecture. *J Comp Neurol*. (1995) 359:490–506. doi: 10.1002/cne.903590310

85. Pruszynski JA, Scott SH. Optimal feedback control and the long-latency stretch response. *Exp Brain Res*. (2012) 218:341–59. doi: 10.1007/s00221-012-3041-8

86. Dickenson AH. Editorial I. *Br J Anaesth*. (2002) 88:755–7. doi: 10.1093/bja/88.6.755

87. Bueti D, Walsh V, Frith C, Rees G. Different brain circuits underlie motor and perceptual representations of temporal intervals. *J Cogn Neurosci*. (2008) 20:204–14. doi: 10.1162/jocn.2008.20017

88. D'Angelo E. Physiology of the cerebellum. In: Manto M, Huisman TAGM, editors. *Handbook of Clinical Neurology*, Vol. 154. Amsterdam: Elsevier (2018). p. 85–108. doi: 10.1016/B978-0-444-63956-1.00006-0

89. Rao SM, Harrington DL, Haaland KY, Bobholz JA, Cox RW, Binder JR. Distributed neural systems underlying the timing of movements. *J Neurosci*. (1997) 17:5528–35. doi: 10.1523/JNEUROSCI.17-14-05528.1997

90. Lang EJ, Sugihara I, Welsh JP, Llinás R. Patterns of spontaneous purkinje cell complex spike activity in the awake rat. *J Neurosci*. (1999) 19:2728–39. doi: 10.1523/JNEUROSCI.19-07-02728.1999

91. Manning CD, Tolhurst SA, Bawa P. Proprioceptive reaction times and long-latency reflexes in humans. *Exp Brain Res*. (2012) 221:155–66. doi: 10.1007/s00221-012-3157-x

92. Gross J, Timmermann L, Kujala J, Dirks M, Schmitz F, Salmelin R, et al. The neural basis of intermittent motor control in humans. *Proc Natl Acad Sci USA*. (2002) 99:2299–302. doi: 10.1073/pnas.032682099

93. Bays PM, Wolpert DM. Computational principles of sensorimotor control that minimize uncertainty and variability: Computational principles of sensorimotor control. *J Physiol*. (2007) 578:387–96. doi: 10.1113/jphysiol.2006.120121

94. Johansson RS. How is grasping modified by somatosensory input? In: Humphrey DR, Freund HJ, editors. *Motor Control: Concepts and Issues*. New York, NY: John Wiley (1991). p. 331–55.

95. Todorov E. Optimality principles in sensorimotor control. *Nat Neurosci*. (2004) 7:907–15. doi: 10.1038/nn1309

96. Gire DH, Restrepo D, Sejnowski TJ, Greer C, De Carlos JA, Lopez-Mascaraque L. Temporal processing in the olfactory system: Can we see a smell? *Neuron*. (2013) 78:416–32. doi: 10.1016/j.neuron.2013.04.033

97. Shepherd GM. *The Synaptic Organization of the Brain*. Oxford: Oxford University Press (2004).

98. Kugelberg E, Eklund K, Grimby L. An electromyographic study of the nociceptive reflexes of the lower limb. Mechanism of the plantar responses. *Brain*. (1960) 83:394–410. doi: 10.1093/brain/83.3.394

99. Nijs J, Daenen L, Cras P, Struyf F, Roussel N, Oostendorp RAB. Nociception affects motor output: A review on sensory-motor interaction with focus on clinical implications. *Clin J Pain*. (2012) 28:175–81. doi: 10.1097/AJP.0b013e318225daf3

100. Patterson BK, Guevara-Coto J, Yogendra R, Francisco EB, Long E, Pise A, et al. Immune-based prediction of COVID-19 severity and chronicity decoded using machine learning. *Front Immunol*. (2021) 12:700782. doi: 10.3389/fimmu.2021.700782

# Frontiers in Medicine

**Translating medical research and innovation into improved patient care**

A multidisciplinary journal which advances our medical knowledge. It supports the translation of scientific advances into new therapies and diagnostic tools that will improve patient care.

## Discover the latest Research Topics

See more →


**Frontiers**

Avenue du Tribunal-Fédéral 34
1005 Lausanne, Switzerland
frontiersin.org

**Contact us**

+41 (0)21 510 17 00
frontiersin.org/about/contact